Comprehensive Two-Dimensional Liquid Chromatographic Analysis of Phenolics

by

Kathithileni Martha Kalili

Dissertation submitted for the degree of

Doctor of Philosophy (PhD) in Chemistry *in the*

Faculty of Science

at

Stellenbosch University

Supervisor: Prof. André de Villiers

December 2013

Declaration

By submitting this dissertation electronically, I declare that the entirety of the work contained therein is my own, original work, that I am the sole author thereof (save to the extent explicitly otherwise stated), that reproduction and publication thereof by Stellenbosch University will not infringe any third party rights and that I have not previously in its entirety or in part submitted it for obtaining any qualification.

Date: December 2013

Abstract

Phenolic chemistry is quite complex; natural phenolic compounds vary widely in terms of size and chemical properties. The high structural diversity within this family presents severe analytical challenges. High performance liquid chromatography (HPLC) is the preferred method for phenolic analysis; however, conventional HPLC methods offer limited separation power and often provide incomplete separation of the large number of components present in natural phenolic extracts. Multi-dimensional chromatographic techniques have proven much more effective in the analysis of complex samples. The current study explored the potential of comprehensive two-dimensional liquid chromatography (LC×LC) for the characterisation of phenolic compounds in complex natural products, with the emphasis on proanthocyanidins (PACs).

Initial work focused on the evaluation of the state of the art in phenolic analysis, to allow information which was used in the development of optimal 1-D separations for use in LC×LC. The combination of hydrophilic interaction chromatography (HILIC) in the first dimension with reversed-phase liquid chromatography (RP-LC) in the second dimension afforded an orthogonal and powerful separation system for phenolics, providing separation on the basis of hydrophilicity and hydrophobicity, respectively. A detailed and systematic procedure was therefore developed to allow the optimisation and evaluation of on-line, off-line and stop-flow HILIC×RP-LC methods. Results showed that all three approaches provide much better separation performance than conventional one-dimensional LC (1-D LC) techniques. On-line HILIC×RP-LC offers automation, shorter analysis times, better reproducibility and minimal sample exposure. The off-line and stop-flow methods are characterised by much higher peak capacities, but relatively long analysis times. It was also demonstrated that stop-flow operation results in negligible additional band broadening for procyanidins (PCs), implying that this method is an attractive alternative to the off-line method as it offers automation and minimal sample handling. Experimental verification of the predictions based on fundamental principles confirmed the validity of the optimisation procedure for cocoa PCs.

The hyphenation of on-line HILIC×RP-LC separation with fluorescence (FL) and mass spectrometry (MS) detection methods provided enhanced resolution in a practical analysis time with the added benefit of selective detection and greater certainty in compound identification. This strategy proved much more powerful, as demonstrated by the identification of the highly complex PACs in grape seeds based on chromatographic retention data in two dimensions and accurate mass information. It was further shown that on-line coupling of HILIC×RP-LC separation with an optimised radical scavenging assay provides an improved approach for screening of individual radical scavengers in complex phenolic fractions, as demonstrated for cocoa, grape seed and green tea extracts.

Opsomming

Fenoliese chemie is baie kompleks; natuurlike fenoliese verbindings varieer in terme van beide grootte en chemiese eienskappe. Hierdie hoë strukturele diversiteit binne die familie bied daadwerklike analitiese uitdagings. Hoëverrigtingvloeistofchromatografie (HPLC) is die voorkeur-metode vir fenoliese analises, maar konvensionele HPLC metodes bied egter 'n beperkte skeidingsvermoë en verskaf dikwels onvolledige skeiding van die groot aantal komponente teenwoordig in natuurlike fenoliese ekstrakte. Multi-dimensionele chromatografiese tegnieke is bewys om baie meer effektief te wees met betrekking tot die ontleding van komplekse monsters. Hierdie studie ondersoek die potensiaal van omvattende twee-dimensionele vloeistof chromatografie (LC×LC) vir die karakterisering van fenoliese verbindings in komplekse natuurlike produkte, met die fokus op pro-antosianidiëne (PAC's).

Aanvanklike werk het gefokus op die evaluering van moderne tegnieke vir fenoliese analise – inligting wat in die ontwikkeling van optimale 1-D skeidings vir die toepasing in LC×LC gebruik is. Die kombinasie van hidrofiliese interaksie chromatografie (HILIC) in die eerste dimensie met omgekeerde-fase vloeistof chromatografie (RP-LC) in die tweede dimensie verleen 'n ortogonale en kragtige skeidingsisteem vir fenoliese komponente en verskaf skeiding op grond van onderskiedelik hidrofiliteit en hidrofobiteit. 'n Gedetailleerde en sistematiese prosedure is dus ontwikkel om die optimisering en evaluering van aan-lyn, af-lyn en stop-vloei HILIC×RP-LC metodes uit te voer. Resultate het getoon dat al drie benaderings baie beter skeidingsvermoë bied as konvensionele een-dimensionele LC (1-D LC) tegnieke. Aan-lyn HILIC×RP-LC bied outomatisering, korter ontledingstyd, beter herhaalbaarheid en minimale monster blootstelling. Die af-lyn en stop-vloei metodes word gekenmerk deur 'n veel hoër piekkapasiteit, maar relatief lang ontledingstye. Daar is ook getoon dat die stop-vloei prosedure geringe bykomende bandverbreding vir prosianodiniëne (PC's) tot gevolg het, wat beteken dat hierdie metode 'n aantreklike alternatief is vir die af-lyn metode aangesien dit outomatisering bied en minimale monster hantering behels. Eksperimentele verifiëring van die voorspellings gebaseer op fundamentele beginsels bevestig die geldigheid van die optimalisering proses vir kakao PCs. Die koppeling van aan-lyn HILIC×RP-LC skeiding met fluoressensie (FL) en massaspektrometrie (MS) deteksie verskaf verbeterde resolusie binne 'n praktiese ontledingstyd saam met die bykomende voordeel van selektiewe opsporing en groter sekerheid betreffende die verbindings se identifikasie. Hierdie strategie was baie meer kragtig, soos gedemonstreer deur die identifisering van die hoogs komplekse PAC's in druiwepitte gebaseer op chromatografiese behoud van die integriteit van die data in twee dimensies tesame met akkurate massa inligting. Daar is verder getoon dat aanlyn koppeling van HILIC×RP-LC skeiding met 'n geoptimiseerde radikale vangers deteksie-metode 'n beter benadering bied om die gedrag van individuele radikale vangers in komplekse fenoliese fraksies te bestudeer, soos bewys is vir kakao, druiwepitte en groen-tee ekstrakte.

Acknowledgements

First and foremost, I would like to thank the Almighty, our Heavenly Father for the protection, mercy, grace, guidance and for making everything possible.

I would also like to express my sincere gratitude to the following individuals and institutions for their invaluable contributions to this study:

I would forever be indebted to my supervisor and chromatography teacher, Prof André de Villiers, first of all, for welcoming me in his research group, despite the fact that I had very limited knowledge on the subject. Thanks for believing in me, I could not have done this without you. Thanks for your guidance, patience and immense help throughout the years. I am thankful for the many wonderful opportunities I have had to attend conferences, both locally and internationally, and for the research visit to Belgium (that was an experience I will treasure for life, many thanks!). Thanks for the financial support and for sharing your knowledge and experience, not only on academic issues but on other aspects of life as well, I have learned so much from you. I could go on and on, but the truth is, I don't think I will ever be able to thank you enough.

I am very grateful to my financial supporters: Stellenbosch University (Harry Crossley Foundation, Merit bursary), National Research Foundation (NRF) and the Postgraduate and International Office (PGIO).

The Separation Science Group (Stellenbosch University) for providing a friendly and conducive working environment, for all the discussions, for offering help when needed and for those little chit-chats, it has really been a pleasure and blessing to have you guys around.

Many thanks to the academic, technical and administrative staff of the Chemistry and Polymer Science (Stellenbosch University) for all the assistance. A special thanks to Shafiek Mohamed, Deidre Davids and Roger Lawrence for taking care of the administrative and laboratory matters.

Thanks to Dr Marietjie Stander, Fletcher Hiten and Meryl Adonis for assistance with the LC–MS experiments and data analysis.

Thanks to Prof Deirdre Cabooter for helping with the kinetic plot program and many other things, thanks for looking out for me during my visit in Belgium and also for the many crazy things we did together, I owe you for so much.

I am thankful to Jochen Vestner for assisting with the processing of the LC×LC–MS data and also for putting up with my constant nagging, really greatly appreciated.

Thanks to Prof Harald Pasch for serving as an internal examiner, and also Prof Paola Dugo and Dr Stefan Louw for serving as external examiners.

Thanks to Mr Alexander Whaley of LECO Africa for assistance with the ChromaTOF software.

Ms Renate Smit of the Department of Horticulture, Drs James Lloyd and Christell van der Vyver of the Institute of Plant Biotechnology (IPB), Dr Dalene de Beer of the Agricultural Research Council (ARC, South Africa) are thanked for putting their freeze-driers at my disposal.

Thanks to Ms Huba Boshoff of PGIO for facilitating my research visit to Belgium and providing me with necessary information and tips I needed to survive Belgium.

I am also greatly indebted to Tom Parlevliet of the Department of Organic Chemistry (Ghent University, Belgium) for the warm welcoming and for taking care of me during my stay in Belgium.

A special thanks to Prof Frédéric Lynen and the entire Separation Science group of Ghent University (Belgium), for welcoming and accommodating me in your research group, for all the help and for making my stay in your laboratory a memorable one.

The Namibian Oshiwambo service group, a special thanks to our pastors for sacrificing their most valuable time to satisfy our spiritual needs, thanks for your unwavering faith and commitment to serve God's people. Your sound knowledge of the gospel, words of wisdom greatly motivated and helped us to remain focused and spiritually uplifted. The discussions at the end of the sermons were very enlightening and life-changing, thanks to everybody who contributed; we have all learned a thing or many. God bless you abundantly.

I thank my parents for their words of wisdom, constant encouragement, support and love.

Last, but not least, my friends, family and anybody else whose name I might have omitted, thanks for your support and for sticking with me even when I was least lovable, you have all contributed to the successful completion of this work.

Table of Contents

Chapter 3

Chapter 4

Addenda

Dissertation Layout

This dissertation is presented in a new format for Stellenbosch University where the bulk of the dissertation is presented as published work. The publications are placed in context by a general introduction familiarising the reader with the relevant fields, followed by concise summaries of the content of the publications and finally some general conclusions and recommendations for future studies. This dissertation is therefore structured as follows:

Chapter 1 provides a general preface to the study, highlighting the research goals.

Chapter 2 provides background information on phenolic compounds with the emphasis on their occurrence, chemistry, importance and methods of analysis. The separation principle and aspects pertaining to multi-dimensional separations are concisely discussed to facilitate interpretation of the results presented in later chapters.

Chapter 3 presents short summaries of the results (Addenda B-F) obtained in this study.

In **Chapter 4**, general conclusions and recommendations for future studies are presented.

Addenda A-F presents the publications resulting from this work and additional supporting information. It must be mentioned that the student was responsible for the execution of the experimental work and the drafting of the manuscripts for all the publications presented in this dissertation except for the popular article entitled “Improving HPLC separation of polyphenols” presented in Addendum A.

Chapter 1

General Introduction and Objectives

This chapter presents a general introduction to the research topic as well as the specific objectives of the study.

1.1. General introduction

Phenolic compounds represent one of the most widespread and most-studied groups of natural compounds. Phenolics are common constituents of a variety of plant-derived foods and beverages and are consumed in large quantities as part of the human diet [1]. These compounds have attracted increasing attention in the past decades, due to their numerous health benefits and also a number of influential roles that they play in food quality. It is also for these reasons that plant extracts are increasingly being used in a variety of nutritional supplements, pharmaceutical, cosmetic and nutraceutical products. To obtain a better understanding of the roles of phenolics in human health and food quality, methods that allow accurate determination of individual compounds in various sample matrices are required since these properties are compound-dependent [2-4]. Despite their importance, no single analytical method is capable of providing complete characterisation of this diverse group of compounds in complex samples. In particular, the large diversity of phenolic structures demands more efficient separation methods.

Extensive research has been focused on the development of suitable analytical methods for phenolics, and notable progress has been made in phenolic research in recent years. Various analytical methods including gas chromatography (GC), thin layer chromatography (TLC) and capillary electrophoresis (CE) have been employed for phenolic analysis, but high performance liquid chromatography (HPLC) is by far the most widely used technique. Although conventional LC methods in combination with common detection methods such as ultraviolet-visible (UV-vis), fluorescence (FL) and mass spectrometry (MS) have greatly contributed to unravelling the phenolic composition of various natural products, these methods remain limited in terms of separation power and therefore do not guarantee complete separation of complex phenolic samples. More recently, new technologies in LC such as ultra high pressure liquid chromatography (UHPLC), high temperature LC (HTLC) and alternative stationary phases such as monolithic and superficially porous packings have also been applied in phenolic analysis for improved performance. While these strategies provide better separation efficiency and/or speed compared to conventional methods, these performance gains are not commensurate with the complexity of the phenolic composition of natural products. This is in essence due to the limited separation space and selectivity provided by single chromatographic separations [5]. Coupling multiple separation methods not only results in increased separation space, but also increases selectivity through the use of a secondary separation mechanism, which effectively delivers improved resolution [5,6]. The benefit of multi-dimensional (MD) separation techniques has been demonstrated for a variety of complex biological and natural product samples in recent years.

Against this background, the current study was aimed at developing specifically more powerful comprehensive two-dimensional LC (LC×LC) methods for the analysis of phenolics. As primary target analytes, proanthocyanidins (PACs) were used. PACs represent one of the most complex

families of phenolic compounds, since they vary significantly in terms of isomeric distribution as well as molecular weight (MW). Oligomeric PACs are important constituents of various natural products such as cocoa, apples, grapes, green tea, etc. Yet, as a result of their complexity, oligomeric PACs cannot be separated by conventional HPLC.

1.2. Aims and Objectives of the study

This study was aimed at developing novel and powerful LC×LC methodologies that would allow detailed chemical investigation of phenolic compounds in natural products, with particular emphasis on oligomeric PACs. To achieve this aim, the following specific objectives were formulated:

(i) To evaluate the performance of the latest generation of chromatographic supports and/or column formats in order to select the best chromatographic support and experimental conditions for improved phenolic separation in one and two dimensions.

(ii) To select the best-suited one-dimensional separation methods and evaluate their separation performance in the LC×LC analysis of phenolics using on-line, off-line and stop-flow approaches. This would entail development of a theoretical optimisation strategy for each of these LC×LC modes, followed by experimental verification of the findings using a real-life complex phenolic sample as application.

(iii) To develop hyphenated techniques combining LC×LC separation with UV, FL and MS detection methods as a means of enhancing the utility of LC×LC by providing selective detection and simplifying compound identification. The applicability of this approach will be demonstrated by the qualitative analysis of a highly complex phenolic sample.

(iv) To assess the potential of coupling LC×LC to a radical scavenging assay as a novel and powerful method for the identification of individual radical scavenging species in complex phenolic extracts.

References

[1] M. D'Archivio, C. Filesi, R. Di Benedetto, R. Gargiulo, C. Giovannini, R. Masella, Ann Ist Super Sanità 43 (2007) 348.
[2] E. Haslam, Biochem. J. 139 (1974) 285.
[3] J. Rigaud, M.T. Escribano-Bailon, C. Prieur, J.-M. Souquet, V. Cheynier, J. Chromatogr. A 654 (1993) 255.
[4] G. Tucker, K. Robards, Crit. Rev. Food Sci. Nutr. 48 (2008) 929.
[5] J.C. Giddings, in H.J. Cortes (Editor), Multidimensional Chromatography: techniques and applications, Marcel Dekker, Inc., New York, 1990, p. 1.
[6] H.J. Cortes, L.D. Rothman, in H.J. Cortes (Ed.), Multidimensional Chromatography: Techniques and Applications, Marcel Dekker, Inc., New York, USA, 1990, p. 219.

Chapter 2

State of the art in Phenolic Analysis

This chapter introduces the reader to the world of phenolic compounds, providing an overview on the occurrence, basic chemistry and importance of phenolics. Conventional as well as current analytical approaches for phenolic compounds are also outlined.

Since the goal of the research presented in this dissertation was to develop improved methods for phenolic analysis, the first step was to obtain a comprehensive overview of current trends in phenolic analysis, with the emphasis on recent developments and current limitations. This chapter summarises the information provided in two publications (Addendum A). The first is a review of literature reports on phenolic analysis covering the period 2000-2010, while the second is a more popular article discussing means of improving phenolic analyses by LC. These reports discuss the beneficial application of ultra high pressure liquid chromatography (UHPLC), high temperature LC (HTLC), multi-dimensional LC (MDLC) as well as new stationary phase morphologies (monolithic and superficially porous packings) to phenolic analysis. Since this is a highly active research field, a list of additional references covering the period 2011-2013 has also been added to Addendum A.

2.1. Phenolic compounds: occurrence, basic chemistry and importance

Phenolic compounds (also referred to as phenolics or polyphenols) are natural molecules occurring widely throughout the plant kingdom [1]. Phenolics constitute a significant portion of plant secondary metabolites and are present in relatively high amounts in various plant tissues. As such, phenolic constituents form a significant part of the human diet, as they are present in a variety of plant-derived products such as fruits and vegetables [2,3].

The term “phenolic compounds” encompasses a diverse family of chemical structures; more than 8000 compounds have been isolated to date [1,4,5], all of which possess at least one aromatic ring comprising one or more hydroxyl groups. Phenolic compounds range from simple phenols to highly polymerised forms and can be broadly classified into flavonoids and non-flavonoids on the basis of their structural features (**Figure 2.1**). Flavonoids represent the largest group of plant phenolics and are sub-divided into various classes whose structures are characterised by a C_6-C_3-C_6 backbone, with variations occurring at the central heterocyclic ring [6]. These include flavones, flavonols, isoflavones, flavanones, flavanonols, anthocyanidins and flavanols (catechins and tannins). Non-flavonoids are sub-divided into simple phenols, phenolic acids, coumarins, xanthones, chalcones, stilbenes, lignins and lignans. It should be mentioned that further sub-division within individual classes is possible based on differences in hydroxylation patterns and stereochemistry, and that significant additional structural diversity occurs due to glycosylation, acylation, prenylation, alkylation, etc [4].

Phenolic compounds have been the subject of extensive research due to ever-increasing scientific evidence suggesting a diverse array of roles that these compounds play in human health and food quality. For example, phenolics purportedly exhibit anti-oxidant, anti-microbial, anti-inflammatory, anti-carcinogenic and anti-hypertensive effects [7,8]. In addition, these compounds are involved in a number of other roles, including but not limited to, defensive mechanisms against pathogens in plants [5], protecting plants against UV radiation and oxidation [5], imparting colour to flowers, fruits and vegetables [5,9] as well as colour stabilisation in natural products and their derived commodities [10,11].

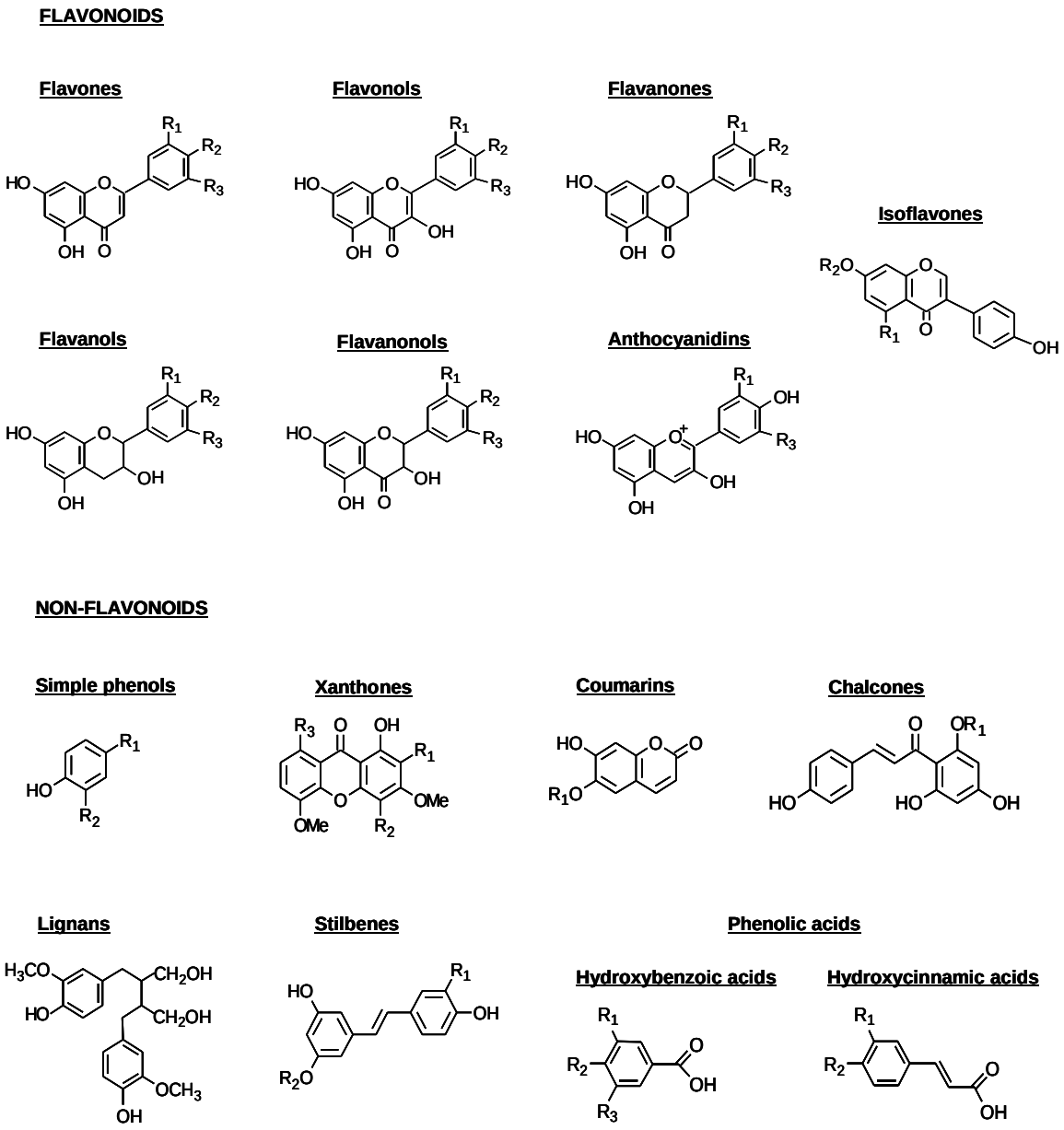

Figure 2.1. General chemical structures for the major classes of natural phenolic compounds [12].

2.2. Conventional strategies in phenolic analysis

2.2.1. Sample preparation methods

Sample preparation is often the most important and critical part of an analysis. Different sample preparation procedures may be used for phenolic analysis depending on the sample matrix and/or analytical method of choice. For this reason, the discussion will be limited to sample preparation methods pertaining to liquid chromatographic analyses.

Although procedures vary widely depending on the type of sample and target analytes, a few generalisations can be made with respect to types of samples. For solid samples, isolation of

phenolics is generally achieved using conventional methods such as Soxhlet extraction (SE) or solid-liquid extraction (SLE). SLE is more often used and typically involves homogenisation of the dried or frozen material, followed by extraction with a suitable solvent. Relatively apolar solvents such as dichloromethane, chloroform, ethyl acetate and diethyl ether are commonly used for extraction of less polar phenolics, while more polar solvents such as methanol, acetone, ethanol, ethyl acetate or aqueous mixtures of these are used for more polar compounds. In some cases, extraction with hexane or dichloromethane may be necessary to remove fatty materials and/or chlorophyll before phenolic extraction [13], while addition of small amounts of acidic modifiers may facilitate the extractability and/or enhance stability of certain compounds [14]. Acidic solvents should however be used with caution as they might induce hydrolysis of the acid labile interflavanoid bonds present in highly condensed tannins [1]. Extraction is normally performed by shaking or magnetic stirring, although alternative extraction approaches such as microwave-assisted, ultrasound-assisted, pressurised solvent and supercritical fluid extraction have also been investigated as means of enhancing the extraction efficiency and/or speed. Each approach has its benefits and limitations, therefore the choice would depend on the analysis goals. Parameters such as temperature, solvent composition, sample weight to solvent volume ratio, pH and extraction time have all been found to influence the extraction efficiency of phenolics from their matrices [4, 15-17], therefore careful optimisation of extraction conditions is often required for optimum yield.

Liquid samples such as fruit juices, beers and wines generally require minimal sample preparation steps, sometimes only centrifugation, filtration and/or dilution (or de-alcoholisation for alcoholic products) is necessary prior to analysis. Where sample pre-concentration or clean-up is necessary, this can be performed using solid-phase extraction (SPE), liquid-liquid extraction (LLE) or column chromatography (CC). SPE is the preferred method for purification, fractionation and/or enrichment of crude phenolic extracts and liquid samples due to its simplicity, versatility, high recoveries and good reproducibility [4]. Alkyl-bonded silica (mostly C18) or co-polymeric sorbents are normally used for this purpose. SPE can also be coupled on-line with HPLC separation, thus allowing automation and increased sample throughput [18]. Countercurrent chromatography (CCC) has also been used for fractionation of phenolic extracts [19].

2.2.2. Analytical methods

Although analytical techniques such as thin layer chromatography (TLC), capillary electrophoresis (CE) and gas chromatography (GC) have all found application in the qualitative and/or quantitative determination of phenolic compounds, high performance liquid chromatography (HPLC) is the most extensively used method. In the next section, brief overviews of each of these methods will be presented.

Thin layer chromatography. TLC offers a relatively simple, rapid and cost-effective method for preliminary screening of phenolic constituents in crude plant extracts [20-22]. Separation in TLC generally entails spotting of the extract onto a layer of an adsorbent immobilised on a glass plate or plastic sheet support, followed by development of the plate in a suitable solvent. The separated bands are then visualised under UV light, by spraying the plate with a suitable reagent or exposing the plate to iodine vapour [22]. Silica, cellulose and polyamide plates are commonly used, and a wide range of solvent systems have been described. A number of one- (1-D) and two-dimensional (2-D) TLC methods have been developed for different classes of phenolics. For example, Lea [23] achieved good separation of catechins and procyanidin oligomers ranging from monomers to heptamers on silica plates. Mueller-Harvey *et al* [20] developed a 2-D TLC method for condensed and hydrolysable tannins based on a cellulose plate and solvent mixtures containing acetic acid and water in the first dimension and 1-butanol, acetic acid and water in the second dimension. On-going developments in TLC have led to significant improvement in the technique in recent years; better coating materials as well as novel sample application and solvent feeding methods have become available. This technique is now known as high performance TLC (HPTLC), and is preferred as it offers automation, faster and improved separation and requires less solvent compared to classical TLC [24]. TLC however remains a screening and/or preparative tool for crude phenolic extracts due to its relatively poor separation performance.

Gas chromatography. Despite its superior separation power, GC has only found limited application in phenolic analysis. This is primarily due to the low volatility and/or thermal lability of many phenolic compounds [4,22]. To be made amenable to GC analysis, polyphenols are commonly transformed into more volatile species by converting hydroxyl groups through methylation, ethylation or silylation [4]. Silylation is preferred over methylation because it is applicable to a much wider range of compounds [25] and since methylated and/or methoxylated derivatives frequently occur in nature [26]. Derivatisation normally involves heating (60-120 °C) of the phenolic extract in the presence of a suitable derivatising agent for a defined period (10 to 120 min). Derivatisation reagents such as diazomethane, ethyl- and methylchloroformate, trimethylchlorosilane, dimethyldichlorosilane, bis-(trimethylsilyl)-trifluoroacetamide are commonly used. Separation is generally achieved on apolar capillary columns (such as (5%-phenyl)-methylpolysiloxane [27-30]) using temperature gradients with flame ionisation and/or mass spectrometric detection. Multi-dimensional GC (MDGC) methods have also recently been applied to phenolic analysis. For example, Gao *et al* [31] reported a comprehensive two-dimensional GC (GC×GC)-flame ionisation detection–time-of-flight mass spectrometry (FID–TOF-MS) method combining polar and apolar columns for the analysis of trimethylsilylated flavonoids and chalcones. Although derivatisation is an effective means of improving volatility and extending the utility of GC to phenolic analysis, the potential formation of multiple derivatives from a single compound

represents a significant drawback [32,33]. Furthermore, these procedures are mostly time-consuming and labour-intensive, although alternative methods such as microwave heating can be used to reduce the derivatisation time [34].

Nonetheless, a few studies have reported the GC analysis of phenolics without derivatisation. For example, Schmidt and Merfort [35] developed a GC–MS method which allowed separation and identification of 49 underivatised flavones, flavonols, flavanones and chalcones. Dos Santos Pereira and co-workers [36,37] also successfully characterised flavonoids and rotenoids in various plant extracts using high temperature GC–MS without the need of derivatisation.

The GC analysis of particularly flavonoid glycosides, even after derivatisation, is a challenging task [4,33]. With the availability of improved derivatisation approaches, high temperature GC and MDGC, the application of GC to phenolic analysis is expected to continue, although it is highly unlikely that the technique will replace HPLC as the method of choice for this purpose.

High performance liquid chromatography. HPLC currently represents the most widespread method for polyphenol analysis, both for analytical and preparative purposes [22]. Reversed-phase LC (RP-LC) is the mode of choice for phenolic analysis. Separation is usually achieved on 3-5 µm C18 (and less commonly, C8) columns using gradient elution with aqueous methanol or acetonitrile mobile phases. Acidic modifiers are normally added to suppress ionisation of phenolic acids and improve analyte stability and peak shapes. More acidic mobile phases (pH<2) are required for better chromatographic efficiency for anthocyanin analysis [38,39]. While RP-LC generally provides good separation of low molecular weight compounds on the basis of hydrophobicity, this method fails to resolve highly condensed isomeric compounds [7]. Alternative HPLC modes such as normal-phase LC (NP-LC) and hydrophilic interaction chromatography (HILIC) have also been employed in phenolic analysis. These methods rely on the use of polar supports such as silica, bonded amide and diol phases in combination with relatively apolar eluents such as dichloromethane-methanol-water-formic acid [40] or acetonitrile-methanol-water-acetic acid [41] mixtures. Separation occurs on the basis of polarity [40], although isomeric structures or compounds with similar polarity are not resolved. Thorough optimisation of chromatographic conditions is required for optimum performance with regard to target analytes and no single method provides complete resolution of all the phenolics. HPLC is most often coupled with detection methods such as ultraviolet-visible (UV-vis) or diode-array (DAD) and MS to allow on-line identification of phenolics.

Capillary electrophoresis. Since the 90's, capillary electromigration techniques have also been applied for the separation of phenolic compounds, often with promising results. Different CE modes such as capillary zone electrophoresis (CZE), micellar electrokinetic chromatography (MEKC), microemulsion electrokinetic chromatography (MEEKC), capillary electrochromatography (CEC),

capillary isotachophoresis (CITP) and non-aqueous CE (NACE) have been described for phenolics. Although these methods differ in terms of separation principles, they all rely on the use of an electric field to bring about differential electromigration of analytes [19,42]. Of these modes, CZE and MEKC are by far the most extensively used in phenolic analysis. Separation is generally carried out in fused silica capillaries using borate and phosphate buffers for CZE, while surfactants like sodium dodecyl sulphate (SDS) are commonly added in MEKC. Detection is mostly performed using UV-vis or DAD; fluorescence (FL), electrochemical (EC) and MS detection methods have also been described.

CZE has been used for the determination of phenolics in various samples including olive oil [43,44], green tea infusions [45] and wines [46], while MEKC has been used for phenolic separation in black and green tea extracts [47-49], cacao and chocolate [50,51] and various food samples [52]. Acidic, basic and neutral conditions have all been evaluated, although the instability of phenolics under basic conditions makes acidic conditions preferable [48,52,53].

CE can provide peak capacities orders of magnitude higher than those achievable in HPLC, coupled to the advantages of alternative selectivity, shorter analysis times and low sample and solvent consumption [49]. However, well documented drawbacks of the technique include lower sensitivity and poor reproducibility compared to HPLC [54]. In addition, method development in CE is relatively complicated.

Alternative methods. In addition to the analytical methods discussed above, spectrophotometric methods such as the Prussian-Blue [55], Folin-Ciocalteu [56], vanillin, butanol-acid and dimethylaminocinnamaldehyde (DMACA) assays are also frequently used in the measurement of the phenolic contents of samples [57]. While these assays differ with respect to the reagents used, the operation principles are somewhat similar, typically involving the reaction of a sample with a specific reagent to form a coloured species, which is then quantified spectrophotometrically [58]. Although some assays are specific for certain classes of compounds, most lack specificity and detect all phenolic compounds present in a sample. Therefore, sample fractionation may be necessary if quantification of a certain class of phenolics is desired. Depolymerisation assays such as thiolysis and phloroglucinolysis are also used for the determination of constituent units of proanthocyanidin oligomers and their mean degree of polymerisation (mDP) [58]. Essentially, these reactions involve acid-catalysed hydrolysis of the sample in the presence of a suitable nucleophile (thiol or phloroglucinol), which provides a free terminal unit and a nucleophile adduct of the extension unit [59]. Degradation is usually followed by HPLC analysis to allow identification of constituent units.

2.2.3. Detection methods

Detection constitutes an essential aspect of any analysis. Several chromatographic detection methods are available; this discussion will focus on detectors used in combination with HPLC for phenolic compounds, including UV-vis or DAD, FL and MS. Electrochemical detection (ECD) has also been employed to a lesser extent, while nuclear magnetic resonance (NMR) spectroscopy plays an important role in the structural elucidation of phenolic compounds.

Despite the fact that UV-vis detectors may suffer from interferences, this detection method is most widely used in phenolic analysis. Owing to differences in structural features, phenolic compounds often exhibit distinctive UV absorbance maxima [22]. For example, flavan-3-ols absorb maximally around 270-290 nm, flavones and flavonols exhibit two absorption bands around 310-380 nm and 250-295 nm [38], phenolic acids show two bands in the regions 225-235 nm and 290-330 nm [6], while anthocyanins are characterised by a maximum in the visible region around 460-560 nm [38]. This makes DAD useful, since multiple wavelengths can be monitored for selective detection of different phenolic classes, and tentative identification of individual compounds can be performed based on characteristic absorption spectra. Absorption spectra are also helpful for peak purity determination.

Because of the lack of fluorescence properties of most native phenolics, fluorescence detection (FLD) is not as widely used in phenolic analysis. Where applicable, FLD is beneficial due to the inherent selectivity and sensitivity of the technique. Some phenolic classes such as flavan-3-ols, phenolic acids, stilbenes, flavones and isoflavones do possess native fluorescence. For example, FLD has proven useful in the detection of phenolic acids, stilbenes and flavan-3-ols in wine samples [11,60], phenolic acids in plant materials and pharmaceutical preparations [61], flavones in orange and mandarin essential oils [62], polymethoxylated flavones in orange juices [63,64], isoflavones in a red clover extract [65] and procyanidins in a variety of samples [7,41,66]. Furthermore, derivatisation has been used to extend the utility of fluorescence in phenolic detection. For example, Hollman *et al* [67] and Gutierrez *et al* [68] found post-column complexation of some flavonols (which lack native fluorescence) with aluminium ions to result in highly fluorescent complexes.

ECD has also demonstrated its usefulness in phenolic detection. This method is suitable for detection of compounds containing electroactive groups (such as the phenolic group) which can easily be oxidised or reduced at low potentials [69]. For example, ECD has been applied in the detection of phenolic compounds in various matrices such as orange juice [70], tea samples [71], beer [69,72,73] as well as cacao beans and chocolates [74]. Compared to UV detection, both fluorescence and electrochemical detection have been shown to provide better selectivity, sensitivity and reduced interferences.

MS detection has also found considerable use, and in recent years has become indispensable in the analysis of complex phenolic fractions. MS allows compounds to be identified based on their molecular ions and/or characteristic fragment ions. Several ionisation methods such as atmospheric pressure electrospray ionisation ((AP)ESI), atmospheric pressure chemical ionisation (APCI), thermospray (TSP), continuous flow fast atom bombardment (CF-FAB) and matrix-assisted laser desorption ionisation (MALDI) have been used. Owing to its high ionisation efficiency, ESI has found widespread use in phenolic analysis, although APCI and MALDI are increasingly becoming popular. All methods provide efficient ionisation in both positive and negative modes depending on analysis conditions. The most common mass analysers are the quadrupole (Q) and time-of-flight (TOF) instruments. Quadrupole instruments are cheap and robust, however they are limited in terms of resolution. TOF instruments on the other hand are more costly, but their high resolution allows much higher certainty in compound identification based on accurate mass information. Tandem MS (MS/MS) instruments such as triple quadrupole and Q-TOF systems are increasingly being used as highly selective detectors and for structural elucidation purposes.

Owing to the low energy involved in the ionisation process, soft ionisation methods such as ESI and MALDI mostly produce intact molecular ions with minimal fragmentation [75]. Fragmentation processes such as collision-induced dissociation (CID) may be used in combination with MS/MS to induce fragmentation of molecular ions to allow determination of structural features. LC-MS/MS has been extensively used to provide structural information on phenolics. For example, Gu *et al* [76-77] and Li *et al* [78] employed ESI-MS/MS in the characterisation of proanthocyanidins in various foods. These authors were able to establish the connection sequence of individual flavanol units, the type(s) of interflavan linkages as well as substitution patterns for different proanthocyanidin oligomers on the basis of their fragmentation patterns. MS/MS and CID-MS methods are also useful in the determination of the nature of the aglycone and position of sugar units in *O*- and *C*-glycosylated phenolic compounds [22,32].

MALDI-TOF-MS has also proven to be a sensitive and efficient approach for the analysis of highly polymerised phenolic molecules such as tannins. For example, MALDI-TOF allowed identification of proanthocyanidins with degrees of polymerisation (DPs) ranging between 13 and 30 in different sample matrices [79-82]. More recently, MALDI-TOF-CID-MS has also been shown to be useful in the determination of the sequence of flavanol units in tannin oligomers, thereby allowing unambiguous assignment of isobaric structures in complex wood-based tannin extracts [83].

In addition to the detection methods described above, NMR spectroscopy also provides an invaluable structural elucidation tool for phenolic compounds. Through the use of 1-D and 2-D proton (^{1}H) and carbon-13 (^{13}C) NMR techniques, chemical environment information of each proton and carbon nucleus in a molecule as well as correlation between the different nuclei can be established. Deuterated dimethyl sulfoxide (DMSO-d_6) and methanol (CD_3OD) are the most

commonly used solvents for phenolic compounds. The potential of on-line coupling of HPLC with NMR has also been investigated recently, although this approach is generally characterised by low sensitivity and high instrumental complexity [84].

The coupling of separation techniques with multiple, complementary detection methods is a powerful means of rapid and unambiguous identification of compounds, since compounds can be identified based on different properties. Obviously, some combinations are more informative than others, while certain combinations are not feasible due to the destructive nature of some detectors. As an example, Abad-Garcia *et al* [85] reported a useful systematic identification strategy for phenolic compounds based on HPLC with DAD and MS/MS detection. In this study, UV spectra and fragmentation patterns for 72 phenolic compounds including phenolic acids, flavonols, flavan-3-ols, procyanidins, flavanones, coumarins, flavones, anthocyanins, chalcones as well as glycosylated derivatives were determined, and the applicability of the method was demonstrated for 17 different fruit juices. Such studies clearly demonstrate that selective and sensitive detection methods are essential for the detailed characterisation of phenolics in complex matrices. Of more benefit is the fact that this places less demand on rigorous sample preparation procedures, which can potentially result in loss of low level analytes or degradation of labile compounds.

2.3. Recent trends in phenolic analysis

Although conventional HPLC methods often provide adequate results, the relatively low separation power delivered by these methods does not allow complete separation of highly complex natural phenolic extracts. There is a high demand for improved methods for polyphenol analysis. In the past decade, a number of important developments in HPLC such as ultra high pressure liquid chromatography (UHPLC), high temperature liquid chromatography (HTLC), multi-dimensional LC (MDLC) as well as new stationary phase chemistries and morphologies, have provided new possibilities for improving the speed and efficiency of HPLC separations. These technologies have also been applied to phenolic analysis in recent years. Each of these technologies will be described briefly and their application in phenolic analysis will be discussed.

2.3.1. UHPLC and HTLC

From chromatographic theory, it is well-known that a reduction in particle size results in increased separation performance of packed columns. This is due to the fact that smaller particles pack more closely, thus providing shorter diffusion distances and more uniform flow through the column, consequently minimising band broadening [86,87]. This results in reduced A- and C-terms of the van Deemter (VD) equation, as can be seen in the experimental plate height curves for different particles shown in **Figure 2.2A**.

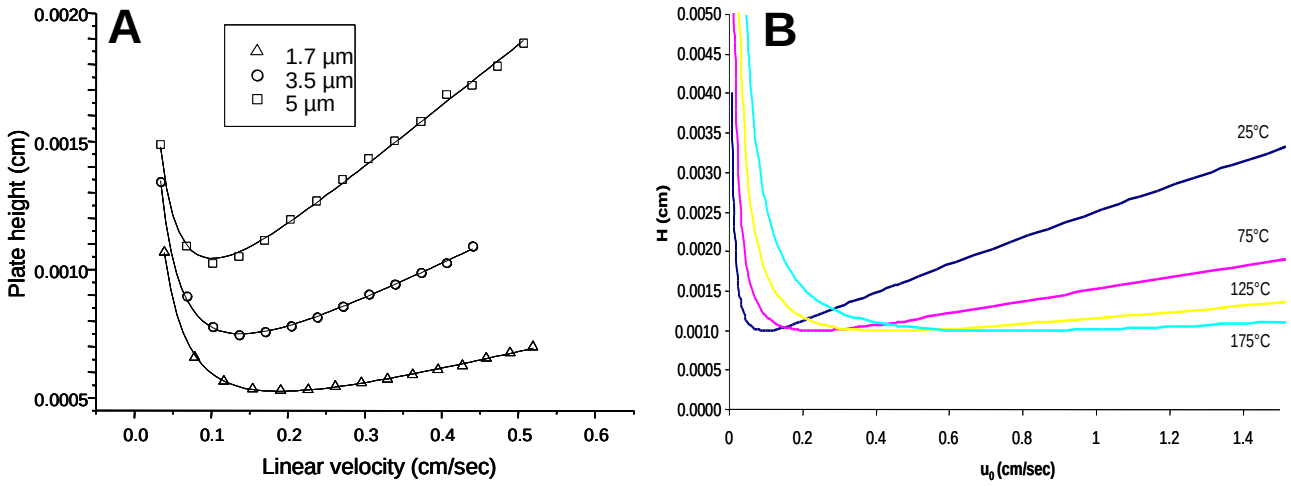

Figure 2.2. Experimental plate height curves obtained on 1.7, 3.5 and 5 µm HPLC columns (A) [88] and theoretical plate height curves illustrating the effect of temperature on the performance of a 5 µm HPLC column (B) [89].

Reducing the particle size is however coupled with an increase in pressure, since smaller particles have higher resistance to solvent flow. This is illustrated by Darcy's law [86,90], which correlates the pressure drop across the column (ΔP) to the mobile phase viscosity (η), column length (L), linear velocity (u_0), particle diameter (d_p) and column permeability (K_0):

$$\Delta P = \frac{K_0 \eta L}{d_p^{\,2}} u_0 = \frac{K_0 \eta N H}{d_p^{\,2}} u_0 \qquad (2.1)$$

Equation (2.1) illustrates that the pressure drop across a column is directly proportional to the column length and inversely proportional to the square of the particle size. This implies that reduction in particle size should be accompanied by reduction in column length, linear velocity or an increase in temperature (to lower the mobile phase viscosity) in order to keep the pressure drop the same. Reduction in d_p is therefore often accompanied by a similar reduction in column length to keep within the instrumental pressure limits. Shorter columns packed with small particles offer the benefit of speeding up separations – since higher optimal linear velocities can be used – although the gain in efficiency is minimal. When keeping the column length constant, higher efficiencies are achievable on columns packed with small particles, however at the cost of increased operating pressure. The practical exploitation of this approach only came to be realised in the late 1990s when Jorgenson and co-workers [86,91] developed an LC system capable of operating at pressures up to 5000 bar. This technology, which became known as "ultra high pressure liquid chromatography (UHPLC)" subsequently led to the commercial introduction of columns packed with sub-2 µm particles and instruments with pressure capabilities up to 1300 bar.

Temperature is another important parameter that holds promise to improve LC separations. An increase in temperature results in reduced mobile phase viscosity and increased mass transfer kinetics, providing enhanced efficiency at higher flow rates and therefore faster separations [92,93]. This benefit is clearly evident from the plate height curves obtained at different temperatures shown in **Figure 2.2B**. From the figure, it can be seen that while the maximum achievable efficiency remains roughly unchanged (as indicated by the minimum plate height), this value is achieved at higher mobile phase linear velocities when the temperature is increased, which effectively results in faster analyses. Although the benefits of HTLC have long been known [92] this parameter has, until recently, been under-utilised. This is partially due to the lack of thermally stable stationary phases and suitable instrumentation [92,93] as well as concerns relating to analyte stability. In the past decade, columns with improved thermal stability and dedicated HTLC instruments have become available; HTLC now finds considerable use in various application areas.

UHPLC and HTLC have also been exploited for improved phenolic separation. UHPLC is often complemented with high analysis temperatures (up to 80 °C) for even faster separations. A large number of reports are available on the applications of UHPLC and HTLC to phenolic analysis which cannot be covered in the content of this dissertation; rather, several pertinent examples will be highlighted. Several authors reported good separations of diverse phenolic compounds on reversed-phase columns packed with sub-2 µm particles in a variety of samples such as flowers [94], milk-based products [95], tea samples [96,97] and various plant extracts [98-101]. Analysis temperatures ranging between 30 and 80 °C were employed in these studies and between 8 and 27 compounds were separated using analysis times ranging between 0.5-10 min. Schwarz *et al* [102] described UHPLC and HPLC methods for the analysis of polyphenols and furanic derivatives in brandy. In this study, separation of 14 polyphenols was achieved in 6.5 min by UHPLC, while 60 min were required for HPLC. Moreover, the solvent consumption per analysis for HPLC was 60 mL, compared to 4.55 mL for the UHPLC method. Although strict comparison between these techniques is often difficult due to significant differences in operational parameters, UHPLC methods typically demonstrate better sensitivity, minimal solvent consumption as well as higher analytical throughput, with analysis time shortened by a factor up to 10 in some cases. When used in combination with short UHPLC columns, high temperature allows for further reduction in analysis times. Several authors have also shown that higher analysis temperatures can be applied to achieve highly efficient separations on longer UHPLC columns (150-200 mm) while providing analysis times similar to HPLC [103,104]. It should be noted that high temperature should be used with caution, as some phenolics are thermolabile. Therefore, the thermal stability of both analytes and stationary phases should be ascertained before practical implementation of this technique [92,105]. As a good example, de Villiers and co-workers [39,106] studied the thermal stability of

anthocyanins, and confirmed that analysis temperatures up to 70 °C could be used without the risk of on-column degradation for analysis times less than 120 min.

2.3.2. Alternative stationary phases for phenolic analysis

As is well-documented in HPLC literature, fully porous silica packings are the most widely used supports for most applications. Increasing column performance through further reduction in particle size is eventually limited by factors such as excessively high pressures and frictional heating that occurs at ultra high pressures [107]. Research into alternative stationary phase morphologies is aimed at overcoming some of the limitations of porous silica. Although a number of alternative packing materials are available, superficially porous and monolithic columns have received the most attention, therefore the following discussion will be limited to these technologies.

Superficially porous (also known as partially porous or core-shell) particles comprise a non-porous solid core coated with a thin porous layer. The fused-core technology was introduced back in the 1960s [108-110], however it was only around 2000 that this technology was revisited with great success, leading to commercialisation of a new generation of superficially porous columns [111]. Several column chemistries are currently available, with particle sizes ranging from 1.3 to 5 µm. The solid core to outer layer ratio is critical in determining the performance of these columns, and this differs somewhat between manufacturers. Although the exact reason(s) for the performance of superficially porous phases are the subject of some debate, the consensus is that the reasons are not only associated with shorter diffusion distances in the porous layer (i.e. reduced C-term of the van Deemter equation) [112], but also due to improved A- and B-terms on this phase. The principal benefit of these phases is that they provide similar performance to UHPLC columns, but on larger particle sizes and therefore at lower operating pressures. As a result, these particles are generally exploited for one of several benefits [107]: (i) using smaller particles to provide higher efficiencies and shorter analysis times (compared to similarly-sized fully porous counterparts), when higher pressure is available, (ii) using larger particles to provide performance similar to smaller fully porous particles at reduced pressures or (iii) using longer columns packed with larger particles to provide higher efficiencies under pressure constrained conditions, at the cost of analysis time. Furthermore, with the exception of sub-2 µm superficially porous particles, these benefits can be realised on conventional HPLC instruments.

From the limited number of reports that have appeared on the application of superficially porous phases in phenolic analysis, the trend seems to be geared towards achieving faster separations. For example, Manchón and co-workers [113] achieved a fast separation (6 min) of 12 target isoflavones on a 2.6 µm Kinetex superficially porous C18 column. Boros *et al* [114] and Dugo *et al* [115] employed 2.7 µm Ascentis Express superficially porous C18 columns for the rapid analysis of

phenolic compounds in various plant extracts. Shen *et al* [116] also used a 2.7 µm Halo superficially porous C18 column for the quantification of caffeoylquinic acid derivatives in artichoke heads and leaf extracts. Furthermore, Kinetex and Ascentis Express C18 columns have also been employed in the second dimension of LC×LC separations of phenolic compounds in a number of samples (see further); good separations were achieved in analysis times ranging between 0.42 and 2 min [73,115,117-121]. In all instances, these columns demonstrated similar benefits to UHPLC, providing enhanced resolution, sensitivity and shorter analysis times compared to conventional HPLC columns.

Monolithic columns are chromatographic supports characterised by a continuous macroporous structure [122]. Unlike conventional silica-based porous particles, these through-pore structures have far less resistance to solvent flow, which greatly improves the mass transfer and permeability of the column. Therefore, long monolithic columns can be used to achieve highly efficient separations, or short columns can be operated at high flow rates for gains in analysis speed. Although this technology has been known for decades, the first generation commercial monolithic columns were only introduced in 2000 [107]. This technology has also received attention in phenolic analysis in the past years.

As in the case of superficially porous particles, monolithic phases have mostly been utilised to speed up phenolic separations. For example, Apers *et al* [123] used two coupled 100 mm monolithic columns at a flow rate of 4 mL/min to provide improved resolution and an analysis time three times shorter than conventional HPLC. Rostagno *et al* [124] achieved a rapid separation (10 min) of 12 isoflavones on two coupled 100 mm monolithic columns at a flow rate of 5 mL/min and 35 °C. Chinnici *et al* [125] also achieved a good separation of phenolic acids, flavanols, chalcones and flavonols in apple extracts on a C18 monolithic column using a flow rate of 2.5 mL/min. Monolithic columns have also been evaluated for separation of phenolic compounds in lemon oil [126], beer and wines [117,127-129], grapes and must [130], red cabbage [16] and plant extracts [131,132]. These separations were achieved either on one or two coupled columns and analysis times ranged between 1 and 20 min, although higher flow rates were necessary. The use of high flow rates does represent a major drawback for monolithic columns, since large volumes of costly solvents are required. As a means of taking advantage of the benefits provided by monolithic columns while reducing solvent consumption, Jandera and co-workers [133-135] developed a series of capillary monolithic columns with various chemistries by means of *in-situ* polymerisation, which were also evaluated in the analysis of phenolic compounds. Despite the inherent advantage that monoliths hold for high-efficiency separations, this technology has not been applied for this purpose in phenolic analyses, while UHPLC has found much more widespread application in speeding up polyphenol analyses.

2.3.3. Multi-dimensional LC

As discussed in the precedent sections, several modern HPLC technologies provide significant gains in separation performance compared to conventional approaches. Even so, highly optimised one-dimensional chromatographic methods still fail to provide adequate resolving power to allow complete separation of complex real-world samples. This is a consequence of the large number of compounds present in these samples and the uneven distribution of peaks across the separation space [136]. Davis *et al* [136-139] studied component overlap phenomena in both one- and two-dimensional systems using the statistical method of overlap (SMO) theory and showed that a chromatogram should be 95% empty for a single component to have a 90% probability of appearing as a single peak. This suggests that any separation system should be capable of generating peak capacities (i.e. the number of peaks that can theoretically be separated by a given method at unit resolution, see further) which far exceed the number of components to be resolved. To achieve this in single chromatographic systems would require excessively long columns and impractically long analysis times.

Multi-dimensional separations are an alternative means of enhancing peak capacity. In a MD separation, multiple separation techniques are applied to a sample. Coupling multiple separations results in increased separation space and consequently, increased peak capacity. This approach allows maximum exploitation of selectivity differences between the selected separation modes, effectively reducing peak overlap [140]. MD separations can be performed in either comprehensive or heart-cutting modes [141]. In the comprehensive MD chromatography, the entire sample is analysed in both dimensions, whereas in the heart-cutting mode, only part of the sample (the area of interest) is analysed in both dimensions. For a system to be designated as truly comprehensive, (i) the selected methods should be based on different separation mechanisms (i.e. they should be orthogonal), (ii) any two components separated in the first dimension must remain separated in consecutive dimensions and (iii) the elution profiles from both dimensions should be preserved [141-143]. In order to meet these criteria and ensure optimum performance, thorough optimisation of several inter-related operation parameters is generally required. Three experimental configurations may be used for comprehensive two-dimensional chromatography: on-line, off-line and stop-flow. In the on-line set-up, fractions from the primary dimension are continuously transferred and analysed in the secondary dimension at defined time intervals. In the off-line system, fractions from the first dimension are collected and analysed in the second dimension at a later time. The stop-flow configuration entails direct transfer of the first dimension fractions onto the second dimension column, after which the primary flow is stopped while the transferred fraction is analysed in the second dimension. Once separation in the second dimension is completed, the primary flow is resumed again for the transfer of the next fraction, etc. In the next section, a short account of some of the most important aspects relating to MDLC separations will be given. For

simplicity, the discussion will be limited to comprehensive two-dimensional LC (LC×LC), as this falls within the scope of the dissertation.

2.3.3.1. General aspects of LC×LC

Sample dimensionality. Sample dimensionality (*s*) is a parameter initially proposed by Giddings [144] that can be used as a measure of sample amenability to a multi-dimensional separation. According to Giddings, the retention of analytes in a sample is influenced by their structural properties (referred to as "dimensions"), whereby each unique chemical characteristic according to which analytes can be separated represents an independent dimension. This means that if sample components can only be separated on the basis of one structural property, the sample is mono-dimensional. Subjecting such a sample to multiple separation dimensions would be pointless as the additional dimensions would provide no useful information. On the other hand, if the sample dimensionality exceeds the system dimensionality, a disordered peak distribution or chaotic separation would result, since components would not be systematically separated. Ideally, the system dimensionality should match the sample dimensionality in order to fully benefit from the separation. It is expected that *s* for most complex samples would be high, and since it is practically difficult to increase the system dimensionality above two, a balance between the system- and sample dimensionalities will have to be made. Although the sample dimensionality can only be determined by trial and error, the concept provides a useful guide for designing multi-dimensional separations [145].

Sampling rate. Sampling of first dimension peaks is a key aspect that requires optimisation in LC×LC separations. As a rule of thumb, it is required that peaks eluting from the primary column be sampled multiple times to avoid loss of resolution in the first dimension due to under-sampling. Murphy and co-workers [146] studied the effect of the sampling rate on resolution in LC×LC systems and found that optimal 2-D resolution is achieved when each first dimension peak is sampled at least three times (when the sampling is in-phase i.e. "when sampling starts exactly at the beginning of the peak"). This number should be increased to four when sampling is maximally out-of-phase. In his theoretical study, Seeley [147] investigated the effect of sampling on the first dimension resolution in LC×LC systems and came to a conclusion that loss in resolution is minimal when each primary peak is sampled at least three times, which was in agreement with the findings of Murphy and co-workers. In a later study, Horie *et al* [148] demonstrated that the best compromise between sampling rate and second dimension analysis time is achieved when each first dimension peak is sampled at least two times. This is because, while higher sampling rates may be required for preservation of first dimension resolution, the use of shorter analysis times in the second dimension results in lower peak capacity in this dimension and consequently lower overall peak capacity. This aspect is of critical importance in on-line LC×LC, since the second dimension separation should be completed within the sampling period. Therefore, a compromise

between the sampling rate and the second dimension analysis time is necessary for optimum system performance. The transfer of small fraction volumes may also have a detrimental impact on sensitivity (this aspect depends on the first dimension column dimensions). In off-line and stop-flow LC×LC, the two separations are performed independently, and therefore the sampling rate can be selected independent of the second dimension analysis time. However, higher sampling rates would mean a larger number of fractions for analysis in the second dimension, which would result in extremely long analysis times for off-line and stop-flow systems.

Peak capacity. Peak capacity is defined as the number of peaks that can theoretically be separated by a given method at unit resolution [141,142]. This is a quantitative parameter used to measure the quality of chromatographic separations [149]. The prime benefit of performing multi-dimensional separations is the increased peak capacity achieved by the combination of independent (orthogonal) separation mechanisms. In principle, the total peak capacity for an "ideal" LC×LC separation system ($n_{c,2D}$) is equal to the product of peak capacities in the first (^1n_c) and second (^2n_c) dimensions, expressed as:

$$n_{c,2D} = {}^1n_c \times {}^2n_c \qquad (2.2)$$

However, perfect orthogonality is hard to realise in practice because of retention similarities which always occur between different separation mechanisms [145,150]. This means that the benefits of LC×LC are not always fully realised as the entire separation space is not effectively used. In addition to orthogonality, other peak broadening effects such as under-sampling of the first dimension peaks results in loss of peak capacity in 2-D separations. Because of these phenomena, several mathematical metrics have been developed to allow correction for lack of orthogonality [151-154] and under-sampling [155-157] in the calculation of practical peak capacities. It is not within the scope of this dissertation to provide a comprehensive overview of these methods; only concise summaries of the methods used for correction of orthogonality and under-sampling in this study will be described. Interested readers are referred to dedicated reports [158,159] for more detailed descriptions of these methods.

To account for orthogonality in the calculation of peak capacity, the method of Liu *et al* [151] was used. This is a statistical method based on the geometric approach to factor analysis which assumes that each set of independent retention data obtained in each dimension can be regarded as an independent vector. The correlation between the vectors can be calculated using normalised retention factors of compounds in each dimension. Graphically, this approach is illustrated in **Figure 2.3**, where the gridded region represents the area of the two-dimensional separation space occupied by peaks, while the non-shaded areas (D and E) are unavailable because of correlation.

Following computation of angles α, α', β and γ as well as areas D and E (see [151]), the corrected 2-D peak capacity ($n'_{c,2D}$) is then calculated according to:

$$n'_{c,2D} = n_{c,2D} - \frac{1}{2}\left[{}^{2}n_c \tan\gamma + {}^{1}n_c \tan\alpha\right] \qquad (2.3)$$

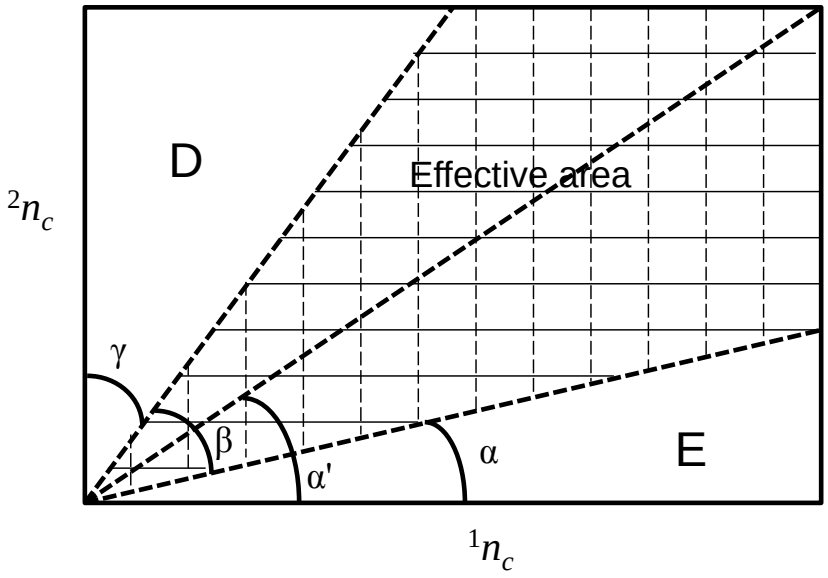

Figure 2.3. A graphical illustration of the effective 2-D retention plane used for estimation of orthogonality according to [151].

To account for under-sampling, the method of Carr and co-workers [156] was used. This method is an extension of the method developed by the same research group [155], which incorporates the under-sampling correction factor (<*β*>) to account for under-sampling of first dimension peaks. According to this method, the corrected peak capacity of an on-line LC×LC system is given by:

$$n'_{c,2D} = \frac{{}^{1}n_c \times {}^{2}n_c}{<\beta>} = \frac{{}^{1}n_c \times {}^{2}n_c}{\sqrt{1 + 3.35\left(\frac{{}^{2}t_c \, {}^{1}n_c}{{}^{1}t_g}\right)^2}} \qquad (2.4)$$

where ${}^{1}t_g$ is the first dimension gradient time and ${}^{2}t_c$ is the second dimension cycle time (i.e. the sum of the second dimension gradient time (${}^{2}t_g$) and the column re-equilibration time (${}^{2}t_{re\text{-}eq}$)), which is equal to the sampling time. ${}^{2}t_c$ is substituted by the sampling time for off-line and stop-flow systems.

Both orthogonality and under-sampling are important aspects that should be accounted for in the calculation of LC×LC peak capacity. Yet, literature reports often account for only one, or even none, of these aspects. This inconsistency in terms of performance metrics for LC×LC separation currently hampers comparison of results obtained in different studies.

2.3.3.2. Instrumental aspects of LC×LC

Different instrumental configurations may be used in LC×LC separations, which differ in terms of the mode of fraction transfer between the primary and secondary columns. In on-line LC×LC, automation is normally achieved through the use of eight-port, ten-port or two six-port switching valve(s) equipped with trapping loops or columns. In all instances, the fraction from the first dimension is trapped in one of the loops (or columns), while the content of the second loop (or column) is being analysed in the second dimension, and this is repeated for the duration of the first dimension separation. It is required that separation in the second dimension be complete before transfer of the next fraction in order to avoid chaotic band displacement or the "wrap-around" effect [160]. In cases where higher peak capacities are desired, two parallel columns can be employed in the second dimension for longer second dimension analysis times, although additional instrumentation is required for this configuration [161].
In the stop-flow mode, the two dimensions are usually connected by means of a switching valve with no trapping loops. For the off-line set-up, an automated fraction collector is often used. While off-line LC×LC analysis can be performed on a single instrument, two pumps are required for the on-line and stop-flow configurations. Illustrations of typical instrumental configurations used for on-line, off-line and stop-flow systems are shown in **Figure 2.4**.

LC offers a wide range of separation mechanisms which provides flexibility in tuning selectivity and hence numerous possibilities for LC×LC separations [140]. It should however be noted that some combinations are limited due to solvent immiscibility and/or mobile/stationary phases mismatches [143]. In addition, the injection of large volumes of immiscible solvents, solvents differing significantly in viscosity or solvents of high eluotropic strength in the second dimension, can detrimentally affect the second dimension performance [162,163]. While this is not a major issue for off-line analyses, since evaporation and redissolution is possible between the two dimensions (provided it does not result in sample alteration), careful optimisation of parameters is necessary for effective operation in the on-line and stop-flow modes. To account for these effects, microbore columns operated at low flow rates are often used in the first dimension to ensure minimal sample dilution and provide small enough fractions for injecting onto the second dimension column. Conventional-bore (4.6 mm i.d.) columns are then employed in the second dimension for higher loadability. Especially in on-line LC×LC, elevated temperatures are commonly used in the second dimension to reduce the system backpressure and speed up separations. Because of their high permeabilities, monolithic and superficially porous columns are also viable alternatives for faster separations in the second dimension.

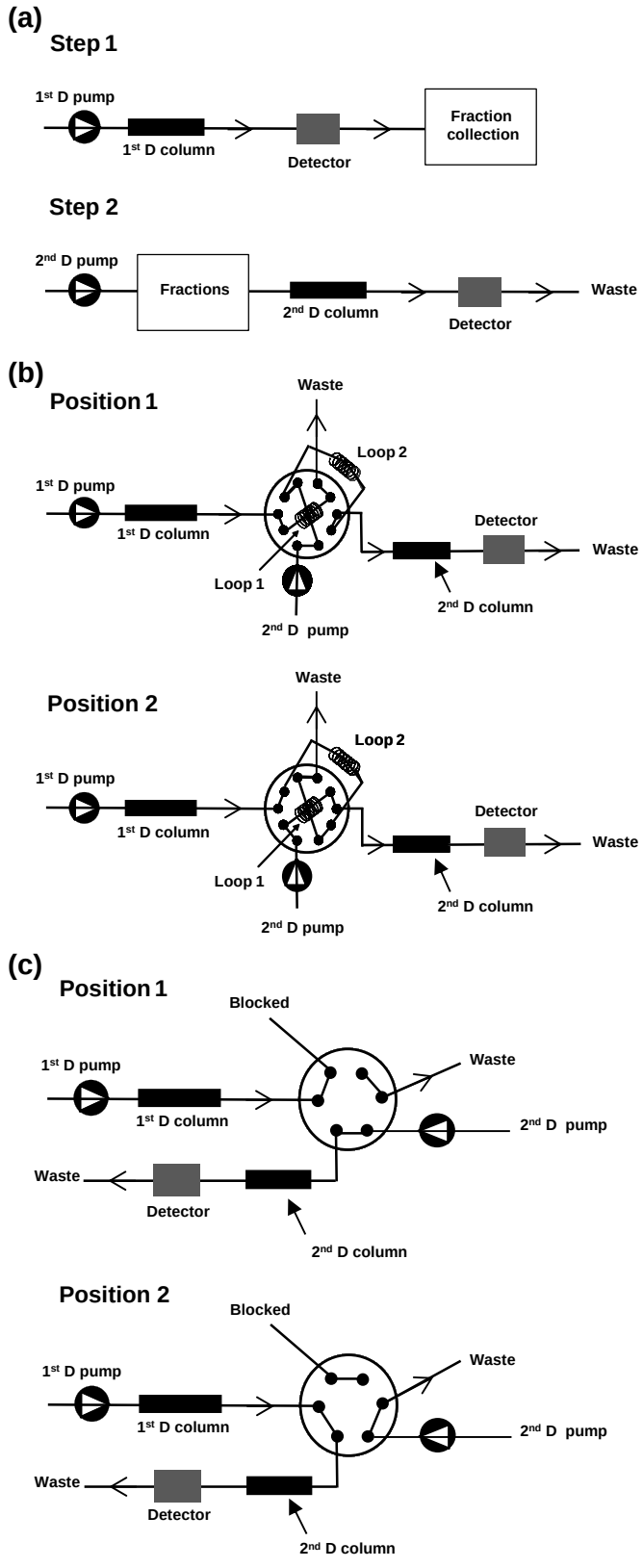

Figure 2.4. Schematic representation of typical instrumental configurations used for (a) off-line, (b) on-line and (c) stop-flow LC×LC. 1st– and 2nd D indicate first and second dimensions, respectively.

2.3.3.3. Applications of LC×LC to phenolic analysis

Since the revolutionary work of Erni and Frei [164] on the LC×LC separation of complex plant extracts, the technique has been receiving increasing attention in various fields; application of LC×LC has grown quite substantially in recent years. The technique has also found widespread application in phenolic analysis. Good results have been obtained using various column combinations in either on-line, off-line or stop-flow modes, and both heart-cutting and comprehensive approaches have been employed. Selected applications of LC×LC for phenolic analysis will be highlighted briefly below.

Mondello and co-workers [115,117,118,128,165-167], Hájek *et al* [73] as well as Kivilompolo *et al* [168] described a series of on-line RP-LC×RP-LC systems based on different stationary phase chemistries (C18, phenyl, amide, cyano, polyethylene glycol (PEG) or zirconia-carbon phases) and different mobile phases for analysis of phenolic acids and/or flavonoid compounds in wines, beers and various plant extracts. Good separations and peak capacities (>300) higher than those obtainable using 1-D LC methods were reported for these systems, despite the fact that these methods suffer from lack of orthogonality in some cases.

HILIC and NP-LC offer alternative selectivity to RP-LC, which potentially makes them attractive combinations for LC×LC separations. However, combination of these methods is challenging due to the nature of solvents used. While combining NP-LC and RP-LC is somewhat limited due to solvent immiscibility, HILIC×RP-LC is complicated by the relative elution strength of solvents used (i.e. HILIC solvents have high eluotropic strength in RP-LC and vice-versa). In spite of these limitations, both approaches have been successfully used for on-line analysis of phenolic compounds. For example, Francois *et al* [161,169] successfully characterised psolarens and flavones in citrus oil using NP-LC×RP-LC and achieved peak capacities in excess of 450, representing significant gains compared to peak capacities of less than 50 for the individual 1-D methods. As a way of dealing with the solvent issues in HILIC×RP-LC systems, Jandera *et al* [170] developed an on-line HILIC×RP-LC method employing a capillary HILIC column (0.5 mm i.d.) in the first dimension and various 3.0 mm i.d. superficially porous C18 columns in the second dimension. This method provided good separation and demonstrated good sensitivity for phenolic acids and flavonoid standards.

Kalili *et al* [171-173] developed off-line HILIC×RP-LC methods which provided good separation of a diverse range of phenolic compounds including proanthocyanidins, phenolic acids, flavonols and flavones in cocoa, apples and green and rooibos teas. Practical peak capacities in excess of 3000 were reported for these systems, which are much higher than for on-line LC×LC systems.

Unlike on-line and off-line LC×LC, the stop-flow approach has received limited attention in phenolic analysis. This is largely due to the risk of additional band broadening associated with this technique [160]. Blahová *et al* [174] investigated a stop-flow RP-LC×RP-LC method for the

analysis of phenolic standards. Although the effect of stopping the flow was not quantified, these authors achieved good separations of 14 phenolic antioxidants when using a 19-min gradient in the second dimension. In a later study [167], the same authors used heart-cutting stop-flow RP-LC×RP-LC to compare the effects of temperature and solvent gradients in phenolic separation. The authors found that temperature programming under isocratic conditions on zirconia-carbon (Zr-C) columns was as effective as solvent gradients for the studied compounds.

In another interesting application, the comprehensive combination of LC and CE separations was evaluated for phenolic analysis. Cesla *et al* [175] devised an off-line 2-D method based on RP-LC and MEKC, which provided a good separation of 25 phenolic acids and flavone standards. In this study, fractions from the LC column were automatically collected every 15 s using a CE autosampler and subsequently analysed on a 48 cm fused silica capillary using a 25mM borate buffer (pH 9.05) containing 10 g/L SDS and 1.85 g/L heptakis(6-O-sulfo)-β-CD. This method demonstrated higher orthogonality and peak capacity than an on-line RP-LC×RP-LC method [119] previously developed by the same authors, although a longer analysis time was required.

These and other studies clearly demonstrate the potential of LC×LC for improving separation of phenolic compounds. It should also be acknowledged that the availability of selective and sensitive detection methods that allow on-line identification of compounds greatly complement these analyses.

References

[1] W. Hümmer, P. Schreier, Mol. Nutr. Food Res. 52 (2008) 1381.
[2] C. Santos-Buelga, A. Scalbert, J. Sci. Food Agric. 80 (2000) 1094.
[3] J. Wollgast, E. Anklam, Food Res. Int. 33 (2000) 423.
[4] C.D. Stalikas, J. Sep. Sci. 30 (2007) 3268.
[5] V. Lattanzio, P.A. Kroon, S. Quideau, D. Treutter, in F. Daayf, V. Lattanzio (Editors), Recent advances in polyphenol research, Blackwell Publishing Ltd., Chichester, 2008, p. 1.
[6] P. Ribereau-Gayon, Plant Phenolics, Hafner Publishing Company, Inc., New York, 1972.
[7] S.A. Lazarus, G.E. Adamson, J.F. Hammerstone, H.H. Schmitz, J. Agric. Food Chem. 47 (1999) 3693.
[8] A. Yanagida, T. Kanda, T. Shoji, M. Ohnishi-Kameyama, T. Nagata, J. Chromatogr. A 855 (1999) 181.
[9] K.M. Davies, H. Zhang, K.E. Schwinn, in F. Daayf, V. Lattanzio (Editors), Recent advances in polyphenol research, Blackwell Publishing Ltd., Chichester, 2008, p. 139.
[10] M. Dell'Agli, A. Busciala, E. Bosisio, Cardiovasc. Res. 63 (2004) 593.
[11] S. Gómez-Alonso, E. García-Romero, I. Hermosín-Gutiérrez, J. Food Comp. Anal. 20 (2007) 618.
[12] K.M. Kalili, A. de Villiers, J. Sep. Sci. 34 (2011) 854.
[13] I. Mueller-Harvey, Animal Feed Sci. Technol. 91 (2001) 3.
[14] S. Peng, C. Jay-Allemand, J. Chem. Ecol. 17 (1991) 887.
[15] M.A. Rostagno, M. Palma, C.G. Barroso, Anal. Chim. Acta 588 (2007) 274.
[16] P. Arapitsas, C. Turner, Talanta 74 (2008) 1218.
[17] T. Yue, D. Shao, Y. Yuan, Z. Wang, C. Qiang, J. Sep. Sci. 35 (2012) 2138.
[18] M. Papagiannopoulos, B. Zimmermann, A. Mellenthin, M. Krappe, G. Maio, R. Galensa, J. Chromatogr. A 958 (2002) 9.
[19] J. Valls, S. Millán, M.P. Martí, E. Borràs, L. Arola, J. Chromatogr. A 1216 (2009) 7143.
[20] I. Mueller-Harvey, J.D. Reed, R.D. Hartley, J. Sci. Food Agric. 39 (1987) 1.
[21] G. Cimpan, S. Gocan, J. Liq. Chromatogr. Rel. Technol. 25 (2002) 2225.
[22] A. Marston, K. Hostettmann, in Ø.M. Andersen, K.R. Markham (Editors), Flavonoids: chemistry, biochemistry and applications, CRC Press, New York, 2006, p. 1.
[23] A.G.H. Lea, J. Sci. Food Agric. 29 (1978) 471.
[24] P.S. Variyar, S. Chatterjee, A. Sharma, in M. Srivastava (Editor), High performance Thin-Layer Chromatography (HPTLC), Springer-Verlag Berlin Helderberg, 2011, p. 27.
[25] Y. Nolvachai, P.J. Marriott, J. Sep. Sci. 36 (2013) 20.
[26] A. Khoddami, M.A. Wilkes, T.H. Roberts, Molecules 18 (2013) 2328.
[27] J.L. Donovan, J.R. Bell, S. Kasim-Karakas, J.B. German, R.L. Walzem, R.J. Hansen, A.L. Waterhouse, J. Nutr. 129 (1999) 1662.
[28] M. Stobiecki, P. Wojtaszek, K. Gulewicz, Phytochem. Anal. 8 (1997) 153.
[29] Y. Zuo, C. Wang, J. Zhan, J. Agric. Food Chem. 50 (2002) 3789.
[30] K. Zhang, Y. Zuo, J. Agric. Food Chem. 52 (2004) 222.
[31] X. Gao, S.J. Williams, O.L. Woodman, P.J. Marriott, J. Chromatogr. A 1217 (2010) 8317.
[32] T. Fossen, Ø.M. Andersen, in Ø.M. Andersen, K.R. Markham (Editors), Flavonoids: chemistry, biochemistry and applications, CRC Press, New York, 2006, p. 37.
[33] E. de Rijke, P. Out, W.M.A. Niessen, F. Ariese, C. Gooijer, U.A.T. Brinkman, J. Chromatogr. A 1112 (2006) 31.
[34] T.Y. Chu, C.H. Chang, Y.C. Liao, Y.C. Chen, Talanta 54 (2001) 1163.
[35] T.J. Schmidt, I. Merfort, J. Chromatogr. 634 (1993) 350.
[36] A. dos Santos Pereira, M.A. Afonso Serrano, F.R. de Aquino Neto, A. da Cunha Pinto, J. Chromatogr. Sci. 38 (2000) 174.
[37] A. Branco, A. dos Santos Pereira, J.N. Cardoso, F.R. de Aquino Neto, A.C. Pinto, R. Braz-Filho, Phytochem. Anal. 12 (2001) 266.
[38] C. Santos-Buelga, C. Garcia-Viguera, F.A. Tomas-Barberan, in C. Santos-Buelga, G. Williamson (Editors), Methods in polyphenol analysis, The Royal Society of Chemistry, Cambridge, 2003, p. 93.

[39] A. de Villiers, D. Cabooter, F. Lynen, G. Desmet, P. Sandra, J. Chromatogr. A 1216 (2009) 3270.
[40] J. Rigaud, M.T. Escribano-Bailon, C. Prieur, J.M. Souquet, V. Cheynier, J. Chromatogr. A 654 (1993) 255.
[41] M.A. Kelm, J.C. Johnson, R.J. Robbins, J.F. Hammerstone, H.H. Schmitz, J. Agric. Food Chem. 54 (2006) 1571.
[42] M. Naczk, F. Shahidi, J. Pharm. Biomed. Anal. 41 (2006) 1523.
[43] A. Carrasco-Pancorbo, D. Arráez-Román, A. Segura-Carretero, A. Fernández-Gutiérrez, Electrophoresis 27 (2006) 2182.
[44] A.M. Gómez Caravaca, A. Carrasco Pancorbo, B. Cañabate Díaz, A. Segura Carretero, A. Fernández Gutiérrez, Electrophoresis 26 (2005) 3538.
[45] H. Horie, T. Mukai, K. Kohata, J. Chromatogr. A 758 (1997) 332.
[46] H. Franquet-Griell, A. Checa, O. Núñez, J. Saurina, S. Hernández-Cassou, L. Puignou, J. Agric. Food Chem. 60 (2012) 8340.
[47] H. Horie, K. Kohata, J. Chromatogr. A 802 (1998) 219.
[48] C.C.T. Wörth, M. Wießler, O.J. Schmitz, Electrophoresis 21 (2000) 3634.
[49] M. Bonoli, M. Pelillo, T.G. Toschi, G. Lercker, Food Chem. 81 (2003) 631.
[50] R. Gotti, S. Furlanetto, S. Pinzauti, V. Cavrini, J. Chromatogr. A 1112 (2006) 345.
[51] R. Gotti, J. Fiori, F. Mancini, V. Cavrini, Electrophoresis 25 (2004) 3282.
[52] A. Cifuentes, B. Bartolomé, C. Gómez-Cordovés, Electrophoresis 22 (2001) 1561.
[53] R. Pomponio, R. Gotti, B. Luppi, V. Cavrini, Electrophoresis 24 (2003) 1658.
[54] I. Ignat, I. Volf, V.I. Popa, Food Chem. 126 (2011) 1821.
[55] M.L. Price, L.G. Butler, J. Agric. Food Chem. 25 (1977) 1268.
[56] E.A. Ainsworth, K.M Gillespie, Nat. Protoc. 2 (2007) 875.
[57] M. Naczk, F. Shahidi, J. Chromatogr. A 1054 (2004) 95.
[58] M.J. Herderich, P.A. Smith, Austr. J. Grape Wine Res. 11 (2005) 205.
[59] J.A. Kennedy, G.P. Jones, J. Agric. Food Chem. 49 (2001) 1740.
[60] M.A. Rodríguez-Delgado, S. Malovaná, J.P. Pérez, T. Borges, F.J. García Montelongo, J. Chromatogr. A 912 (2001) 249.
[61] G. Zgórka, S. Kawka, J. Pharm. Biomed. Anal. 24 (2001) 1065.
[62] E. Buiarelli, G.R Cartoni, E. Coccioli, E. Ravazzi, Chromatographia 31 (1991) 489.
[63] B. Heimhuber, R. Galensa, K. Herrmann, J. Chromatogr. 439 (1988) 481.
[64] R.L. Rouseff, S.V. Ting, J. Chromatogr. 176 (1979) 75.
[65] E. de Rijke, H.C. Joshi, H.R. Sanderse, F. Ariese, U.A.T. Brinkman, C. Gooijer, Anal. Chim. Acta 468 (2002) 3.
[66] R.J. Robbins, J. Leonczak, J.C. Johnson, J. Li, C. Kwik-Uribe, R.L. Prior, L. Gu, J. Chromatogr. A 1216 (2009) 4831.
[67] P.C. H. Hollman, J.M.P. van Trijp, M.N.C.P. Buysman, Anal. Chem. 68 (1996) 3511.
[68] A.C. Gutierrez, M.H. Gehlen, Spectrochim. Acta A 58 (2002) 83.
[69] P.J. Hayes, M.R. Smyth, I. McMurrough, Analyst 112 (1987) 1197.
[70] M. Careri, L. Elviri, A. Mangia, M. Musci, J. Chromatogr. A 881 (2000) 449.
[71] H. Long, Y. Zhu, T. Huang, L.A. Coury, P.T. Kissinger, J. Liq. Chromatogr. Rel. Technol. 24 (2001) 1105.
[72] P.J. Hayes, M.R. Smyth, I. McMurrough, Analyst 112 (1987) 1205.
[73] T. Hájek, V. Skeríková , P. Cesla, K. Vynuchalová, P. Jandera, J. Sep. Sci. 31 (2008) 3309.
[74] A. Subagio, P. Sari, N. Morita, Phytochem. Anal. 12 (2001) 271.
[75] R.M. Smith, Understanding mass spectra: a basic approach, 2nd edition, John Wiley & Sons, Inc., Hoboken, New Jersey, 2004.
[76] L. Gu, M.A. Kelm, J.F. Hammerstone, Z. Zhang, G. Beecher, J. Holden, D. Haytowitz, R.L. Prior, J. Mass Spectrom. 38 (2003) 1272.
[77] L. Gu, M.A. Kelm, J.F. Hammerstone, G. Beecher, J. Holden, D. Haytowitz, R. L. Prior, J. Agric. Food Chem. 51 (2003) 7513.
[78] H.-J. Li, M.L. Deinzer, Anal. Chem. 79 (2007) 1739.
[79] N.E. Es-Safi, S. Guyot, P.H. Ducrot, J. Agric. Food Chem. 54 (2006) 6969.

[80] M. Ohnishi-Kameyama, A. Yanagida, T. Kanda, T. Nagata, Rapid Commun. Mass Spectrom. 11 (1997) 31.
[81] T. Shoji, S. Masumoto, N. Moriichi, T. Kanda, Y. Ohtake, J. Chromatogr. A 1102 (2006) 206.
[82] Y. Takahata, M. Ohnishi-Kameyama, S. Furuta, M. Takahashi, I. Suda, J. Agric. Food Chem. 49 (2001) 5843.
[83] N. Radebe, K. Rode, A. Pizzi, H. Pasch, J. Appl. Polym. Sci. 127 (2013) 1937.
[84] J.-L. Wolfender, K. Ndjoko, K. Hostettmann, in C. Santos-Buelga, G. Williamson (Editors), Methods in polyphenol analysis, The Royal Society of Chemistry, Cambridge, 2003, p. 128.
[85] B. Abad-García, L.A. Berrueta, S. Garmón-Lobato, B. Gallo, F. Vicente, J. Chromatogr. A 1216 (2009) 5398.
[86] J.E. MacNair, K.C. Lewis, J.W. Jorgenson, Anal. Chem. 69 (1997) 983.
[87] D.C. Harris, Quantitative Chemical Analysis, W.H. Freeman and Co., New York, 1999.
[88] A. de Villiers, F. Lestremau, R. Szucs, S. Gelebart, F. David, P. Sandra, J. Chromatogr. A 1127 (2006) 60.
[89] F. Lestremau, A. de Villiers, F. Lynen, A. Cooper, R. Szucs, P. Sandra, J. Chromatogr. A 1138 (2007) 120.
[90] G. Guiochon, J. Chromatogr. A 1126 (2006) 6.
[91] J.E. MacNair, K.D. Patel, J.W. Jorgenson, Anal. Chem. 71 (1999) 700.
[92] F.D. Antia, C. Horvath, J. Chromatogr. 435 (1988) 1.
[93] H. Chen, C. Horvath, J. Chromatogr. A 705 (1995) 3.
[94] N. Kumar, P. Bhandari, B. Singh, S.S. Bari, Food Chem. Toxicol. 47 (2009) 361.
[95] K.I. Nagy, K. Redeuil, R. Bertholet, H. Steiling, M. Kussmann, Anal. Chem. 81 (2009) 6347.
[96] W. Pongsuwan, T. Bamba, K. Harada, T. Yonetani, A. Kobayashi, E. Fukusaki, J. Agric. Food Chem. 56 (2008) 10705.
[97] D. Guillarme, C. Casetta, C. Bicchi, J.-L. Veuthey, J. Chromatogr. A 1217 (2010) 6882.
[98] B. Klejdus, J. Vacek, L. Benesová, J. Kopecky, O. Lapcik, V. Kuban, Anal. Bioanal. Chem. 389 (2007) 2277.
[99] B. Klejdus, J. Vacek, L. Lojková, L. Benesová , V. Kubán, J. Chromatogr. A 1195 (2008) 52.
[100] G. Du, H.Y. Zhao, Q.W. Zhang, G.H. Li, F.Q. Yang, Y. Wang, Y.C. Li, Y.T. Wang, J. Chromatogr. A 1217 (2010) 705.
[101] W. Oleszek, A. Stochmal, B. Janda, J. Agric. Food Chem. 55 (2007) 8095.
[102] M. Schwarz, M.C. Rodríguez, D.A. Guillén, C.G. Barroso, J. Sep. Sci. 32 (2009) 1782.
[103] M. Gómez-Romero, A. Segura-Carretero, A. Fernández-Gutiérrez, Phytochem. 71 (2010) 1848.
[104] C. Cavaliere, P. Foglia, R. Gubbiotti, P. Sacchetti, R. Samperi, A. Laganá, Rapid Commun. Mass Spectrom. 22 (2008) 3089.
[105] S. Ahuja, M. Dong, Separation Science and Technology, Academic Press, 2005, p. 611.
[106] A. de Villiers, K.M. Kalili, M. Malan, J. Roodman, LC-GC Eur. 23 (2010) 466.
[107] T.L. Chester, Anal. Chem. 85 (2013) 579.
[108] C.G. Horvath, B.A. Preiss, S.R. Lipsky, Anal. Chem. 39 (1967) 1422.
[109] C.G. Horvath, S.R. Lipsky, Anal. Chem. 41 (1969) 1227.
[110] J.J. Kirkland, Anal. Chem. 41 (1969) 218.
[111] J.J. Kirkland, F.A. Truszkowski, C.H. Dilks Jr., G.S. Engel, J. Chromatogr. A 890 (2000) 3.
[112] A. Liekens, J. Denayer, G. Desmet, J. Chromatogr. A 1218 (2011) 4406.
[113] N. Manchón, M. D'Arrigo, A. García-Lafuente, E. Guillamón, A. Villares, A. Ramos, J.A. Martínez, M.A. Rostagno, Talanta 82 (2010) 1986.
[114] B. Boros, S. Jakabová, Á. Dörnyei, G. Horváth, Z. Pluhár, F. Kilár, A. Felinger, J. Chromatogr. A 1217 (2010) 7972.
[115] P. Dugo, F. Cacciola, P. Donato, R.A. Jacques, E.B. Caramão, L. Mondello, J. Chromatogr. A 1216 (2009) 7213.
[116] Q. Shen, Z. Dai, Y. Lu, J. Sep. Sci. 33 (2010) 3152.
[117] P. Dugo, F. Cacciola, M. Herrero, P. Donato, L. Mondello, J. Sep. Sci. 31 (2008) 3297.
[118] P. Dugo, F. Cacciola, P. Donato, D. Airado-Rodríguez, M. Herrero, L. Mondello, J. Chromatogr. A 1216 (2009) 7483.

[119] P. Cesla, T. Hájek, P. Jandera, J. Chromatogr. A 1216 (2009) 3443.
[120] P. Jandera, P. Cesla, T. Hájek, G. Vohralík, K. Vynuchalová, J. Fischer, J. Chromatogr. A 1189 (2008) 207.
[121] P. Jandera, T. Hájek, P. Česla, J. Sep. Sci. 33 (2010) 1382.
[122] Y. Li, P. Aggarwal, H.D. Tolley, M.L. Lee, in E. Grushka, N. Grinberg (Editors), Advances in chromatography; CRC Press, Boca Raton, FL, 2012, p. 237.
[123] S. Apers, T. Naessens, K. Van Den Steen, F. Cuyckens, M. Claeys, L. Pieters, A. Vlietinck, J. Chromatogr. A 1038 (2004) 107.
[124] M.A. Rostagno, M. Palma, C.G. Barroso, Anal. Chim. Acta 582 (2007) 243.
[125] F. Chinnici, A. Gaiani, N. Natali, C. Riponi, S. Galassi, J. Agric. Food Chem. 52 (2003) 3.
[126] P. Dugo, O. Favoino, R. Luppino, G. Dugo, L. Mondello, Anal. Chem. 76 (2004) 2525.
[127] P. Jandera, K. Vynuchalová, T. Hájek, P. Cesla, G. Vohralík, J. Chemometr. 22 (2008) 203.
[128] F. Cacciola, P. Jandera, E. Blahová, L. Mondello, J. Sep. Sci. 29 (2006) 2500.
[129] M.A. Vian, V. Tomao, S. Gallet, P.O. Coulomb, J.M. Lacombe, J. Chromatogr. A 1085 (2005) 224.
[130] A. Liazid, G.F. Barbero, M. Palma, J. Brigui, C.G. Barroso, Chromatographia 72 (2010) 417.
[131] M. Krizman, D. Baricevic, M. Prosek, J. Pharm. Biomed. Anal. 43 (2007) 481.
[132] N. Troncoso, H. Sierra, L. Carvajal, P. Delpiano, G. Günther, J. Chromatogr. A 1100 (2005) 20.
[133] Z. Kučerovv, M. Szumski, B. Buszewski, P. Jandera, J. Sep. Sci. 30 (2007) 3018.
[134] V. Skeríková, P. Jandera, J. Chromatogr. A 1217 (2010) 7981.
[135] P. Jandera, J. Urban, V. Skeríková, P. Langmaier, R. Kubícková, J. Planeta, J. Chromatogr. A 1217 (2010) 22.
[136] J.M. Davis, J.C. Giddings, Anal. Chem. 55 (1983) 418.
[137] J.M. Davis, J.C. Giddings, Anal. Chem. 57 (1985) 2168.
[138] K. Rowe, J.M. Davis, Anal. Chem. 67 (1995) 2981.
[139] J.M. Davis, J.C. Giddings, Anal. Chem. 57 (1985) 2178.
[140] H.J. Cortes, L.D. Rothman, in H.J. Cortes (Editor), Multidimensional Chromatography: techniques and applications, Marcel Dekker, Inc., New York, 1990, p. 219.
[141] J.C. Giddings, in H.J. Cortes (Editor), Multidimensional Chromatography: techniques and applications, Marcel Dekker, Inc., New York, 1990, p. 1.
[142] J.C. Giddings, Anal. Chem. 56 (1984) 1258A.
[143] P.Q. Tranchida, P. Dugo, G. Dugo, L. Mondello, J. Chromatogr. A 1054 (2004) 3.
[144] J.C. Giddings, J. Chromatogr. A 703 (1995) 3.
[145] S.P. Dixon, I.D. Pitfield, D. Perrett, Biomed. Chromatogr. 20 (2006) 508.
[146] R.E. Murphy, M.R. Schure, J.P. Foley, Anal. Chem. 70 (1998) 1585.
[147] J.V. Seeley, J. Chromatogr. A 962 (2002) 21.
[148] K. Horie, H. Kimura, T. Ikegami, A. Iwatsuka, N. Saad, O. Fiehn, N. Tanaka, Anal. Chem. 79 (2007) 3764.
[149] U.D. Neue, J. Chromatogr. A 1184 (2008) 107.
[150] P. Dugo, F. Cacciola, T. Kumm, G. Dugo, L. Mondello, J. Chromatogr. A 1184 (2008) 353.
[151] Z. Liu, D.G. Patterson, M.L. Lee, Anal. Chem. 67 (1995) 3840.
[152] P.J. Slonecker, X. Li, T.H. Ridgway, J.G. Dorsey, Anal. Chem. 68 (1996) 682.
[153] M. Gilar, P. Olivova, A.E. Daly, J.C. Gebler, Anal. Chem. 77 (2005) 6426.
[154] N.E. Watson, J.M. Davis, R.E. Synovec, Anal. Chem. 79 (2007) 7924.
[155] J.M. Davis, D.R. Stoll, P.W. Carr, Anal. Chem. 80 (2008) 461.
[156] X. Li, D.R. Stoll, P.W. Carr, Anal. Chem. 81 (2009) 845.
[157] G. Vivó-Truyols, S. van der Wal, P.J. Schoenmakers, Anal. Chem. 82 (2010) 8525.
[158] P.W. Carr, J.M. Davis, S.C. Rutan, D.R. Stoll, in E. Grushka, N. Grinberg (Editors), Advances in chromatography, CRC Press, Boca Raton, FL, 2012, p. 139.
[159] M. Gilar, J. Fridrich, M.R. Schure, A. Jaworski, Anal. Chem. 84 (2012) 8722.
[160] A.R. Shalliker, M.J. Gray, in E. Grushka, N. Grinberg (Editors), Advances in Chromatography, CRC Press, New York, 2006, p. 177.

[161] I. François, A. de Villiers, B. Tienpont, F. David, P. Sandra, J. Chromatogr. A 1178 (2008) 33.
[162] S. Udrescu, A. Medvedovici, V. David, J. Sep. Sci. 31 (2008) 2939.
[163] S. Keunchkarian, M. Reta, L. Romero, C. Castells, J. Chromatogr. A 1119 (2006) 20.
[164] F. Erni, R.W. Frei, J. Chromatogr. A 149 (1978) 561.
[165] F. Cacciola, P. Jandera, Z. Hajdu, P. Cesla, L. Mondello, J. Chromatogr. A 1149 (2007) 73.
[166] F. Cacciola, P. Jandera, L. Mondello, J. Sep. Sci. 30 (2007) 462.
[167] F. Cacciola, P. Jandera, L. Mondello, Chromatographia 66 (2007) 661.
[168] M. Kivilompolo, T. Hyotylainen, J. Chromatogr. A 1145 (2007) 155.
[169] I. François, A. de Villiers, P. Sandra, J. Sep. Sci. 29 (2006) 492.
[170] P. Jandera, T. Hájek, M. Staňkova, K. Vyňuchalova, P. Česla, J. Chromatogr. A 1268 (2012) 91.
[171] K.M. Kalili, A. de Villiers, J. Chromatogr. A 1216 (2009) 6274.
[172] K.M. Kalili, A. de Villiers, J. Sep. Sci. 33 (2010) 853.
[173] T. Beelders, K.M. Kalili, E. Joubert, D. de Beer, A. de Villiers, J. Sep. Sci. 35 (2012) 1808.
[174] E. Blahová, P. Jandera, F. Cacciola, L. Mondello, J. Sep. Sci. 29 (2006) 555.
[175] P. Cesla, J. Fischer, P. Jandera, Electrophoresis 31 (2010) 2200.

Chapter 3

Results and Discussion

This chapter presents a short overview of the results obtained in this study. Detailed descriptions of experimental procedures and results can be found in the attached publications and accompanying supporting information at the end of the dissertation.

3.1. Introduction

The goal of this study was to develop comprehensive two-dimensional liquid chromatographic (LC×LC) methods for the improved analysis of proanthocyanidins (PACs) in natural products. To achieve this, a systematic approach was used. First, it was important to know the performance limits of state of the art HPLC methods for polyphenol analysis. Reversed-phase LC (RP-LC), being the most powerful separation method for phenolic compounds, was specifically evaluated in this regard, as this was to be used in the second dimension in LC×LC analysis. Subsequently, a systematic optimisation procedure was developed for the coupling of hydrophilic interaction chromatography (HILIC) and RP-LC in each of the three coupling configurations i.e. on-line, off-line and stop-flow. Experimental verification of the findings of this optimisation study was performed for cocoa procyanidins (PCs). Having established the optimal experimental conditions, on-line HILIC×RP-LC separation was hyphenated with high resolution mass spectrometric detection to provide a powerful method for the analysis of grape seed PACs. As a "spin off" of this work, the feasibility of hyphenating HILIC×RP-LC with an on-line radical scavenging assay was explored. The findings of the study are briefly summarised in the following sections.

3.2. Kinetic optimisation of the reversed-phase liquid chromatographic separation of proanthocyanidins

(K.M. Kalili, D. Cabooter, G. Desmet, A. de Villiers, J. Chromatogr. A 1236 (2012) 63-76, Addendum B).

An understanding of the analytes' chromatographic behaviour is of key importance when designing methods for their separation. This follows from the fact that compounds may display different chromatographic behaviours depending on their physico-chemical properties [1]. In view of this, it was necessary to gain insight into the chromatographic behaviour of phenolic compounds in order to determine optimal conditions for their separation. This was especially important under RP-LC conditions, as this mode will be used in the second dimension of LC×LC, where optimal conditions for fast analyses are essential.

In this study, the kinetic plot method (KPM) was used to evaluate a new generation of C18 columns packed with different particle sizes and with different porosity properties. These included UPLC 1.7 µm and Zorbax 1.8 µm fully porous columns, a Kinetex 2.6 µm superficially porous column and an Xbridge 5 µm fully porous column (used as reference for conventional RP-LC analyses). A representative sample of nine proanthocyanidin molecules spanning a range of molecular weights (290-1155 g/mol) was used. Plate height data were obtained for all compounds on each column using isocratic mobile phases consisting acetonitrile (ACN) and 0.1% formic acid

in water (*v/v*), selected such that the retention factors (*k*) for all the compounds were between 3.5 and 15, and similar retention factors were ensured on all columns. Experiments were performed at two temperatures, 25 and 50 °C, to assess the effect of temperature on phenolic analysis.

Plate height data showed comparable performances for the 2.6 µm superficially porous column and the sub-2 µm fully porous columns. These columns provided minimum plate height (H_{min}) values between 3.74 and 5.20 µm for smaller molecules and 6.62 to 7.70 µm for larger molecules. The 5 µm fully porous column on the other hand provided H_{min} values ranging between 10.86 and 14.79 µm. These values were all in agreement with theoretical expectations ($H_{min} = 2d_p$) for the fully porous particle columns. However, the values obtained on the superficially porous column (with the exception of a tetrametric procyanidin, MW = 1155 g/mol) were much lower than the norm for fully porous particles, indicating better column packing efficiency and/or a more uniform particle size distribution. It was further noted that optimal performance was achieved at low linear velocities for high MW compounds, while smaller MW compounds were efficiently separated at higher linear velocities. These observations are consistent with expectations based on differences in diffusion coefficients of these molecules. Fully porous sub-2 µm as well as the 2.6 µm superficially porous particles provided significant speed gains compared to the conventional 5 µm fully porous particles in order of 4.7-5.0 times for small molecules, and 3.3-3.8 times for the tetrameric procyanidin.

Kinetic plots showed that for a fixed analysis time, the 2.6 µm Kinetex column performed better than all the other columns across the entire range of practical efficiencies (~25 000-250 000 theoretical plates), while the UPLC 1.7 µm column provided faster separations in the efficiency range of 10 000 to 25 000. When analysing small molecules, efficiencies greater than 160 000 theoretical plates are not achievable on columns packed with sub-2 µm fully porous particles under the specified pressure limitations for these columns (600 or 1000 bar). However, when used at optimal linear velocities for the larger molecule, these columns are superior to the 5 µm fully porous column in the efficiency range up to 250 000 plates. Due to favourable pressure characteristics of the superficially porous particles, long Kinetex columns (2.9 m) can be employed to reach efficiencies up to ~280 000 when analysing small molecules, while this value can be increased to ~485 000 (on a 3.6 m column) for large molecules. Extremely long analysis times will however be required. It is only for efficiencies in excess of 300 000 for small molecules and 500 000 for large molecules that the fully porous 5 µm column performs better than all the other columns. These efficiencies are however impractical for HPLC separations, as columns longer than 5 m are required.

The Kinetex column provided the lowest separation impedance number (E_0) of 2084, which is indicative of the higher permeability and good packing quality of this column. For smaller molecules, an increase in temperature resulted in improved efficiencies at higher linear velocities, while the minimum plate height remained unchanged, implying that high temperature is beneficial for speeding up analyses. Elevated temperature proved much more useful for high molecular

weight compounds, resulting in analysis speed gains of between 1.4 and 3 times and efficiency gains of between 5-39% for larger compounds on all columns. The 1.7 µm fully porous column provided the highest speed gain, while the highest efficiency gain was achieved on the superficially porous column at high temperature. The unexpected improvement in efficiency measured at high temperatures for larger compounds was proposed to be caused by temperature-dependent rotation of (epi)catechin units around the inter-flavanoid bond of oligomeric B-type PCs [2]. This hypothesis was supported by differences in the plate height curves for A- and B-type PCs (where for the former molecule rotation is not possible due to the second ether bond between flavanol units).

The column internal diameter (i.d.) was also found to have a significant effect on performance. A comparison of plate height data for three analytes with *k* values of roughly 3.5, 7.5 and 13.1 on 2.1 and 4.6 mm i.d. columns before and after accounting for the system contribution to band broadening showed no significant differences in performance for the 4.6 mm i.d. column, while efficiency losses of more than 40% were obtained for the weakly retained analyte on the narrow-bore column, even on a low-dispersion instrument. The extra-column contribution to band broadening decreased gradually with increasing retention and was insignificant for the most retained compound (k = 13.1) on all columns, suggesting that particular attention needs to be paid when working with narrow bore columns to avoid significant loss in efficiency. This also stresses the need for operating such columns on systems with highly optimised extra-column volumes.

In summary, the kinetic evaluation of several modern high performance LC (HPLC) columns showed that the 2.6 µm superficially porous column provides efficiencies similar to the fully porous sub-2 µm columns, however at lower pressures. The data obtained in this study revealed that analyte properties, particles size, column packing quality as well as analysis temperature all have a significant influence on the performance of a chromatographic support. Similar chromatographic behaviour was observed for small phenolic molecules on all columns; however, marked differences were evident between small and large phenolics on all studied supports. Smaller molecules are optimally separated on shorter columns at higher linear velocities, while optimal conditions for larger molecules involve longer columns operated at lower linear velocities. This suggests that a compromise between chromatographic efficiency and analysis speed would be necessary when analysing phenolic extracts containing analytes with widely varying physico-chemical properties if optimum performance is to be realised. High analysis temperature proved much more advantageous for high MW compounds, providing significant improvements in speed and efficiency for larger PCs. However, analyte and column stability have yet to be ascertained. Extra-column band broadening was shown to have a detrimental effect on the performance on narrow bore columns, particularly for weakly retained analytes ($k \leq 7$); this effect is negligible on conventional i.d. columns. These results indicate that the combination of high temperature and small-particle porous and superficially porous phases, when used under optimal conditions for the target

analytes, are capable of providing significant speed and/or efficiency gains for the RP-LC analyses of phenolic compounds.

3.3. Systematic optimisation and evaluation of on-line, off-line and stop-flow comprehensive hydrophilic interaction chromatography × reversed phase liquid chromatographic analysis of procyanidins, Part I: Theoretical considerations

(K.M. Kalili, A. de Villiers, J. Chromatogr. A 1289 (2013) 58-68, Addendum C).

LC×LC can be performed using one of three configurations, namely on-line, off-line and stop-flow. In our previous work [3-5], the off-line combination of HILIC and RP-LC methods has been shown to be a powerful method for the analysis of PCs. This is as a result of complementary information provided by the two methods, with HILIC allowing separation on the basis of molecular weight (or degree of polymerisation (DP)) and RP-LC providing separation of isomeric compounds. Although the off-line HILIC×RP-LC method is easy to perform and offers high peak capacities, this approach is characterised by relatively long analysis times and the sample integrity may be compromised by sample handling steps between the two dimensions. The work reported here and in a related paper [6] therefore investigated the on-line and stop-flow coupling of the HILIC and RP-LC separations, as these set-ups allow automation, less risk for sample alteration and better reproducibility. To enable the selection of the best method for a particular application, a systematic optimisation strategy was developed to compare the on-line, off-line and stop-flow HILIC×RP-LC modes in terms of resolution and separation performance per unit time. Cocoa PCs were used as model analytes for this purpose. The optimisation protocol involved the use of pre-defined first dimension (HILIC) parameters while varying those of the second dimension (RP-LC) separation, taking the coupling scheme, degree of orthogonality, under-sampling and stop-flow band broadening into account.

HILIC and RP-LC gradients, column dimensions and chromatographic conditions were optimised in a previous study [3]; therefore these were adopted with minor changes in the current work. Firstly, due to concerns regarding additional first dimension band broadening during stop-flow experiments [7-11], it was necessary to quantify the effect of the stop-flow operation on the first dimension performance for the analytes under investigation. This information was required to inform the choice of analysis time in the second dimension, since this determines the stop-flow period and the extent of additional band broadening experienced by each first dimension peak. To quantify the effect of the stop-flow operation, a cocoa extract was analysed under HILIC conditions using the so-called arrested elution method [7] and peak variances for PCs of DPs 1 to 4 were obtained for different stop times. From these data, a relationship between DP and the effective diffusion coefficient (D_{eff}) of PCs was determined ($D_{eff} = 4.91\times10^{-10}\times DP^{-2.334}$, $r^2 = 0.961$). D_{eff} values for PCs

of DP 5-8 were extrapolated from this relationship. An inverse correlation was obtained between DP and D_{eff}, as expected. This proved advantageous since higher DP PCs, which are retained longer on the HILIC column, exhibit smaller D_{eff} values, which counteracts the fact that these compounds will be subjected to the longest effective stop-flow times.

Secondly, the relationship between peak capacity and analysis time in the second dimension was established by analysing a cocoa extract on a 50 mm × 4.60 mm, 1.8 µm C18 (RP-LC) column using different gradient times at two flow rates, 0.8 and 1.5 mL/min. The relationship between peak capacity (n_c) and gradient time (t_g) is approximated by the following empirical equation [12]:

$$n_{c,1D} = 1 + \frac{a t_g}{b + t_g} \qquad (3.1)$$

where the respective values for constants *a* and *b* were found to be 357.3 and 12.3 for experimental data (r^2 = 0.987) measured at a flow rate of 1.5 mL/min. This flow rate provided higher peak capacities than 0.8 mL/min for a constant gradient time and was therefore used in the second dimension for all experiments (higher flow rates were not possible due to pressure limitations in the on-line configuration). The HILIC method provided a peak capacity (n_c) of ~14 for a 50 min gradient time at a flow rate of 50 µL/min. Orthogonality was estimated by the degree of correlation (r^2) between the two methods, determined as 0.05 according to the method of Liu *et al* [13]. With this information available, it was possible to calculate the total peak capacity and total analysis time (t_{tot}) required for HILIC×RP-LC analysis when using each of the different coupling modes.

For the off-line system, the second dimension gradient time (^2t_g) was used a primary variable and ^2n_c was calculated according to **equation (3.1)** for each ^2t_g value while keeping the first dimension sampling time (^1t_s) constant. The two-dimensional peak capacity ($n_{c,2D}$) was then calculated as outlined in **chapter 2**, followed by correction for under-sampling according to Li *et al* [14] and orthogonality according to Liu *et al* [13]. For each ^2t_g value, the total analysis time and the peak production rate were calculated and this procedure was repeated for a number of sampling times. From these calculations, it was clear that for a fixed sampling time, the highest corrected 2-D peak capacity ($n'_{c,2D}$) was obtained at the longest second dimension cycle time (^2t_c), while the shortest sampling time provided the highest $n'_{c,2D}$ when keeping ^2t_c constant. This is expected considering the dependence of peak capacity on the gradient time and also that resolution loss due to under-sampling is reduced when shorter sampling times are used. However, there is a point beyond which an increase in ^2t_c no longer leads to a proportional gain in peak capacity, irrespective of the sampling time used. It was further clear that reducing the sampling time below 1 min provided little gain in peak capacity, which is also undesirable considering the concomitant increase in the total analysis time with an increase in the number of fractions to be analysed. Furthermore, it was noted that the peak production rate varies with the second dimension cycle time and that for a fixed ^2t_c,

there was a unique sampling time that delivered the optimal peak production rate. For the specific sample and column combination studied here, a second dimension cycle time of 6.5 min delivered the highest peak production rate of 4.21 peaks/min when using a sampling time of 2.5 min in the off-line set-up.

Optimisation for the stop-flow LC×LC system was performed in a manner analogous to the off-line method, taking additional first dimension band broadening due to stop-flow operation into account. The effect of stopping the flow on the first dimension peak capacity was estimated from the total band widths for PCs with different DPs, approximated using their effective diffusion coefficients and stop-flow times. These calculations were performed for various ${}^2t_c$ values (since ${}^2t_c$ determines the effective stop-flow time experienced by each first dimension band). This was followed by calculation of corrected 2-D peak capacities for different second dimension cycle times, and correction for under-sampling and orthogonality as for the off-line method. A comparison of the results for the off-line and stop-flow methods showed comparable corrected peak capacities for ${}^2t_c$ values up to 15 min, implying that similar performance should be obtained for the two set-ups for ${}^2t_c$ less than or equal to this value. For longer ${}^2t_c$ values, small differences were obtained, up to a maximum of 3.6% at ${}^2t_c$ equals to 60 min. Comparable peak production rates were also obtained for the two systems.

Since the first dimension sampling time and flow rate determine the volume of first dimension fractions transferred to the second dimension column in the stop-flow and on-line set-ups, a flow-splitter was incorporated to decouple the two dimensions and to allow optimisation of individual separations to be performed independently. This is an especially serious constraint for the HILIC×RP-LC combination used here since only ~2 µL of HILIC fractions could be injected onto the 50 mm × 4.60 mm RP column used in this work to avoid band broadening (due to the high eluotropic strength of HILIC solvents in RP-LC). Flow splitting was also essential to allow the HILIC separation to be performed at optimal flow rate – flow rates commensurate with these small fraction volumes (i.e. 1 or 2 µL/min) would result in longer overall analysis times and loss of first dimension peak capacity due to the use of sub-optimal flow rates.

For the on-line system, ${}^2t_c$ was used as the primary variable since this parameter determines the second dimension peak capacity, the extent of first dimension under-sampling (because ${}^2t_c$ is equal to ${}^1t_s$ in the on-line set-up) as well as the overall analysis time. For each ${}^2t_c$ value, ${}^2n_c$ was calculated using **equation (3.1)** and corrected two-dimensional peak capacities were calculated by taking under-sampling and orthogonality into account as outlined previously. Calculations based on initial HILIC parameters i.e. those used for the off-line and stop-flow methods (flow rate of 50 µL/min and a gradient time of 50 min) provided a maximum corrected two-dimensional peak capacity of 292, achievable when using an optimal ${}^2t_c$ of 3 min. However, this value represented no benefit compared to a one-dimensional RP separation, which can be used to provide a peak capacity of ~280 in a similar analysis time. For this reason, and in view of the fact that longer

gradient times in the first dimension provide higher total peak capacities [15,16], a gradient time of 100 min and a flow rate of 25 µL/min were used in the HILIC dimension to improve the performance of the on-line system. These conditions resulted in an increased first dimension peak capacity of ~28 and ultimately doubled the corrected two-dimensional peak capacities, a phenomenon which was attributed to the combined use of a low injection volume and a near-optimal linear velocity for PCs. A $^{2}t_{c}$ of ~3 min provided the highest overall two-dimensional peak capacity (569) at a peak production rate of 5.53 peaks/min, despite the fact that this sampling time is associated with a higher degree of under-sampling (first dimension peak widths ranged between 2.91-5.02 min). This suggests that $^{1}t_{s}$ should be optimised relative to $^{2}t_{c}$, since longer analysis times in the second dimension result in higher peak capacities, which counteracts the loss in first dimension peak capacity due to under-sampling. For cycle times above this value, under-sampling becomes critical, resulting in a reduction in the overall peak capacity.

This work therefore delivered a systematic optimisation procedure that allowed the detailed evaluation and comparison of different LC×LC coupling modes based on the HILIC×RP-LC analysis of cocoa PCs. Under the conditions utilised in this study, one-dimensional RP-LC provided the best performance for peak capacities up to ~300, although this value is deceptive considering that extensive co-elution occurs under these conditions. For required peak capacities in excess of ~300 up to ~600 and for analysis times up to 2 hours, on-line HILIC×RP-LC provides better separation performance than 1-D RP-LC and should preferentially be used, as an additional dimension of information is provided. On the other hand, the separation performance offered by the off-line and stop-flow methods is unrivalled by either 1-D RP-LC or on-line HILIC×RP-LC. These methods provide much higher peak capacities, although this benefit is realised at a cost of significantly longer analysis times and lower peak production rates. Therefore, these methods are ideally suited for the in-depth analysis of samples with much more complex PC profiles. The additional band broadening associated with the stop-flow approach proved to be less of a concern for PCs, as it was shown that negligible peak capacity loss is expected for stop-flow times up to 60 min.

3.4. Systematic optimisation and evaluation of on-line, off-line and stop-flow comprehensive hydrophilic interaction chromatography × reversed phase liquid chromatographic analysis of procyanidins, Part II: Application to cocoa procyandins

(K.M. Kalili, A. de Villiers, J. Chromatogr. A 1289 (2013) 69-79, Addendum D).

Following the development of an optimisation protocol and theoretical comparison of the on-line, off-line and stop-flow HILIC×RP-LC methods described in **section 3.3**, this work was aimed at the

experimental verification of these findings. For this purpose, a cocoa extract was analysed using optimal conditions for each of the HILIC×RP-LC configurations established in [17].

Theoretical calculations indicated that similar separation performance should be achieved for the off-line and stop-flow methods for second dimension analysis times up to 60 min. To allow a quantitative comparison of the two methods, identical flow rates, sampling- and analysis times were used in the two dimensions. Analysis conditions used for the calculations, i.e. a flow rate of 50 µL/min, a gradient time of 50 min and an injection volume of 9 µL were used in the HILIC dimension. A sampling time of 1 min was selected in order to satisfy the sampling requirement of at least 3 fractions per first dimension peak [18-21] to avoid loss of first dimension peak capacity due to under-sampling. This was also necessary to keep the number of fractions to a minimum to avoid unnecessarily long analysis times. Although longer second dimension cycle times could be employed for higher peak capacities, a ${}^2t_c$ of 15 min was used here as this provided high resolution at acceptable total analysis times (~13.3 hours). For the off-line method, 1-min fractions (50 µL) were collected and 1.5 µL of each fraction was injected onto the second dimension column. For the stop-flow method, the HILIC effluent was split ~1:32[a] after the first dimension column for a direct transfer of ~1.5 µL onto the second dimension column. Flow-splitting was necessary to allow the use of equivalent flow rates in the first dimension and to avoid injection of large volumes of strong HILIC solvents in the second dimension, which could lead to band broadening or peak distortion. Comparison of the two-dimensional contour plots obtained for off-line and stop-flow HILIC×RP-LC analyses of the cocoa extract showed comparable elution profiles, confirming that band broadening due to stop-flow is negligible for PCs, at least for the stop-flow times used here. These results therefore confirm the validity of the theoretical approach [17] used for the optimisation of stop-flow analysis.

For the on-line system, operating the HILIC dimension at 25 µL/min using a gradient time of 100 min provided much better performance [17]; therefore those conditions were used here. A flow-splitter (1:32[a] or 1:49[b]) was also incorporated after the first dimension column so that ~1.5 µL would be injected onto the second dimension. For on-line LC×LC, the sampling time should be optimised in relation to ${}^2t_c$, since longer second dimension separations provide improved resolution. However, the use of longer cycle times in the second dimension is only beneficial up to a point where it does not negatively impact on the degree of first dimension under-sampling. Calculations indicated that a second dimension cycle time of 3 min would provide the best compromise between the sampling time and the second dimension peak capacity. However, seeing that this cycle time implied a high degree of under-sampling for later eluting compounds whose widths ranged between 2.91 and 3.05 min in the HILIC dimension, two sampling times of 2 and 3 min were used in on-line experiments. Compared to off-line and stop-flow methods, results obtained using the two

[a] Note that in the published paper [6] the split ratio was incorrectly reported as 1:33.
[b] Note that in the published paper [6] the split ratio was incorrectly reported as 1:50.

sampling times in the on-line set-up showed a significant reduction in resolution, which is expected given that shorter analysis times were used in the second dimension. A detailed examination of the contour plots obtained using the two cycle times revealed a significant loss of resolution in the HILIC dimension in case of a 3 min sampling time, which was more noticeable for the high molecular weight compounds (DP 5-8, peak widths between 2.91-3.05 min). The two systems were however characterised by very similar practical peak capacities, 462 for a 2 min sampling time *vs* 470 for a 3 min sampling time. This suggests that the effective two-dimensional separation of individual compounds was not accurately reflected in the theoretical calculations, since an average under-sampling correction factor was used. Experimental data showed that preserving the first dimension resolution is more important than indicated by theoretical calculations in the specific case of HILIC×RP-LC analysis of PCs. Although theoretical calculations provide a useful starting point for method optimisation, they may not necessarily reflect optimal performance in practice.

Although minor differences were obtained between theoretical and experimental peak capacity values, the trends were consistent with the predictions reported in **section 3.3**, allowing some conclusions to be drawn with regard to HILIC×RP-LC analysis of PCs. All three HILIC×RP-LC systems provided higher practical peak capacities than those achievable using 1-D LC. While the performance of the on-line system was significantly lower than the off-line and stop-flow methods, this approach provides much more useful information compared to 1-D separations in terms of both size and isomeric distribution of the sample PCs. Therefore, this method is ideally suited for the analysis of samples with relatively simple PC content and can be used as a quick screening tool. The off-line and stop-flow methods on the other hand provided much higher resolution, although there is a price to pay in terms of analysis times. Hence, these methods are better suited for the detailed analysis of highly complex samples. It has been experimentally demonstrated that stop-flow operation has a negligible effect on band broadening for PCs, making this an effective alternative to the more labour-intensive off-line method as it offers automation and minimal sample exposure between the two dimensions. Moreover, the fact that compounds are eluted in order of increasing size in HILIC makes this an ideal method for use in the first dimension of a stop-flow experiment as the most retained compounds exhibit the smallest effective diffusion coefficients, thereby offsetting the fact that these analytes experience the longest effective stop-flow times.

3.5. Towards unravelling grape tannin composition: Application of on-line hydrophilic interaction chromatography × reversed phase liquid chromatography – time-of-flight mass spectrometry to grape seed analysis

(K.M. Kalili, J. Vestner, M.A. Stander, A. de Villiers, Anal. Chem. 85 (2013) 9107-9115, Addendum E).

HILIC×RP-LC has been shown to be an effective tool for the analysis of PCs (**section 3.4**). This work focused on the extension of the same methodology to grape seed PACs. PACs comprise grape and wine tannins, which are responsible for determining important sensory characteristics such as bitterness and astringency in wines [22,23]. The chromatographic separation of tannins is exceptionally challenging due to their complexity, yet of importance, since the biological and organoleptic properties of tannins depend on individual chemical structures [24-26].

Although off-line and stop-flow HILIC×RP-LC separations offer much higher separation power, the on-line method provides a fast, automated system better suited for hyphenation with mass spectrometry (MS). Therefore, on-line HILIC×RP-LC hyphenated to high resolution MS (HR-MS) was explored here to allow the in-depth analysis of grape seed tannins. Experimental conditions used were based on those derived in **sections 3.3 and 3.4**. HILIC separation was performed using a 100 min gradient, a flow rate of 25 µL/min with a 1:24 flow-splitter after the first dimension column. The RP-LC separation was performed at 1.5 mL/min using a cycle time of 2 min (to ensure sufficient sampling of first dimension peaks; peak widths ranged from 3.08 to 7.61 min) and a column temperature of 50 °C. Fluorescence (FL) and MS data were acquired on-line after the second dimension separation. The RP-LC effluent was split ~1:1.14 before the mass spectrometer to ensure efficient ionisation.

Raw HILIC×RP-LC–MS data were converted to network common data form (NetCDF) and HILIC×RP-LC–FL data to comma separated (CSV) files before importing the data into Matlab 7.14 for processing and interpretation. Contour plots obtained for the MS and fluorescence data depicted a clear picture of the grape seed proanthocyanidin distribution, both in terms of molecular weight and isomeric composition. Hyphenation of HILIC×RP-LC separation with especially HR-MS revealed the complexity of the sample. Thorough study of the data showed that the investigated grape seed extract comprised a diverse family of tannins, notably PCs and galloylated PCs spanning a wide range of DPs. The selective nature of fluorescence detection provided a clear fingerprint of the PC content of the sample, and simplified compound identification as distinction between fluorescent PCs and non-fluorescent PACs was facilitated. Given the fact that fluorescence response for PCs decreases as a function of DP [27], only PCs of DP up to 9 were detected by fluorescence.

HR-MS detection proved much more powerful and sensitive, allowing confirmation of the presence of low level PCs of DP up to 12 as well as monogalloylated to octagalloylated PCs of DPs as high

as 16. Furthermore, MS detection allowed an in-depth analysis of the chemical composition as the distribution of different classes of compounds in the sample could be obtained through extracted ion contour plots. This approach allowed tentative identification as single chromatographic peaks of 78 PACs, including 33 PCs, 25 monogalloylated-, 11 digalloylated-, 6 trigalloylated- and 1 tetragalloylated PCs as well as 2 (epi)catechin monoglycosides. Compounds were detected either as singly, doubly or triply charged species, and were identified on the basis of their respective accurate masses.

Although the relative elution pattern of compounds was generally maintained in HILIC, it was evident that overlap was unavoidable between high MW PCs and galloylated PCs because of the extreme complexity of these compound classes. It was further evident that the resolving power of the 2-min RP-LC gradient was not sufficient for separation of individual isomers of DP greater than 5, resulting in unresolved bumps for these compounds. This is expected in light of the exponential increase in the number of isomeric structures with increasing DP [28]. This situation was further exacerbated by the extensive co-elution involving PCs and galloylated PCs under HILIC conditions. Subjecting the grape seed extract to phloroglucinolysis indicated a mean degree of polymerisation (mDP) of 3.6, which is in agreement with previous values [29,30] and signifies that the majority of grape seed PACs are low molecular weight compounds. Phloroglucinolysis data further showed that the grape seed tannins comprised catechin, epicatechin and epicatechin gallate units, with catechin (46%) and epicatechin (44%) as the major terminal units. Epicatechin (73%) was the main extension unit, followed by catechin (19%) and epicatechin gallate (8%).

Summarising this work, on-line HILIC×RP-LC-FL–MS separation allowed grape seed PACs to be fractionated according to size in the HILIC dimension followed by separation into individual isomers in the RP-LC dimension, which reduces peak overlap and simplifies data interpretation. Combining HILIC×RP-LC with MS allows compounds to be identified much more accurately as individual compounds are represented by two independent chromatographic retention times and corresponding mass spectral information. The fact that these methods provide complementary information allows the benefits of individual methods to be exploited where others are constrained. For example, HILIC and MS fail to differentiate between compounds with similar MW (particularly stereoisomers present in grape seeds), while RP-LC provides separation of these isomers based on hydrophobicity. In contrast, compounds with different MW which are not resolved in RP-LC were clearly distinct in HILIC and MS. Although HILIC separates PCs of different DPs, co-elution between different classes of PCs and galloylated PCs was unavoidable, therefore complete resolution of the large number of isomers present in these HILIC fractions could not be achieved using a 2-min RP-LC gradient. Combining the two separation methods in either off-line and stop-flow modes to allow the use of longer RP-LC analysis times would be beneficial in this regard as better isomeric separation could be achieved. Based on these data, it is clear that MS is an indispensable detection method for the detailed investigation of complex phenolic extracts and that

the high complexity of grape PACs require a combination of complementary analytical techniques if complete characterisation of individual compounds is to be realised. Nonetheless, HILIC×RP-LC–MS is currently the most effective single analytical method for the detailed characterisation of grape seed PACs.

3.6. Comprehensive two-dimensional liquid chromatography coupled to the ABTS radical scavenging assay: A powerful method for the analysis of phenolic antioxidants

(K.M. Kalili, F. Lynen, S. de Smet, T. van Hoeylandt, A. de Villiers, 2013, submitted for publication in Anal. Bioanal. Chem., Addendum F).

Amongst the many health effects reported for phenolics, their antioxidant and/or radical scavenging activities have thus far received most attention. This is because antioxidant activity is viewed as the most potent indicator of bioactivity and is also a property that can be easily monitored throughout the production process [31,32]. Several methods have been developed for the determination of antioxidants or radical scavengers in various sample matrices. HPLC coupled on-line to antioxidant assays with UV detection has become a routine method for the identification of radical scavengers in complex mixtures. However, single chromatographic methods do not provide sufficient resolving power for complete separation of the large number of compounds typically encountered in crude phenolic extracts. As illustrated in **sections 3.4 and 3.5**, LC×LC clearly offers improved resolution for such samples. Therefore, this study investigated the feasibility of the on-line coupling of HILIC×RP-LC separation with the 2,2'-azino-bis(3-ethylbenzothiazoline)-6 sulfonic acid (ABTS) radical scavenging assay as a more powerful approach for profiling of radical scavengers in complex mixtures. The ABTS assay was selected here as it has previously demonstrated better sensitivity, faster reaction kinetics and its suitability for the detection of both hydrophilic and lipophilic radical scavengers over a wider range of pH and solvent compositions compared to alternative methods [33-35].

Prior to on-line coupling of the HILIC×RP-LC system with the ABTS assay, parameters such as the reaction time, reactor dimensions and the ABTS flow rate were optimised. A 2.8 m polytetrafluoroethylene (PTFE) reaction coil with an internal diameter (i.d.) of 0.01" was used, since it provided the best compromise between reaction time and maintaining chromatographic efficiency. A 0.07 mM ABTS solution was used and detection was performed at 280 (detection of phenolics) and 414 nm (detection of radical scavenging species). The ABTS assay was characterised by sufficiently fast reaction kinetics to provide good sensitivity for reaction times of 4.26 and 5.32 s in the on-line and off-line analyses, respectively. Cocoa, red grape seed and green tea extracts were analysed using both on-line and off-line HILIC×RP-LC–ABTS configurations. By comparing contour plots obtained at 280 and 414 nm it was immediately possible to identify radical

scavengers in the different samples. From the 2-D data it was also evident that extensive peak overlap occurred in both HILIC and RP-LC dimensions, suggesting that for highly complex samples such as these, measurement of radical scavenging activities by either HILIC– or RP-LC–ABTS would provide inaccurate results due to co-elution. The data further showed that most compounds in the investigated cocoa, grape seed and green tea extracts display radical scavenging activity, with the exception of a few minor components which either lacked activity or exhibit much slower reaction kinetics. Judging from the peak intensities, it appeared that the activity was directly correlated to the relative concentrations of individual compounds. Quantitative evaluation of relative radical scavenging activity for individual compounds, not attempted in this study, would make an interesting subject for future studies as it would allow important structural-radical scavenging activity relationships to be drawn.

To the best of our knowledge, this work represents the first report on the combination of LC×LC separation with radical scavenging detection. It was demonstrated that on-line coupling of LC×LC separation with a radical scavenging assay provides a much more powerful and accurate approach for the screening of active compounds in complex matrices compared to 1-D LC, where extensive co-elution is unavoidable. The on-line HILIC×RP-LC–ABTS method requires shorter analysis times and offers reduced resolution compared to the off-line approach, but this method is superior to 1-D LC as it reduces component overlap. This method is suitable for analysis of samples with simpler phenolic profiles or as a quick screening tool for radical scavenging activity. The off-line HILIC×RP-LC–ABTS method offers high resolution at the cost of relatively long analysis times. Therefore, this method can serve as an alternative to the tedious and time-consuming conventional assay-guided isolation of bioactive molecules in complex mixtures.

References

[1] A. de Villiers, F. Lynen, P. Sandra, J. Chromatogr. A 1216 (2009) 3431.
[2] A.C. Fletcher, L.J. Porter, E. Haslam, R.K. Gupta, J. Chem. Soc., Perkin Trans. 1 (1977) 1628.
[3] K.M. Kalili, A. de Villiers, J. Chromatogr. A 1216 (2009) 6274.
[4] K.M. Kalili, A. de Villiers, J. Sep. Sci. 33 (2010) 853.
[5] T. Beelders, K.M. Kalili, E. Joubert, D. de Beer, A. de Villiers, J. Sep. Sci. 35 (2012) 1808.
[6] K.M. Kalili, A. de Villiers, J. Chromatogr. A 1289 (2013) 69.
[7] J.H. Knox, H.P. Scott, J. Chromatogr. 282 (1983) 297.
[8] J.H. Knox, J. Chromatogr. A 831 (1999) 3.
[9] B. Tran, E. Lundanes, T. Greibrokk, Chromatographia 64 (2006) 1.
[10] F. Bedani, W.T. Kok, H.-G. Janssen, J. Chromatogr. A 1133 (2006) 126.
[11] K. Miyabe, H. Kobayashi, D. Tokuda, N. Tanaka, J. Sep. Sci. 29 (2006) 2452.
[12] J.N. Fairchild, K. Horvath, G. Guiochon, J. Chromatogr. A 1216 (2009) 1363.
[13] Z. Liu, D.G. Patterson, M.L. Lee, Anal. Chem. 67 (1995) 3840.
[14] X. Li, D.R. Stoll, P.W. Carr, Anal. Chem. 81 (2009) 845.
[15] L.W. Potts, D.R. Stoll, X. Li, P.W. Carr, J. Chromatogr. A 1217 (2010) 5700.
[16] Y. Huang, H. Gu, M. Filgueira, P.W. Carr, J. Chromatogr. A 1218 (2011) 2984.
[17] K.M. Kalili, A. de Villiers, J. Chromatogr. A 1289 (2013) 58.
[18] R.E. Murphy, M.R. Schure, J.P. Foley, Anal. Chem. 70 (1998) 1585.
[19] J.V. Seeley, J. Chromatogr. A 962 (2002) 21.
[20] P. Schoenmakers, P. Marriott, J. Beens, LC-GC Eur. 16 (2003) 335.
[21] K. Horie, H. Kimura, T. Ikegami, A. Iwatsuka, N. Saad, O. Fiehn, N. Tanaka, Anal. Chem. 79 (2007) 3764.
[22] A.L. Waterhouse, Ann. N.Y. Acad. Sci. 957 (2002) 21.
[23] M.J. Herderich, P.A. Smith, Austr. J. Grape Wine Res. 11 (2005) 205.
[24] E. Haslam, Biochem. J. 139 (1974) 285.
[25] J. Rigaud, M.T. Escribano-Bailon, C. Prieur, J.-M. Souquet, V. Cheynier, J. Chromatogr. A 654 (1993) 255.
[26] G. Tucker, K. Robards, Crit. Rev. Food Sci. Nutr. 48 (2008) 929.
[27] W.J. Hurst, B. Stanley, J.A. Glinski, M. Davey, M.J. Payne, D.A. Stuart, Molecules 14 (2009) 4136.
[28] R. Mayer, G. Stecher, R. Wuerzner, R.C. Silva, T. Sultana, L. Trojer, I. Feuerstein, C. Krieg, G. Abel, M. Popp, O. Bobleter, G.K. Bonn, J. Agric. Food Chem. 56 (2008) 6959.
[29] J.A. Kennedy, G.P. Jones, J. Agric. Food Chem. 49 (2001) 1740.
[30] F. Mattivi, U. Vrhovsek, D. Masuero, D. Trainotti, Austr. J. Grape Wine Res. 15 (2009) 27.
[31] E.J. Borowska, Plant Foods Hum. Nutr. 63 (2008) 147.
[32] B. Kusznierewicz, A. Piasek, A. Bartoszek, J. Namiesnik, Phytochem. Anal. 22 (2011)392.
[33] R. Re, N. Pellegrini, A. Proteggente, A. Apnnal, M. Yang, C. Rice-Evans, Free Radic. Biol. Med. 26 (1999) 1231.
[34] I.I. Koleva, H.A.G. Niederländer, T.A. van Beek, Anal. Chem. 73 (2001) 3373.
[35] H.A.G. Niederländer, T.A. van Beek, A. Bartasiute, I.I. Koleva, J. Chromatogr. A 1210 (2008) 121.

Chapter 4

General Conclusions and Recommendations

This chapter presents general conclusions of the results obtained in this study. Recommendations for future work are also made.

4.1. General conclusions

Phenolic analysis is a challenging task. Although significant progress has been made in phenolic research, a great challenge remains in developing improved methods for the analysis of these compounds. As is apparent from the phenolic extracts dealt with in this study and an overview of the most recent developments in the field, the complexity of these samples far exceed the separation capability of any single analytical method. This suggests that combining multiple, complementary analytical techniques is necessary for the detailed investigation of phenolics in complex samples. From the results obtained in this study it can be concluded that LC×LC holds significant promise for improving phenolic separations. HILIC×RP-LC in particular, provides a powerful combination for proanthocyanidin analysis, allowing compounds to be pre-fractionated according to molecular size in HILIC before their isomeric separation in RP-LC.

The systematic optimisation procedures for on-line, off-line and stop-flow HILIC×RP-LC systems developed in this study point to the relative complexity of these methods. Optimisation of several inter-related parameters is required for optimal performance. All three HILIC×RP-LC methods provided superior performance compared to individual HILIC and RP-LC methods. The on-line HILIC×RP-LC method offered high throughput and automation, although at slightly reduced resolution relative to the off-line and stop-flow methods. This method is therefore suited for analysis of samples with simple phenolic compositions or as a quick screening tool. The off-line and stop-flow HILIC×RP-LC methods provided much higher resolving power, although these analyses are costly in terms of analysis time. These methods are suitable for the analysis of highly complex phenolic fractions. Significantly, this study demonstrated that additional band broadening due to stop-flow operation is negligible for procyanidins when analysis times up to 15 min are used in the second dimension, suggesting that stop-flow HILIC×RP-LC is a viable alternative to the more labour-intensive off-line method.

Combining on-line HILIC×RP-LC with fluorescence (FL) and mass spectrometry (MS) detection provided an additional dimension of separation and increased specificity, exploiting the complementary benefits of each of the methods. The power of this approach was demonstrated for the analysis of highly complex PACs in grape seeds. Although complete separation of particularly high molecular weight PACs could not be achieved, partly due to the limitations of on-line LC×LC operation, this approach provided important insights into the complexity of the grape seed tannin chemistry. This methodology was found to represent the most powerful analytical strategy for grape PAC analysis reported to date.

In the last experimental chapter, the hyphenation of LC×LC with alternative detection strategies was explored. It was demonstrated that on-line coupling of LC×LC method with a radical scavenging assay offers a much more powerful approach than conventional HPLC-radical scavenging systems for the screening of individual radical scavengers in complex matrices.

Based on the results reported in this dissertation, it can be concluded that for natural product phenolics, where the sample complexity exceeds the resolving power of individual separation methods, combining optimal LC×LC separation with complementary detection methods such as fluorescence, high resolution MS and/or radical scavenging assays, holds significant promise to allow the more detailed characterisation of complex phenolic fractions.

4.2. Recommendations for future studies

Given the complexity of natural phenolic samples and the demonstrated benefits of LC×LC, more research is clearly required to improve and/or extend the methods developed in this study. First of all, while the benefits of HILIC×RP-LC for PAC separation have been shown, the combination of alternative separation mechanisms should be explored, also for different phenolic classes. HILIC separations, especially on conventional 5 µm phases such as the diol phase used in this study, are generally characterised by relatively low chromatographic efficiency. A new generation of HILIC columns packed with sub-2 µm particles have recently been introduced; these may be used to improve efficiency in the first dimension. Similarly, alternative stationary phases such as sub-2 µm superficially porous columns also hold potential to improve separation performance in the second dimension.

In addition, the use of a capillary HILIC column in the first dimension would be helpful. Although this might not necessarily provide better sensitivity, it would avoid the requirement of flow-splitting between the two dimensions and therefore improve the robustness of the methodology.

Considering the importance of tannins in wine chemistry and the separation difficulties associated with these compounds, it is worth extending the analytical methodologies developed in this study to the analysis of grape skin and wine tannins, as this could potentially provide more information on the evolution of these influential molecules in wine.

This study demonstrated the feasibility of coupling LC×LC with radical scavenging assays. It would be interesting to extend this to a quantitative method suitable for the evaluation of the radical scavenging activities for individual compounds. Also in this regard, the use of a capillary HILIC column would be highly beneficial by ensuring the quantitative transfer of the HILIC fractions to the secondary column for more accurate results.

Finally, the combination of LC (or LC×LC) with entirely different separation methods for phenolic analysis would also be interesting, such as combining CE and LC separations for example.

Addenda

Research Publications and Additional

Supporting Information

Addendum A

1. Recent developments in the HPLC separation of phenolic compounds

K.M. Kalili, A. de Villiers, J. Sep Sci. 34 (2011) 854-876.

2. Improving HPLC separation of polyphenols

A. de Villiers, K.M. Kalili, M. Malan, J. Roodman, LC-GC Eur. 466-478.

3. Additional references

Kathithileni M. Kalili
André de Villiers

Department of Chemistry and Polymer Science, Stellenbosch University, Matieland, South Africa

Received November 17, 2010
Revised November 17, 2010
Accepted December 29, 2010

Review Article

Recent developments in the HPLC separation of phenolic compounds

Phenolic compounds represent a class of highly complex naturally occurring molecules that possess a range of beneficial health properties. As a result, considerable attention has been devoted to the analysis of phenolics in a variety of samples. HPLC is the workhorse method for phenolic separation. However, conventional HPLC methods provide insufficient resolving power when faced with the complexity of real-world phenolic fractions. This limitation has been traditionally circumvented by extensive sample fractionation, multiple analysis methods and/or selective detection strategies. On the other hand, there is an increasing demand for improved throughput and resolving power from the chromatographic methods used for phenolic analyses. Fortunately, during the last decade, a number of important technological advances in LC have demonstrated significant gains in terms of both speed and resolution. These include ultra high-pressure liquid chromatography (UHPLC), high-temperature liquid chromatography (HTLC), multi-dimensional separations as well as various new stationary phase chemistries and morphologies. In recent years, these technologies have also found increasing application for phenolic analysis. This review seeks to provide an updated overview of the application of recent advances in HPLC to phenolic separation, with the emphasis on how these methodologies can contribute to improve performance in HPLC analysis of phenolics.

Keywords: Comprehensive two-dimensional liquid chromatography (LC × LC) / High-temperature liquid chromatography / Phenolic compounds / Superficially porous columns / Ultra high-pressure liquid chromatography
DOI 10.1002/jssc.201000811

1 Introduction

The growing interest in natural phenolic compounds in recent years can largely be ascribed to evidence of the beneficial health properties that these compounds have demonstrated, in addition to various roles that they are known to play in food quality. This has in turn spurned the development of a vast array of chromatographic methods for phenolic analysis, although the high complexity and chemical diversity of natural phenolics continues to present analytical challenges [1, 2]. Improved analytical techniques for phenolic compounds are required to enable, for example, in vitro and in vivo studies of their purported health benefits [3, 4], considering that these physico-chemical properties are compound-dependent [5]. Superior separation methods would also allow investigation of the mechanisms of action and bioavailability of these molecules in order to fully understand the roles they play in human health and food quality [6, 7]. This knowledge is of particular relevance in recent times considering that phenolics are increasingly being used as ingredients in functional foods and beverages as well as in cosmetics and pharmaceutical formulations. HPLC is the most widely used separation technique for phenolic analysis. Although promising results have, in the past, been achieved using conventional LC methods, the high complexity of real-world phenolic samples has placed sustained pressure on improved chromatographic performance to meet increasing analytical demands in terms of resolving power, selectivity and sensitivity.

During the last decade, a number of developments in LC have delivered a quantum leap in the performance attainable on commercial LC instrumentation. The most important developments include ultra high-pressure liquid chromatography (UHPLC), high-temperature liquid chromatography (HTLC), multi-dimensional LC (MDLC) separations as well as new column supports including monolithic and superficially porous stationary phases. These technologies have also been applied to phenolic analysis in recent years.

Correspondence: Dr. André de Villiers, Department of Chemistry and Polymer Science, Stellenbosch University, Private Bag X1, Matieland 7602, South Africa
E-mail: ajdevill@sun.ac.za
Fax: +27-21-808-3360

Abbreviations: HSS, high-strength silica; **HTLC**, high temperature liquid chromatography; **LC × LC**, comprehensive two-dimensional liquid chromatography; **UHPLC**, ultra high-pressure liquid chromatography; **Zr**, zirconia

The focus of this review is therefore on the application of the recent developments in packed column HPLC to phenolic separation, with the emphasis on practical benefits associated with their implementation. Clearly, this topic is rather defined in scope, encompassing as it does only a relatively small part of the field of phenolic analysis. A number of up-to-date overview articles on the extraction, sample preparation, general separation and MS analysis of phenolic compounds may be consulted for more information on these topics, for example [8–10]. Furthermore, it should be noted that the dedicated reviews or overviews dealing with UHPLC [11], HTLC [12, 13], multidimensional LC [14, 15], monolithic [16] and superficially porous [17] stationary phases may be found elsewhere. Only the work reported during the last 10 years is covered in this review.

2 Phenolic compounds: Occurrence, basic chemistry and importance

Phenolic compounds, also often referred to as polyphenols, embody a class of widely distributed and chemically diverse secondary metabolites synthesised in plants at different developmental stages [18]. Owing to their wide distribution in nature, these compounds constitute an essential part of the human diet [19, 20]. For this reason, phenolic compounds have been the focus of extensive research ultimately aimed at understanding the role they play in human health and food quality.

Phenolic compounds encompass compounds whose chemical structures possess an aromatic ring with one or more hydroxyl functional groups. These are loosely classified into flavonoids and non-flavonoids. Flavonoids, whose structures are based on a C_6-C_3-C_6 skeleton, are the most abundant group of phenolic compounds, and are sub-divided into different classes differing in the oxidation state of the central heterocyclic ring [21]. These comprise flavonols, flavones, isoflavones, flavanones, anthocyanidins and flavanols (catechins and tannins). Tannins are classified into hydrolysable and non-hydrolysable or condensed tannins (proanthocyanidins). Hydrolysable tannins are esters of phenolic acids and sugars or their derivatives, which yield a sugar and a phenolic acid moiety upon hydrolysis [21]. The sugar is usually glucose or a polysaccharide, whereas the phenolic acid is either gallic acid in the case of gallotannins or ellagic acid in the case of ellagitannins [19, 21]. Proanthocyanidins are oligomers and polymers of flavan-3-ol monomeric units which form coloured anthocyanidins when subjected to acidic hydrolysis [19, 21].

Non-flavonoids comprise simple phenols, phenolic acids, coumarins, xanthones, chalcones, stilbenes, lignins and lignans. Phenolic acids are further divided into benzoic acid derivatives, based on a C_6-C_1 skeleton, and cinnamic acid derivatives, which are based on a C_6-C_3 skeleton [21]. The coumarins are phenolic acid derivatives composed of a benzene ring fused with an oxygen heterocycle [21]. Xanthones consist of a C_6-C_1-C_6 basic structure and stilbenes are composed of a C_6-C_2-C_6 skeleton with various hydroxylation patterns [22]. Chalcones contain a C_6-C_3-C_6 basic structure lacking a heterocyclic C-ring [22], lignins are polymers of C_6-C_3 units [23], whereas lignans are made up of two phenylpropane units [7, 24]. The general structures of each of these classes are shown in Fig. 1. Note that further sub-division of each of these classes is possible depending on hydroxylation patterns and stereochemistry.

Extensive research has shown that phenolic compounds exhibit a wide range of biological activities and play an important role in determining food properties. For example, red wine procyanidins were found to inhibit atherosclerosis through suppression of endothelin-1 [25], whereas grape seed procyanidins were found to exhibit antioxidant activity in vivo [26]. Green tea catechins were found to show, among others, antioxidant, anti-hypertensive, anti-depressant and anti-inflammatory activities [27, 28]. A cacao pentameric procyanidin was reported to selectively inhibit the growth of human breast cancer cells [29]. Proanthocyanidins are also believed to be involved in defense against ultraviolet radiation or aggression by pathogens [7, 19]. Isoflavones have been shown to exhibit anti-inflammatory [30], estrogenic and anti-proliferation effects [31].

Flavones, flavonols and anthocyanidins are believed to attract pollinating insects in flowers [32], whereas lignins and lignans are believed to be involved in plant growth and defense [24]. Phenolic compounds also play influential roles in determining the quality of plant-derived food products such as colour and chemical stability, astringency, bitterness, etc. [19, 33]. Flavanols are involved in browning reactions in various natural products including grapes and wine [34]. In red wine, flavanols react with anthocyanins to form complex pigments, resulting in colour stability [35, 36] and loss of astringency [34] during ageing.

To date, more than 4000 flavonoids have been identified [37]. Many natural products contain large numbers of phenolics of different classes, clearly highlighting the challenges associated with their analysis.

3 Applications of recent advances in HPLC to phenolic analysis

3.1 1-D analyses

3.1.1 UHPLC and HTLC

It has long been known that a reduction in particles size (d_p) for packed column HPLC is beneficial. This is due to the fact that small particles provide a more uniform flow and shorter diffusion distances, which increases mass transfer kinetics and implies that high efficiency can be attained in a short time. This knowledge has been the driving force behind the continuous decrease in d_p evident from HPLC literature since the 1960s. However, as a decrease in d_p is associated with an important concomitant reduction in

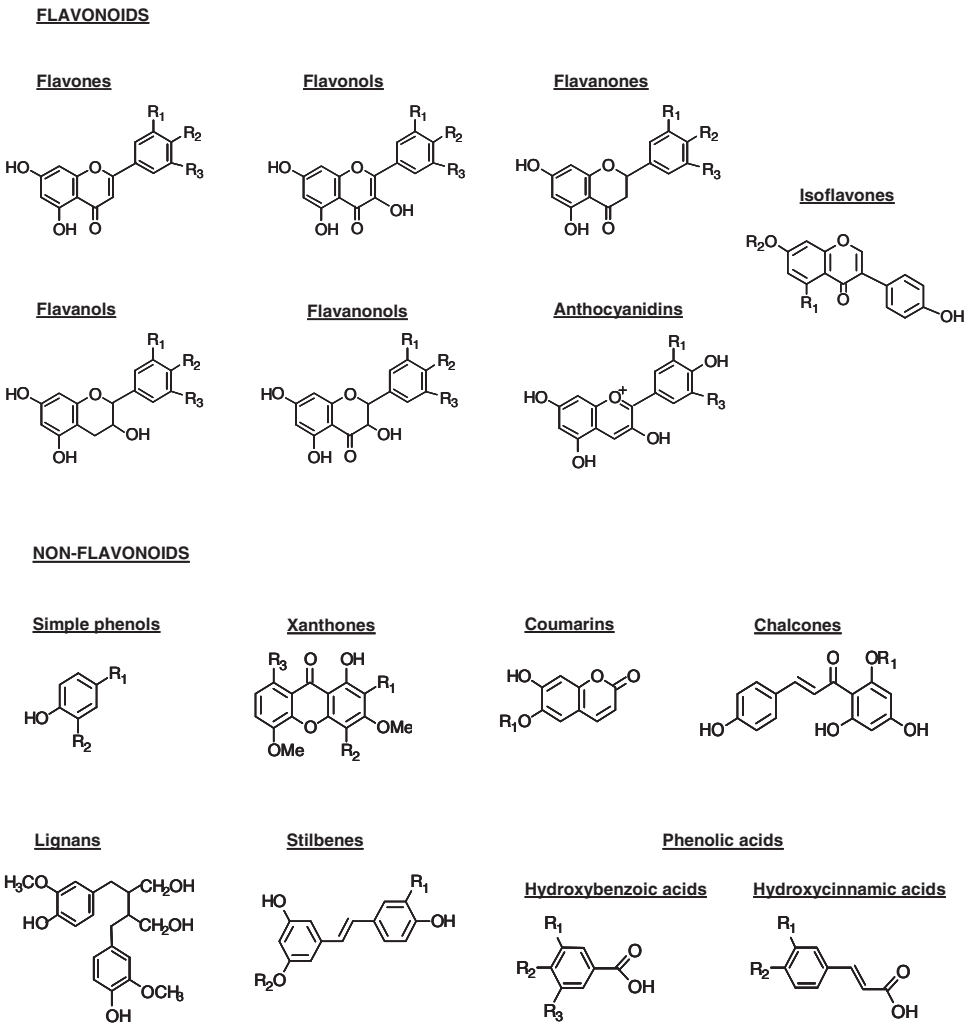

Figure 1. Chemical structures of the principal classes of natural flavonoid and non-flavonoid phenolic compounds.

column permeability, it has been common practice to reduce both d_p and column length due to the instrumental pressure constraints. Thus, the primary benefit of this approach are faster analyses (a result of both shorter column lengths and higher optimal flow rates), with negligible gains in efficiency. The seminal study of Jorgenson and co-workers demonstrated for the first time the practical benefits of a combination of sub-2 μm particles and ultra high pressures (up to 5000 bar or 72 000 psi) [38, 39]. This was followed in 2004 by the first commercial instruments capable of pressures above 500 bar. Since this time, a wide variety of sub-2 μm phases and instruments dedicated for separation using these columns have become available – this technology is generally referred to as UHPLC.

Extensive fundamental research has shown the benefits of UHPLC compared with ''conventional'' HPLC (i.e. 3–5 μm phases and pressures up to 400 bar) to be twofold: (i) improved speed for relatively low-plate counts (due to the characteristics of the small packings referred to above), and (ii) a shift of the optimal performance of any given phase to better performance for high-efficiency analysis. In fact, the combination of small particles and pressure up to 1250 bar (the highest pressures currently available on commercial instrumentation) will provide better results for the analysis up to ~100 000 theoretical plates [40, 41]. For conventional HPLC analysis (in the region of 15 000–25 000 theoretical plates), gains in analysis time in the order of three to nine times can be achieved using this approach. UHPLC can also be utilised to improve the efficiency for a given analysis time compared with conventional HPLC although this approach has received less attention to date.

The effect of temperature on HPLC separations has been known since the 1980s [42] although it is only in the past decade that the use of temperature as an additional parameter for the improvement of HPLC separations has gained general acceptance. In the past, the benefits of elevated temperature in LC analyses have not been widely explored, partly not only due to the lack of suitable columns and instrumentation [42, 43], but also due to the concerns regarding analyte stability. With the recent availability of

thermally stable stationary phases and suitable instrumentation, HTLC has taken on a new relevance.

Analysis temperature affects the selectivity, retention and mobile-phase viscosity in HPLC [12, 42]. The most important effect of an increase in temperature is the reduction of the mobile-phase viscosity and concomitant increase in mass transfer kinetics, resulting in higher optimal flow rates and therefore faster analyses [12, 42]. One approach to benefit from the reduction in mobile-phase viscosity with increasing temperature is to use longer columns to deliver higher efficiency. It should be noted, however, that because of the increase in optimal linear velocity associated with an increase in temperature, this does require higher pressure capabilities. In fact, under pressure-constrained conditions, the primary benefit of elevated temperature is to improve the speed of HPLC separations [12].

From the precedent discussion, it is evident that UHPLC and HTLC are in fact complementary techniques, with the former providing efficiency gains for a given phase (in addition to the well-documented gains in analysis time when used in combination with smaller d_p phases), and the latter providing gains in terms of analysis speed. In fact, due to the high backpressures generated by small particles, much of the UHPLC research performed on the analysis of phenolics also involve the use of elevated analysis temperatures. For this reason, UHPLC and HTLC are considered together in this section. For the purpose of this review, UHPLC is defined as separation performed on columns packed with 2.5 μm particles or less (i.e. not defined in terms of pressure), whereas HTLC as used in this contribution refers to the analyses carried out at 40°C and above. It is mostly in the last 5 years that reports dealing with the application of UHPLC and HTLC for polyphenol analysis have appeared in the literature. Below is a brief summary of these reports grouped according to the different classes of phenolic compounds, which are summarised in Table 1.

3.1.1.1 Procyanidins

Procyanidins (and catechins), being the most abundant class of phenolic compounds in nature, are among the most studied. These compounds also present one of the most severe challenges in terms of chromatographic separation: with an increase in molecular weight, the number of potential isomers increases exponentially. In fact, especially for high-molecular-weight procyanidins, there is currently no known separation method, as recently summarised [44]: ''polymeric procyanidins … cannot be separated through conventional HPLC.'' Various researchers have investigated the combination of UHPLC and elevated temperature for improved procyanidin analysis. Most of this work has focussed on reversed-phase (RP) separation on C18 phases using acidified acetonitrile/water phases. For example, Spácil *et al.* [45] achieved a rapid separation of eight tea catechins within 2.5 min using a 100 mm 1.7 μm BEH C18 column operated at 35°C, whereas Pongsuwan et al. [46] reported a UHPLC method for tea catechins and other metabolites using a 150 mm 1.7 μm C18 column and a column temperature of 40°C. The latter method has proved to be useful in the metabolic profiling of 56 Japanese green tea samples.

Alternative RP phases have also been investigated. Guillarme et al. [47] developed a UHPLC-MS method employing a 1.7 μm shield RP18 column, which was found to provide better selectivity and resolution than the corresponding C18 phase. These authors demonstrated the separation of eight tea catechins in about 30 s; the gradient was adapted to 8 min for better separation of highly complex tea samples. Serra et al. [48] used a 100 mm 1.8 μm high-strength silica (HSS) T3 column for the determination of procyanidins and their metabolites in rat plasma samples, following off-line solid-phase extraction (SPE). The method demonstrated high sensitivity and allowed accurate quantification of procyanidins and metabolites in plasma samples within 5 min. More recently, Marti et al. [49] used a similar column for the simultaneous analysis of procyanidins and anthocyanins in the rat plasma samples following μSPE.

3.1.1.2 Flavones and isoflavones

Isoflavones are a class of phytoestrogenic flavonoids associated with various protective effects against cardiovascular diseases, cancer, menopausal symptoms and osteoporosis, among others [8, 50]. Flavones, on the other hand, are well known for their potent anti-oxidative activity [51]. It is due to these beneficial properties that significant research effort has been devoted to the analysis of flavones and isoflavones in recent years. Notable in isoflavone analysis is the study of Klejdus et al. [52, 53] who used a combination of small particles and high temperatures to achieve efficient, rapid resolution of isoflavones and phenolic acids on different stationary phases. In an earlier study, these authors [52] used a 1.8 μm Zorbax C18 column along with acidified water–methanol mobile phases and a temperature of 80°C to achieve the separations of up to 13 isoflavones in various soy preparations and plant extracts in less than 1 min. Subsequently, the same authors [53] investigated the simultaneous separation of isoflavones and phenolic acids on various RP stationary phases. Satisfactory results were achieved on a cyanopropyl column (50 × 2.1 mm, 1.8 μm) thermostated at 58°C using acidified water–methanol mobile phases and separation of up to 19 compounds in various plant extracts was obtained in 1.9 min (Fig. 2).

Du et al. [54] employed a short 1.8 μm C18 column and a column temperature of 46°C for the analysis of isoflavones in the extracts of the herbal medicine and dietary supplement *Radix Puerariae*, achieving a separation of 14 compounds in 8 min. Using a 100 mm C18 column packed with 1.7 μm particles at 40°C and acidified water–methanol mobile phase, Deng et al. [55] resolved 28 compounds (including eight flavones) in 20 min, whereas Wang et al. [56] used the same column in combination with buffered water–methanol mobile phases and a column temperature

Table 1. Summary of recent applications of UHPLC and HTLC for the analysis of phenolic compounds

Sample	Compound class(es)	Column and temperature	Detection[a)]	Analysis time (no. of compounds)	Reference
Plasma samples	Procyanidins and metabolites	HSS T3 column (100 × 2.1 mm, 1.8 μm)[b)]	DAD ESI-MS/MS	5 min (6 compounds)	[48]
Plasma samples	Procyanidins Anthocyanins	HSS T3 column (100 × 2.1 mm, 1.8 μm)[b)]	ESI-MS/MS	12.5 min[c)]	[49]
Chamomile extract	Phenolic acids Flavonols	Acquity BEH C18 (100 × 2.1 mm, 1.7 μm)[b)]	ESI-MS/MS	20 min (12 compounds)	[70]
Burdock leaves	Phenolic acids Flavonols Flavones	Acquity BEH C18 (150 × 2.1 mm, 1.7 μm)[b)]	DAD ESI-MS/MS	25 min (10 compounds)	[78]
Cocoa, chocolate	Procyanidins	Acquity BEH C18 (50 × 2.1 mm, 1.7 μm)[b)]	DAD ESI-MS	3 min (6 compounds)	[86]
Grape extracts	Anthocyanins	Zorbax SB C18 (50 × 4.6 mm, 1.8 μm)[b)]	DAD ESI-MS/MS	15 min (40 compounds)	[65]
Milk-based food products	Anthocyanins Flavonols	Acquity BEH C18 (50 × 2.1 mm, 1.7 μm), ambient	DAD ESI-MS/MS	10 min (27 compounds)	[76]
Soy foods	Isoflavones	Acquity BEH C18 (50 × 1 mm, 1.7 μm), ambient	ESI-MS/MS	5 min (9 compounds)	[83]
Wines	Phenolic acids Catechin Flavonols	Agilent Rapid Resolution HT C18 (50 × 2.1 mm, 1.8 μm), 20°C	ESI-MS/MS	10 min (11 compounds)	[79]
Chinese medicine	Flavonoids	Acquity BEH C18 (50 × 2.1 mm, 1.7 μm), 25°C	DAD	13 min (15 compounds)	[68]
Red cabbage	Anthocyanins	Zorbax SB C18 (50 × 4.6 mm, 1.8 μm), 27°C	DAD ESI-MS/MS	34 min (24 compounds)	[64]
Tea extract	Catechins	Acquity BEH Shield RP18 (100 × 2.1 mm, 1.7 μm), 30°C	UV ESI-MS/MS	8 min (8 compounds)	[47]
Rat plasma	Isoflavones Flavones	Acquity BEH C18 (100 × 2.1 mm, 1.7 μm), 30°C	ESI-MS	6 min (6 compounds)	[56]
Tea	Catechins Flavonoids Phenolic acids	Acquity BEH C18 (100 × 2.1 mm, 1.7 μm), 30°C	DAD	20 min (29 compounds)	[69]
Different rose species	Hydrolysable tannins Flavonols and glycosides	Acquity BEH C18 (100 × 2.1 mm, 1.7 μm), 30°C	DAD ESI-MS/MS	3 min (21 compounds)	[71]
White wine, grapefruit juice, green tea infusion	Phenolic acids	Acquity BEH C18 (150 × 2.1 mm, 1.7 μm), 30°C	DAD ESI-MS/MS	10 min (17 compounds)	[77]
Cocoa samples	Procyanidins	HSS T3 column (100 × 2.1 mm, 1.8 μm), 30°C	ESI-MS/MS	12.5 min (11 compounds)	[85]
Vanilla extract	Various constituents	Acquity BEH C18 (50 × 2.1 mm, 1.7 μm), 30°C	DAD	6.5 min[c)]	[87]
Almond skin extracts	Phenolic acids Flavonoids	Phenomenex Synergi Fusion-RP100A (50 × 2 mm, 2.5 μm), 35°C	ESI-MS	9 min (23 compounds)	[66]
R. Paeoniae	Monoterpene glycosides Galloyl glucoses Phenolic compounds	HSS T3 column (100 × 2.1 mm, 1.8 μm), 35°C	DAD MS	12 min (40 compounds)	[73]
Tomato extracts	Organic acids Amino acids Nucleosides Phenolic acids Phenolic alcohols Flavonoids Fatty acids Triterpenoid glycosides	Zorbax Eclipse Plus C18 (150 × 4.6 mm, 1.8 μm), 37°C	DAD ESI-MS/MS	46 min (135 compounds)	[72]
Tea	Catechins	Acquity BEH C18 (100 × 2.1 mm, 1.7 μm), 40°C	ESI-MS/MS	2.5 min (8 compounds)	[45]

Table 1. Continued.

Sample	Compound class(es)	Column and temperature	Detection[a)]	Analysis time (no. of compounds)	Reference
Japanese green tea extracts	Catechins	Acquity BEH C18 (150 × 2.1 mm, 1.7 μm), 40°C	ESI-MS	10 min[c)]	[46]
Different honey samples	Phenolic acids Flavonoids	Acquity BEH C18 (100 × 2.1 mm, 1.7 μm), 40°C	DAD ESI-MS	14 min (37 compounds)	[74]
Phenolic antioxidants	Phenolic acids	Discovery Zr-carbon (150 × 4.6 mm, 5 μm), 40°C	UV	26 min (6 compounds)	[81]
	Flavones	Discovery Zr-carbon C18 (150 × 4.6 mm, 5 μm), 40°C		25 min (8 compounds)	
		Discovery Zr-polystyrene (150 × 4.6 mm, 5 μm), 40°C		10 min (8 compounds)	
Tobacco	Various polyphenols Organic acids	Acquity BEH C18 (100 × 2.1 mm, 1.7 μm), 45°C	DAD ESI-MS/MS	12 min[c)]	[80]
R. Puerariae	Isoflavones	Zorbax SB C18 (50 × 4.6 mm, 1.8 μm), 46°C	DAD ESI-MS	9 min (14 compounds)	[54]
Brandy	Various polyphenols	Acquity BEH C18 (100 × 2.1 mm, 1.7 μm), 47°C	DAD	6.5 min (14 compounds)	[88]
Cocoa, apple	Procyanidins Phenolic acids Flavonols Alkaloids	Acquity BEH C18 (100 × 2.1 mm, 1.7 μm), 50°C	UV Fluorescence ESI-MS	25 min (46 compounds)	[94]
Green tea	Proanthocyanidins Phenolic acids Flavonols	Acquity BEH C18 (100 × 2.1 mm, 1.7 μm), 50°C	UV ESI-MS/MS	25 min (67 compounds)	[95]
Red wine	Anthocyanins	Acquity BEH C18 (200 × 2.1 mm, 1.7 μm), 50°C	UV	98 min[c)]	[63]
T. ledibouri Reichb flower	Flavonoids	Acquity BEH C18 (100 × 2.1 mm, 1.7 μm), 50°C	ESI-MS/MS NMR	20 min (15 compounds)	[67]
Isatis indigotica leaves	Flavones	Acquity BEH C18 (100 × 2.1 mm, 1.7 μm), 50°C	DAD ESI-MS/MS	20 min (28 compounds)	[55]
Trifolium species	Isoflavones Phenolic acids Flavonoids Clovamides	Acquity BEH C18 (50 × 2.1 mm, 1.7 μm), 50°C	DAD	8.5 min (23 compounds)	[57]
Horse chestnut extract	Flavonols and derivatives	Acquity BEH C18 (50 × 2.1 mm, 1.7 μm), 50°C	DAD ESI-MS/MS MALDI-TOF/MS NMR	4.5 min (13 compounds)	[58]
Different plant species	Phenolic acids Isoflavones	Zorbax SB-CN (50 × 2.1 mm, 1.8 μm), 58°C	DAD	1.9 min (19 compounds)	[53]
Blueberries	Anthocyanins	Xbridge C18 (250 × 4.6 mm, 5 μm), 70°C	UV MS	55 min (20 compounds)	[63]
Grape berries	Flavonols Flavanols Anthocyanins Stilbenes	Zorbax Eclipse Plus C18 2 × (100 × 2.1 mm, 1.8 μm), 70°C	ESI-MS/MS	35 min (33 compounds) 27 min (11 compounds)	[75]
Soy preparations, plant extracts	Isoflavones	Zorbax SB C18 (30 × 2.1 mm, 1.8 μm), 80°C	DAD ESI-MS	1 min (13 compounds)	[52]
Yerba Santa (*E. californicum*) and honeybush tea (*C. intermedia*) extracts	Flavanones	Hamilton PRP-1 (250 × 10 mm, 10 μm), 120°C	DAD	50 min[c)]	[82]

a) DAD, diode array detection; ESI, electrospray ionisation; UV, ultraviolet/visible detection.
b) Analysis temperature is not specified.
c) Target analytes are not specified.

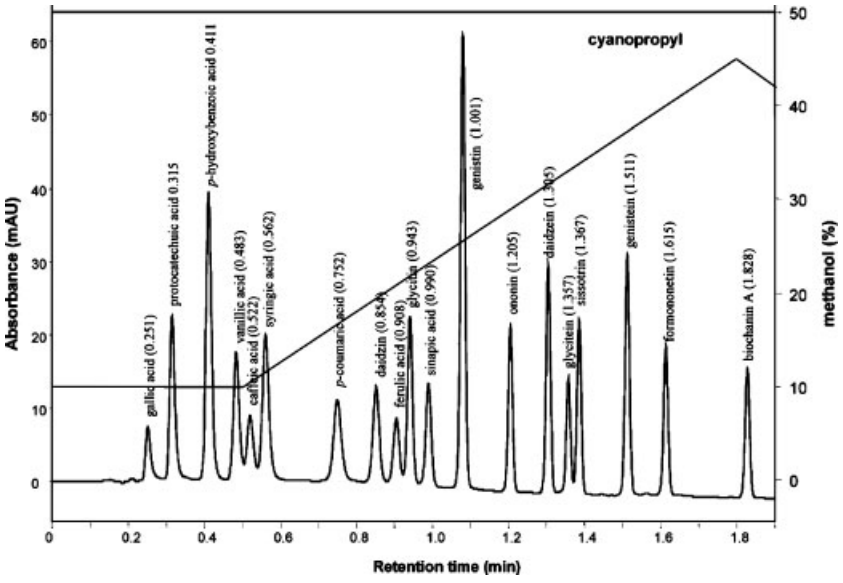

Figure 2. UHPLC separation of phenolic acid and isoflavone standards on a 50 × 2.1 mm 1.8 μm cyanopropyl column. A 3-min gradient analysis was performed at a flow rate of 0.9 mL/min and at a temperature of 58°C. UV detection was performed at 270 nm. Reproduced from [53] with permission from Elsevier.

of 30°C to achieve a separation of six isoflavones and flavones in rat plasma in 6 min. Oleszek et al. [57] developed a UHPLC method utilising a 1.7 μm C18 column and acidified water–acetonitrile mobile phases at 50°C for the simultaneous separation of isoflavones, phenolic acids, flavonoids and clovamides in 57 *Trifolium* plant species of different origins. A total of 23 compounds were separated in less than 8.5 min and were identified based on co-chromatography with standards and their respective UV spectra. In another study, the same authors [58] used an identical column with a slightly modified gradient to achieve a separation of 13 flavonoids and derivatives in a horse chestnut extract in less than 5 min.

3.1.1.3 Anthocyanins

Anthocyanins (anthocyanidin-glycosides) are coloured phenolic compounds whose analysis by conventional HPLC methods is often problematic. Past research has elucidated the pH-dependant equilibria of the various forms of anthocyanins that occur in solution [59, 60]. The solution chemistry of anthocyanins has important implications for their separation by HPLC. Horváth and co-workers demonstrated how similar secondary equilibria affect chromatographic separation: for slow inter-conversion reactions (relative to the chromatographic timescale), individual species are separated, whereas fast inter-conversion leads to the detection as a single peak [61]. de Villiers et al. [62] demonstrated that on-column inter-conversion between flavylium cationic and carbinol pseudo-basic species of anthocyanins is responsible for the relatively poor chromatographic efficiency commonly observed for these compounds under conventional RP-LC conditions. These authors showed how a reduction in particle size and increase in the temperature (used in this instance to speed up secondary equilibria) could be used to enhance the chromatographic efficiency of anthocyanins. In a subsequent report [63], they showed how the analysis on a 200 mm 1.7 μm column at 50°C provides significantly improved resolution for the analysis of red wine anthocyanins.

In other anthocyanin-related work, Arapitsas et al. [64] developed a 34-min UHPLC-DAD/MS method employing a 1.8 μm C18 column and aqueous formic acid–acetonitrile mobile phases for the analysis of 24 cyanidin derivatives in red cabbage. Pati et al. [65] reported a method utilising similar column- and mobile-phase combinations to achieve good separation of 18 monomeric and 22 dimeric anthocyanins in grape extracts inside 15 min, which allowed the tentative identification of six new acylated anthocyanins in grapes.

3.1.1.4 Miscellaneous

Arraez-Roman et al. [66] separated 23 phenolic acids and flavonoids in almond skin extracts by HPLC-TOF-MS in 9 min using a 2.5 μm C18 column. Li et al. [67] and Chen et al. [68] reported a good separation of 15 flavonoids in *Trollius ledibouri* Reichb flowers and *Epimedium* herbs using 1.7 μm C18 columns. Nováková et al. [69] also employed a 1.7 μm C18 column and acidified water–methanol mobile phases for the separation of 29 catechins, flavonoids and phenolic acids in 20 min. In a subsequent study, these authors [70] used the same approach to separate 12 phenolic acids and flavonols in chamomile flower and tea extracts. Kumar et al. [71] achieved simultaneous separation of 21 hydrolysable tannins, flavonols and flavonol-glycosides in three rose species in 3 min. Gómez-Romero et al. [72] tentatively identified a total of 135 phenolic compounds (of which 21 were new) in different tomato extracts using a 46-min

gradient analysis on a 150 mm 1.8 μm column operated at 37°C. Li et al. [73] employed a 1.8 μm HSS T3 column and acidified aqueous acetonitrile mixtures for the chemical profiling of *R. paeoniae* plant extracts. In this study, chemical structures of 40 compounds were elucidated with the help of collision-induced dissociation (CID) MS and comparison to an in-house library. Trautvetter et al. [74] also used a combination of a 1.7 μm C18 column, a temperature of 40°C and Q-TOF-MS for the identification of 37 phenolic acids and flavonoids in different honey samples using a 20-min gradient. Another study by Cavaliere et al. [75] reported a UPLC-MS method based on two serially coupled 100 mm 1.8 μm C18 columns, a temperature of 70°C and acidified water–methanol–acetonitrile mobile phases for the determination and quantification of flavonols, flavanols, anthocyanins and stilbenes in grape skins and seeds. More than 30 compounds were detected by ESI-MS in the grape skins extract, whereas eleven compounds were identified in the seed extract.

The use of selective detectors places less strict demands on chromatographic separation. Of particular relevance in this regard is the application of UHPLC in combination with tandem mass spectrometric (MS/MS) detection for the target analysis of phenolics. For example, Nagy et al. [76] reported a RP UHPLC-MS/MS method based on a 1.7 μm C18 column and acidified aqueous acetonitrile mobile phases that allowed good separation and quantification of 27 anthocyanins and flavonols in milk-based food products in 10 min following ultrafiltration. Gruz et al. [77] successfully characterised and quantified 17 phenolic acids in various beverages inside 10 min using a 1.7 μm C8 column at 30°C and MS/MS detection, whereas Lou et al. [78] used a combination of MS/MS and a 1.7 μm C18 column with acidified aqueous methanol–acetonitrile mobile phases to achieve good separation of phenolic acids and flavonols in burdock leaves in 25 min. Jaitz et al. [79] also developed a RP LC-MS/MS method that allowed simultaneous detection of catechins, phenolic acids and flavonols in various red wines in 10 min using a 1.8 μm column and acidified aqueous acetonitrile mobile phases. Xiang et al. [80] used a 1.7 μm C18 column at 45°C together with acidified aqueous methanol mixtures and MS/MS for the identification of polyphenols and organic acids in tobacco following SPE.

Because of their excellent thermal and chemical stability, zirconia (Zr)-based columns have also been investigated in the HTLC analysis of phenolic compounds [81]. Although these columns were found to offer alternative selectivity compared with silica-based columns, most flavone antioxidants were too strongly retained on the Zr-carbon and Zr-carbon C18 columns. On the other hand, the Zr-polystyrene stationary phase provided good separation of phenolic compounds in a reasonable time and was recommended for routine analysis of such compounds. An interesting application of HTLC was reported by Reichelt et al. [82], who developed a novel LC taste system for the detection of flavour- and taste-modulating substances. These authors used high temperature (120°C) and aqueous ethanol mobile phases to affect a separation of homoeriodictyol, sterubin, hesperetin and lactisol in *Yerba Santa* (*Eriodictyon californicum*) and honeybush tea (*Cyclopia intermedia*) plant extracts. The high temperature used here allows the use of aqueous–ethanol mobile phases (rarely used due to the high viscosity of these phases), which in turn provides the option of direct sensory assessment of collected fractions by a sensory tester or sensory panel. An analysis temperature of 70°C was used to improve the separation of blueberry anthocyanins on a conventional column (XBridge C18, 250 × 4.6 mm, 5 μm) [63]. Because of the effect of temperature on anthocyanin secondary equilibria, better resolution and different selectivities were obtained compared with analysis on the same column at 25°C.

Several studies have focussed on the comparison of UHPLC and conventional HPLC analysis of phenolic compounds, generally with the emphasis on the benefits offered by the use of small particles and high pressures. For example, Churchwell et al. [83] compared HPLC-MS and UHPLC-MS for the analysis of isoflavones in a soy nutritional supplement, whereas Spácil and co-workers [84] compared UHPLC and HPLC analyses of phenolic acids, catechins, coumarins and flavonoids using C18 columns and column temperatures of up to 50°C. In accordance with expectations, these studies demonstrated that UHPLC generally provided significantly enhanced sensitivity, speed and/or resolution. Sensitivity gains by up to a factor of 10 and speed improvements by up to a factor of 5 have been reported. The high efficiency offered by sub-2 μm phases has been exploited to resolve diastereomers which are not resolved by conventional HPLC [83]. The same authors demonstrated how the analysis times could be shortened by a factor of between 2 and 5, whereas solvent consumption is reduced by up to a factor of 10 by switching from HPLC to UHPLC.

Ortega et al. [85] evaluated HPLC and UHPLC for the analysis of procyanidins in a cocoa extract in normal phase or RP-LC modes. The HPLC method employed a silica column (250 × 4.60 mm, 5 μm) and dichloromethane–methanol–water–acetic acid mobile phases, whereas the UHPLC method utilised a HSS T3 column (100 × 2.1 mm, 1.8 μm) and mobile phases containing acetonitrile–water–acetic acid; both methods were coupled to a triple quadrupole mass spectrometer. In this study, the analysis time was reduced by up to a factor 7 (from 80 to 12.5 min). The UHPLC method was also characterised by improved efficiency and better sensitivity: procyanidin oligomers up to hexamers could be detected by HPLC, whereas the UHPLC method allowed the detection of oligomers up to nonamers. Similar results were obtained by de Villiers and co-workers [63] in RP mode. These authors showed how the combination of small particles, elevated temperature (50°C) and high pressures could be used to shorten the analysis time by up to a factor of 3, as illustrated using cocoa procyanidins and green tea flavonols. Cooper et al. [86] also described a UHPLC-MS method that allowed the separation of six procyanidins in 3 min by employing a 1.7 μm C18 column

and acidified aqueous THF–acetonitrile mobile phases. This method provided improved speed, sensitivity and resolution compared with an HPLC method, which achieved similar separation in 20 min.

Cicchetti and Chaintreau [87] compared HPLC and UHPLC analyses of vanilla constituents. UHPLC analysis employed a 50 mm 1.7 μm C18 column, whereas a conventional 250 mm 5 μm C18 column was used in HPLC analysis. In this report, the UHPLC method demonstrated better sensitivity and peak resolution than the HPLC method and the analysis time was shortened by a factor of 4. Similarly, Schwarz et al. [88] reported a comparative study between HPLC and UHPLC for the determination of polyphenols and furanic derivatives in brandy. A highly efficient separation of 14 polyphenols was achieved in only 6.5 min, which is a significant reduction in analysis time compared with 60 min for HPLC. In addition, solvent consumption was greatly reduced: 4.55 mL used in UHPLC as opposed to 60 mL in HPLC. The UHPLC method was applied for the characterisation of phenolic contents of 33 different commercial brandies.

Although objective comparison of HPLC and UHPLC performance is not always feasible, given that the analysis parameters may vary significantly, it can be concluded that in general UHPLC is advantageous in terms of analysis time, solvent consumption and sensitivity. This has been demonstrated in practice by numerous authors. UHPLC therefore holds particular promise for improving throughput in polyphenol analysis, considering that typical HPLC analysis times range between 20 and 80 min [89].

Several authors have demonstrated how the use of longer columns (150–200 mm in length) packed with sub-2 μm phases (often in combination with elevated temperature) may be used to improve resolution compared with conventional HPLC columns for similar analysis times [63, 72, 75]. However, it is interesting to note that to date, the application of UHPLC technology to provide improved efficiency has not been exploited extensively for polyphenol analysis.

Practical implementation of the technology is relatively straightforward with the commercial availability of dedicated UHPLC instrumentation. Also, the continued increase in the number of UHPLC stationary phases available implies that adaptation of HPLC methods to UHPLC conditions is greatly facilitated. However, it is also relevant to point out certain impediments to the general application of UHPLC instrumentation and columns. Although sub-2 μm phases may in principal be utilised on conventional instrumentation under certain conditions [63], pressures above 400 bar are most often required to reap the benefits of these columns. Moreover, due to the significantly lower volumes of UHPLC columns, their effective operation requires extensive alteration of conventional instrumentation in order to avoid excessive extra-column band broadening [90]. Low-volume detectors providing high (>10 Hz) acquisition rates are also essential to deliver optimum performance.

It can also be concluded that the use of elevated temperature offers an attractive approach, especially in combination with UHPLC, to further speed up separations. Most reports make use of relatively modest increases in temperature (up to ~80°C). This can partly be ascribed to the limited temperature range available on commercial HPLC and UHPLC instrumentation (though it should be pointed out that the benefits of HTLC are most pronounced for relatively mild increases in temperature, in the region 25–80°C). Equally important in terms of HTLC analysis of polyphenols are concerns regarding their stability. It is known, for example, that anthocyanins in particular are thermally labile. This aspect, coupled to the fact that the benefits of elevated temperature have, only in recent years, received increasing attention (the technique is therefore not yet commonly employed in routine laboratories), is partly responsible for the fact that HTLC has received relatively little attention in the literature, especially compared with UHPLC. However, concerns regarding on-column degradation, whereas remaining relevant for polyphenol analysis, could pose less of a problem than commonly perceived. Using the criteria proposed by Thompson and Carr [91] for ascertaining the risk of on-column degradation, de Villiers and co-workers have shown that temperature up to 70°C is feasible for anthocyanin analysis without the risk of degradation, provided that the analysis times remain less than 120 min [62, 63].

Other potential drawbacks of HTLC include the need for dedicated instrumentation, especially in terms of effective mobile phase pre-heating, and column stability at elevated temperature which could result in shortened column lifetimes [42, 92]. Therefore, it is important that thorough studies on the thermal stability of analytes and stationary phases be carried out if the benefits of this application are to be realised in practice [42, 93].

3.1.2 The use of alternative column formats in phenolic analysis

Although porous silica currently remains the phase of choice for most HPLC applications due to the numerous advantages of this material, extensive research into alternative stationary phase materials and morphologies is ongoing. Much of this research is aimed at providing alternative packing materials without some of the limitations of porous silica, such as limited temperature and chemical stability and relatively low permeability. Although it is beyond the scope of this review to present a comprehensive overview of the different stationary phases used for phenolic analyses, two alternative column formats which have been applied to provide improved separation of polyphenols will be considered: monolithic columns and superficially porous particles.

3.1.2.1 Monolithic stationary phases

Although monolithic columns have been introduced over two decades ago, these phases have not been widely used for polyphenol determination. Compared with conventional

silica-based stationary phases, monolithic columns offer the advantage of much lower flow resistance due to higher external porosities. In some ways, monolithic columns may therefore be considered an alternative approach to UHPLC, where instrumental pressure capabilities are used to overcome the high flow resistance of small particle-packed columns. In fact, the use of monolithic phases and elevated pressure capabilities has very similar effects on kinetic performance: both approaches provide more pronounced benefits for high-efficiency analyses [41]. However, as in the case of UHPLC, monolithic columns are most often employed for the purposes of obtaining faster separations compared with conventional HPLC. This is possible due to the combination of favourable mass transfer characteristics at high linear velocities and the high permeability of monolithic columns, which allows the use of high flow rates.

As an example, Apers et al. [96] compared conventional RP-LC analysis with the use of monolithic columns for isoflavone analyses. Similar results were achieved on both columns, and although coupling of two 100 mm monolithic columns was necessary to improve resolution of some compounds, flow rates as high as 4 mL/min could be used to shorten the analysis time by a factor of almost 3. Rostagno et al. [97] also coupled two 100-mm monolithic columns for the analysis of isoflavones in soybeans following SPE. This separation was completed in 35 min at a flow rate of 0.8 mL/min. The same authors later speeded up this separation by increasing the flow rate to 5 mL/min on two coupled columns thermostated at 35°C, achieving separation of 12 isoflavones in less than 10 min [98]. Subsequently, they adapted their method to a single column, maintaining the same resolution at a flow rate of 3 mL/min (Fig. 3) [99, 100].

Biesaga et al. [101] developed a method employing a Chromolith Performance RP-18e (100 × 4.6 mm) monolithic column and acetonitrile–phosphate buffer (pH 2.2) mobile phases for the separation and quantification of phenolic acids in plums. This separation was performed at 1 mL/min using a 35 min gradient. Krizman et al. [102] used the same column and acidified water–acetonitrile mobile phases at a flow rate of 3 mL/min to achieve a good separation of phenolic acids from fennel plant extracts inside 10 min. Castellari et al. [103] employed a multistage gradient of buffered methanol–water mixtures and a Chromolith Perfomance RP-18e monolithic column for the separation of phenolic acids, catechins, flavonols and stilbenes in red and white wines. In addition, simultaneous separation of phenolic acids, flavanols, chalcones and flavonols in apple extracts was achieved on a C18 monolithic column operated at 25°C and at a flow rate of 2.5 mL/min [104]. Monolithic columns have also been applied in the determination of phenolics in lemon oil [105], rosemary leaf extract [106], traditional Chinese medicines [107], propolis, *Ginkgo biloba*, red wine and green tea extracts [108], red cabbage [109], vanilla pods [110], beer and wines [111–114] and grapes and must [115]. Analysis times for these separations varied between 1 min (for a 25 mm Chromolith Flash column) and 20 min (on two 100-mm columns). A summary of selected applications is provided in Table 2.

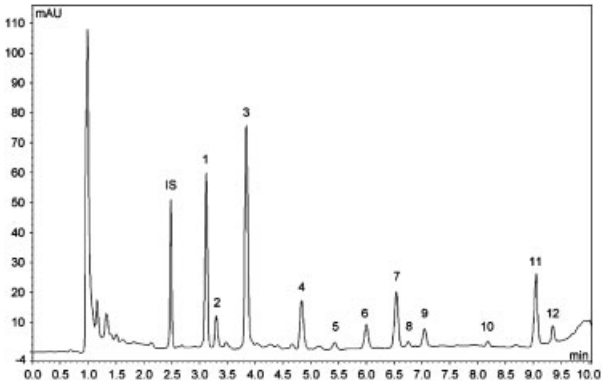

Figure 3. HPLC analysis of a soy extract on a Chromolith TH Performance RP-18e monolithic column (100 × 4.6 mm). A 15-min gradient analysis was performed at a flow rate of 3 mL/min. UV detection at 254 nm. Peak labels correspond to: IS, internal standard; 1, daidzin; 2, glycitin; 3, genistin; 4, malonyl daidzin; 5, malonyl glycitin; 6, acetyl daidzin; 7, acetyl glycitin; 8, malonyl genistin; 9, daidzein; 10, glycitein; 11, acetyl genistin; and 12, genistein. Reproduced from [99] with permission from Elsevier.

Due to their high external porosity and low resistance to solvent flow, monolithic columns are ideally suited to very high flow rates to speed up the separations without loss of resolution and/or efficiency [116]. The disadvantage of this is, however, very high solvent consumption, which is a drawback from economical and ecological points of view. High flow rates are also not compatible with MS detectors, whereas flow splitting compromises sensitivity [93]. Miniaturisation of the column bore size is an established approach to reducing solvent consumption in HPLC, and in fact several authors have developed narrow-bore monolithic columns, which have also found application in the analysis of phenolic compounds. Jandera and co-workers [117] prepared alkylated (C18 chains) poly(styrene-divinylbenzene) monolithic columns for micro-HPLC (μ-HPLC) and capillary electrochromatographic (CEC) separation of phenolic acids. The columns provided good efficiencies with minimum plate heights in the range of 7–11 μm for micro-HPLC and 5 μm for CEC. In a more recent study, the same group [118] prepared zwitterionic (ZIC) polymethacrylate monolithic columns for micro-HPLC by *in situ* co-polymerisation in fused silica capillaries. These columns exhibited mixed-mode HILIC-RP separation mechanisms, properties similar to the conventional commercial zwitterionic-HILIC silica-based columns, but had higher retention and better selectivity under RP conditions. The columns also displayed good thermal stability (up to 80°C) and provided good separations of seven out of eleven phenolic acid standards in the RP mode and ten acids in the HILIC mode at 60°C using a flow rate of 5 μL/min. The HILIC methodology was used for the quantification of phenolic

Table 2. Summary of the recent applications of monolithic columns and superficially porous columns for phenolic analysis

Sample	Phenolic class(es)	Column type, flow rate and temperature	Analysis time (no. of compounds)	Reference
Soy extracts	Isoflavones	2 × Chromolith TH Performance RP-18e (100 × 4.6 mm), 3–4 mL/min[a)]	25 min (9 target compounds)	[96]
Soybeans	Isoflavones	2 × Chromolith TH Performance RP-18e (100 × 4.6 mm), 0.8 mL/min[a)]	35 min (12 compounds)	[97]
Soybeans and derived products	Isoflavones	2 × Chromolith Performance RP-18e 5 mL/min, 35°C	10 min (12 compounds)	[98]
Soybeans	Isoflavones	Chromolith TH Performance RP-18e (100 × 4.6 mm), 3 mL/min[a)]	10 min (12 compounds)	[99]
Soy beverages	Isoflavones	Chromolith TH Performance RP-18e (100 × 4.6 mm), 3 mL/min[a)]	16 min (13 compounds)	[100]
Plums	Phenolic acids	Chromolith Performance RP-18e (100 × 4.6 mm), 2 mL/min[a)]	35 min (7 compounds)	[101]
Fennel extract	Phenolic acids	Chromolith Performance RP-18e (100 × 4.6 mm), 3 mL/min, 22°C	10 min (10 compounds)	[102]
Red and white wines	Phenolic acids Catechins Flavonols Stilbenes	Chromolith Performance RP-18e (100 × 4.6 mm), 2.1 mL/min, 30°C	36 min (17 compounds)	[103]
Apple extract	Phenolic acids Flavanols Chalcones Flavonols	Chromolith Performance RP-18e (100 × 4.6 mm), 2.5 mL/min, 25°C	20 min[b)]	[104]
Lemon oil	Coumarins	Chromolith Flash (25 × 4.6 mm), 4 mL/min[a)]	1 min[b)]	[105]
Rosemary leaf extract	Phenolic antioxidants	Chromolith Performance RP-18e (100 × 4.6 mm), 1.5 mL/min[a)]	10 min (3 compounds)	[106]
Traditional Chinese medicines	Phenolic antioxidants	Chromonolith Speed ROD (50 × 4.6 mm), 3 mL/min[a)]	5 min (5 compounds)	[107]
Propolis *G. biloba* Red wine Green tea	Flavanols Flavonols Flavanones	Chromolith Performance C18 (100 × 4.6 mm), 2 mL/min, 25°C	15 min (11 compounds)	[108]
Red cabbage	Anthocyanins	Chromolith Performance RP-18e (100 × 4.6 mm), 4 mL/min, 27°C	18 min (24 compounds)	[109]
Vanilla pods	Phenolic compounds	Chromolith RP-18e (100 × 4.6 mm), 2 mL/min, 25°C	2.5 min (4 target compounds)	[110]
Phenolic and flavone standards Beer Wines	Phenolic acids Phenolic alcohols Flavones Flavanones Flavonols Flavanols Benzoic aldehydes Coumarins Stilbenes	Chromolith Speed ROD RP-18e (50 × 4.6 mm), 2–4 mL/min 40°C or Chromolith Flash RP-18e (25 or 50 × 4.6 mm), 2–4 mL/min, 40 or 45°C	1–9 min	[111–113, 120, 121]
Must Wine	Stilbenes	2 × Chromolith Performance RP-18e (100 × 4.6 mm), 4–7 mL/min[a)]	20 min (4 target compounds)	[114]
Grapes Must	Phenolic acids Flavones	Chromolith Performance RP-18e (100 × 4.6 mm), 2–5 mL/min, 15–40°C	8 min (13 compounds)	[115]
Phenolic acids standards	Phenolic acids	Poly(styrene-divinylbenzene) or alkylated poly(styrene-divinylbenzene) monolithic capillary (250 or 335 × 0.10 mm)	2 or 10 min (3 or 5 target compounds)	[117]
Phenolic acids standards	Phenolic acids	Zwitterionic polymethacrylate monolithic capillary (149, 173 or 181 × 0.32 mm), 0.05 mL/min, 25–80°C or hybrid particle-monolithic polymethacrylate capillary	16–35 min (9 target compounds)	[118, 119]

Table 2. Continued.

Sample	Phenolic class(es)	Column type, flow rate and temperature	Analysis time (no. of compounds)	Reference
		(132–193 × 0.32 or 0.50 mm), 0.15–18.5 μL/min, ambient		
Thymus species	Catechins Phenolic acids Flavanones Flavones Flavonols	Ascentis Express C18 (50 × 2.1 mm, 2.7 μm), 0.2 mL/min, 50°C	15 min (15 compounds)	[122]
Cynara scolymus	Phenolic acids	Halo C18 (50 × 2.1 mm, 2.7 μm), 0.8 mL/min, 25°C	3.5 min (3 compounds)	[123]
Soybeans and derived products	Isoflavones	Kinetex C18 (100 × 4.6 mm, 2.6 μm), 2.7 mL/min, 50°C	5.8 min (12 compounds)	[124]
Mate extracts	Phenolic acids Xanthines	Ascentis Express C18 (150 × 4.6 mm, 2.7 μm), 4 mL/min, 45°C	50 min (21 compounds)	[125]

a) Analysis temperature is not specified.
b) Target analytes are not specified.

acids in a beer sample. In another recent study by the same group [119], hybrid particle–monolithic polymethacrylate columns for micro-HPLC were prepared by *in situ* polymerisation in fused silica capillaries pre-packed with 3–5 μm C18 and aminopropyl silica-bonded particles. The efficiency and permeability properties of the hybrid columns were generally intermediate between those of particle-packed and pure monolithic columns. Some columns provided good separations in comparison to conventional fully porous C18 and aminopropyl columns in the RP mode, whereas zwitterionic hybrid columns allowed good separations in shorter analysis times than either reference column in the HILIC mode. These columns have been employed in the analysis of phenolic acids and good separations were achieved.

Comparison of Tables 1 and 2 shows that UHPLC has found more application for phenolic analyses, and in general provides faster analyses than have been reported using monolithic columns. This is in part due to the inherent kinetic properties of these phases [41] coupled to the more widespread acceptance of UHPLC technology in applications laboratories and the fact that similar separations (in terms of selectivity) may be obtained using this approach, which facilitates method adaptation. However, monolithic columns have been extensively used in the second dimension of comprehensive 2-D LC analysis (see below). Monolithic columns have not yet been extensively applied for high-efficiency analysis of polyphenols, despite the intrinsic advantages of monoliths for these analyses.

3.1.2.2 Superficially porous stationary phases

Although a reduction in particle size provides numerous advantages in HPLC, the price to pay for increased performance is a decrease in column permeability. Superficially porous particles (also known as partially porous, pellicular or shell particles) have been the focus of intensive research in recent years as a means of optimally exploiting this compromise. These particles consist of a thin porous shell and a solid fused core, effectively providing shorter diffusion distances coupled with permeability values comparable to those of conventional 3 μm particles. This technology has been known for decades [126–128], but has been revisited with some success in the past years. It has been demonstrated in practice [17] that these columns provide chromatographic performance comparable to sub-2 μm phases, yet permeability values corresponding to the total particle size (i.e. typically ~2.7 μm), which allows their operation at optimal flow rates on conventional instrumentation. The low mass transfer resistance of these phases essentially provides similar advantages to sub-2 μm porous phases: higher efficiency per unit column length, higher optimal mobile-phase velocities and less efficiency loss for flow rates above the optimal value. A limited number of reports on the application of these phases for polyphenol analysis have appeared in recent years (Table 2).

Boros et al. [122] recently described an HPLC-MS method based on a 2.7 μm Ascentis Express C18 superficially porous column and acidified aqueous–methanol mobile phases for the simultaneous determination of catechins, phenolic acids, flavanones, flavones and flavonols in *Thymus* plant species. This method allowed the characterisation of 15 phenolic compounds in 15 min. Shen et al. [123] developed a rapid RP method for the analysis and quantification of caffeoylquinic acid derivatives in artichoke heads and leaf extracts using a 2.7 μm Halo C18 superficially porous column and acidified aqueous–acetonitrile mobile phases. Manchón et al. [124] also reported a method for the analysis of isoflavones using a 2.6 μm Kinetex C18 superficially porous column to achieve the separation of 12 target isoflavones in less than 6 min. Dugo *et al.* reported the

Table 3. Recent applications of multi-dimensional LC methods for the analysis of phenolic compounds

Sample(s)	Compound class(es)	Mode	First-dimension column	Second-dimension column	Interface	Modulation time (min)	Total analysis time	Peak capacity (n_p)	Reference
M. ilicifolia leaves	Flavonol glycosides	Heart cutting	Waters Ultrahydrogel 120 (300 × 7.8 mm), 60°C	SupelCosil LC-18 (250 × 4.6 mm, 5 μm), 60°C	Fraction collection	19	n.r.[a)]	n.r.[a)]	[134]
Phenolic and flavone standards Beer Wine	Phenolic acids	On-line and heart-cutting stop-flow	Purospher Star RP-18e (125 × 4.0 mm, 5 μm) or (250 × 4.6 mm, 5 μm)	Two parallel Zr carbon columns (50 × 2.1 mm, 5 μm), 120°C	6-Port valve	3	80 min	n.r.[a)]	[143]
Phenolic and flavone standards Beer Red wine	Phenolic acids Phenols Flavones Flavanols Flavonols Flavanones	On-line	Discovery HS PEG (150 × 2.1 mm, 5 μm)	Chromolith Speed ROD RP-18e (50 × 4.6 mm), 40°C	10-Port valve	2	140 min	n.r.[a)]	[111]
Phenolic and flavonoid standards Beer	Phenolic acids Flavonols Flavanols Benzoic aldehydes Coumarins	On-line	A single Discovery HS PEG (150 × 4.6 mm, 5 μm), 40°C or serially coupled Discovery HS PEG (150 × 4.6 mm, 5 μm) and ACE 3 C18 (100 × 2.1 mm, 3 μm), 40°C	Chromolith Speed ROD RP-18e (50 × 4.6 mm), 40°C, or Discovery Zr-carbon (50 × 2.1 mm), 120°C, or Purospher STAR RP-18e (150 × 4.6 mm), 40°C	10-Port valve	1,5,6 or 9	n.r.[a)]	n.r.[a)]	[112]
Polyphenolic standards Wines	Phenolic acids Phenolic alcohols Flavones Flavanones Flavonols Stilbenes Coumarins	On-line	Ascentis Phenyl (250 × 1.0 mm, 5 μm), 25°C	Ascentis Express C18 (30 × 4.6 mm; 2.7 μm), or Chromolith Flash RP-18e (25 or 50 × 4.6 mm), 45°C	10-Port valve	2	80 min	386–516[b),c)]	[113, 120]
Phenolic and flavone standards Beer	Phenolic acids Flavones Flavanones Flavonols Flavanols	On-line	Discovery HS PEG (150 × 2.1 mm, 5 μm), 40°C	Ascentis Express C18 (30 × 4.6 mm; 2.7 μm), or Chromolith Flash RP-18e (25 or 50 × 4.6 mm), 40°C	10-Port valve	1, 2 or 4	70, 140 or 280 min	n.r.[a)]	[121]
Phenolic and flavone standards	Phenolic acids Flavones Flavanones Flavonols Flavanols Coumarins	On-line	Discovery HS PEG (150 × 2.1 mm, 5 μm), 40°C	Ascentis Express C18 (30 × 3 mm; 2.7 μm), 60°C	10-Port valve	0.417, 2	30 or 140 min	280[b),d)]	[129]

Table 3. Continued.

Sample(s)	Compound class(es)	Mode	First-dimension column	Second-dimension column	Interface	Modulation time (min)	Total analysis time	Peak capacity (n_p)	Reference
Phenolic and flavone standards	Phenolic acids Flavonols Flavanols Flavones Flavanones Benzoic aldehydes Coumarins	On-line	Discovery HS PEG (150 × 2.1 mm, 5 μm), 40°C	Purospher STAR RP-18e (30 × 4.0 mm), 40°C	10-Port valve	2	140 min	n.r.[a]	[130]
Phenolic and flavone standards	Phenolic acids Flavonols Flavanols Flavones Flavanones Benzoic aldehydes Coumarins	On-line	Discovery HS PEG (150 × 2.1 mm, 5 μm), 40°C	Ascentis Express C18 (30 × 3.0 mm, 2.7 μm), or Kinetex C18 (50 × 3.0 mm, 2.7 μm), 50°C	10-Port valve	0.42–2	30–150 min	n.r.[a]	[131]
Mate extracts (medicinal plant)	Phenolic acids Flavanols Xanthines Flavonol glycosides	On-line	RP-Amide column (250 × 1.0 mm, 5 μm), 25°C	Ascentis Express C18 (30 × 4.6 mm; 2.7 μm), 40°C	10-Port valve	2	70 min	503[b),d)]	[125]
Phenolic and flavone standards Beer Wines	Phenolic acids Phenolic alcohols Flavones Flavanones Flavonols Stilbenes Coumarins	On-line	Various columns	Various columns	10-Port valve	1,3,6,7 or 8	150–200 min	n.r.[a]	[141]
Phenolic antioxidant standards		On-line	Zorbax-SB C18 (150 × 0.5 mm, 5 μm), 40°C	Two parallel Zr carbon columns (50 × 2.1 mm, 5 μm), 120°C	10-Port valve	3	85 min	n.r.[a]	[142]
Lemon oil Orange oil Citrus oil	Psoralens Flavones	On-line	Thermo Electron Diol (250 × 1 mm, 5 μm), 30°C	Zorbax C18 (50 × 4.6 mm, 3.5 μm), 30°C	10-Port valve	1	90 min	453[b),c)]	[144]
Lemon oil	Coumarins Psoralens	On-line	Thermo electron Diol (250 × 1 mm, 5 μm), 30°C	2 × Zorbax C18 (50 × 4.6 mm, 3.5 μm), 30°C	2 × 10-Port valves	2	90 min	1095[b),c)]	[145]
Phenolic acid standards Wines Juices	Phenolic acids	On-line	Various columns	Various columns	10-Port valve	1.5 and 2	51 min	330–616[b),d)]	[146]
Wines Fruit juices	Phenolic acids Flavanols Flavonols	On-line	Atlantis C18 (150 × 2.1 mm, 3 μm), 40°C	XBridge (50 × 3 mm, 2.5 μm) with an ion-pair reagent, 40°C	10-Port valve	2	70 min	572[b),d)]	[147]

Table 3. Continued.

Sample(s)	Compound class(es)	Mode	First-dimension column	Second-dimension column	Interface	Modulation time (min)	Total analysis time	Peak capacity (n_p)	Reference
Lamiaceae herbs	Phenolic acids	On-line	Atlantis C18 (150 × 2.1 mm, 3 μm), 35°C	Ultrasphere CN (75 × 4.6 mm, 3 μm), 45°C	10-Port valve	0.5–1	60 min	735[b),d)]	[148]
Cocoa extract Apple extract Green tea extract	Proanthocyanidins Phenolic acids Flavonols	Off-line	Develosil diol (250 × 1.0 mm, 5 μm), ambient	Zorbax-SB C18 (50 × 4.6 mm, 1.8 μm), 50°C	Fraction collector	30	1350 min	2493–3512[b),c)] 2334–3137[b),e)]	[94, 95]
Phenolic and flavone standards Green tea extract	Phenolic acids Flavones Flavanols Flavonols Flavanones	Off-line	MEKC	Discovery HS PEG (50 × 2.1 mm, 5 μm), 40°C	6-Port valve	2	630 min	450[b),d)]	[151]
Phenolic standards Beer Hop extract	Phenolic acids Flavanones Flavanols Coumarins	Stop-flow	Discovery HS PEG (50 × 2.1 mm, 3 μm)	Purospher STAR RP-18e (125 × 2.0 mm)	6-Port valve	17	n.r.[a)]	n.r.[a)]	[150]

a) Not reported.
b) Calculated according to [154].
c) Calculated according to Liu *et al.* [153].
d) $n_T = n_1 \times n_2$.
e) Calculated according to Li *et al.* [152].

analysis of mate extracts on a 150 mm Ascentis Express column, obtaining a peak capacity of 195 for a 50-min gradient [125]. Similar advantages to UHPLC were observed for these analyses in terms of sensitivity, resolution and speed (reduction in analysis times by up to a factor of 10 compared with conventional HPLC). Importantly, these advantages were achieved on conventional HPLC instrumentation [123, 124].

Due to their innate properties, superficially porous phases have also been utilised in comprehensive two-dimensional chromatography (LC × LC) separation of phenolics (Table 3). For instance, Jandera and co-workers [121, 129, 130] employed an 2.7 μm Ascentis Express C18 column in the second dimension for LC × LC separation of phenolic and flavone antioxidants, reporting good separations in less than 2 min. In a more recent study, the same authors [131] developed a series of LC × LC systems with various gradient types in the second dimension using two superficially porous columns (Ascentis Express and Kinetex). These columns provided rapid, highly efficient separations, with the analysis times ranging between 0.42 and 2 min. The Ascentis Express column has also been employed in the second dimension for the LC × LC characterisation of phenolic compounds in wine samples [113, 120] and a mate extract [125].

3.2 Multi-dimensional LC in phenolic analysis

Clearly, advances in column design and instrumentation have greatly improved the performance of uni-dimensional LC analyses. In the application of these techniques for phenolic analysis, the focus of most literature reports is on exploiting the benefits of UHPLC, HTLC and new column formats for high-throughput analysis. Therefore, similar or slightly improved resolution is obtained compared with conventional HPLC methods, but much faster. Use of these techniques for improved resolution has received much less attention, despite the evidence of fundamental studies indicating the potential of each of these technologies for improving efficiency compared with conventional HPLC. However, efficiency gains in 1-D LC remain relatively minor. For example, long UHPLC and monolithic columns may be used to obtain efficiencies of up to 100 000 theoretical plates in reasonable analysis times. Under gradient conditions, this translates into a peak capacity gain of a factor 2 (due to the dependence of peak capacity on the square root of the number of theoretical plates). Compared with conventional RP-LC methods, which typically deliver peak capacities in the region of 100–150, this implies that peak capacities in the region of 300 may be obtained using these techniques. Taking into account that the peak capacity of a separation should be significantly larger than the number of randomly distributed compounds to be separated [132], coupled to the known complexity of natural phenolics [37], it is clear that this resolving power remains entirely insufficient for the analysis of the large numbers of phenolic compounds encountered in natural products.

Multi-dimensional, and in particular comprehensive multi-dimensional LC methods represent an alternative strategy capable of providing much higher peak capacities. In a multi-dimensional separation, two or more separation mechanisms are combined to improve resolution [133]. This may be done for only a fraction of the sample which is of interest, using heart-cutting 2-D LC. An example of this approach applied to phenolic analysis was reported by de Souza et al. [134]. These authors achieved good separation of flavonol glycosides in *Maytenus ilicifolia* plant extracts using off-line heart-cutting 2-D LC-MS combining size exclusion chromatography (SEC) in the first dimension and RP-LC in the second dimension. In this system, fractions from the first dimension were automatically collected and pre-concentrated prior to re-injection on the second-dimension column. High resolution was obtained, and with the help of MS detection a large number of flavonol glycosides (including some new compounds) could be identified.

In LC × LC, as opposed to 2-D LC, each part of the sample is subjected to two different separations. In principal, provided the first-dimension separation is essentially maintained and the two separation mechanisms are orthogonal, the resolving power (peak capacity) of an LC × LC is the product of peak capacities in each dimension [133, 135–137]. In this manner, peak capacities in the region of a few thousand may be obtained, rendering this technique ideally suited to the analysis of complex samples. It is therefore not surprising that since the pioneering study of Erni and Frei [138] in 1978, a large number of LC × LC systems for the analysis of complex real-life samples, particularly in the areas of food and beverages [139, 140] and biomedical research [133] have been developed. Especially during the last 5 years, LC × LC has also extensively been applied for the analysis of complex phenolic samples (Table 3).

LC × LC separations may be performed in three different ways: on-line, off-line or stop-flow modes. In on-line LC × LC, fractions from the first dimension are sequentially transferred to the second dimension for subsequent analysis. Switching valves equipped with sampling loops or trapping columns are generally used as interfaces to alternately trap fractions from the first dimension at defined time intervals (the sampling rate). Off-line LC × LC involves collection of fractions from the first dimension, which are subsequently injected on the second-dimension column. In the stop-flow mode, the two columns are coupled without trapping or sampling loops. Following transfer of a specific fraction from the primary to the second-dimension column, the flow in the first dimension is stopped, whereas separation in the second dimension is completed. This process is repeated for the duration of the first-dimension separation. Off-line LC × LC requires very long analysis times (roughly equal to the product of the number of first-dimension fractions and the second-dimension analysis time), but provides the highest

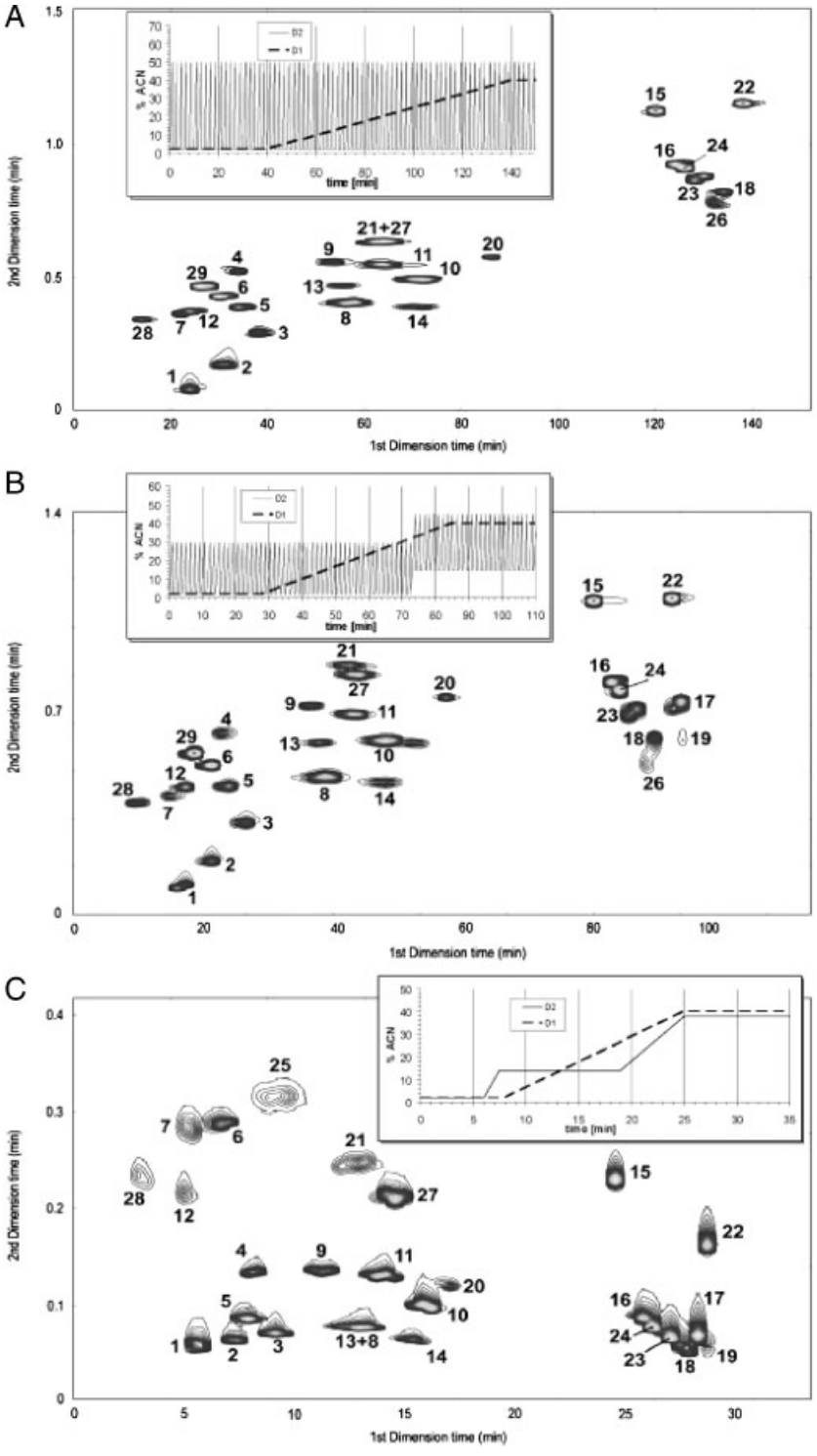

Figure 4. UV contour plots for the LC × LC separation of phenolic acid and flavone standards obtained using full-in-fraction (A), segment-in-fraction (B) and continuously shifting (C) parallel gradients in the second dimension. A PEG column was employed in the first dimension, whereas an Ascentis Express C18 column was used in the second dimension. Reproduced from [131] with permission from Wiley-VCH Verlag GmbH & Co. KGaA.

overall peak capacity. Analysis times for on-line LC × LC are similar to 1-dimensional analyses, although the peak capacity is generally less than can be achieved by the off-line approach. The stop-flow method is characterised by analysis times and peak capacities intermediate between on- and off-line approaches.

Numerous on-line LC × LC systems have been described for phenolic analysis. Mondello and co-workers [112, 113, 121, 141–143] have developed a number of on-line LC × LC methods for the analysis of phenolic acids and/or flavonoid antioxidants. These authors used the combinations of single or serially coupled polyethylene glycol (PEG),

phenyl and C18 columns in the first dimension and single or two parallel monolithic C18 or Zr carbon columns in the second dimension. The applicability of these methods was demonstrated for beer and wine samples. By using two parallel columns in the second dimension, the second-dimension separation could be improved to provide better resolution [142, 143]. Jandera and co-workers [131] compared the use of different gradients in the second dimension of an on-line LC × LC for the separation of phenolic acid and flavonoid standards. Continuously shifting, full-in-fraction and segment-in-fraction gradient were each found to have advantages and disadvantages in terms of maximum coverage of the 2-D plane, peak width and risk of wraparound (Fig. 4).

François et al. [144] developed a LC × LC method combining normal-phase LC (NP-LC) and RP-LC for the analysis of psoralens and flavones in citrus oil. In this study, a microbore diol column with a hexane/ethyl acetate mobile phase was employed in the first dimension, whereas a C18 column with water–acetonitrile mobile phases was used in the second dimension. Good separations were achieved in less than 1 min in the second dimension using a monolithic column. A peak capacity of 453 was measured for the LC × LC system, compared with the individual 1-D peak capacities of 46 and 15 calculated for the first and second dimensions, respectively. In a subsequent report [145], the same authors used an additional 10-port valve and two parallel 3.5 μm fully porous columns in the second dimension to allow longer analysis times in the second dimension. The benefit of this set-up was demonstrated by an enhanced peak capacity of 1095 for the same sample.

Kivilompolo et al. [146, 147] reported an on-line RP-LC × RP-LC method using ion-pair chromatography in the second dimension for the analysis of phenolic acids and monomeric procyanidins in wines and juices. A relatively low retention-time correlation was measured between these methods, and theoretical peak capacities in excess of 300 were obtained. In another study, the same group [148] described an on-line RP-LC × RP-LC method for quantitative analysis of phenolic acids in *Lamiaceae* herbs. A C18 column was coupled to a cyano column in this instance and theoretical peak capacities as high as 735 were reported. Dugo et al. [113] used a microbore phenyl column in the first dimension coupled to a monolithic or superficially porous C18 column in the second dimension for the on-line comprehensive LC × LC analysis of standards and red wine phenolics. Although low practical peak capacities (compared with the theoretical values) were measured for this system due to high correlation ($r^2 > 0.8$) between the selected separation mechanisms, these values (386–516) are still much higher than those that can be achieved by 1-D LC. In a recent report, Dugo et al. [125] used an RP-amide column in the first dimension and a partially porous C18 column in the second dimension for the LC × LC separation of phenolic compounds in a mate extract. A highly efficient separation was obtained, with a theoretical peak capacity of 503, which represents a significant gain compared with a value of 195 obtained on a 150 mm 2.7 μm superficially porous phase for the same sample.

Although on-line LC × LC provides the advantages of speed, automation, less risk of sample loss and/or alteration and better reproducibility [15, 137, 138], off-line LC × LC offers the benefit of longer second-dimension analyses, and

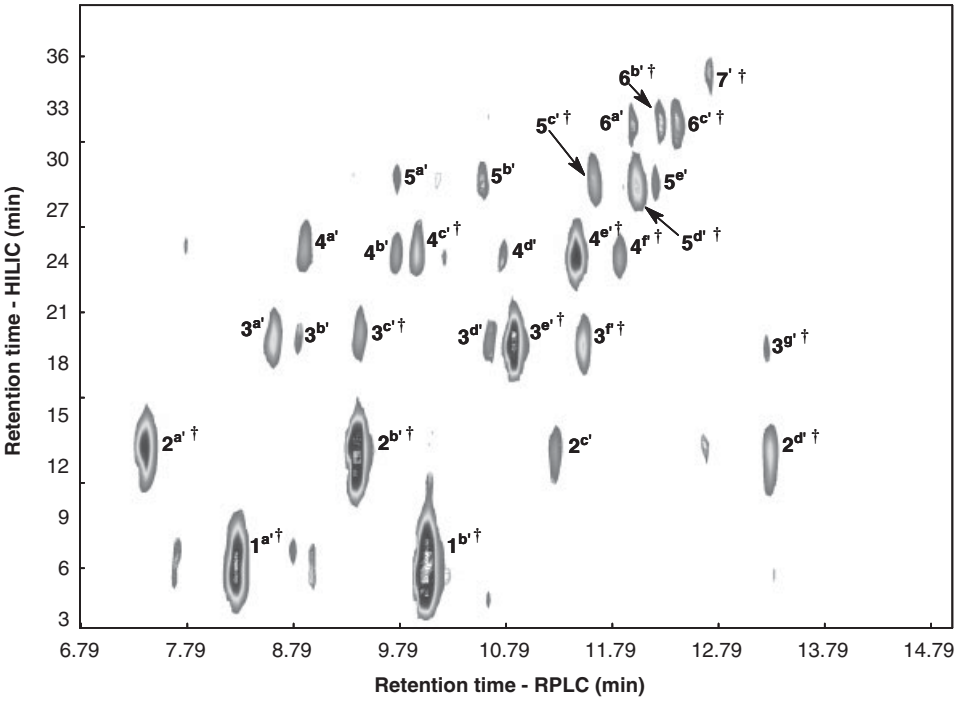

Figure 5. A fluorescence contour plot obtained for the off-line HILIC × RP-LC analysis of apple procyanidins. HILIC separation was performed on a 250 × 1 mm Diol column at a flow rate of 0.05 mL/min. Briefly, 1-min fractions were collected and injected onto two 50 × 4.6 mm 1.8 μm C18 columns operated at 50°C and 0.8 mL/min in the second dimension. Peak labels correspond to degree of polymerisation for procyanidin isomers as identified by ESI-MS. Reproduced from [94] with permission from Elsevier.

therefore higher overall resolving power at the cost of longer analysis times. Kalili and de Villiers [94, 95] developed an off-line 2-D LC method combining HILIC and RP-LC for the analysis of phenolic compounds in cocoa, apple and green tea extracts (Fig. 5). This approach proved suitable for the analysis of a wide range of analytes, including procyanidins, proanthocyanidins, flavonols and glycosylated derivatives. These 2-D systems offered practical peak capacities in excess of 3000, which far exceeds the peak capacities reported for most on-line systems (<1000).

Compared with the off-line approach, stop-flow LC × LC provides the benefits of complete automation and less risk of sample alteration. Stop-flow LC × LC also allows the use of longer analysis time in the second dimension and hence improved peak capacities compared with on-line LC × LC. The drawbacks of the technique include long analysis times (similar to off-line LC × LC) and the risk of excessive band broadening in the first dimension [149]. Stop-flow LC × LC has also been applied to phenolic analysis. In a preliminary study, Blahová et al. [150] considered the combinations of octadecyl (C18), pentafluorophenylpropyl (F5) and PEG silica-based columns for the separation of phenolic standards. Retention of these compounds on the C18 and F5 columns was found to be strongly correlated ($r^2 = 0.999$), which was not the case for the C18 and PEG columns ($r^2 = 0.657$). It was also established that serial coupling of the PEG and C18 columns provided improved resolution for compounds that were not well separated on single columns. In the optimised stop-flow LC × LC set-up, a PEG column was coupled to a C18 column in the second dimension using a 6-port valve as the interface. A 19-min gradient was used in the second dimension to achieve good separations of 14 phenolic antioxidants. In a subsequent study [143], the same group used a C18 column in the first dimension and a Zr carbon column in the second dimension and a heart-cutting stop-flow approach for the separation of phenolic standards. The effects of both temperature and solvent gradients on the separation were assessed. It was concluded that on Zr columns temperature programming in combination with isocratic elution could be used as an alternative to solvent gradients. This did not lead to significant loss of resolution and importantly saved the time required for column re-equilibration when performing solvent gradient separations.

LC may also be combined with alternative separation methods. For example, Cesla et al. [151] recently reported an interesting off-line 2-D method combining LC and micellar electrokinetic capillary chromatography (MEKC) for the analysis of 25 phenolic acids and flavone standards. In this set-up, fractions from the first-dimension HPLC column (Discovery HS PEG) were automatically collected using a CE autosampler, which was programmed to rotate every 15 s. The collected fractions were subsequently analysed by MEKC using a background electrolyte containing 25 mM borate buffer (pH 9.05), 10 g/L SDS and 1.85 g/L heptakis(6-*O*-sulfo)-β-CD on a 48 cm capillary. The authors calculated a practical peak capacity of 450 for this set-up, which is almost double that of the on-line LC × LC system previously developed by the same authors [129].

As summarized in Table 3, LC × LC methods effectively provide much higher resolving power than even optimised 1-D methods. This is especially true for off-line LC × LC methods although this performance is obtained at the cost of very long analysis times. On-line LC × LC has found much wider application for phenolic analysis. Analysis times for these methods are comparable to conventional 1-D LC methods although not to optimised UHPLC or HTLC methods. Due to the inherent compromise between sampling rate and second-dimension peak capacity, the performance of on-line LC × LC is invariably lower than equivalent off-line methods, yet this performance remains much larger than that which can be achieved using a single column, and also offers complete automation. Stop-flow LC × LC has been less applied for phenolic compounds, and typically offers analysis times and peak capacities intermediate between the on- and off-line approaches.

A word of caution should be mentioned relating to the interpretation of peak capacities reported for LC × LC methods. These values are calculated in any one of the variety of ways, varying between reporting theoretical peak capacities based on the multiplication rule (which is never met in real-life systems), to methods used to take into account first-dimension under-sampling [152], orthogonality [153] or both of these phenomena. This means that often the reported performance does not accurately reflect the experimental gain in resolution, and objective comparison of different methods is thereby complicated.

The design and implementation of LC × LC is also rather complicated, requiring as it does the consideration of a wide range of experimental parameters such as column dimensions, flow rates, mobile-phase compatibility, *etc.* Coupled to the instrumental complexity (and cost) of especially on-line LC × LC, this means that practical implementation of the technique is far from straightforward in a routine environment. Moreover, LC × LC produces complex and relatively large data sets (especially when used in combination with MS), which complicates data analysis and quantitative analysis. For these reasons, despite the obvious advantages of the technique, LC × LC will remain in the foreseeable future primarily a research tool. In this context, it is also worth revisiting Giddings' concept of sample dimensionality [132], which implies that the application of multi-dimensional separation methods only makes sense for samples containing compounds of more than one chemical characteristic. Fortunately or unfortunately, however, most natural phenolic fractions consist of a wide range of compounds, and as a result, multi-dimensional chromatographic methods will certainly play a significant role in future phenolic research.

4 Concluding remarks

This review was aimed at presenting an overview of the recent applications of advances in HPLC for polyphenol

analysis. From the reports cited herein, a few general conclusions may be reached.

First of all, the recent trend in HPLC of a reduction in particle size, coupled to increases in operating pressure, has also found beneficial application in the analysis of phenolics. The most important advantage of this approach, as applied in the literature reports, is one of the increased throughput. In addition, separation efficiency and sensitivity may be improved, and in general solvent consumption is largely reduced. Together with the known benefits of RP-LC which remain applicable, such as robust columns and a well-understood separation mechanism, this renders the methodology ideally suited for routine analysis, and it is expected that UHPLC will find increased application in the field of polyphenol analysis in the near future.

The use of elevated temperature in HPLC offers very similar advantages to those of UHPLC. The reduction in mobile-phase viscosity associated with higher temperatures has as primary advantage faster analysis, while organic solvent consumption may also be reduced. As such, HTLC is, in many ways, complementary to UHPLC and is often applied in conjunction with smaller particle-packed phases. However, certain constraints apply to the use of high temperature for phenolic analysis. Most important of these are the concerns regarding analyte stability, which needs further investigation (although initial investigations indicate that this aspect is of less importance than commonly believed to be). In any case, it seems likely that the benefits of temperature for polyphenol analysis will be limited to a fairly modest range (i.e. below 100°C) in the near future. In addition, instrumental constraints and the need for suitably stable stationary phases currently limit the widespread application of HTLC, even if on-going developments in these fields will surely facilitate the future application of the technique.

Monolithic columns have been used extensively for the fast analysis of phenolics, although based on the available literature for the current generation of phases, the UHPLC approach provides better performance for this purpose. Nevertheless, the use of monolithic columns, due to their inherent compatibility with high flow rates, holds particular promise for application in LC × LC. Superficially porous particles, on the other hand, offer excellent kinetic properties, which make them an attractive alternative to fully porous particles for fast and efficient HPLC separations. It is envisioned that future research will extend the application of these phases for polyphenol analysis to exploit these advantages.

The high resolution offered by comprehensive LC methods has also, in recent years, found the application for phenolic analysis. Despite the fact that this performance comes at the price of instrumental complexity or analysis time [149], without doubt LC × LC will play an increasingly important role in the future investigation of complex phenolic samples.

It should be noted in conclusion that HPLC separation constitutes only part of the analysis of polyphenols. Sample pre-treatment is especially relevant for phenolic analysis, as this step influences the demands placed on chromatographic separation. Often, extensive pre-fractionation of natural extracts may serve to simplify the analysis of specific groups of phenolics. In addition, the modern trend of the application of MS as detection technique in polyphenol analysis is expected to continue. Apart from the obvious power of MS for identification purposes, MS/MS methods continue to find extensive application for target analysis of selected phenolics, in this instance greatly simplifying the demands placed on chromatographic separation. Finally, other techniques such as gas chromatography and especially capillary electrophoresis are also applied for phenolic separation, and the developments in these fields are ongoing.

The authors gratefully acknowledge Stellenbosch University, the Third World Academy of Science (TWAS, 08-077 RG/CHE/AF/AC), the International Foundation of Science, Stockholm, Sweden (IFS, F/4904-1), the National Research Foundation (NRF, South Africa) and SASOL for financial support.

The authors have declared no conflict of interest.

5 References

[1] Schieber, A., Keller, P., Carle, R., *J. Chromatogr. A* 2001, *910*, 265–273.

[2] Sun, B., Leandro, M. C., de Freitas, V., Spranger, M. I., *J. Chromatogr. A* 2006, *1128*, 27–38.

[3] Yanagida, A., Kanda, T., Takahashi, T., Kamimura, A., Hamazono, T., Honda, S., *J. Chromatogr. A* 2000, *890*, 251–259.

[4] Yanagida, A., Murao, H., Ohnishi-Kameyama, M., Yamakawa, Y., Shoji, A., Tagashira, M., Kanda, T., Shindo, H., Shibusawa, Y., *J. Chromatogr. A* 2007, *1143*, 153–161.

[5] Tucker, G., Robards, K., *Crit. Rev. Food Sci. Nutr.* 2008, *48*, 929–966.

[6] Barbosa, D. S., *J. Consum. Protect. Food Safety* 2007, *2*, 407–413.

[7] Manach, C., Scalbert, A., Morand, C., Remesy, C., Jimenez, L., *Am. J. Clin. Nutr.* 2004, *79*, 727–747.

[8] Valls, J., Millán, S., Martí, M. P., Borràs, E., Arola, L., *J. Chromatogr. A* 2009, *1216*, 7143–7172.

[9] Hümmer, W., Schreier, P., *Mol. Nutr. Food Res.* 2008, *52*, 1381–1398.

[10] Abad-García, B., Berrueta, L. A., Garmón-Lobato, S., Gallo, B., Vicente, F., *J. Chromatogr. A* 2009, *1216*, 5398–5415.

[11] Wu, N., Clausen, A. M., *J. Sep. Sci.* 2007, *30*, 1167–1182.

[12] Heinisch, S., Rocca, J.-L., *J. Chromatogr. A* 2009, *1216*, 642–658.

[13] Teutenberg, T., *High-Temperature Liquid Chromatography: A User's Guide for Method Development,* The Royal Society of Chemistry, Cambridge, UK 2010.

[14] François, I., Sandra, K., Sandra, P., *Anal. Chim. Acta* 2009, *641*, 14–31.

[15] Dugo, P., Cacciola, F., Kumm, T., Dugo, G., Mondello, L., *J. Chromatogr. A* 2008, *1184*, 353–368.

[16] Guiochon, G., *J. Chromatogr. A* 2007, *1168*, 101–168.

[17] Gritti, F., Leonardis, I., Abia, J., Guiochon, G., *J. Chromatogr. A* 2010, *1217*, 3819–3843.

[18] Macheix, J.-J., Fleuriet, A., Billot, J., *Fruit Phenolics*, CRC Press, Inc., Florida, USA 1990.

[19] Santos-Buelga, C., Scalbert, A., *J. Sci. Food Agric.* 2000, *80*, 1094–1117.

[20] Gu, L., Kelm, M. A., Hammerstone, J. F., Zhang, Z., Beecher, G., Holden, J., Haytowitz, D., Prior, R. L., *J. Mass Spectrom.* 2003, *38*, 1272–1280.

[21] Ribereau-Gayon, P., *Plant Phenolics*, Hafner Publishing Company, Inc., New York 1972.

[22] Andres-Lacueva, C., Medina-Remon, A., Llorach, R., Mireia, U.-S., Khan, N., Chiva-Blanch, G., Zamora-Ros, R., Rotches-Ribalta, M., Lamuela-Raventos, R. M., in: de la Rosa, L. A., Alavarez-Parrilla, E., Gonzalez-Aguilar, G. A. (Eds.), *Fruit and Vegetable Phytochemicals. Chemistry, Nutritional Value and Stability*, Blackwell Publishing, Iowa, USA 2010.

[23] Stafford, H. A., *Phytochemistry* 1988, *27*, 1–6.

[24] Willför, S. M., Smeds, A. I., Holmbom, B. R., *J. Chromatogr. A* 2006, *1112*, 64–77.

[25] Corder, R., Mullen, W., Khan, N. Q., Marks, S. C., Wood, E. G., Carrier, M. J., Crozier, A., *Nature* 2006, *444*, 566.

[26] García-Marino, M., Rivas-Gonzalo, J. C., Ibáñez, E., García-Moreno, C., *Anal. Chim. Acta* 2006, *563*, 44–50.

[27] Lunder, T. L., in: Mou-Tang, H., Chi-Tang, H., Lee, C. Y. (Eds.), *Phenolic Compounds in Food and Their Effects on Health II*, American Chemical Society, New York 1992, pp. 114–120.

[28] Jeong, W.-S., Kong, A.-N., *Pharm. Biol.* 2004, *42*, 84–93.

[29] Ramljak, D., Romanczyk, L. J., Metheny-Barlow, L. J., Thompson, N., Knezevic, V., Galperin, M., Ramesh, A., Dickson, R. B., *Mol. Cancer Ther.* 2005, *4*, 537–546.

[30] Kao, T. H., Wu, W. M., Hung, C. F., Wu, W. B., Chen, B. H., *J. Agric. Food Chem.* 2007, *55*, 11068–11079.

[31] Zhang, E. J., Ng, K. M., Luo, K. Q., *J. Agric. Food Chem.* 2007, *55*, 6940–6950.

[32] Stalikas, C. D., *J. Sep. Sci.* 2007, *30*, 3268–3295.

[33] Wollgast, J., Anklam, E., *Food Res. Int.* 2000, *33*, 423–447.

[34] Pati, S., Losito, I., Gambacorta, G., La Notte, E., Palmisano, F., Zambonin, P. G., *J. Mass Spectrom.* 2006, *41*, 861–871.

[35] Gómez-Alonso, S., García-Romero, E., Hermosín-Gutiérrez, I., *J. Food Comp. Anal.* 2007, *20*, 618–626.

[36] Dell'Agli, M., Busciala, A., Bosisio, E., *Cardiovasc. Res.* 2004, *63*, 593–602.

[37] Strack, D., Wray, V., in: Harborne, J. B. (Ed.), *The Flavonoids*, Chapman & Hall, London, UK 1994.

[38] MacNair, J. E., Lewis, K. C., Jorgenson, J. W., *Anal. Chem.* 1997, *69*, 983–989.

[39] MacNair, J. E., Patel, K. D., Jorgenson, J. W., *Anal. Chem.* 1999, *71*, 700–708.

[40] de Villiers, A., Lestremau, F., Szucs, R., Gélébart, S., David, F., Sandra, P., *J. Chromatogr. A* 2006, *1127*, 60–69.

[41] Desmet, G., Cabooter, D., Gzil, P., Verelst, H., Mangelings, D., Heyden, Y. V., Clicq, D., *J. Chromatogr. A* 2006, *1130*, 158–166.

[42] Antia, F. D., Horvath, C., *J. Chromatogr.* 1988, *435*, 1–15.

[43] Chen, H., Horvath, C., *J. Chromatogr. A* 1995, *705*, 3–20.

[44] Touriño, S., Fuguet, E., Jáuregui, O., Saura-Calixto, F., Cascante, M., Torres, J. L., *Rapid Commun. Mass Spectrom.* 2008, *22*, 3489–3500.

[45] Spácil, Z., Nováková, L., Solich, P., *Food Chem.* 2010, *123*, 535–541.

[46] Pongsuwan, W., Bamba, T., Harada, K., Yonetani, T., Kobayashi, A., Fukusaki, E., *J. Agric. Food Chem.* 2008, *56*, 10705–10708.

[47] Guillarme, D., Casetta, C., Bicchi, C., Veuthey, J.-L., *J. Chromatogr. A* 2010, *1217*, 6882–6890.

[48] Serra, A., Maciá, A., Romero, M.-P., Salvadó, M.-J., Bustos, M., Fernández-Larrea, J., Motilva, M.-J., *J. Chromatogr. B* 2009, *877*, 1169–1176.

[49] Marti, M.-P., Pantaleo, A., Rozek, A., Soler, A., Valls, J., Macia, A., Romero, M.-P., Motilva, M.-J., *J. Sep. Sci.* 2010, *33*, 2841–2853.

[50] Robles-Sardin, A. E., Bolanos-Villar, A. V., Gonzalez-Aguilar, G. A., De la Rosa, L. A., in: Laura, A d. l. R., Emilio, A.-P., Gustavo, A. G.-A. (Eds.), *Fruit and Vegetable Phytochemicals: Chemistry, Nutritional Value And Stability*, Blackwell Publishing, Singapore 2010, pp. 155–175.

[51] Pratt, D. E., *Phenolic, Sulfur, and Nitrogen Compounds in Food Flavors*, American Chemical Society, Washington, DC 1976, pp. 1–13.

[52] Klejdus, B., Vacek, J., Benesova, L., Kopecky, J., Lapcik, O., Kuban, V., *Anal. Bioanal. Chem.* 2007, *389*, 2277–2285.

[53] Klejdus, B., Vacek, J., Lojková, L., Benesová, L., Kubán, V., *J. Chromatogr. A* 2008, *1195*, 52–59.

[54] Du, G., Zhao, H. Y., Zhang, Q. W., Li, G. H., Yang, F. Q., Wang, Y., Li, Y. C., Wang, Y. T., *J. Chromatogr. A* 2010, *1217*, 705–714.

[55] Deng, X., Gao, G., Zheng, S., Li, F., *J. Pharm. Biomed. Anal.* 2008, *48*, 562–567.

[56] Wang, Y., Yao, Y., An, R., You, L., Wang, X., *J. Chromatogr. B* 2009, *877*, 1820–1826.

[57] Oleszek, W., Stochmal, A., Janda, B., *J. Agric. Food Chem.* 2007, *55*, 8095–8100.

[58] Kapusta, I., Janda, B., Szajwaj, B., Stochmal, A., Piacente, S., Pizza, C., Franceschi, F., Franz, C., Oleszek, W., *J. Agric. Food Chem.* 2007, *55*, 8485–8490.

[59] Brouillard, R., Delaporte, B., *J. Am. Chem. Soc.* 1977, *99*, 8461–8468.

[60] Brouillard, R., Dubois, J.-E., *J. Am. Chem. Soc.* 1977, *99*, 1359–1364.

[61] Melander, W. R., Lin, H. J., Jacobson, J., Horváth, C., *J. Phys. Chem.* 1984, *88*, 4527–4536.

[62] de Villiers, A., Cabooter, D., Lynen, F., Desmet, G., Sandra, P., *J. Chromatogr. A* 2009, *1216*, 3270–3279.

[63] de Villiers, A., Kalili, K. M., Malan, M., Roodman, J., *LC-GC Eur.* 2010, *23*, 466–478.

[64] Arapitsas, P., Sjöberg, P. J. R., Turner, C., *Food Chem.* 2008, *109*, 219–226.

[65] Pati, S., Liberatore, M. T., Gambacorta, G., Antonacci, D., La Notte, E., *J. Chromatogr. A* 2009, *1216*, 3864–3868.

[66] Arraez-Roman, D., Fu, S., Sawalha, S. M. S., Segura-Carretero, A., Fernandez-Gutierrez, A., *Electrophoresis* 2010, *31*, 2289–2296.

[67] Li, X., Xiong, Z., Ying, X., Cui, L., Zhu, W., Li, F., *Anal. Chim. Acta* 2006, *580*, 170–180.

[68] Chen, X. J., Ji, H., Zhang, Q. W., Tu, P. F., Wang, Y. T., Guo, B. L., Li, S. P., *J. Pharm. Biomed. Anal.* 2008, *46*, 226–235.

[69] Nováková, L., Spácil, Z., Seifrtová, M., Opletal, L., Solich, P., *Talanta* 2010, *80*, 1970–1979.

[70] Nováková, L., Vildová, A., Mateus, J. P., Gonçalves, T., Solich, P., *Talanta* 2010, *82*, 1271–1280.

[71] Kumar, N., Bhandari, P., Singh, B., Bari, S. S., *Food Chem. Toxicol.* 2009, *47*, 361–367.

[72] Gómez-Romero, M., Segura-Carretero, A., Fernández-Gutiérrez, A., *Phytochemistry* 2010, *71*, 1848–1864.

[73] Li, S.-L., Song, J.-Z., Choi, F. F. K., Qiao, C.-F., Zhou, Y., Han, Q.-B., Xu, H.-X., *J. Pharm. Biomed. Anal.* 2009, *49*, 253–266.

[74] Trautvetter, S., Koelling-Speer, I., Speer, K., *Apidologie* 2010, *40*, 140–150.

[75] Cavaliere, C., Foglia, P., Gubbiotti, R., Sacchetti, P., Samperi, R., Laganà, A., *Rapid Commun. Mass Spectrom.* 2008, *22*, 3089–3099.

[76] Nagy, K. I., Redeuil, K., Bertholet, R., Steiling, H., Kussmann, M., *Anal. Chem.* 2009, *81*, 6347–6356.

[77] Gruz, J., Novák, O., Strnad, M., *Food Chem.* 2008, *111*, 789–794.

[78] Lou, Z., Wang, H., Zhu, S., Zhang, M., Gao, Y., Ma, C., Wang, Z., *J. Chromatogr. A* 2010, *1217*, 2441–2446.

[79] Jaitz, L., Siegl, K., Eder, R., Rak, G., Abranko, L., Koellensperger, G., Hann, S., *Food Chem.* 2010, *122*, 366–372.

[80] Xiang, G., Yang, L., Zhang, X., Yang, H., Ren, Z., Miao, M., *Chromatographia* 2009, *70*, 1007–1010.

[81] Beldean-Galea, M. S., Jandera, P., Hodisan, S., *J. Liq. Chromatogr. Relat. Technol.* 2008, *31*, 807–818.

[82] Reichelt, K. V., Peter, R., Paetz, S., Roloff, M., Ley, J. P., Krammer, G. E., Engel, K.-H., *J. Agric. Food Chem.* 2010, *58*, 458–464.

[83] Churchwell, M. I., Twaddle, N. C., Meeker, L. R., Doerge, D. R., *J. Chromatogr. B* 2005, *825*, 134–143.

[84] Spácil, Z., Nováková, L., Solich, P., *Talanta* 2008, *76*, 189–199.

[85] Ortega, N., Romero, M.-P., Macià, A., Reguant, J., Anglès, N., Morelló, J.-R., Motilva, M.-J., *J. Food Comp. Anal.* 2010, *23*, 298–305.

[86] Cooper, K. A., Campos-Gimenez, E., Jimenez-Alvarez, D., Nagy, K., Donovan, J. L., Williamson, G., *J. Agric. Food Chem.* 2007, *55*, 2841–2847.

[87] Cicchetti, E., Chaintreau, A., *J. Sep. Sci.* 2009, *32*, 3043–3052.

[88] Schwarz, M., Rodríguez, M. C., Guillén, D. A., Barroso, C. G., *J. Sep. Sci.* 2009, *32*, 1782–1790.

[89] Klejdus, B., Lojková, L., Lapčík, O., Koblovská, R., Moravcová, J., Kubáň, V., *J. Sep. Sci.* 2005, *28*, 1334–1346.

[90] Gritti, F., Sanchez, C. A., Farkas, T., Guiochon, G., *J. Chromatogr. A* 2010, *1217*, 3000–3012.

[91] Thompson, J. D., Carr, P. W., *Anal. Chem.* 2002, *74*, 1017–1023.

[92] Harris, D. C., *Quantitative Chemical Analysis*, W. H. Freeman and Co., New York 1999.

[93] Ahuja, S., Dong, M., *Separation Science and Technology*, Academic Press 2005, pp. 611–629.

[94] Kalili, K. M., de Villiers, A., *J. Chromatogr. A* 2009, *1216*, 6274–6284.

[95] Kalili, K. M., de Villiers, A., *J. Sep. Sci.* 2010, *33*, 853–863.

[96] Apers, S., Naessens, T., Van Den Steen, K., Cuyckens, F., Claeys, M., Pieters, L., Vlietinck, A., *J. Chromatogr. A* 2004, *1038*, 107–112.

[97] Rostagno, M. A., Palma, M., Barroso, C. G., *J. Chromatogr. A* 2005, *1076*, 110–117.

[98] Rostagno, M. A., Palma, M., Barroso, C. G., *Anal. Chim. Acta* 2007, *582*, 243–249.

[99] Rostagno, M. A., Palma, M., Barroso, C. G., *Anal. Chim. Acta* 2007, *588*, 274–282.

[100] Rostagno, M. A., Palma, M., Barroso, C. G., *Anal. Chim. Acta* 2007, *597*, 265–272.

[101] Biesaga, M., Ochnik, U., Pyrzynska, K., *J. Sep. Sci.* 2007, *30*, 2929–2934.

[102] Krizman, M., Baricevic, D., Prosek, M., *J. Pharm. Biomed. Anal.* 2007, *43*, 481–485.

[103] Castellari, M., Sartini, E., Fabiani, A., Arfelli, G., Amati, A., *J. Chromatogr. A* 2002, *973*, 221–227.

[104] Chinnici, F., Gaiani, A., Natali, N., Riponi, C., Galassi, S., *J. Agric. Food Chem.* 2003, *52*, 3–7.

[105] Dugo, P., Favoino, O., Luppino, R., Dugo, G., Mondello, L., *Anal. Chem.* 2004, *76*, 2525–2530.

[106] Troncoso, N., Sierra, H., Carvajal, L., Delpiano, P., Günther, G., *J. Chromatogr. A* 2005, *1100*, 20–25.

[107] Hu, L., Chen, X., Kong, L., Su, X., Ye, M., Zou, H., *J. Chromatogr. A* 2005, *1092*, 191–198.

[108] Repollés, C., Herrero-Martínez, J. M., Ràfols, C., *J. Chromatogr. A* 2006, *1131*, 51–57.

[109] Arapitsas, P., Turner, C., *Talanta* 2008, *74*, 1218–1223.

[110] Sharma, U. K., Sharma, N., Sinha, A. K., Kumar, N., Gupta, A. P., *J. Sep. Sci.* 2009, *32*, 3425–3431.

[111] Jandera, P., Vynuchalová, K., Hájek, T., Cesla, P., Vohralík, G., *J. Chemometr.* 2008, *22*, 203–217.

[112] Cacciola, F., Jandera, P., Blahová, E., Mondello, L., *J. Sep. Sci.* 2006, *29*, 2500–2513.

[113] Dugo, P., Cacciola, F., Herrero, M., Donato, P., Mondello, L., *J. Sep. Sci.* 2008, *31*, 3297.

[114] Vian, M. A., Tomao, V., Gallet, S., Coulomb, P. O., Lacombe, J. M., *J. Chromatogr. A* 2005, *1085*, 224–229.

[115] Liazid, A., Barbero, G. F., Palma, M., Brigui, J., Barroso, C. G., *Chromatographia* 2010, *72*, 417–424.

[116] Ikegami, T., Tanaka, N., *Curr. Opin. Chem. Biol.* 2004, *8*, 527–533.

[117] Kučerovv, Z., Szumski, M., Buszewski, B., Jandera, P., *J. Sep. Sci.* 2007, *30*, 3018–3026.

[118] Skeríková, V., Jandera, P., *J. Chromatogr. A* 2010, *1217*, 7981–7989.

[119] Jandera, P., Urban, J., Skeríková, V., Langmaier, P., Kubícková, R., Planeta, J., *J. Chromatogr. A* 2010, *1217*, 22–33.

[120] Dugo, P., Cacciola, F., Donato, P., Airado-Rodríguez, D., Herrero, M., Mondello, L., *J. Chromatogr. A* 2009, *1216*, 7483–7487.

[121] Hájek, T., Skeríková, V., Cesla, P., Vynuchalová, K., Jandera, P., *J. Sep. Sci.* 2008, *31*, 3309.

[122] Boros, B., Jakabová, S., Dörnyei, Á., Horváth, G., Pluhár, Z., Kilár, F., Felinger, A., *J. Chromatogr. A* 2010, *1217*, 7972–7980.

[123] Shen, Q., Dai, Z., Lu, Y., *J. Sep. Sci.* 2010, *33*, 3152–3158.

[124] Manchón, N., D'Arrigo, M., García-Lafuente, A., Guillamón, E., Villares, A., Ramos, A., Martínez, J. A., Rostagno, M. A., *Talanta* 2010, *82*, 1986–1994.

[125] Dugo, P., Cacciola, F., Donato, P., Jacques, R. A., Caramão, E. B., Mondello, L., *J. Chromatogr. A* 2009, *1216*, 7213–7221.

[126] Horvath, C. G., Lipsky, S. R., *Anal. Chem.* 1969, *41*, 1227–1234.

[127] Horvath, C. G., Preiss, B. A., Lipsky, S. R., *Anal. Chem.* 1967, *39*, 1422–1428.

[128] Kirkland, J. J., *Anal. Chem.* 1969, *41*, 218–220.

[129] Cesla, P., Hájek, T., Jandera, P., *J. Chromatogr. A* 2009, *1216*, 3443–3457.

[130] Jandera, P., Cesla, P., Hájek, T., Vohralík, G., Vynuchalová, K., Fischer, J., *J. Chromatogr. A* 2008, *1189*, 207–220.

[131] Jandera, P., Hájek, T., Česla, P., *J. Sep. Sci.* 2010, *33*, 1382–1397.

[132] Giddings, J. C., *J. Chromatogr. A* 1995, *703*, 3–15.

[133] Dixon, S. P., Pitfield, I. D., Perrett, D., *Biomed. Chromatogr.* 2006, *20*, 508–529.

[134] de Souza, L. M., Cipriani, T. R., Sant'Ana, C. F., Iacomini, M., Gorin, P. A. J., Sassaki, G. L., *J. Chromatogr. A* 2009, *1216*, 99–105.

[135] Schoenmakers, P. J., Vivo-Truyols, G., Decrop, W. M. C., *J. Chromatogr. A* 2006, *1120*, 282–290.

[136] Bushey, M. M., Jorgenson, J. W., *Anal. Chem.* 1990, *62*, 161–167.

[137] Tranchida, P. Q., Dugo, P., Dugo, G., Mondello, L., *J. Chromatogr. A* 2004, *1054*, 3–16.

[138] Erni, F., Frei, R. W., *J. Chromatogr. A* 1978, *149*, 561–569.

[139] Herrero, M., Ibáñez, E., Cifuentes, A., Bernal, J., *J. Chromatogr. A* 2009, *1216*, 7110–7129.

[140] Dugo, P., Kumm, T., Cacciola, F., Dugo, G., Mondello, L., *J. Liq. Chromatogr. Rel. Technol.* 2008, *31*, 1758–1807.

[141] Cacciola, F., Jandera, P., Hajdu, Z., Cesla, P., Mondello, L., *J. Chromatogr. A* 2007, *1149*, 73–87.

[142] Cacciola, F., Jandera, P., Mondello, L., *J. Sep. Sci.* 2007, *30*, 462–474.

[143] Cacciola, F., Jandera, P., Mondello, L., *Chromatographia* 2007, *66*, 661–667.

[144] François, I., de Villiers, A., Sandra, P., *J. Sep. Sci.* 2006, *29*, 492–498.

[145] François, I., de Villiers, A., Tienpont, B., David, F., Sandra, P., *J. Chromatogr. A* 2008, *1178*, 33–42.

[146] Kivilompolo, M., Hyötyläinen, T., *J. Sep. Sci.* 2008, *31*, 3466.

[147] Kivilompolo, M., Oburka, V., Hyotylainen, T., *Anal. Bioanal. Chem.* 2008, *391*, 373–380.

[148] Kivilompolo, M., Hyotylainen, T., *J. Chromatogr. A* 2007, *1145*, 155–164.

[149] Shalliker, A. R., Gray, M. J., in: Grushka, E., Grinberg, N. (Eds.), *Advances in Chromatography*, CRC Press, New York 2006, pp. 177–236.

[150] Blahová, E., Jandera, P., Cacciola, F., Mondello, L., *J. Sep. Sci.* 2006, *29*, 555–566.

[151] Cesla, P., Fischer, J., Jandera, P., *Electrophoresis* 2010, *31*, 2200–2210.

[152] Li, X., Stoll, D. R., Carr, P. W., *Anal. Chem.* 2009, *81*, 845–850.

[153] Liu, Z., Patterson, D. G., Lee, M. L., *Anal. Chem.* 1995, *67*, 3840–3845.

[154] Neue, U. D., *J. Chromatogr. A* 2005, *1079*, 153–161.

Improving HPLC Separation of Polyphenols

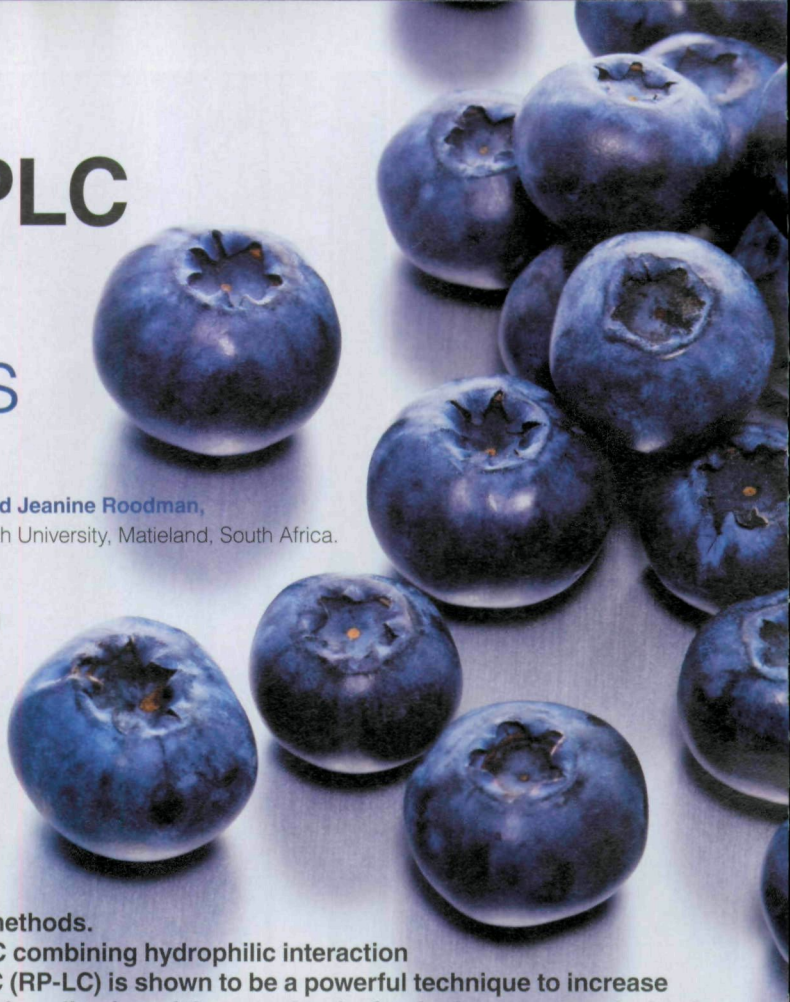

André de Villiers, Kathithileni M. Kalili, Mareta Malan and Jeanine Roodman,
Department of Chemistry and Polymer Science, Stellenbosch University, Matieland, South Africa.

The in-depth study of polyphenols is hampered by their sheer complexity, combined with the inherent limitations of conventional high performance liquid chromatography (HPLC) separation methods. In this paper, the beneficial application of a number of recent developments in HPLC for polyphenol analysis is highlighted. Small particle-packed columns operated at elevated pressures and temperatures are used to improve the speed and/or resolving power of conventional HPLC methods. In addition, comprehensive two-dimensional LC combining hydrophilic interaction chromatography (HILIC) and reversed phase LC (RP-LC) is shown to be a powerful technique to increase the resolving power. Examples of the successful application of these technologies for improved analysis of procyanidins, flavonols and anthocyanins in wine, tea, cocoa and blueberry samples are presented.

Polyphenols represent one of the most studied classes of natural compounds. Interest in these ubiquitous secondary metabolites, in recent times in particular, stems from their physiological contribution to the human diet and the numerous health benefits associated with their consumption. In addition, polyphenols are responsible for a range of organoleptic properties, including colour, astringency, bitterness and mouth-feel, as well as ageing properties.[1]

Clearly, the analysis of these compounds is of significant importance in various fields, particularly in the food and beverage and neutraceutical industries. However, the accurate analytical determination of phenolic compounds is hampered by the sheer complexity of the numerous chemical classes and species classified as polyphenols. These broadly include phenolic acids (hydroxybenzoic and cinnamic acids) and flavonoids, the latter class being subdivided into flavonols, flavanols (and their polymeric derivatives, the proanthocyanidins) and anthocyanins (anthocyanin-glycosides) (Figure 1).

The investigation of polyphenols is therefore closely related to the development of suitable analytical techniques for their identification and quantification. High performance liquid chromatography (HPLC), and reversed phase LC (RP-LC) in particular, is most often used for the routine analysis of phenolics, while in recent years the hyphenation of HPLC to mass spectrometry (MS) has become an indispensable tool for the detailed investigation of these compounds.[2]

The resolving power of chromatographic methods is commonly measured in terms of peak capacity: the

KEY POINTS

- The determination of natural phenolic compounds represents a severe analytical challenge.
- Recent developments in HPLC may be exploited to improve phenolic analysis.
- The combination of UHPLC and elevated temperature provide faster peak capacity production rates, particularly beneficial from the perspective of routine phenolic analysis.
- Comprehensive 2-dimensional LC (LC×LC), in particular off-line HILIC×RP-LC, delivers much higher separating power required for the investigation of complex phenolic fractions.
- The judicious application of recent advances in HPLC shows significant promise for improving phenolic analysis, providing the tools for the in-depth investigation of phenolic compounds in natural products.

number of peaks that can theoretically be resolved with unit resolution using a given separation method. The peak capacity (n_p) for gradient separations can be calculated according to:[3]

$$n_p = 1 + \frac{t_g}{\bar{w}}$$

where t_g is the gradient run time and $\bar{w}$ the average (4σ) peak width. Common gradient RP-LC methods typically provide peak capacities in the order of 100–150 (for ~1 h analysis times). Considering that the peak capacity should significantly exceed the number of randomly distributed analytes in a given sample to provide a high likelihood of separation,[4] and the fact that typical phenolic extracts contain in excess of 100 species, the limitations of HPLC are evident.

Importantly, in recent years a number of significant developments in HPLC have contributed to deliver improved performance. These include the use of ultra high pressure liquid chromatography (UHPLC), new developments in stationary phase morphologies (monolithic columns and superficially porous particles), high temperature liquid chromatography (HTLC) and multidimensional LC separations. In this contribution we discuss the beneficial application of some of these new technologies to improve the analysis of polyphenols in a variety of samples.

Experimental

Reagents and materials: Cocoa beans, wine, blueberries and green tea were purchased from a local supermarket. Epicatechin, catechin and uracil standards were from Sigma-Aldrich (Atlasville, South Africa), and anthocyanin standards from Polyphenols Laboratories (Sandnes, Norway). Dimeric procyanidins were isolated by HILIC fractionation from a cocoa extract. Mobile phases were prepared from HPLC-grade solvents (Sigma) and Milli-Q deionized water (Millipore, Milford, Massachusetts, USA).

Sample preparation: Extracts of green tea and cocoa were prepared as reported previously.[5,6] For extraction of blueberry anthocyanins, 6.681 g blueberries were frozen and ground under liquid nitrogen and extracted with methanol/water/formic acid (60:37:3), followed by evaporative pre-concentration. Filtered wine samples were directly injected.

Figure 1: General structures of the principal classes of phenolics. R is commonly H, OH or OCH_3, while R_1 may be OH, O-glycosyl, or O-acyl-glycosyl.

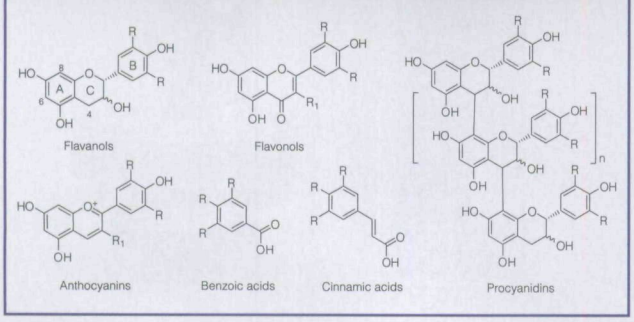

Instrumentation: HPLC–UV analyses were performed on an Alliance 2690 HPLC equipped with a photodiode array (PDA) detector (Waters, Milford, Massachusetts, USA). UHPLC experiments were performed on an Acquity UPLC system with PDA detector (Waters). HPLC–ESI-MS analyses were performed on a UPLC system coupled to a Waters Ultima Q-TOF mass spectrometer operated in positive ionization (PI) mode.[6] Blueberry anthocyanins were tentatively identified by MS and MS^2 spectra and comparison of retention times with literature reports.[7] The following columns were used: XBridge C18 (250 × 4.6 mm, 5 µm) and Acquity BEH C18 (50 and 100 × 2.1 mm, 1.7 µm, both Waters), Zorbax SB C18 (50 × 4.6 mm, 1.8 µm, Agilent, Waldbronn, Germany) and Develosil Diol-100 (250 × 1 mm, 5 µm, Nomura Chemical, Japan).

Chromatographic Conditions

Cocoa procyanidins and green tea flavonols: HPLC analyses at 25 °C were performed using 0.1% formic acid (A) and acetonitrile (B) at a flow rate of 1 mL/min: 0–0.63 min (2%B), 0.63–27 min (2–18%B), 27–45 min (18–25%B), 45–51.75 min (25–100%B), 51.75–56.25 min (100%B). UHPLC analyses were performed on a 100 mm Acquity column at 50 °C using the following gradient at 0.3 mL/min: 0–0.17 min (2%B), 0.17–7.4 min (2–18%B), 7.4–12.48 min (18–25%B), 12.48–14.53 min (25–100%B), 14.53–15.6 min (100%B). UV detection was performed at 280 and 370 nm for procyanidins and flavonols, respectively.

Wine anthocyanins: Mobile phases consisted of 7.5% formic acid (A) and acetonitrile (B). HPLC analyses were performed on the XBridge column at 25 °C and 1 mL/min using the following gradient: 0–1 min (1%B), 1–12 min (1–13.5%B),

Figure 2: (a) Comparison of van Deemter curves for procyanidin dimer on 5 and 1.7 µm columns at 25 °C and 50 °C; (b) Corresponding kinetic plots of efficiency versus analysis time.

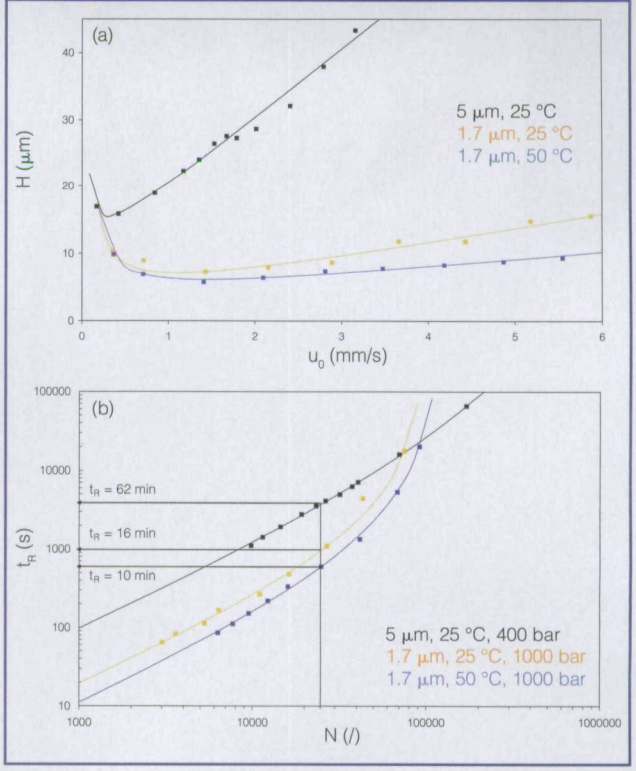

12–24 min (13.5–23.5%B), 24–28 min (23.5–28.5%B), 28–35 min (28.5%B). UHPLC analyses were performed on two coupled 100 mm Acquity columns at 50 °C and 0.06 mL/min as follows: 0–3 min (1%B), 3–34 min (1–13.5%B), 34–67 min (13.5–23.5%B), 67–78 min (23.5–28.5%B), 78–98 min (28.5%B). UV detection was performed at 500 nm.

Blueberry anthocyanins: Analyses were performed on the XBridge column using the same mobile phases as for wine anthocyanins. A flow rate of 1 mL/min was used throughout with the following gradients: 0–50 min (1–25%B), 50–55 min (25–40%B) at 25 °C; and 0–50 min (1–20%B), 50–55 min (25–40%B) at 70 °C. A post-column split (1:4) was used prior to eluent introduction into the MS.

HILIC×RP-LC: Conditions were as reported elsewhere.[5,6]

van Deemter Experiments

For procyanidins, experiments were performed on the XBridge column at 25 °C and on a 50 mm Acquity column at 25 °C and 50 °C, and for anthocyanins on the XBridge column at 25 °C and 70 °C. Mobile phases were as specified for each of these samples above, with the composition varied to ensure similar retention factors at all temperatures. Uracil was used as unretained marker, and all experiments were performed in duplicate. van Deemter curves and kinetic plots were constructed according to reference 8.

Results and Discussion

Uni-dimensional HPLC analyses: Since the inception of HPLC, there has been a continuous drive to improve the performance of the technique. The most widely practiced approach is to reduce the particle size (d_p) of column packing. The benefit of this approach is illustrated by the van Deemter curve, which plots chromatographic efficiency, in terms of plate height ($H = L/N$, where N is the number of theoretical plates) as a function of linear velocity of the mobile phase, u_0. The optimal linear velocity, u_{opt}, is that mobile phase velocity (flow rate) which delivers the minimum plate height (H_{min}) and therefore maximum efficiency. The effect of d_p on the van Deemter curve is demonstrated in Figure 2(a) for a dimeric procyanidin analysed on 5 µm and 1.7 µm columns. It is clear that u_{opt} increases and H_{min} decreases with a reduction in d_p, implying that faster and more efficient analyses are possible on the smaller phase for equal column lengths.

In fact, this picture is not entirely accurate, since decreasing d_p leads to a very important decrease in column permeability. Pressure constraints ultimately limit the column length and therefore efficiency attainable, so that very high efficiencies are easier to achieve for larger particle sizes (a result of the higher permeability of the larger d_p phases). Note though that the price to pay for such high efficiencies is a very significant increase in analysis time.

This dilemma has been partially overcome by the availability of a new generation of high-pressure instrumentation. In Figure 2(b) the isocratic efficiency as a function of total analysis time for the procyanidin dimer is compared for the same 5 µm and 1.7 µm columns, the latter operated at pressures up to 1000 bar. Note the significant

Figure 3: Comparison of HPLC analysis of cocoa procyanidins and green tea flavonols at 25 °C on a 5 µm XBridge column (a) and (b) respectively, and at 50 °C on a 1.7 µm column (c) and (d) respectively. Detection was performed at 280 nm and 370 nm for procyanidins and flavonols, respectively. ΔP_{max} = 193 and 505 bar for HPLC and UHPLC analyses.

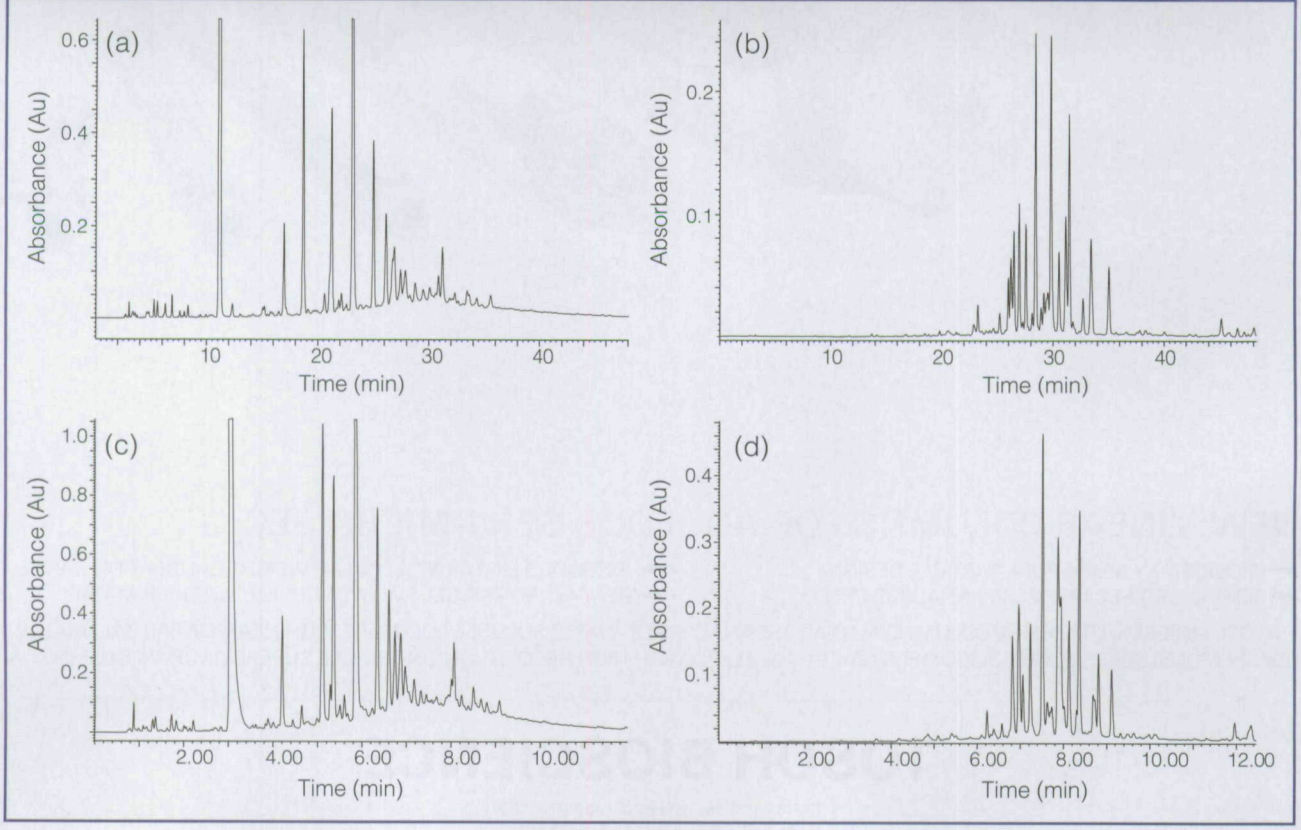

Figure 4: van Deemter plots for four anthocyanins on a 5 μm XBridge column at (a) 25 °C and (b) 70 °C and (c) corresponding kinetic plots of efficiency versus retention time for malvidin-3-O-glucoside

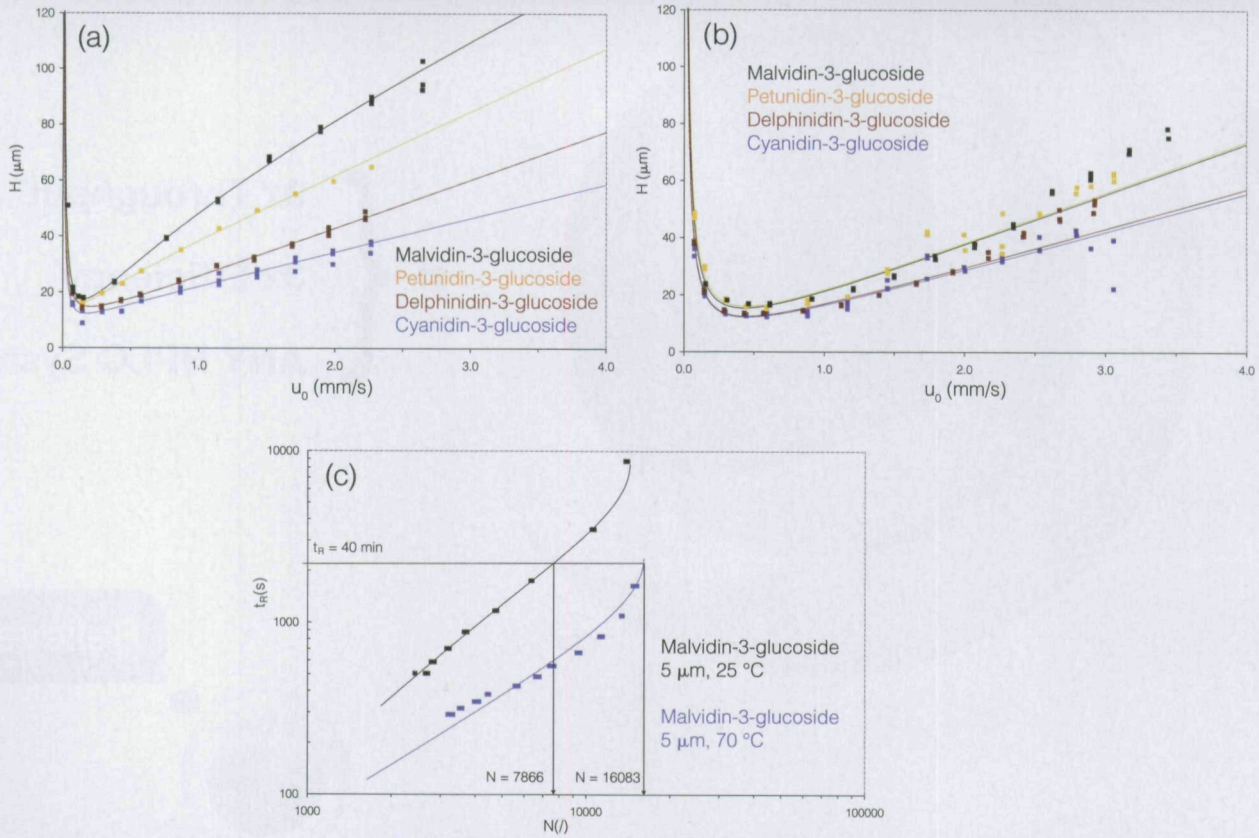

Figure 5: Extracted ion chromatograms for the gradient HPLC—MS analysis of blueberry anthocyanins on a 5 μm XBridge column: (a) at 25 °C, and (b) at 70 °C, both at 1 mL/min. Cy = cyanidin, Dp = delphinidin, Pt = petunidin, Pe = peonidin and Mv = malvidin.

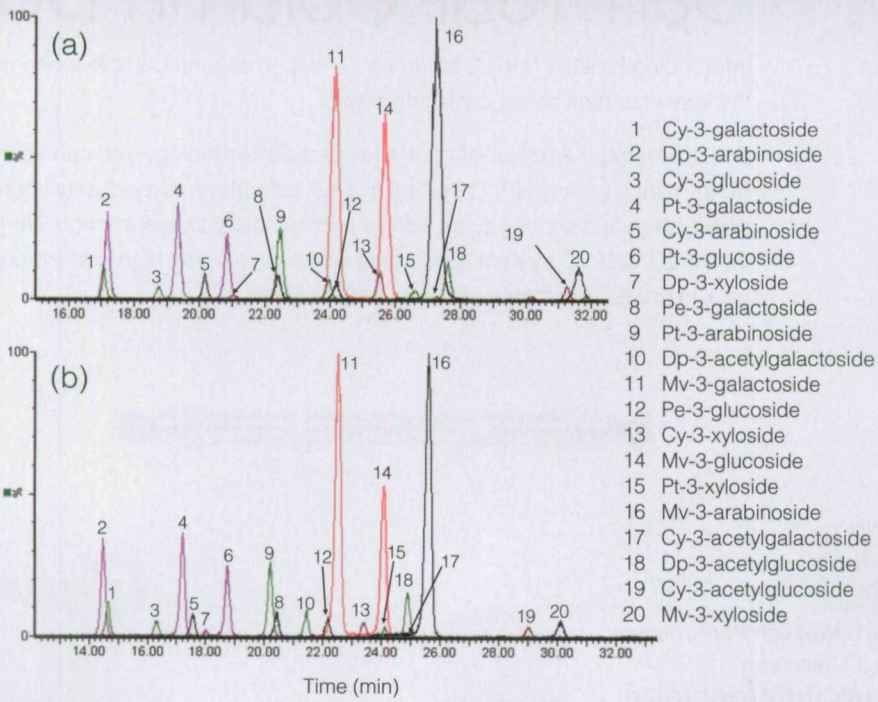

decrease in analysis time achieved on the UHPLC column for an efficiency of 25000 plates (equal to that provided by a conventional 250 mm, 5 µm column). Moreover, UHPLC clearly offers faster analysis for efficiencies up to $N \sim 80000$.

It is relatively straightforward to practically exploit the benefits of UHPLC because HPLC methods may nowadays easily be adapted to UHPLC column formats and instrumentation, essentially providing the same separation mechanism. To date this approach has received comparatively little attention for polyphenol analysis,[9,10] with the focus primarily on very fast analysis on short columns, essentially providing the same efficiency as conventional HPLC columns.

Increasing the temperature of HPLC separations provides an additional means of improving performance.[11] This is primarily a result of faster analyte diffusion in the mobile phase at higher temperatures. The effect of this on plate height behaviour is demonstrated once again for the dimeric procyanidins on the 1.7 µm column in Figure 2: while the maximum column efficiency (= L/H_{min}) remains roughly unchanged, the optimal linear velocity increases and efficiency-loss at high flow rates is reduced. At higher analysis temperature the flow rate should be increased to operate close to u_{opt}, in this manner providing the same efficiency faster. Note that even though the mobile phase viscosity is inversely proportional to temperature, the requirement of operating at higher flow rates means that the overall pressure remains roughly constant.

In fact, elevated temperature offers a complementary means of further increasing the speed of UHPLC separations for efficiencies up to $N \sim 80000$. The benefits of this approach are illustrated in Figure 3, where conventional HPLC analysis of cocoa procyanidins and green tea flavonols are compared to UHPLC analysis at 50 °C. This approach provides similar separation in a third of the analysis time, demonstrating obvious advantages for routine analysis of polyphenols.

For anthocyanins (anthocyanidin-glycosides, Figure 1), analysis temperature plays a particularly important role. These compounds are known to exist in solution in a number of different chemical forms.[12] On-column inter-conversion between these species causes significant band broadening,[13] leading to the relatively poor efficiency commonly observed for HPLC analyses of anthocyanins. Higher analysis temperatures speed up the inter-conversion reactions — leading to less band-broadening and improved efficiency. This is demonstrated for the van Deemter curves

Figure 6: Comparison of gradient RP-LC analysis of red wine anthocyanins on a (a) 5 µm XBridge column at 25 °C and 1 mL/min and a (b) 1.7 µm Acquity column at 50 °C and 0.06 mL/min.14 UV detection at 500 nm. ΔP_{max} = 190 and 295 bar for HPLC and UHPLC analyses.

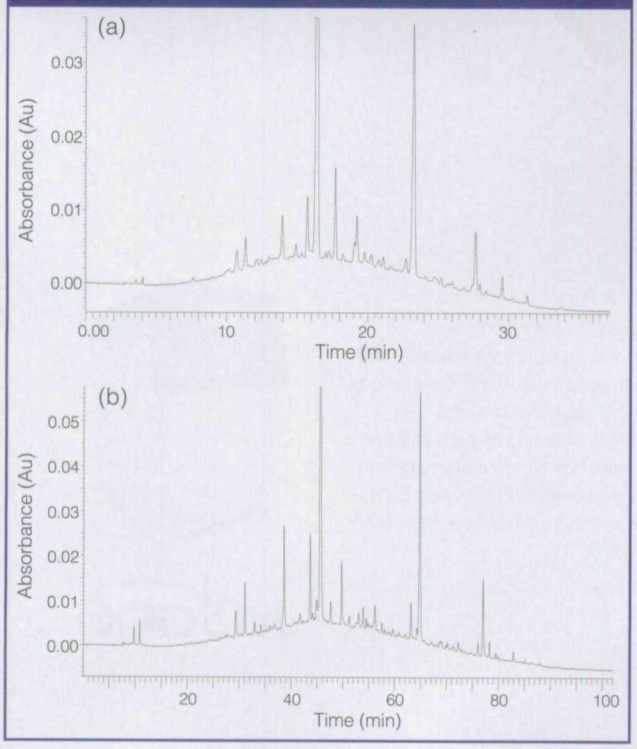

Figure 7: HILIC×RP-LC analysis of cocoa procyanidins. Numbers correspond to degree of polymerisation of procyanidins, A indicates A-type procyanidins. Refer to reference 5 for further details.

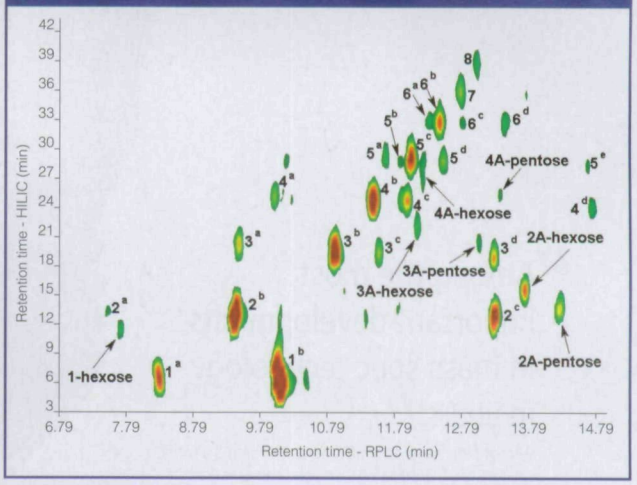

Figure 8: HILIC×RP-LC analysis of green tea flavonols. Data taken from reference 6. Myr = myricetin, Q = querectin, K = kaempferol, gal = galactoside, glc = glucoside, rha = rhamnoside, xyl = xyloside, rut = rutinoside and hex = unkown hexose.

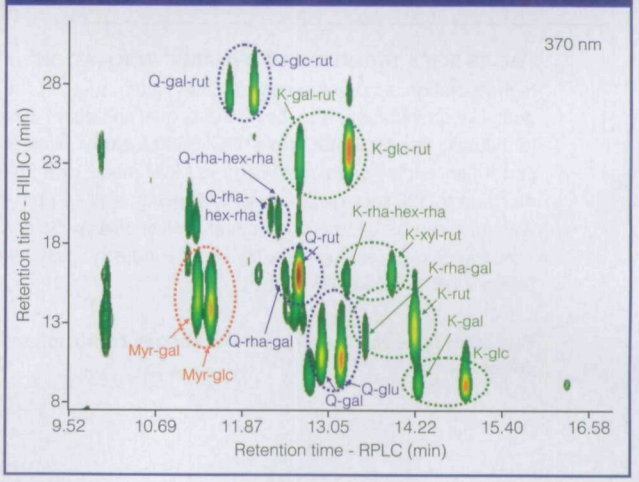

of four common anthocyanins in Figure 4. At conventional flow rates (i.e., 1 mL/min on 4.6 mm i.d. columns), an improvement in efficiency of between 25 and 130% is achieved at 70 °C compared with 25 °C. In this manner elevated temperature may be used to improve the efficiency of conventional gradient RP-LC analysis of anthocyanins, as demonstrated for blueberry anthocyanins in Figure 5. Also note that temperature may affect the selectivity of the separation, as is evident from the relative elution order of some anthocyanins in Figure 5.

The previous examples demonstrate how analysis speed for polyphenol analysis may be increased (for the same efficiency) or efficiency increased for the same analysis time. Another approach especially suited for complex phenolic fractions, is to exploit the benefits of UHPLC and elevated temperature for high-efficiency analysis. This is demonstrated for the analysis of red wine anthocyanins on a 200 mm 1.7 µm column operated at 50 °C in Figure 6.[14] This set-up provides isocratic efficiencies of up to 40000 plates, and gradient analysis delivers much improved resolution for an acceptable analysis time of 90 min. Note that this analysis is performed at pressures below 300 bar, implying that conventional instrumentation may be used (provided system delay and void volumes are optimized for such analyses).

However, caution should be exercised in the application of elevated temperature for phenolic analysis. As is well documented in literature, anthocyanins in particular are readily degraded at relatively mild temperatures. Fortunately this aspect may be evaluated quantitively. Using the approach of Thompson et al.[15] it at can be demonstrated that analysis times of less than 2 hours at 70 °C do not lead to on-column degradation of anthocyanins.[13]

Finally, in the context of uni-dimensional HPLC analysis, it should be mentioned that a number of additional developments in column technology in recent years hold some promise for HPLC analysis of polyphenols. These include the use of monolithic[16] and superficially porous particles.[17] However, limited application of these column formats to polyphenol determination has been reported to date.[18]

Comprehensive two-dimensional liquid chromatography (LC×LC)

The challenges associated with HPLC analysis of phenolics may be demonstrated using an example: procyanidins (Figure 1) consist of a mixture of monomeric, oligomeric and polymeric compounds composed of flavanol building blocks. As the degree of polymerization (DP) increases, the number of possible isomers increases exponentially (a result of the possible combinations of monomers as well as different inter-flavanol bonds). For example, 48 isomers of dimeric procyanidins containing catechin and epicatechin building blocks are possible.[19] Considering that optimized high-efficiency HPLC methods provide peak capacities of maximally 400, no uni-dimensional HPLC method is capable of providing complete separation of higher molecular weight (MW) procyanidins in a single analysis.

Comprehensive two-dimensional HPLC (LC×LC) is a promising method for the separation of such complex samples. LC×LC delivers peak capacities an order of magnitude or more than uni-dimensional LC. In LC×LC, two separation methods are combined in such a manner that the separation in each dimension is retained. As a consequence, the overall peak capacity in a two-dimensional space is (ideally) the product of peak capacities in each dimension. Admittedly, this ideal is only achieved if certain criteria are met, most importantly that both separations are based on different (orthogonal) mechanisms.

Comprehensive 2-D LC may be performed in off-line, on-line or stop-flow modes.[19] In on-line LC×LC, fractions from the first dimension are transferred in real time to the second dimension column, usually using multi-port two-position switching valves. This approach provides relatively fast (approximately equal to 1-D HPLC methods) separations, although resolution in the second dimension is sacrificed to meet sampling rate requirements. Off-line LC×LC, by contrast, results in much longer analysis times, but since no constraints are placed on the second dimension separation much higher peak capacities may be obtained. (Stop-flow LC×LC is less often applied, and provides peak capacities and analysis times in between the off-line and on-line approaches).

In fact, the application of on-line LC×LC using a variety of separation modes has been demonstrated for diverse phenolics in wine, beer and herb samples.[18,21,22] In our group, we have investigated the off-line coupling of hydrophilic interaction chromatography (HILIC) and RP–LC to improve procyanidin determination.[5] Off-line coupling was chosen to obtain the maximal practical peak capacity through optimal second-dimension analyses. In HILIC, procyanidins are separated according to polarity, which effectively provides molecular weight separation based on the number of hydroxyls (individual isomers are co-eluted).[23] RP-LC, in contrast, provides isomeric separation according to hydrophobicity — although complete separation of isomers in not possible in a single analysis. HILIC and RP-LC therefore

Table 1: Comparison of peak capacities and peak capacity production rates for conventional HPLC, UHPLC, elevated temperature LC and LC×LC analysis of phenolic compounds in various samples.

	Peak capacity (np)[a]	Time (min)	np/min
Cocoa procyanidins			
250 mm L, 5 µm, 25 °C RP-LC	118	56.25	2.1
100 mm L, 1.7 µm, 50 °C RP-LC	127	15.6	8.1
HILIC×RP-LC	3512	1555	2.3
Green tea flavonols			
250 mm L, 5 µm, 25 °C RP-LC	151	56.25	2.7
100 mm L, 1.7 µm, 50 °C RP-LC	138	15.6	8.8
HILIC×RP-LC	2535	1555	1.6
Blueberry anthocyanins			
250 mm L, 5 µm, 25 °C RP-LC	110	55	2.0
250 mm L, 5 µm, 70 °C RP-LC	146	55	2.7
Wine anthocyanins			
250 mm L, 5 µm, 25 °C RP-LC	98	35	2.8
200 mm L, 1.7 µm, 50 °C RP-LC	175	98	1.8

[a] Calculated according to reference 3 and reference 23 for 1-D and 2-D separations, respectively.

provide highly orthogonal separations. The off-line comprehensive HILIC×RP-LC analysis of cocoa procyanidins is illustrated in Figure 7, where it is evident that the combination of MW (HILIC, y-axis) and isomeric (RP-LC, x-axis) information delivers a complete picture of the oligomeric procyanidin content of this extract. The practical peak capacity for this separation (according to reference 24) is ~3500.

The same approach may also be used beneficially for the analysis of other classes of phenolic compounds. This is illustrated in Figure 8 for flavonol glycosides in green tea (practical peak capacity 2500). A very structured elution pattern reminiscent of comprehensive GC is evident from this figure: retention in HILIC increases with the number of attached sugars, while the different flavonol moieties as well as individual mono-, di- and tri-glycosides are resolved in the RP-LC dimension. It may be concluded that HILIC×RP-LC, and LC×LC in general, holds significant promise for the in-depth investigation of complex phenolic fractions such as encountered in numerous natural products.

Conclusions

The analysis of polyphenols represents a severe analytical challenge, and important advances in natural phenolic research hinge on the development of suitable separation strategies. Fortunately, recent developments in HPLC show promise for improving polyphenol analysis.

A summarized comparison of conventional HPLC, UHPLC and/or elevated temperature LC and LC×LC analyses of different phenolic compounds is presented in Table 1. These examples demonstrate that the combination of small d_p columns and/or temperature primarily delivers improved peak capacity production rates. This advantage can be practically exploited in one of two ways: (1) to achieve similar peak capacities to conventional HPLC ~3–4× faster (e.g., cocoa procyanidins, green tea flavonols); and (2) to improve the peak capacity for a given analysis time (e.g., blueberry anthocyanins). These techniques show particular promise in improving current routine HPLC methods for polyphenol determination. In addition, application of UHPLC columns operated at elevated temperatures allows improved total peak capacity for complex phenolic fractions (e.g., red wine anthocyanins).

For very demanding separations, off-line comprehensive 2-D LC offers greatly improved separation power compared with HPLC (>20× higher peak capacities) at similar peak capacity production rates. The choice of the most suitable separation methodology will therefore depend on the requirements for a particular phenolic sample in terms of speed, instrumental simplicity or resolving power.

It should be noted that state-of-the-art mass spectrometric (MS) techniques such as high resolution MS and tandem MS methods, not addressed in the current contribution, represent a complimentary strategy for improving polyphenol analysis. In fact, MS offers an alternative 'separation' dimension (in terms of *m/z* ratio), increased selectivity for target analysis and a powerful structural elucidation tool. Combined with advanced chromatographic separation, LC–MS will prove an even more powerful tool for detailed phenolic determination.

Clearly, the judicious application of recent advances in HPLC demonstrably offers significant benefits for phenolic analyses, and shows promise for the in-depth investigation of the phenolic compounds found in numerous natural products — an endeavour which, to date, has been hampered by the lack of suitable separation methods.

Acknowledgements

The authors gratefully acknowledge Stellenbosch University, the Third World Academy of Science (TWAS, 08-077 RG/CHE/AF/AC) and NRF for financial assistance.

References

1. E. Haslam, *Practical Polyphenolics: From Structure to Molecular Recognition and Physiological Action*, (Cambridge University Press, Cambridge, 1998).
2. C. Santos-Buelga and G. Williamson, *Methods in Polyphenol Analysis* (The Royal Society of Chemistry, Cambridge, 2003).
3. U.D. Neue, *J. Chromatogr. A*, **1079**(1–2), 153–161 (2005).
4. J.M. Davis and J.C. Giddings, *Anal. Chem.*, **55**(3), 418–424 (1983).
5. K.M. Kalili and A. de Villiers, *J. Chromatogr. A*, **1216**(35), 6274–6284 (2009).
6. K.M. Kalili and A.de Villiers, *J. Sep. Sci.*, **33**(6–7), 853–863 (2010).
7. M.J. Cho et al., *J. Sci. Food Agric.*, **84**(13), 1771–1782 (2004).
8. G. Desmet, D. Clicq and P. Gzil, *Anal. Chem.*, **77**(13), 4058–4070 (2005).
9. B. Klejdus et al., *J. Chromatogr. A*, **1195**(1–2), 52–59 (2008).
10. M. Schwarz et al., *J. Sep. Sci.*, **32**(11), 1782–1790 (2009).
11. F. Lestremau et al., *J. Chromatogr. A*, **1138**(1–2), 120–131 (2007).
12. R. Brouillard and J.-E. Dubois, *J. Am. Chem. Soc.*, **99**(5), 1359–1364 (1977).
13. A. de Villiers et al., *J. Chromatogr. A*, **1216**(15), 3270–3279 (2009).
14. A. de Villiers et al., unpublished results (2010).
15. J.D. Thompson and P.W. Carr, *Anal. Chem.*, **74**(5), 1017–1023 (2002).
16. G. Guiochon, *J. Chromatogr. A*, **1168**(1–2), 101–168 (2007).
17. F. Gritti et al., *J. Chromatogr. A*, **1217**(10), 1589–1603 (2010).
18. P. Dugo et al., *J. Sep. Sci.*, **31**(19), 3297–3308 (2008).
19. R. Mayer et al., *J. Agric. Food Chem.*, **56**(16), 6959–6966 (2008).
20. J.N. Fairchild, K. Horváth and G. Guiochon, *J. Chromatogr. A*, **1216**(9), 1363–1371 (2009).
21. P. Cesla, T. Hájek and P. Jandera, *J. Chromatogr. A*, **1216**(16), 3443–3457 (2009).
22. T. Hájek et al., *J. Sep. Sci.*, **31**(19), 3309–3328 (2008).
23. A. Yanagida et al., *J. Chromatogr. A*, **1143**(1–2), 153–161 (2007).
24. Z. Liu, D.G. Patterson and M.L. Lee, *Anal. Chem.*, **67**(21), 3840–3845 (1995).

André de Villiers is a senior lecturer at the Department of Chemistry and Polymer Science at Stellenbosch University, South Africa. His research activities include fundamental studies and the practical application of HPLC, CE, GC, MS and sample preparation techniques especially to natural product analysis. He is author or co-author of 24 scientific papers, and the recipient of the 2009 Csaba Horvath Award.
Kathithileni M. Kalili is a first year PhD student at Stellenbosch University. Her research focuses on the development of novel comprehensive multi-dimensional high performance liquid chromatography (HPLC) and electromigration methods for the analysis of complex phenolics.
Mareta Malan is a part-time MSc student at Stellenbosch University. She works for Freeworld Coatings Research Centre in Stellenbosch as an analytical chemist where her research is focused on method development for the analysis of surface coatings.
Jeanine Roodman is currently working as a chemical analyst in a food laboratory. She completed her honours degree in chemistry at Stellenbosch University focused on the application of high temperature liquid chromatography to anthocyanin analysis.

Additional references: Applications of UHPLC, HTLC, MDLC, monolithic- and superficially-porous phases in phenolic analysis for the period 2011-2013.

[1] A.R. Kavalier, A. Litt, C. Ma, N.J. Pitra, M.C. Coles, E.J. Kennelly, P.D. Matthews, J. Agric. Food Chem. 59 (2011) 4783.
[2] C. Esteve, C. Del Río, M. Luisa Marina, M.C. García, Anal. Chim. Acta 690 (2011) 129.
[3] F. Xie, A. Yu, D. Hou, H. Liu, L. Ding, S. Zhang, Am. J. Anal. Chem. 2 (2011) 929.
[4] J. Ballesta-Claver, M.C. Valencia, L.F. Capitán-Vallvey, Luminescence 26 (2011) 44.
[5] A. Ribas-Agustí, M. Gratacós-Cubarsí, C. Sárraga, J.-A. García-Regueiro, M. Castellari, Phytochem. Anal. 22 (2011) 555.
[6] A.M. Gómez-Caravaca, A. Segura-Carretero, A. Fernández-Gutiérrez, M.F Caboni, J. Agric. Food Chem. 59 (2011) 10815.
[7] M.A. Rostagno, N. Manchón, M. D'Arrigo, E. Guillamón, A. Villares, A. García-Lafuente, A. Ramosa, J.A. Martínez, Anal. Chim. Acta 685 (2011) 204.
[8] M. Ceymann, E. Arrigoni, H. Schärer, D. Baumgartner, A.B. Nising, R.F. Hurrell, Anal. Methods, 3 (2011) 1774.
[9] I.N. Abreu, M. Ahnlund, T. Moritz, B.R. Albrectsen, J. Chem. Ecol. 37 (2011) 857.
[10] I.B. Linaresa, D. Arráez-Román a, M. Herrero, E. Ibánez, A. Segura-Carretero, A. Fernández-Gutiérrez, J. Chromatogr. A 1218 (2011) 7682.
[11] L.S. Chua, N.A. Latiff, S.Y. Lee, C.T. Lee, M.R. Sarmidi, R.A. Aziz, Food Chem. 127 (2011) 1186.
[12] F. Sánchez-Patán, M. Monagas, M.V. Moreno-Arribas, B. Bartolomé, J. Agric. Food Chem. 59 (2011) 2241.
[13] B. Zimmermann, S.G. Walch, L.N. Tinzoh, W. Stuhlinger, D.W. Lachenmeier, J. Chromatogr. B 879 (2011) 2459.
[14] J. Lee, S.E. Ebeler, J.A. Zweigenbaum, A.E. Mitchell, J. Agric. Food Chem. 60 (2012) 8510.
[15] C.-E. Narváez-Cuenca, J.-P. Vincken, H. Gruppen, Food Chem. 130 (2012) 730.
[16] D.C. Manns, A.K. Mansfield, J. Chromatogr. A 1251 (2012) 111.
[17] P. Jandera, T. Hájek, M. Stanková, K. Vynuchalová, P. Cesla, J. Chromatogr. A 1268 (2012) 91.
[18] C. Engels, D. Gräter, P. Esquivel, V.M. Jiménez, M.G. Gänzle, A. Schieber, Food Res. Int. 46 (2012) 557.
[19] C. Engels, A. Schieber, M.G. Gänzle, Eur Food Res Technol 234 (2012) 535.
[20] H. Shi, H. Yang, X. Zhang, L. Yu, J. Agric. Food Chem. 60 (2012) 12403.
[21] M. Ceymann, E. Arrigoni, H. Schärer, A.B. Nising, R.F. Hurrell, J. Food Comp. Anal. 26 (2012) 128.
[22] S. Ma, Q. Liang, Z. Jiang, Y. Wang, G. Luo, Talanta 97 (2012) 150.
[23] J. Zeng, X. Zhang, Z. Guo, J. Feng, J. Zeng, X. Xue, X. Liang, J. Chromatogr. A 1220 (2012) 50.
[24] T. Beelders, K.M. Kalili, E. Joubert, D. de Beer, A. de Villiers, J. Sep. Sci. 35 (2012) 1808.
[25] L. Mouls, H. Fulcrand, J. Mass Spectrom. 47 (2012) 1450.
[26] Z. Guo, X. Zhang, Y. Liu, X. Liang, J. Sep. Sci. 35 (2012) 1821.
[27] A. Kokotkiewicz, M. Luczkiewicz, P. Sowinski, D. Glod, K. Gorynski, A. Bucinski, Food Chem. 133 (2012) 1373.
[28] C.L. Silva, N. Haesen, J.S. Câmara, J. Chromatogr. A 1260 (2012) 154.
[29] M.I. Alarcón-Flores, R. Romero-González, A.G. Frenich, J.L.M. Vidal, Food Chem. 134 (2012) 2465.
[30] E. Kiyota, P. Mazzafera, A.C.H.F. Sawaya, Anal. Chem. 84 (2012) 7015.
[31] H. Zhang, H. Yang, M. Zhang, Y. Wang, J. Wang, L. Yau, Z. Jiang, P. Hu, J. Food Comp. Anal. 25 (2012) 142.
[32] C.S. Funari, P.J. Eugster, S. Martel, P.A. Carrupt, J.L. Wolfender, D.H.S. Silva, J. Chromatogr. A 1259 (2012) 167.
[33] A.J. Steevensz, S.L. Mackinnon, R. Hankinson, C. Craft, S. Connan, D.B. Stengel, J.E. Melanson, Phytochem. Anal. 23 (2012) 547.
[34] J. Sun, L. Lin, P. Chen, Rapid Commun. Mass Spectrom. 26 (2012) 1123.

[35] C.T. Scoparo, L.M. de Souza, N. Dartora, G.L. Sassaki, P.A.J. Gorin, M. Lacomini, J. Chromatogr. A 1222 (2012) 29.
[36] E.A. Prokudina, L. Havlíček, N. Al-Maharik, O. Lapčik, M. Strnad, J. Gruz, J. Food Comp. Anal. 26 (2012) 36.
[37] P. Mena, L. Calani, C. Dall'Asta, G. Galaverna, C. García-Viguera, R. Bruni, A. Crozier, D. Del Rio, Molecules 17 (2012) 14821.
[38] M.-J. Motilva, A. Serra, A. Macià, J. Chromatogr. A 1292 (2013) 66.
[39] C. Narayan, A. Kumar, Orient. Pharm. Exp. Med. 13 (2013) 51.
[40] G. Haghi, A. Hatami, A. Safaei, M. Mehran, Res. Pharm. Sci. 9 (2013) 31.
[41] M.C. Díaz-García, J.M. Obón, M.R. Castellar, J. Collado, M. Alacid, Food Chem. 138 (2013) 938.
[42] A. Rameshkumar, T. Sivasudha, R. Jeyadevi, B. Sangeetha, G.S.B. Aseervatham, M. Maheshwari, Food Res. Int. 50 (2013) 94.
[43] H.H.F. Koolen, F.M.A. da Silva, F.C. Gozzo, A.Q.L. de Souza, A.D.L. de Souza, Food Res. Int. 51 (2013) 467.
[44] A.V. Pavlović, D.Č. Dabić, N.M. Momirović, B.P. Dojcinović, D.M. Milojković-Opsenica, Ž. Lj. Tešić , M.M. Natić, J. Agric. Food Chem. 61 (2013) 4188.
[45] A. Panusa, A. Zuorro, R. Lavecchia, G. Marrosu, R. Petrucci, J. Agric. Food Chem. 61 (2013) 4162.
[46] M.D.L.L. Cádiz-Gurrea, S. Fernández-Arroyo, J. Joven, A. Segura-Carretero, Food Res. Int. 50 (2013) 197.
[47] C.-L. Lin, B. Singco, C.-Y. Wu, P.Z. Liang, Y.-J. Cheng, H.-Y. Huang, J. Chromatogr. A 1272 (2013) 65.
[48] D. De Paepe, K. Servaes, B. Noten, L. Diels, M. De Loose, B. Van Droogenbroeck, S. Voorspoels, Food Chem. 136 (2013) 368.
[49] B. Bayram, B. Ozcelik, G. Schultheiss, J. Frank, G. Rimbach, Food Chem. 138 (2013) 1663.
[50] J. Wu, Y. Qiana, P. Mao, L. Chen, Y. Lub, H. Wang, J. Chromatogr. B 927 (2013) 173.
[51] M.I. Alarcón-Flores, R. Romero-González, J.L.M. Vidal, A.G. Frenich, Food Chem. 141 (2013) 1120.
[52] C.-E. Narváez-Cuenca, J.-P. Vincken, C. Zheng, H. Gruppen, Food Chem. 139 (2013) 1087.
[53] X. Qiu, J. Zhang, Z. Huang, D. Zhu,W. Xu, J. Chromatogr. A 1292 (2013) 121.
[54] W. Kukula-Koch, N. Aligiannis, M. Halabalaki, A.-L. Skaltsounis, K. Glowniak, E. Kalpoutzakis, Food Chem. 138 (2013) 406.
[55] S. Kečkeš, U. Gašić, T.Ć. Veličković, D. Milojković-Opsenica, M. Natić, Ž. Tešic, Food Chem. 138 (2013) 32.
[56] A. Wojakowska, J. Perkowski, T. Góral, M. Stobiecki, J. Mass Spectrom. 48 (2013) 329.
[57] Q. Ren, C. Wu, J. Zhang, J. Chromatogr. A 1304 (2013) 257.
[58] Q. Ren, C. Wu, Y. Ren, J. Zhang, Food Chem. 136 (2013) 1377.
[59] P. Hou, Y. Zeng, B. Ma, X. Wang, Z. Liu, L. Li, K. Qu, K. Bi, X. Chen, J. Sep. Sci. 36 (2013) 2544.
[60] A. Panusa, A. Zuorro, R. Lavecchia, G. Marrosu, R. Petrucci, J. Agric. Food Chem. 61 (2013) 4162.
[61] A.M. Gómez-Caravaca, V. Verardo, M. Toselli, A. Segura-Carretero, A. Fernandez-Gutiérrez, M.F. Caboni, J. Agric. Food Chem. 61 (2013) 5328.
[62] D.M. de Oliveira, C.B. Pinto, G. Sampaio, L. Yonekura, R.R. Catharino, D.H.M. Bastos, J. Agric. Food Chem. 61 (2013) 6113.
[63] A. Frolov, A. Henning, C. Böttcher, A. Tissier, D. Strack. J. Agric. Food Chem. 61 (2013) 1219.
[64] P. Jandera, M. Staňková, T. Hájek, J. Sep. Sci. 36 (2013) 2430.
[65] E.S.L. Chong, T.K. McGhie, J.A. Heyes, K.M. Stowell, J. Sci. Food Agric. (2013), doi:10.1002/jsfa.6285.
[66] L. Azaroual, A. Liazid, G.F. Barbero, J. Brigui, M. Palma, C.G. Barroso, ISRN Chromatogr. (2013), doi:10.5402/2012/609095.
[67] V. Škeríková, J. Urban, J. Sep. Sci. (2013) ,doi:10.1002/jssc.201300395.

[68] G. Di Lecce, M. Martínez-Huélamo, S. Tulipania, A. Vallverdú-Queralt, R.M. Lamuela-Raventós, J. Agric. Food Chem. (2013), doi:10.1021/jf401953y.
[69] E. Sommella, G. Pepe, F. Pagano, G.C. Tenore, P. Dugo, M. Manfra, P. Campiglia, J. Sep. Sci. (2013), doi:10.1002/jssc.201300591.

Addendum B

Kinetic optimisation of the reversed-phase liquid chromatographic separation of proanthocyanidins on sub-2 µm and superficially porous phases

K.M. Kalili, D. Cabooter, G. Desmet, A. de Villiers, J. Chromatogr. A 1236 (2012) 63-76.

Journal of Chromatography A, 1236 (2012) 63–76

Contents lists available at SciVerse ScienceDirect

Journal of Chromatography A

journal homepage: www.elsevier.com/locate/chroma

Kinetic optimisation of the reversed phase liquid chromatographic separation of proanthocyanidins on sub-2 μm and superficially porous phases

Kathithileni M. Kalili[a], Deirdre Cabooter[b], Gert Desmet[b], André de Villiers[a,*]

[a] Department of Chemistry and Polymer Science, Stellenbosch University, Private Bag X1, Matieland 7602, South Africa
[b] Department of Chemical Engineering, Vrije Universiteit Brussel, Pleinlaan 2, B-1050 Brussels, Belgium

ARTICLE INFO

Article history:
Received 20 December 2011
Received in revised form 27 February 2012
Accepted 28 February 2012
Available online 5 March 2012

Keywords:
Kinetic plots
Phenolic compounds
Proanthocyanidins
Ultra high pressure liquid chromatography
Superficially porous phases
Van Deemter plots

ABSTRACT

Phenolic compounds, and proanthocyanidins in particular, are important natural molecules which are of significant importance due to their sensory and biological activities. The analysis of proanthocyanidins in natural products is very challenging due to their complex nature. In this study, the kinetic performance of a range of recently developed C18 columns, including sub-2 μm fully porous and 2.6 μm superficially porous particle-packed columns, was evaluated for improved proanthocyanidin analysis. The kinetic plot method was employed to compare the ultimate performance limits of each column in terms of efficiency and speed for different maximum pressures and temperatures using representative proanthocyanidins comprising a range of molecular weights and functionalities as test analytes. By combining plate height data with relevant parameters such as column permeability and mobile phase viscosity, plots of practically attainable efficiencies as a function of analysis time for specific experimental configurations were obtained and performance limits for all investigated supports could accurately be compared. Both fully- and superficially porous particles provided significant speed and/or efficiency gains compared to conventional 5 μm particle packed columns. Analyte properties, particle size and packing quality as well as analysis temperature were all found to have a significant influence on the performance of the presently investigated chromatographic supports. For smaller compounds, higher optimal linear velocities and better performance in the low-efficiency range were observed, while the lower diffusion coefficients of larger procyanidins resulted in lower optimal linear velocities and better performance in the high-efficiency regime. Faster analyses become possible at higher temperatures due to decreased eluent viscosity and faster mass transfer, which was especially beneficial for larger compounds and resulted in dramatic improvement in efficiency. A possible explanation of the abnormal behaviour of oligomeric procyanidins is presented. Our findings indicate that new column formats, when used under optimal conditions, significantly improve the speed and/or efficiency of reversed phase liquid chromatographic analyses of proanthocyanidins.

1. Introduction

Phenolic compounds are among the most studied, yet complex group of natural compounds. These molecules are of particular interest due to their wide range of health benefits, including antioxidant, anti-hypertensive, anti-depressant and anti-inflammatory activities [1–3], as well as the influential roles they are known to play in the determination of food quality [4,5]. Despite recent advances in phenolic analysis [6], the high complexity and diversity of chemical properties of these molecules continues to hamper their detailed analysis. In fact, there is a continuous demand for faster and more efficient methods for the routine and in-depth analysis of phenolic compounds.

Proanthocyanidins are a subclass of phenolic compounds, which, due to their complexity, constitute a severe analytical challenge. Natural proanthocyanidins vary widely in terms of molecular weight (MW) and isomeric structures, with the result that current chromatographic methods for their analysis are unable to provide complete resolution. In order to design improved methods for proanthocyanidin analysis, a better understanding of the chromatographic behaviour of these compounds is required.

With recent developments in HPLC column technology and stationary phase chemistries, newly designed and improved HPLC columns continue to be introduced on the market. Of these, the most important developments which have found application for phenolic analysis include the use of smaller particle-packed columns and/or elevated temperatures to improve the HPLC

* Corresponding author. Tel.: +27 21 808 3351; fax: +27 21 808 3360.
E-mail address: ajdevill@sun.ac.za (A. de Villiers).

0021-9673/$ – see front matter © 2012 Elsevier B.V. All rights reserved.
doi:10.1016/j.chroma.2012.02.067

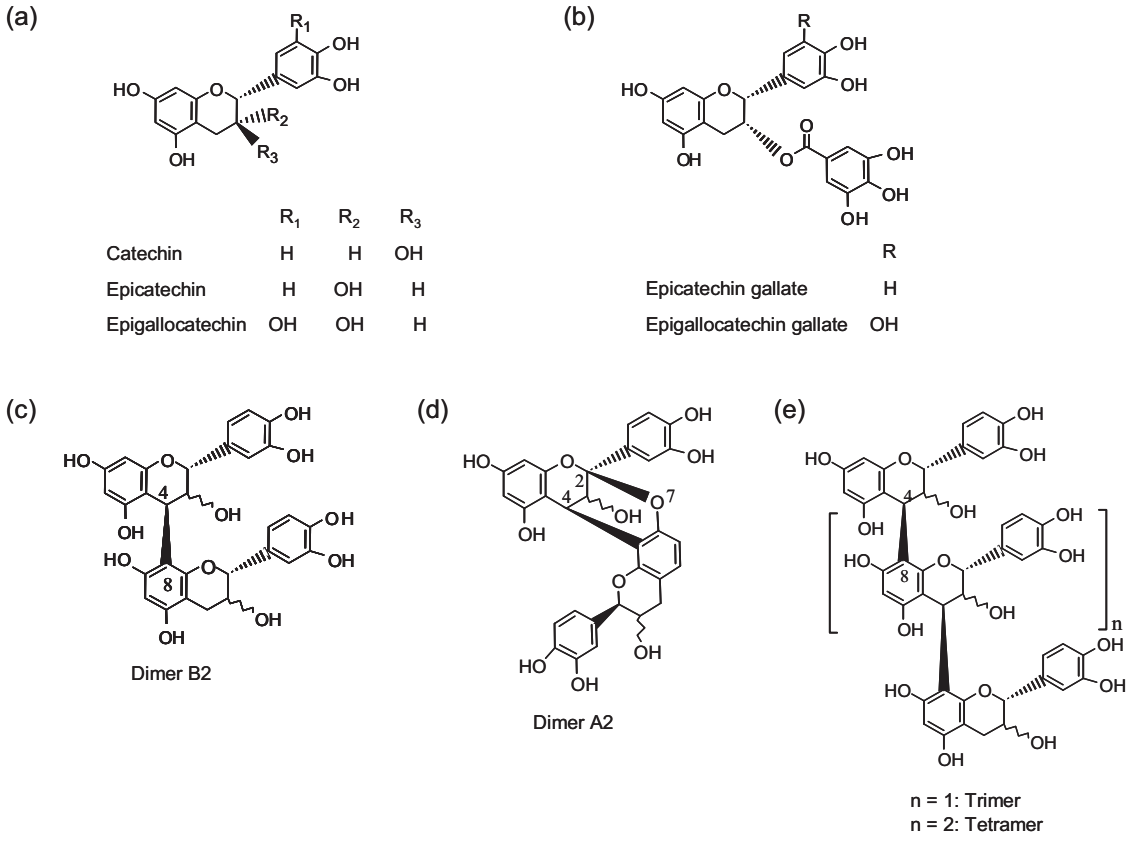

Fig. 1. Chemical structures for different phenolic compounds under investigation.

separation of phenolic compounds [7–21]. However, there remains uncertainty in recent literature about the quantitative benefits of these approaches compared to conventional HPLC methods for phenolic determination.

Given the versatility of new column and instrumental developments, analysts are presented with the challenge of having to select a column and instrument that are best suited for an intended application, as they are faced with a wide range of selectivities and column formats to choose from [22]. As a result, method development becomes a lengthy process and column selection a difficult task.

The availability of methods such as the kinetic plot method (KPM) that allows one to gain a rapid in-depth understanding of the performance limits of different chromatographic supports [23–26] strongly facilitates these assessments. The most attractive feature of the KPM, in relation to classical methods, lies in its ability to combine plate height data with other relevant parameters such as column permeability, mobile phase viscosity and maximum operating pressure to provide plots from which attainable efficiencies and corresponding analysis times for specific system configurations can easily be deduced [23,24]. Inclusion of this information becomes especially relevant when a comparison of the performance of differently shaped and sized chromatographic supports is sought, as there is no need to specify a common reference length [23,24]. This knowledge is invaluable when designing methods for targeted groups of compounds as it helps the analyst to make an informed decision regarding the choice of column and/or analysis conditions. Also of importance is the fact that the chemical composition of real world samples can differ significantly, resulting in widely varying chromatographic behaviours as a function of the physico-chemical properties of the target analytes [7].

In view of the precedent discussion, the current study was aimed at investigating the potential benefits of a new generation of C18 columns packed with both fully porous and superficially porous particles for proanthocyanidin analysis by means of a detailed kinetic evaluation. For this purpose, selected proanthocyanidin compounds covering a range of functionalities and molecular weights were used as test analytes (Fig. 1). A critical comparison of the kinetic performance of the different columns as well as a discussion on the practical implications for proanthocyanidin analysis is presented.

2. Experimental

2.1. Reagents and materials

Standards of (−)-epicatechin (EC) and (±)-catechin (C), (−)-epigallocatechin (EGC) and (−)-epicatechin gallate (ECG) were purchased from Sigma Aldrich (Steinheim, Germany). Procyanidin A2 (dimer A2), procyanidin B2 (dimer B2) and (−)-epigallocatechin gallate (EGCG) standards were purchased from Extrasynthèse (Genay, France). Trimeric and tetrameric procyanidin standards were preparatively isolated and purified in our laboratory by hydrophilic interaction chromatography (HILIC) and reversed-phase liquid chromatography (RP-LC) and characterised using mass spectrometry (MS). HPLC grade acetonitrile and formic acid were purchased from Merck (Darmstadt, Germany). Deionised water was obtained using a Milli-Q water purification system (Millipore, Milford, MA, USA). All solutions were filtered through 0.45 μm HVLP membrane filters (Millipore) and degassed in an ultrasonic bath (Branson Model 3510, Danbury, USA) before use.

Table 1
Retention factors, molecular masses and diffusion coefficients for the phenolic standards used in the study.

Compound	Retention factor (k)	Molecular mass (g/mol)	Diffusion coefficients[a] (m^2/s)
Epigallocatechin (EGC)	3.5 ± 0.2	306	5.15×10^{-10}
Catechin (C)	4.7 ± 0.4	290	5.24×10^{-10}
Epicatechin gallate (ECG)	7.5 ± 0.4	442	4.08×10^{-10}
Procyanidin dimer B2 (dimer B2)	9.2 ± 0.7	578	3.48×10^{-10}
Procyanidin dimer A2 (dimer A2)	9.3 ± 0.6	576	3.49×10^{-10}
Epicatechin (EC)	11.4 ± 0.7	290	5.24×10^{-10}
Epigallocatechin gallate (EGCG)	13.1 ± 1.9	458	4.05×10^{-10}
Procyanidin trimer (trimer)	6.4 ± 0.4	866	2.73×10^{-10}
Procyanidin tetramer (tetramer)	8.3 ± 0.6	1155	2.30×10^{-10}

[a] Diffusion coefficients as calculated at 25 °C according to [27].

2.2. Instrumentation

Plate height data for 5 cm columns were experimentally determined on an Acquity UPLC system consisting of a binary pump, degasser, autosampler, column oven, photodiode array (PDA) detector (500 nL flow cell, 10 mm path length), controlled by Waters Empower software (Waters, Milford, MA, USA). Sample volumes of 5 μL were injected using the full loop injection mode. The extra-column- and dwell volumes for this system were ~20 and 145 μL, respectively. An average external variance (σ^2_{ext}) of 0.11 s^2 was measured at 0.8 mL/min.

Plate height measurements for a 25 cm column were performed on an Alliance 2690 HPLC system equipped with a binary pump, degasser, autosampler, column oven, 996 PDA detector (8 μL flow cell, 10 mm path length), controlled by Millenium software (Waters). The pump and column outlet tubings were replaced with minimal lengths of 0.127 mm i.d. PEEK tubing to minimise the extra-column volume. Stainless steel tubing (83 cm, 0.01 in. i.d.) was connected between the injector and the column to preheat the mobile phase. The extra-column- and dwell volumes for this system were ~96 and 812 μL, respectively. An average external variance (σ^2_{ext}) of 2.22 s^2 was measured at 0.8 mL/min.

2.3. Chromatographic conditions

2.3.1. Plate height and system contribution measurements

Plate heights were measured for nine phenolic compounds on four different C18 columns using an isocratic mobile phase consisting of acetonitrile (ACN) and 0.1% formic acid in water (%v/v). Conditions were selected such that the retention factors for all compounds were between 3.5 and 15 (Table 1). The mobile phase compositions were adjusted in order to keep the retention factors constant on all columns. The column characteristics and the mobile phase compositions used for each column are presented in Table 2.

Stock solutions of 1000 mg/L of each standard were prepared in acetonitrile and individual samples with final concentrations of 25 mg/L of each standard and 1 mg/L of uracil (the unretained marker) were prepared such that the final solvent composition was similar to the mobile phase. Flow rates were systematically increased until the maximum column or instrument pressure was reached to ensure a good fitting of the data in the B- and C-term regions of the plate height curves. The maximum allowable pressures (ΔP_{max}) and permeabilities (K_{t0}) for individual columns are listed in Table 2. Measurements were performed in triplicate at each flow rate and experiments were performed at 25 °C and 50 °C. The average relative standard deviations for linear velocity- and plate height values measured for all compounds on all columns were 0.08 and 1.38%, respectively. For the determination of the system contribution, the column was replaced with a zero-dead volume union and uracil was injected under the same conditions.

2.3.2. Gradient analyses

Peak capacities for the gradient separation of a cocoa extract were calculated at different flow rates by injecting 2 μL of a cocoa extract (prepared using a modified method of Kelm et al. [28]) on the Kinetex column. The relevant gradient profiles are summarised in the Supplementary Information (Table S1). The mobile phases were 0.1% formic acid in water (% v/v) (A) and acetonitrile (B) and the column temperature 50 °C.

2.4. Data analysis and kinetic plots construction

For every component in the sample, the number of theoretical plates was calculated using the peak width at half height with Chemstation software (Agilent, Waldbronn, Germany) and an average of three measurements was used for each point. The linear velocity was calculated using the elution time (t_0) of uracil. All reported plate count (N), linear velocity (u_0, mm/s), column pressure (P, bar) and column permeability (K_{t0}, m^2) values were corrected for the system contribution in accordance with the following equations:

$$N_{corrected} = \frac{(t_R - t_{ext})^2}{(\sigma^2_{tot} - \sigma^2_{ext})} \quad (1)$$

Table 2
Columns and mobile phase compositions used at different temperatures.

Column	ΔP_{max} (bar)	K_{t0} (m^2)[d]	Mobile phase composition (% ACN)					
			25 °C			50 °C		
			Set 1[a]	Set 2[b]	Set 3[c]	Set 1[a]	Set 2[b]	Set 3[c]
Phenomenex Kinetex C18 (50 mm × 4.6 mm, 2.6 μm)	600	0.72×10^{-14}	8.3	14.7	12.3	5.7	11.9	9.4
Waters UPLC C18 (50 mm × 4.6 mm, 1.7 μm)	1000	0.34×10^{-14}	7.1	13.4	10.6	4.2	10.0	7.4
Waters Xbridge C18 (250 mm × 4.6 mm, 5 μm)	400	1.92×10^{-14}	7.5	13.7	10.8	4.0	9.9	7.3
Agilent Zorbax C18 (50 mm × 4.6 mm, 1.8 μm)	600	0.42×10^{-14}	9.1	15.7	13.0	6.5	12.8	10.0

[a] Set 1 contained EGC, C, procyanidin dimer B2, EC and EGCG.
[b] Set 2 contained ECG and procyanidin dimer A2.
[c] Set 3 contained procyanidin trimer and tetramers.
[d] Values given were calculated for set 1 at 25 °C on each of the columns.

where t_R denotes the solute retention time, t_{ext} is the time spent by the solute in the connecting tubing, σ^2_{tot} and σ^2_{ext} represent the total peak variance and external variance, respectively.

$$u_{0corrected} = \frac{L}{t_0 - t_{ext}} \quad (2)$$

where L is the column length.

$$K_{v0} = \frac{d_p^2}{\phi_0} = \frac{u_0 \eta L}{\Delta P_{col}} \quad (3)$$

in which d_p represents the particle diameter (m), ϕ_0 is the column flow resistance (dimensionless) and ΔP_{col} is the column pressure ($Pa = N/m^2$), obtained by subtracting the pressure drop in the connecting tubing (ΔP_{ext}) from the total pressure drop (ΔP_{tot}).

The reduced (dimensionless) plate heights (h) and linear velocities (ν) were calculated using:

$$h = \frac{H}{d_p} \quad (4)$$

$$\nu = \frac{u d_p}{D} \quad (5)$$

where H and u are the experimental plate height and linear velocity, respectively, while D is the diffusion coefficient (D, cm^2/s), calculated using the Wilke–Chang equation [27]:

$$D_{A,B} = 7.4 * 10^{-8} \frac{(\psi_B MW_B)^{0.5} T}{\eta_B \bar{V}_A^{0.6}} \quad (6)$$

where subscripts A and B symbolise the solute and the solvent, respectively, ψ is the association factor of the solvent (dimensionless), MW is the molecular weight of the solvent (g/mol), T is the temperature (K), η_B is the viscosity of the solvent (cP) and $\bar{V}$ is the molar volume of the solute (cm^3/g mol). The mobile phase viscosity for acetonitrile–water mixtures was calculated according to [29] based on the relationship:

$$\eta_{\chi,T} = 10^{(-2.063+(602/T)+0.071\chi+(62/T)\chi+0.504\chi^2-(346/T)\chi^2)} \quad (7)$$

where χ is the volumetric fraction of the organic solvent.

For the construction of kinetic plots, the following two equations, based on experimental parameters, were employed:

$$N = \frac{\Delta P_{\max}}{\eta} \left(\frac{K_{v0}}{u_0 H} \right)_{experimental} \quad (8)$$

$$t_0 = \frac{\Delta P_{\max}}{\eta} \left(\frac{K_{v0}}{u_0^2} \right)_{experimental} \quad (9)$$

Data were fitted using the Giddings model:

$$H = \frac{A u^n}{1 + D u^m} + \frac{B}{u} + Cu \quad (10)$$

where n and m are equal to 1.

3. Results and discussion

The goal of this study was to evaluate a set of new generation support materials for the improved separation of proanthocyanidins. Since it is known that the potential benefits of these phases depend to a large extent on the properties of the analytes under investigation [7], plate height curves and kinetic plots were constructed for a range of standard proanthocyanidins with different properties.

3.1. Van Deemter curves

The kinetic performance of four columns, an Acquity UPLC C18 and an Agilent Zorbax C18-SB, both packed with fully porous sub-2 μm particles, a Kinetex C18 packed with superficially porous 2.6 μm particles and an Xbridge C18 packed with fully porous 5 μm particles, were compared. Each column was operated close to its maximum allowable pressure in order to maximally exploit its ultimate performance limits. To assess the chromatographic performance of the different columns, Van Deemter (VD) curves for different phenolic compounds were constructed and are shown in Fig. 2. Upon inspection of the VD curves for the test analytes, no significant variations were observed in the chromatographic behaviour of low molecular weight compounds C, EC, EGC, ECG and EGCG (data not shown). Notable differences were, however, obvious for high molecular weight compounds (dimeric, trimeric and tetrameric procyanidin isomers) relative to the low molecular weight compounds. For visual clarity, only data for one representative small molecule and those of higher oligomers are therefore presented. The reader is referred to Tables 3a and 3b for summaries of optimal plate heights (H_{min}, h_{min}) and linear velocities (u_{opt}, ν_{opt}) for the individual compounds on each of the columns.

From the H_{min} data, it is evident that comparable performances are obtained for the 2.6 μm superficially porous Kinetex column and the sub-2 μm fully porous particle-packed columns, corresponding to minimum plate heights between 3.74 and 5.20 μm for smaller molecules, and values of 6.62–7.70 μm for the tetrameric procyanidin. On the other hand, the 5 μm column shows minimum plate heights ranging between 10.86 and 14.79 μm. Although these values are well within the theoretically expected H_{min} limits ($H_{min} = 2d_p$) for the respective fully porous particles sizes, the H_{min} values achieved on the Kinetex column (with the exception of the value obtained for the tetrameric procyanidin) are much lower than theoretically expected, indicating a better column packing quality and/or uniform particle size distribution for the superficially porous particles [30–32].

To compare particles with different sizes, columns should preferentially be evaluated in terms of their reduced plate heights ($h = H/d_p$) and reduced linear velocities ($\nu = ud_p/D$) [25,33]. The reduced plate height curves presented in Fig. 2 and the data summarised in Tables 3a and 3b confirm that the 2.6 μm superficially porous column performs significantly better than all other columns, with h_{min} values ranging between 1.4 and 2.0. The sub-2 μm and 5 μm fully porous particles display a similar performance with h_{min} values in the range of 2.0 and 3.0 for small molecules and higher values for the procyanidin tetramer. Previous studies have reported similar low h_{min}-values for the superficially porous particles and have ascribed this to the low eddy dispersion (A-term), resistance to mass transfer (C-term) and recently also to the reduced B-term band broadening associated with the morphology of this particle type [32,34–36].

It is further noted that smaller compounds exhibit higher optimal linear velocities and very flat C-term (resistance to mass transfer) slopes, implying that linear velocities higher than the optimum values can be used without significant losses in efficiency. This trend reverses as the size of the molecule increases. These differences may be partially attributable to inaccuracies in the estimation of diffusion coefficients of especially the larger molecules according to the Wilke–Chang equation. Another possible cause for this unexpected behaviour of the high MW procyanidins may lie in the rotational isomerism of these molecules (refer to Section 3.4). This trend is observed on both small and large particle columns, although the effect is much more detrimental on the 5 μm column due to the dependence of the C-term on the particle size.

Compared to the 5 μm XBridge column, the small-particle packed columns provide minimum plate heights for the small phenolic compounds which are 2.6–2.9 times lower, and optimal linear velocities which are 2.0–2.1 times higher (Table 3a). This implies that by using shorter columns packed with sub-2 μm or superficially porous particles operated at optimal linear velocities, speed gains in the order of 4.7–5.0 times can be obtained compared to

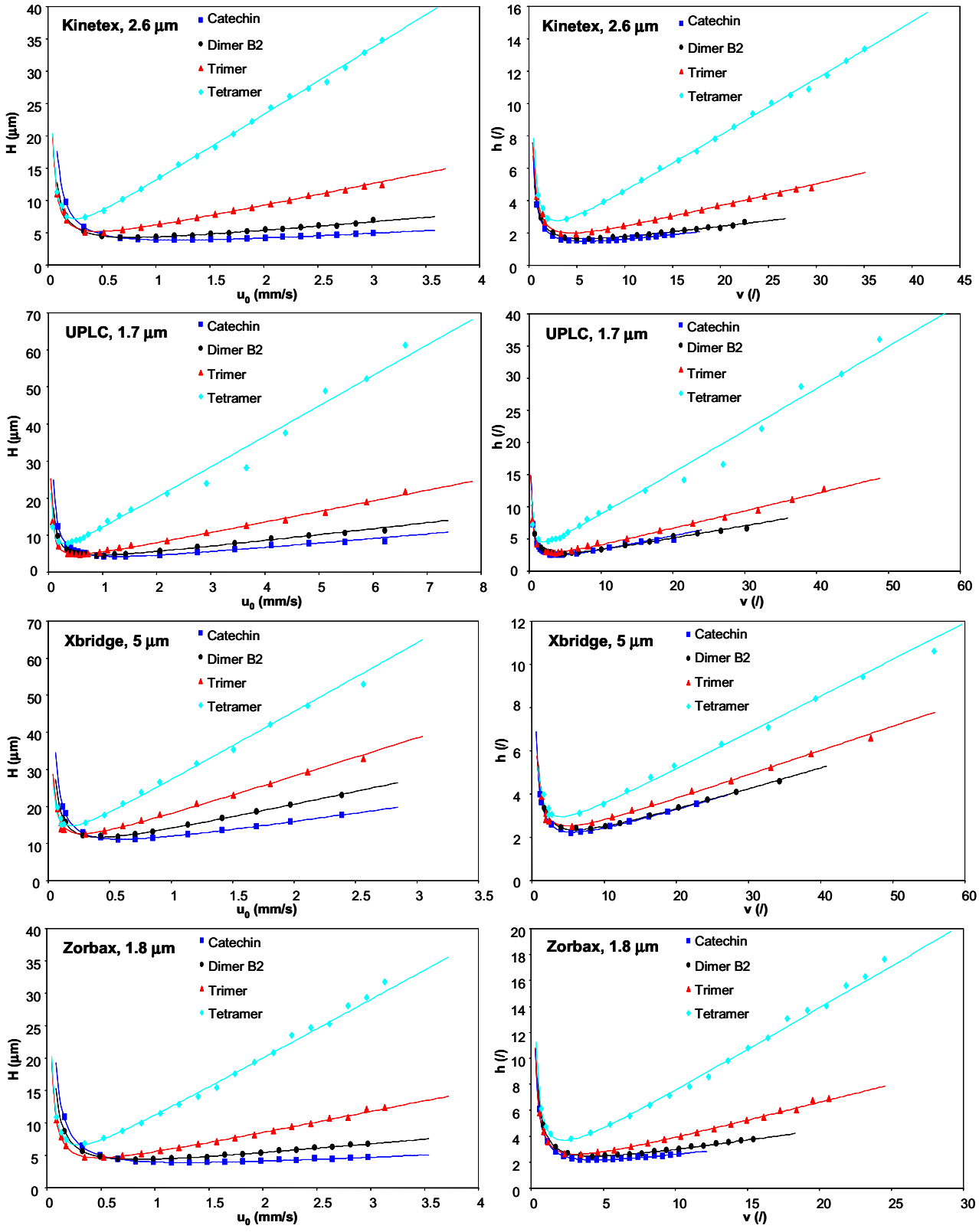

Fig. 2. Van Deemter and reduced plate height curves for catechin (blue), procyanidin dimer B2 (black), trimeric procyanidin (red) and tetrameric procyanidin (cyan) on the four columns under investigation at 25 °C. (For interpretation of the references to colour in this figure legend, the reader is referred to the web version of the article.)

Table 3a
Optimum experimental data obtained for the different phenolic compounds on four different columns at 25 °C.

Compound	Kinetex C18 (d_p = 2.6 μm)				UPLC C18 (d_p = 1.7 μm)				Xbridge C18 (d_p = 5 μm)				Zorbax C18 (d_p = 1.8 μm)			
	H_{min}[a]	u_{opt}[b]	h_{min}	v_{opt}	H_{min}[a]	u_{opt}[b]	h_{min}	v_{opt}	H_{min}[a]	u_{opt}[b]	h_{min}	v_{opt}	H_{min}[a]	u_{opt}[b]	h_{min}	v_{opt}
EGC	3.74	1.07	1.45	5.07	4.14	1.12	2.27	3.37	10.86	0.51	2.18	5.51	3.75	1.06	2.09	4.05
C	3.86	1.18	1.49	5.83	4.24	1.27	2.48	3.98	11.16	0.59	2.21	5.42	3.90	1.30	2.17	4.55
Dimer B2	4.29	0.79	1.63	6.26	4.62	0.90	2.57	4.32	11.72	0.43	2.38	8.15	4.42	0.85	2.43	4.27
EC	4.16	1.53	1.57	8.35	4.94	1.78	2.91	6.69	11.95	0.85	2.39	6.77	4.18	1.76	2.26	6.26
EGCG	4.53	1.36	1.71	7.54	5.06	1.41	2.94	5.98	12.98	0.68	2.57	8.75	4.39	1.51	2.44	6.61
ECG	4.29	1.25	1.63	8.15	4.68	1.31	2.73	4.68	12.25	0.65	2.44	9.57	4.37	1.37	2.41	6.47
Dimer A2	4.16	1.06	1.60	8.17	4.51	1.15	2.65	4.76	12.08	0.56	2.40	6.71	4.37	1.22	2.41	6.62
Trimer	5.20	0.48	1.94	4.93	4.88	0.51	2.76	3.62	12.67	0.28	2.49	5.58	4.67	0.49	2.60	3.46
Tetramer	7.16	0.26	2.85	3.90	7.70	0.27	4.60	2.67	14.79	0.19	3.02	2.30	6.62	0.30	3.82	2.74

[a] H_{min} is given in μm.
[b] u_{opt} is given in mm/s.

Table 3b
Optimum experimental data obtained for the different phenolic compounds on four different columns at 50 °C.

Compound	Kinetex C18 (d_p = 2.6 μm)				UPLC C18 (d_p = 1.7 μm)				Xbridge C18 (d_p = 5 μm)				Zorbax C18 (d_p = 1.8 μm)			
	H_{min}[a]	u_{opt}[b]	h_{min}	v_{opt}	H_{min}[a]	u_{opt}[b]	h_{min}	v_{opt}	H_{min}[a]	u_{opt}[b]	h_{min}	v_{opt}	H_{min}[a]	u_{opt}[b]	h_{min}	v_{opt}
EGC	4.06	1.15	1.54	4.28	4.55	1.85	2.51	2.95	10.65	0.84	2.13	5.24	4.46	1.60	2.41	3.82
C	4.25	1.18	1.64	3.69	4.59	2.20	2.66	2.91	10.91	1.00	2.21	5.16	4.62	1.82	2.52	3.76
Dimer B2	4.24	0.91	1.64	4.75	4.63	1.70	2.65	4.37	11.24	0.75	2.25	6.45	4.66	1.18	2.52	4.14
EC	5.16	1.39	1.97	4.21	4.96	3.54	2.94	8.26	11.59	1.36	2.32	8.55	5.20	2.02	2.83	4.09
EGCG	5.13	1.15	1.93	4.77	4.99	2.76	2.96	7.14	12.20	1.14	2.42	8.87	4.95	1.60	2.67	4.42
ECG	4.54	1.31	1.73	5.20	5.02	2.40	2.96	5.99	11.65	1.08	2.36	9.80	4.79	1.66	2.62	4.93
Dimer A2	4.43	1.20	1.68	6.09	4.77	2.17	2.84	7.02	11.58	0.96	2.34	8.60	4.62	1.51	2.53	4.62
Trimer	4.41	0.69	1.72	5.25	5.11	1.12	2.97	5.18	12.06	0.58	2.37	5.30	5.28	0.74	2.87	3.68
Tetramer	5.16	0.48	2.09	4.99	6.39	0.81	3.74	5.12	12.68	0.46	2.51	6.29	6.04	0.52	3.42	2.62

[a] H_{min} is given in μm.
[b] u_{opt} is given in mm/s.

conventional 5 μm phases (provided that the columns are operated within their respective pressure limitations). This gain is reduced for the larger procyanidins, corresponding to a value of 3.3–3.8 for the tetrameric compound.

3.2. Kinetic plots of phenolic compounds on different columns

Kinetic plots represent one of the best tools currently available to compare the performance of different chromatographic supports [25]. Plotting the plate number (N) as a function of analysis time (t_R), the type of support that offers the fastest separation for a given efficiency or the highest number of plates in a given analysis time can easily be deduced. For an intrinsic evaluation of columns with different packing properties, separation impedance plots representing the separation impedance (E_0) vs the plate count (N), or the reduced form E_0 vs N/N_{opt}, are more suited as they reflect the pure packing quality of the columns, independent of the applied pressure and/or the mobile phase properties [23]. Kinetic plots of t_R vs N and E_0 vs N/N_{opt} for two representative analytes on the four columns are shown in Fig. 3A and B, respectively.

From Fig. 3A, it can be seen that for a fixed analysis time, the 2.6 μm Kinetex column performs better than all other columns over the entire range of practically relevant efficiencies (~25 000–250 000). The 1.7 μm UPLC column provides very fast separations for efficiencies ranging between 10 000 and 25 000. Fig. 3A also shows that optimum performance for small molecules is obtained in the C-term dominated region using short columns packed with small particles. Large molecules are optimally separated at low flow rates (B-term dominated region) and highly efficient separations can be achieved on very long columns, however at the cost of long analysis times. In addition, Fig. 3A shows that efficiencies greater than 160 000 are not attainable on columns packed with sub-2 μm particles under the given pressure constraints when analysing small phenolic molecules. However, when

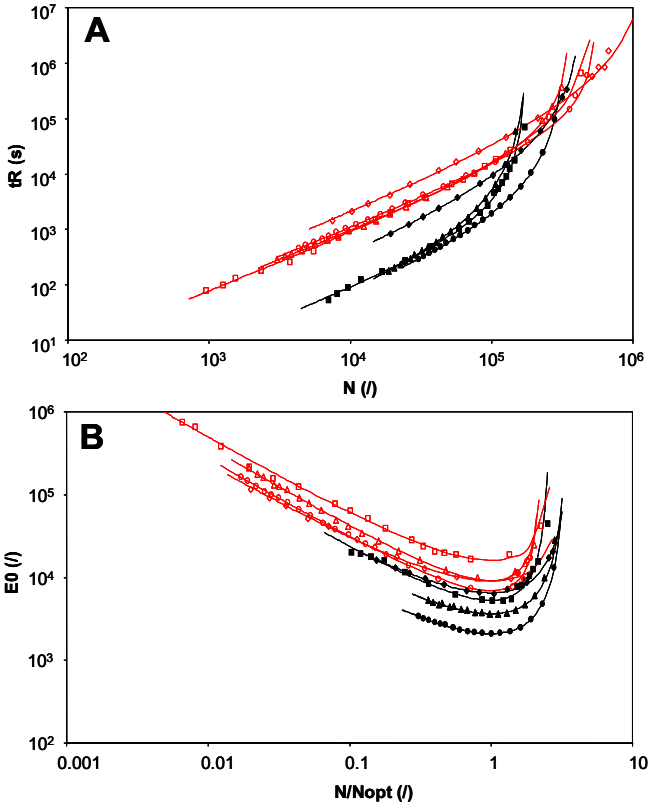

Fig. 3. Kinetic plots of (A) t_R vs N and (B) E_0 vs N/N_{opt} for catechin (black, closed symbols) and the tetrameric procyanidin (red, open symbols) on the 2.6 μm Kinetex (circles), 1.7 μm UPLC (squares), 5 μm Xbridge (diamonds) and 1.8 μm Zorbax (triangles) columns at 25 °C. (For interpretation of the references to colour in this figure legend, the reader is referred to the web version of the article.)

these columns are operated at the optimal flow rate for the larger procyanidins, they outperform the larger particles in the efficiency range up to 250 000 plates. Because of the low backpressures associated with the superficially porous particles, long (2.9 m) Kinetex columns can also be used for small molecule analysis to reach efficiencies up to ~280 000 in an analysis time of roughly 26 h, while this efficiency range can be extended to ~485 000 (on a 3.6 m column) when dealing with large molecules. It is only for efficiencies in excess of 300 000 for small molecules and 500 000 for large molecules that the 5 μm Xbridge column outperforms all other columns. These efficiencies are, however, outside the practical range of most HPLC applications as they require column lengths longer than 5 m. It is clear from Fig. 3A that for separations requiring conventional efficiencies ($N \sim 25\,000$), all three small particle columns will provide much faster analyses compared to the 5 μm phase when operated at optimal conditions and maximum pressure. For small molecules, this translates to a 4.3–5.2 times reduction in analysis time, whereas for the tetrameric procyanidin the gain is reduced to 2.0–2.3. Alternatively, the benefits of these phases (within the range of optimal efficiencies) can be exploited to increase the efficiency for a given analysis time.

Fig. 3B shows reduced separation impedance plots for catechin and the tetrameric procyanidin on the four columns. From these plots, it is clear that the Kinetex column provides the lowest E_0 values, with minimum values of 2084 and 6911 for catechin and the tetramer, respectively, while these values range between 3640 and 6505 for catechin and 9041 and 16 137 for the tetramer on the other columns. From the observed trend, it can be generalised that the separation impedance number for a given column increases as the size of the molecule increases. The E_0 value of around 2000 obtained for the Kinetex column is generally considered to be very good, reflecting the higher permeability and good packing quality of this column [30]. This good performance has been accredited to the uniform particle size distribution achieved during the manufacturing process of these particles, which leads to a very homogeneous packing [37].

3.3. Effect of temperature on plate height behaviour

The benefit of using elevated temperatures in liquid chromatographic separations is well documented in literature. An increase in temperature is associated with a reduction in mobile phase viscosity and a faster analyte diffusion, which improves the mass transfer of analytes between the mobile and stationary phases and therefore results in better efficiency at higher flow rates [38–43]. To study the effect of temperature in phenolic analysis, two temperatures, 25 and 50 °C, were selected for evaluation. A maximum temperature of 50 °C was selected to compare all columns at equivalent temperatures (the maximum temperature of the Kinetex column is 60 °C according to the manufacturer) and to reduce the risk of thermal degradation, since proanthocyanidins are known to be susceptible to thermal degradation and epimerisation reactions [44,45]. Fig. 4 represents Van Deemter plots for phenolic standards on four different columns as obtained at the two temperatures. From these plots, it can immediately be seen that the C-term slope flattens as temperature increases. This results in a broadened range of optimal linear velocities towards high flow rates, implying that faster analyses can be performed at higher temperatures without a significant loss in efficiency. For small molecules, an increase in analysis temperature was only found to be useful for increasing analysis speed, since the maximum attainable efficiencies were roughly unchanged. This behaviour is in agreement with previous reports where it was attributed to decreased resistance to mass transfer due to increased diffusion coefficients at high temperatures as well as improved secondary interaction kinetics [39,40,46–48]. Interesting to note is the differences in reduced plate height curves as a function of temperature for the Kinetex and Zorbax columns in Fig. 4. Since the reduced velocity takes changes in D into account, curves at both temperatures are expected to overlap, as is indeed observed for the small molecules on the UPLC and XBridge columns. The abnormal increase in reduced plate height has previously been observed for superficially porous (Halo) phases, where this behaviour was tentatively ascribed to "unexpected variation of the eddy dispersion with the linear velocity at high temperatures, which might be related to the roughness of the external surface of the superficially-porous particles" [49]. For the Zorbax column, this phenomenon may be a result of the larger internal diameter of this column (4.6 mm i.d.), resulting in less effective preheating of the mobile phase at high flow rates.

Temperature elevation proved to be much more beneficial for larger molecules, leading to a dramatic improvement in efficiency and a significant gain in analysis speed on all particle sizes. This is especially clear from the reduced plate height curves for the larger molecules on all columns. The minimum plate heights for the trimeric and tetrameric procyanidins were reduced, while the optimal linear velocities shifted to higher values at 50 °C compared to 25 °C. A comparison of the kinetic data obtained for the trimeric and tetrameric procyanidin isomers at 25 and 50 °C shown in Tables 3a and 3b indicate efficiency gains ranging between 5 and 18% for the trimer and 17 and 39% for the tetramer, with the highest gain on the superficially porous particles. In addition, analysis speed increased by factors between 1.4 and 2.2 for the trimer and 1.8 and 3 for the tetramer, with the highest gain on the UPLC (1.7 μm) column. Possible reasons for the unexpected decrease in minimum plate height for oligomeric procyanidins as a function of temperature, which cannot be explained based on increased diffusion and lower viscosity, will be discussed in the next section.

In summary, both sub-2 μm fully porous and 2.6 μm superficially porous particles delivered superior performance compared to the 5 μm particles, a fact accredited to the good mass transfer properties of small particles. For 5 μm particles, an increase in temperature resulted in improved chromatographic performance in the high linear velocity region for both small and large molecules. The fact that optimum column performance was only achieved at a much higher temperature for larger compounds indicates that high temperature is necessary for faster, efficient separation of high MW procyanidins, provided that analyte and column stability are ensured.

3.4. Effect of analyte properties and retention factor on kinetic performance

It is well known that the kinetic performance of a chromatographic support is highly influenced by the properties of the analyte under investigation [7]. To better understand the effect of analyte molecular weight on kinetic performance, plots of t_0/N^2 vs N were constructed for four compounds with molecular weights ranging between 290 and 1155 g/mol. From the curves shown in Fig. 5, it is evident that the optimum plate count (N_{opt}) is gradually shifted to higher N values as the weight of the molecule increases. This means that large molecules are optimally separated at low flow rates on long columns (B-term dominated region), while small molecules are optimally separated on short columns at high flow rates (C-term dominated region). These variations are expected for analytes with smaller diffusion coefficients. However, the increase in the minima of the curves observed especially for the tetrameric procyanidin is unexpected.

The abnormal plate height behaviour of the high MW procyanidins (Figs. 2–5), and especially the decrease in minimum plate height observed for these molecules as a function of temperature (Fig. 4), indicates that secondary equilibria may play a role in their chromatographic behaviour [50]. Similar kinetic behaviour was

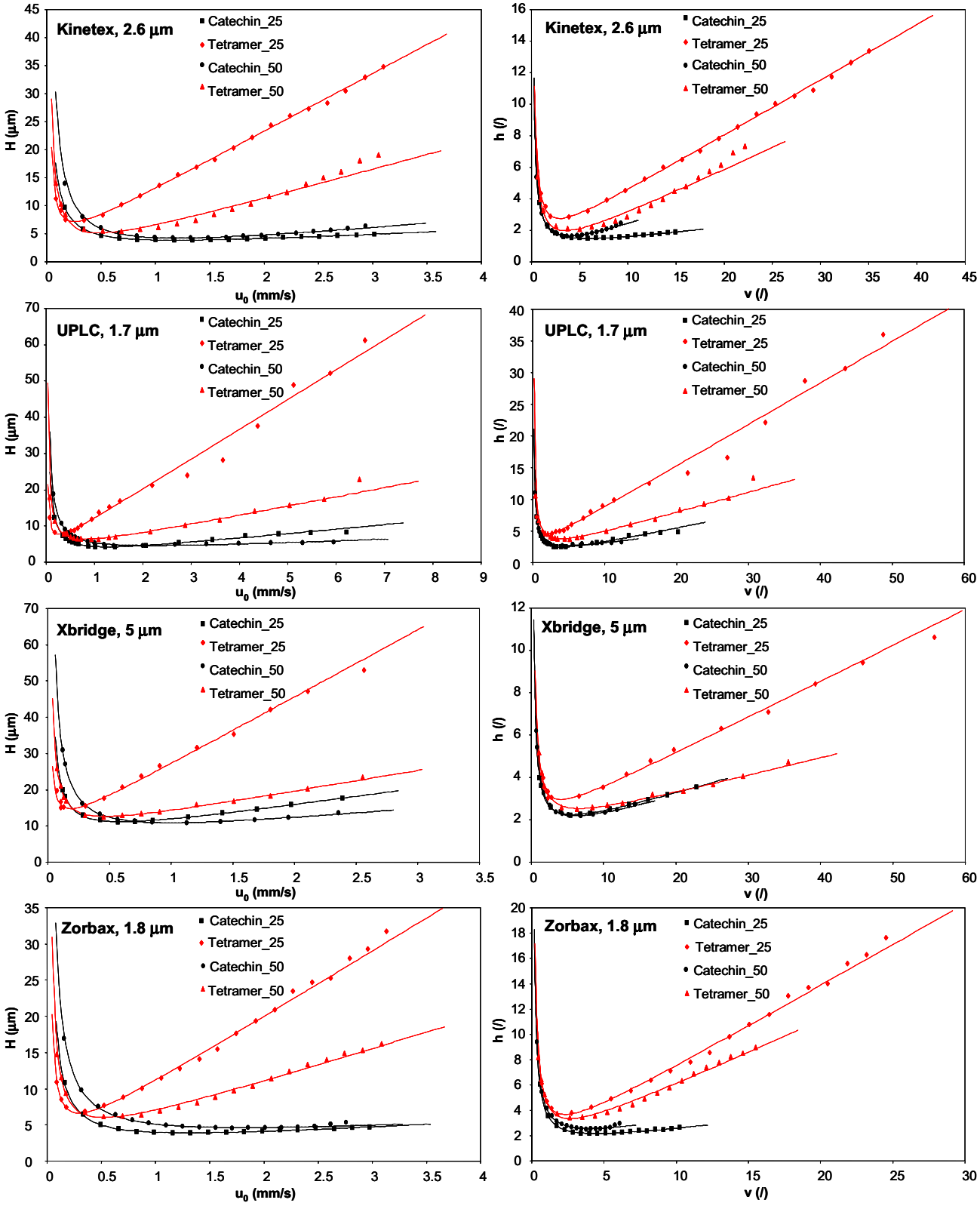

Fig. 4. Experimental Van Deemter plots and reduced VD plots for a small (catechin, black, ■/●) and a big (tetrameric procyanidin, red, ♦/▲) molecule on four columns at 25 and 50 °C. (For interpretation of the references to colour in this figure legend, the reader is referred to the web version of the article.)

previously observed for anthocyanins [12,13], which are known to exist in several chemical forms in solution. We have shown how the pH- and temperature dependant equilibria between these forms are responsible for higher minimum plate heights for anthocyanins [12]. In essence, the interconversion between chemical species on the same time scale as the chromatographic separation is responsible for additional band broadening. In the case of anthocyanins, an increase in temperature results in faster

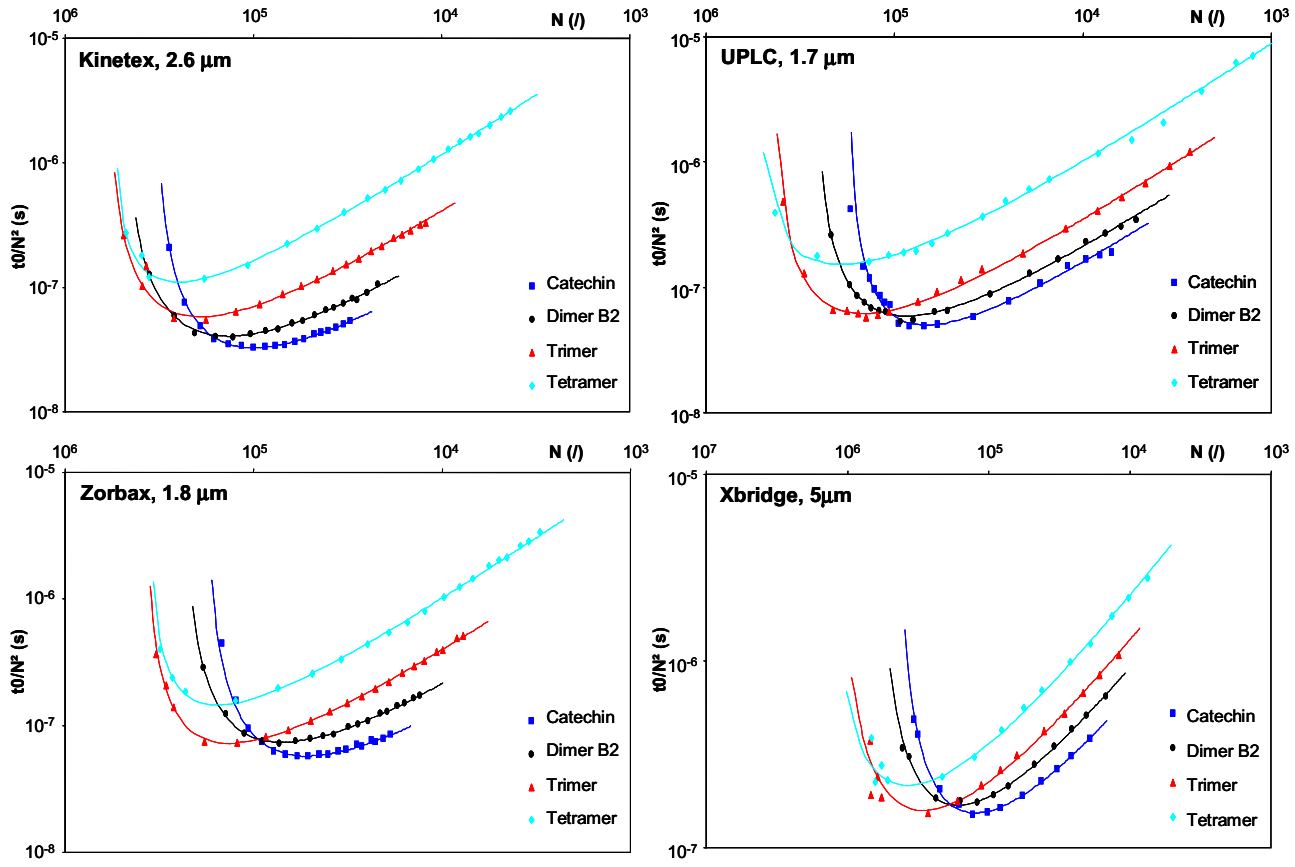

Fig. 5. t_0/N^2 vs N plots for catechin (blue, squares, MW = 290 g/mol), procyanidin B2 (black, circles, MW = 579 g/mol), a procyanidin trimer (red, triangles, MW = 866 g/mol) and a procyanidin tetramer (cyan, diamonds, MW = 1155 g/mol) on the Kinetex, UPLC, Zorbax and Xbridge columns obtained at 25 °C. (For interpretation of the references to colour in this figure legend, the reader is referred to the web version of the article.)

kinetics of the interconversion reaction, and therefore a reduction in the minimum plate height at higher temperatures. A similar phenomenon may be responsible for the same behaviour observed here for the procyanidins.

Proanthocyanidins are subject to epimerisation reactions involving the C-2 carbon (Fig. 1) [51,52]. No kinetic data on epimerisation reactions involving oligomeric procyanidins are available, although for monomeric proanthocyanidins this reaction is very slow (compared to the time scale of chromatographic separation) [52]. It can be confirmed using the approach reported in [12,50] that this reaction is much too slow to affect chromatographic peak shapes. This is supported by the fact that individual isomers are easily separated in RP-LC, which would not be the case if the reaction occurred in the timeframe of the chromatographic separation.

Another more likely explanation for this behaviour may lie in the temperature-dependant rotation of (epi)catechin units around the inter-flavonoid bond of oligomeric B-type procyanidins [53]. This phenomenon may be observed in the detection of rotational isomers of peracylated dimeric procyanidins at ambient temperatures by nuclear magnetic resonance (NMR) [54–56]. For native procyanidins, first-order NMR spectra are observed due to the relatively fast (on the NMR time-scale) interconversion between these rotational isomers, although they may be detected in the fluorescence time domain. Due to a lack of kinetic data on this rotation reaction for higher MW procyanidins, we could not quantitatively confirm that this phenomenon is responsible for band broadening at low temperature chromatographic separations. However, since the individual isomers of procyanidins (catechin and epicatechin) are easily separated in RP-LC, and for higher MW procyanidins retention is primarily affected by the properties of the bottom terminal unit [18,57], it is hypothesised that the individual rotational isomers will display different retention under RP-LC conditions. In this case, rotational isomerism on the same time scale of the chromatographic separation will lead to band broadening. This hypothesis may be tested by comparing the chromatographic behaviour of B-type procyanidins (where rotation occurs freely around the inter-flavonoid bond) with that of the corresponding A-type procyanidin (Fig. 1), where the additional ether linkage is expected to hinder free rotation of the subunits.

Fig. 6A compares the plate height curves measured for A-type and B-type procyanidin dimers on the Zorbax column at 25 °C. A slightly higher minimum plate height and C-term slope are observed in this figure for procyanidin B2. Note that these compounds have virtually identical retention factors and diffusion coefficients (Table 1), and therefore the effect of these parameters on the chromatographic behaviour of these molecules is negligible. Also note that the discrepancy between the plate height behaviour of monomeric- and tetrameric procyanidins is significantly lower for the 5 µm XBridge column. This can be ascribed to the much longer length (and therefore t_R values) of this column, which reduces the effect of secondary equilibria compared to the shorter 50 mm small-particle packed columns [12,13].

Analogously to anthocyanins, it is expected that an increase in temperature will lead to faster interconversion (in this case between rotational isomers) and therefore less band broadening due to secondary equilibria. Indeed, as observed in Fig. 6B, H_{min} and u_{opt} values for the B-type procyanidin dimer are closer to those of the corresponding A-type molecule at 50 °C.

If, as seems likely, this phenomenon is indeed responsible for the abnormal chromatographic behaviour of oligomeric procyanidins,

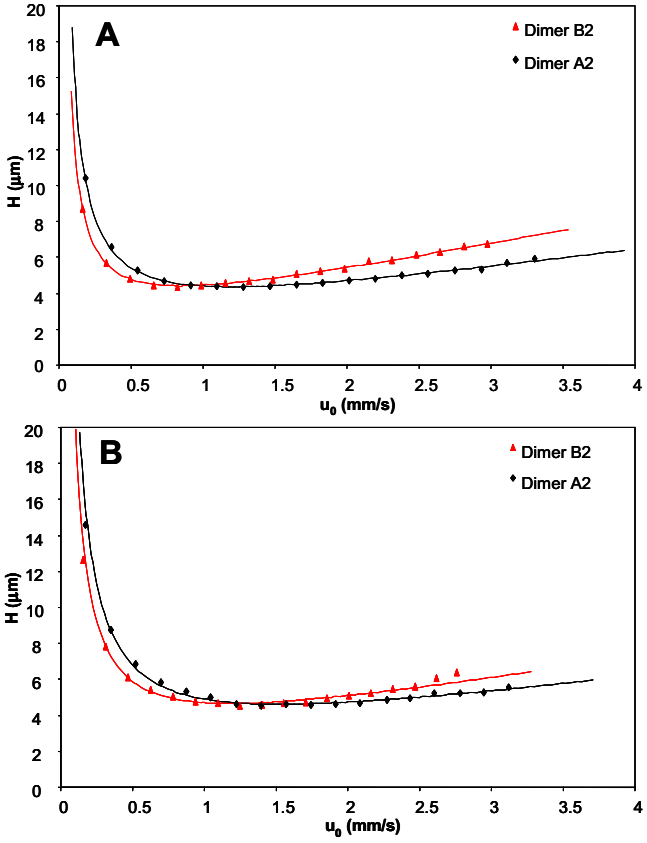

Fig. 6. Experimental Van Deemter plots for dimer B2 (▲) and dimer A2 (♦) obtained on the 1.8 μm Zorbax column at 25 °C (A) and 50 °C (B).

it is expected that the effect will be exacerbated with an increase in the degree of polymerisation (DP) (and therefore the number of interflavonoid bonds). Indeed, this is supported by the increasing H_{min} values observed in the sequence catechin ~ dimer A2 < dimer B2 < trimer < tetramer.

These data confirm that analyte properties significantly influence the performance of a chromatographic support, demonstrating the risk associated with making assumptions on the optimal chromatographic conditions based on a single analyte, even when working with compounds that have similar structures. Rather, when designing chromatographic methods for specific samples, it is essential to base decisions on kinetic data for as many as possible representative analytes of the mixture.

3.5. Effect of retention and the system contribution on plate height

To demonstrate the effect of the retention factor on chromatographic performance, two compounds (catechin (k = 5.1) and epicatechin (k = 11.5) with comparable diffusion coefficients and molecular weights (Table 1) were selected. In the absence of molecular weight and/or diffusion coefficient differences, it is expected that these compounds will exhibit very similar chromatographic behaviour. Van Deemter plots for these compounds on a Zorbax column at 25 °C and 50 °C are presented in Fig. 7. Note that this 4.6 mm i.d. column was selected for this comparison, since the effect of extra-column band broadening is significantly reduced (see further). Comparing the curves for catechin and epicatechin, it is evident that the latter shows a slightly flatter C-term slope at high flow rates, and especially much higher plate heights in the low linear velocities (B-term) region. These discrepancies can be attributed to the differences in retention factors: an increase in

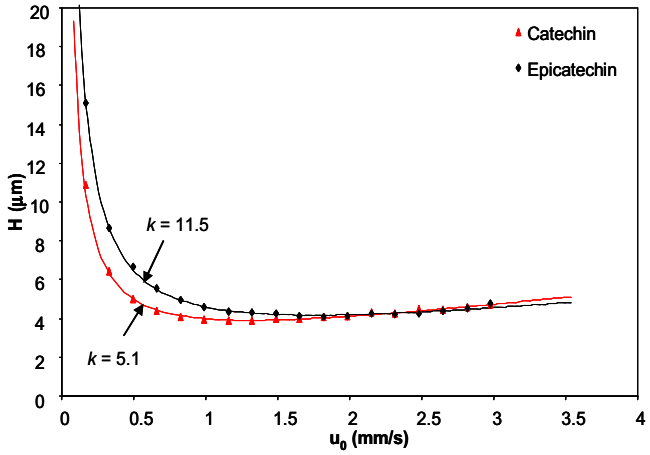

Fig. 7. Experimental Van Deemter plots for catechin (▲) and epicatechin (♦) obtained on the 50 mm × 4.6 mm, 1.8 μm Zorbax column at 25 °C.

retention is expected to lead to an increased B-term, as more time is available for longitudinal diffusion to occur [7], as seen for epicatechin with a k value of 11.5. Higher retention will also lead to a slight reduction in the C-term for the range of k values used here due to the dependence of this term on k. It should be noted that these trends were observed on all columns and that highly retained analytes displayed slightly higher B-terms compared to weakly retained ones. It is also worth mentioning that the differences in the C-term region were greatly reduced at 50 °C, for reasons discussed in Section 3.3.

In a chromatographic system, analyte zones broaden as a result of both the physical processes occurring inside the column, extra-column causes such as injection effects, detector volume, dwell volume between injector and detector as well as time-related effects such as acquisition rate and detector time constant [58–60]. Since the efficiency (N) of a peak in isocratic separations is directly related to its retention volume (V_n) or time (t_R) (as given by [59,61]):

$$N = \left[\frac{V_n}{\sigma}\right]^2 = a\left[\frac{V_n}{w}\right]^2 \quad \text{or} \quad N = \left[\frac{t_R}{\sigma}\right]^2 = a\left[\frac{t_R}{w}\right]^2 \tag{11}$$

where w denotes peak width (a is a constant determined based on the height where the peak width was measured), it is expected that peaks exhibiting smaller elution volumes (earlier eluting peaks with small k values) will be more affected by extra-column contributions. Furthermore, given that the peak elution volume decreases with decreasing column length and internal diameter, the detrimental effects of the extra-column contributions will also be much more pronounced on shorter, small i.d. columns than on conventional i.d. columns.

To quantify the effect of the column internal diameter on column performance, two 5 cm columns, a 1.7 μm, 2.1 mm i.d. UPLC and a 1.8 μm, 4.6 mm i.d. Zorbax column, were compared. Since the experiments were performed for compounds with similar retention factors on the same instrument and the column lengths and particles sizes of the two columns are similar (as per manufacturers specifications), it is expected that differences in performance will mainly be caused by differences in column diameter. Fig. 8 presents VD curves for weakly (EGC, k = 3.5), averagely (ECG, k = 7.5) and strongly retained analytes (EGCG, k = 13.1) on the two columns before and after accounting for extra-column contribution to band broadening according to Eq. (1). Comparing the plots of EGC on the two columns, no significant differences in performance are observed for the Zorbax column between data obtained with and without correction for the system contribution. Noteworthy differences can, however, be seen for the 2.1 mm i.d. UPLC column, where an efficiency loss of more than 40% is obtained for EGC, while the extra-column contribution

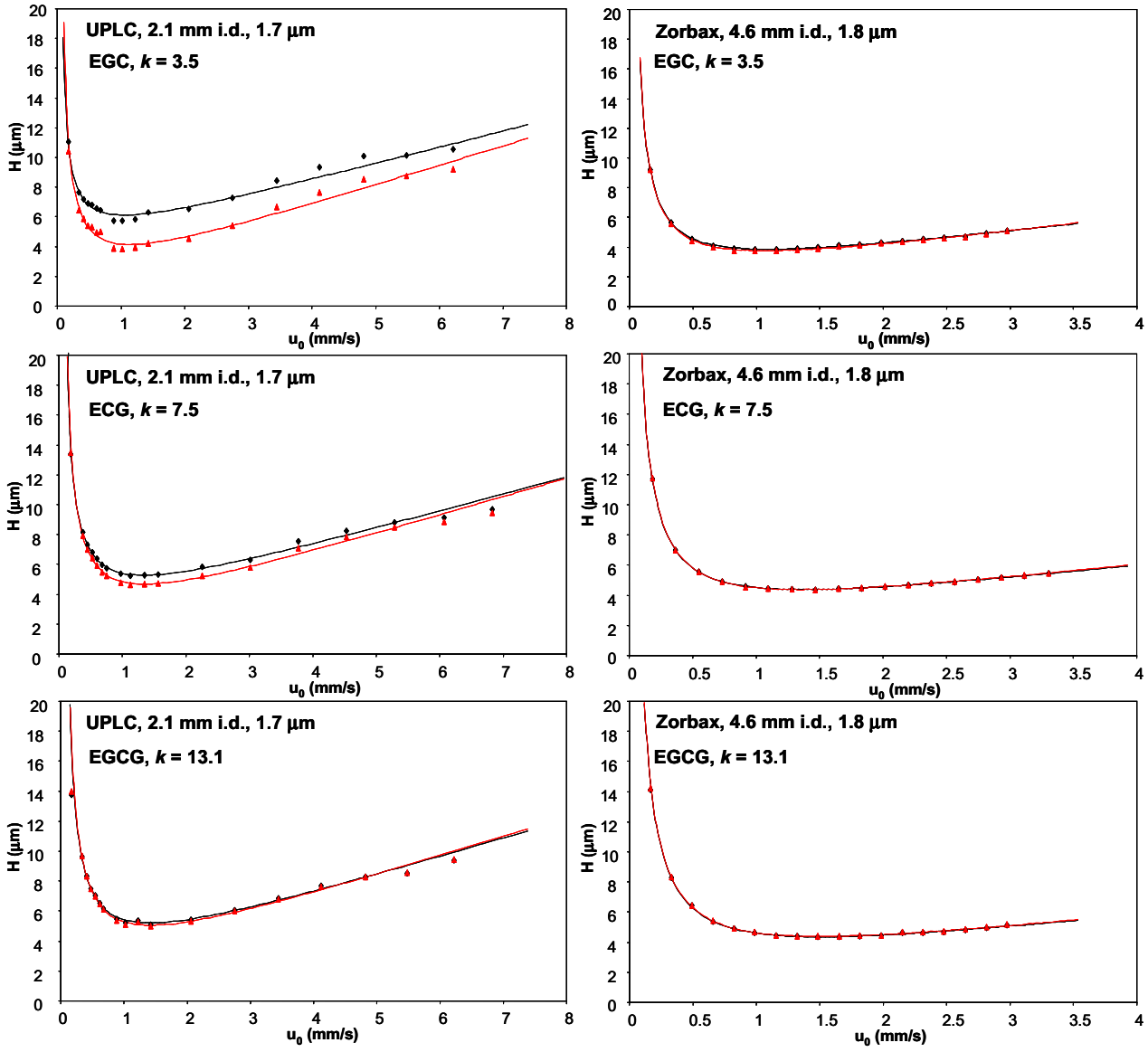

Fig. 8. Experimental Van Deemter curves obtained for the weakly retained (EGC, $k = 3.5$), averagely retained (ECG, $k = 7.5$) and well retained (EGCG, $k = 13.1$) analytes on the 1.7 µm UPLC and 1.8 µm Zorbax columns before (black, diamonds) and after (red, triangles) accounting for system contribution. (For interpretation of the references to colour in this figure legend, the reader is referred to the web version of the article.)

steadily decreases as retention increases. It can also be seen that the extra-column effects on column performance are virtually negligible for the most retained analyte on both columns.

While the efficiency of larger bore columns is not greatly affected by the extra-column effects, particular attention needs to be paid when working with narrow bore columns as significant loss in efficiency can be obtained for small k values ($k \leq 7$). Note that these experiments were performed on an Acquity UPLC system, which has a very low extra-column volume (~20 µL in the set-up used here). This approximates the lowest extra-column volumes of commercially available instrumentation [62,63], which further highlights the importance of using suitable instrumentation when employing short small particle-packed columns. The importance of this aspect is however somewhat reduced in gradient operation due to focussing of analytes at the head of the column.

While extra-column band broadening is of less importance for conventional bore columns (such as the 4.6 mm Zorbax column used here), this benefit is offset by the detrimental effects of frictional heating occurring on wider bore columns operated at high flow rates [64].

3.6. Practical implications of kinetic data on phenolic analysis

The data obtained for proanthocyanidins in this study show that the optimal linear velocity decreases as the particle size and size of the molecule increase. The dependence of the optimal linear velocity on the analyte molecular weight has severe practical implications for isocratic separations, as working outside the optimal velocity range will result in a significant loss of efficiency. As a consequence, for samples containing compounds spanning a wide range of molecular weights such as often encountered in

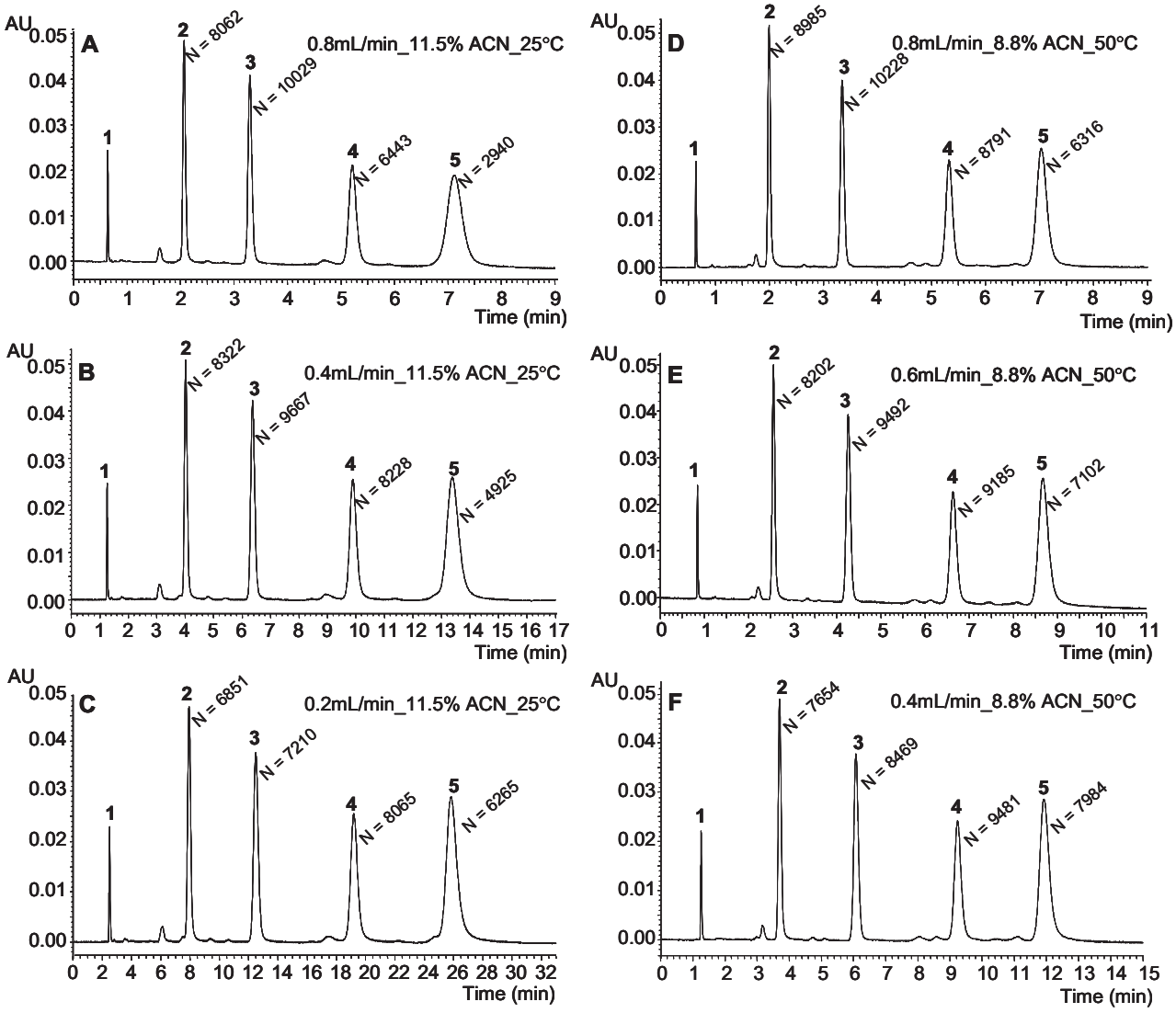

Fig. 9. Chromatograms for isocratic separations of a mixture of large and small procyanidins obtained on a Kinetex column (50 mm × 4.6 mm, 2.6 μm) at 25 and 50 °C using flow rates specified in the figure. Labels—1: uracil; 2: catechin; 3: epicatechin; 4: trimeric procyanidin and 5: tetrameric procyanidin.

phenolic extracts, it will be impossible to find a linear velocity where all compounds are optimally separated. This implies that a compromise between speed and efficiency will have to be made when dealing with samples of this nature.

To quantify this effect, a mixture of low- and high MW procyanidins were analysed at flow rates close to optimal for each set of compounds as well as at an intermediate flow rate (deduced from the kinetic data obtained at the two analysis temperatures used in this study). From the results presented in Fig. 9, it can be seen that an efficiency loss of 28% is obtained for epicatechin when working at (or close to) the optimal conditions for the large procyanidins (F = 0.2 mL/min), while efficiency losses of 20 and 53% are observed for the trimeric and tetrameric procyanidins, respectively, when working at the optimal flow rate for the smaller molecules (F = 0.8 mL/min) at 25 °C. However, when working at an intermediate flow rate (F = 0.4 mL/min), only about 4% and 21% efficiency-loss occurred for epicatechin and the tetrameric procyanidin, respectively.

A similar trend, albeit smaller, is obtained at 50 °C, where efficiency losses of 7 and 20% are obtained for the trimeric and tetrameric procyanidins, respectively, at 0.8 mL/min (close to optimal for small molecules) and 17% for epicatechin when working at 0.4 mL/min (close to optimal for large molecules). However, when an intermediate linear velocity (F = 0.6 mL/min) is used, efficiency losses of about 7, 3 and 11% were obtained for epicatechin and the trimeric and tetrameric procyanidins, respectively. From these results, it seems preferable to tune the chromatographic parameters to the optimal values for higher MW compounds when a mixture of low- and high MW phenolics are analysed, since the loss in efficiency is consistently less for the small molecules.

Most HPLC methods of phenolic analysis are performed on 5 μm columns using flow rates between 0.8 and 1.0 mL/min. While these flow rates are close enough to the optimal linear velocity for smaller molecules, they are clearly above the optimal linear velocity for larger molecules, which, in light of the unique chromatographic behaviour of these compounds, could explain the poor resolution commonly observed for high MW phenolics and procyanidins in particular. For small particle-packed columns, the trend is to further increase the flow rate due to the favourable plate height behaviour for small molecules. However, our results indicate that this will lead to a further reduction in efficiency, and therefore the benefits of these phases for proanthocyanidin analysis are best exploited at relatively low linear velocities, which would still deliver improved performance compared to conventional HPLC methods.

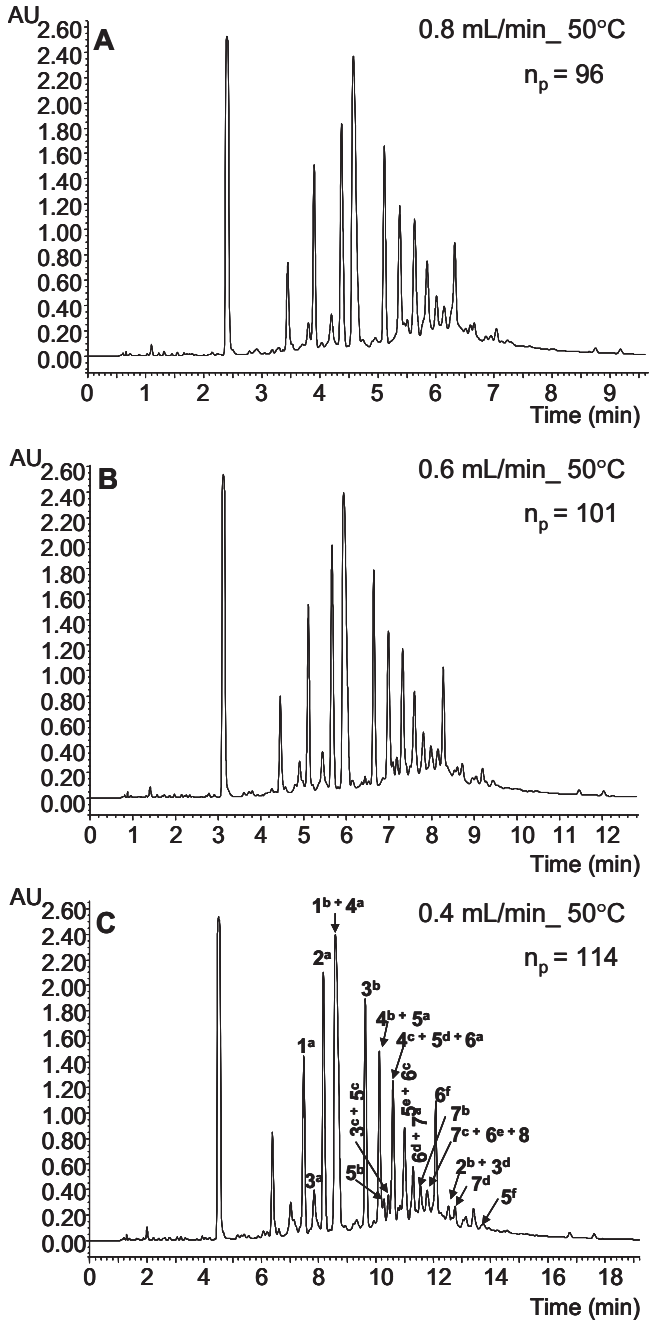

Fig. 10. Chromatograms for the gradient RP separation of a cocoa extract on a Kinetex column (50 mm × 4.6 mm, 2.6 μm) at 50 °C using flow rates specified in the figure. For experimental details, please refer to Section 2.3.2. Peak numbers correspond to the degree of polymerisation of individual procyanidin isomers as identified by LC–MS [17].

Because the optimal linear velocity for high molecular weight compounds is shifted to higher values at high temperatures, elevated operating temperature can be beneficial when analysing samples containing analytes spanning a wide range of molecular weights. A slightly higher linear velocity can then be employed for a faster, efficient separation of high molecular weight compounds while the loss in efficiency for low molecular weight compounds is kept to a minimum.

It should be noted that most routine HPLC methods employ gradient analysis. It has been shown that optimisation of isocratic efficiency leads to equivalent gains in gradient peak capacity (provided the gradient steepness is kept constant), albeit that these values are related via the square root of N [13,65]. For mixtures containing proanthocyanidins comprising a wide range of MWs, the gain in performance will vary due to the divergent effect of chromatographic parameters on the different compounds. In order to evaluate the effect of flow rate on the gradient separation of proanthocyanidins, a cocoa extract containing a wide range of procyanidins of different degrees of polymerisation was analysed under gradient conditions on the Kinetex column at 50 °C. The chromatograms, together with the gradient peak capacities (n_p) calculated according to Neue [66], are presented in Fig. 10A–C. Peak capacity values were calculated using peak widths for a range of molecules of differing DP (indicated in Fig. 10). For this sample, therefore, the average improvement in chromatographic performance is measured. Note that for these analyses, the gradient slope was kept constant for each of the studied flow rates. A gain in peak capacity of 6 and 21% is obtained by decreasing the flow rate from 0.8 to 0.6 and 0.4 mL/min, respectively. Slight changes in selectivity observed in these chromatograms may potentially have been caused by increased longitudinal temperature gradients due to frictional heating at the higher flow rates [64]. Note especially the improvement in resolution obtained under gradient conditions for the higher MW (DP 4–8) compounds in Fig. 10C. These results confirm that the conclusions about the effect of the flow rate drawn from the isocratic kinetic evaluation are also valid for gradient analysis on the same columns. Clearly, for complex mixtures of proanthocyanidins, chromatographic conditions should preferably be selected based on the optimal conditions for the high MW compounds.

4. Conclusions

In light of the increasing interest in the determination of phenolic compounds in natural products, methods aimed at improving the speed and/or resolution of standard RP-LC methods are required. Especially recent developments in sub-2 μm and superficially porous phases show promise for this purpose, although detailed information on the benefits of these phases for phenolic analyses is still lacking. In this study a comprehensive kinetic evaluation of two sub-2 μm and a superficially porous C18 phase was performed using a standard 5 μm phase as reference. The kinetic plot method was used to compare the chromatographic supports and determine optimal analysis conditions for proanthocyanins of differing MWs and chemical properties. Superficially porous 2.6 μm particles provided efficiencies comparable to sub-2 μm fully porous particles, although at lower pressures. It was further shown that analysis temperature, analyte physico-chemical properties, particle size and packing properties all have a strong influence on the performance of a chromatographic support.

Oligomeric procyanidins in particular show much more conservative plate height behaviour (lower H_{min} and u_{opt} values) than expected based on their lower diffusion coefficients alone. We have demonstrated that this behaviour may be explained by the on-column interconversion between rotational isomers. This has important implications for the analysis of higher MW procyanidins, and might indeed be partially responsible for the current lack of suitable 1-dimensional LC methods for the analysis of these compounds. Our results suggest that higher temperatures, longer column lengths and lower flow rates are required for improved procyanidin analysis.

The fact that both the maximum efficiency and the optimum linear velocity decrease as the size of the molecule increases, suggests that a compromise between chromatographic efficiency and analysis speed will have to be made when analysing phenolic extracts containing analytes with widely varying physico-chemical properties if optimum performance is to be achieved. The use of high

temperature is, however, much more beneficial for high molecular weight compounds. Extra-column band broadening was shown to have a large influence on the performance of narrow bore (2.1 mm i.d.) columns for compounds displaying a retention factor below 7, whereas this effect was negligible on conventional bore (4.6 mm i.d.) columns. For the latter columns, however, the detrimental effects of frictional heating have to be considered for analyses performed at very high flow rates.

In summary, our results indicate that the combination of high temperature and new column formats, when used under optimal kinetic conditions for the target analytes, provide significant promise to improve speed and/or efficiency of RP-LC analyses of phenolic compounds compared to conventional HPLC methods.

Acknowledgements

K.M.K. and A.d.V. gratefully acknowledge SASOL, the National Research Foundation (NRF, South Africa, Grant 70995), Harry Crossley Foundation, the Third World Academy of Science (TWAS, 08-077 RG/CHE/AF/AC) and International Foundation of Science, Stockholm, Sweden (IFS, F/4904-1) for funding. D.C. is a fellow of the Research Foundation Flanders (FWO Vlaanderen).

Appendix A. Supplementary data

Supplementary data associated with this article can be found, in the online version, at doi:10.1016/j.chroma.2012.02.067.

References

[1] M. García-Marino, J.C. Rivas-Gonzalo, E. Ibáñez, C. García-Moreno, Anal. Chim. Acta 563 (2006) 44.
[2] T.L. Lunder, in: M.-T. Huang, C.-T. Ho, C.Y. Lee (Eds.), Phenolic Compounds in Food and Their Effects on Health II, American Chemical Society, New York, 1992, p. 114.
[3] W.-S. Jeong, A.-N. Kong, Pharm. Biol. 42 (2004) 84.
[4] C. Santos-Buelga, A. Scalbert, J. Sci. Food Agric. 80 (2000) 1094.
[5] J. Wollgast, E. Anklam, Food Res. Int. 33 (2000) 423.
[6] K.M. Kalili, A. de Villiers, J. Sep. Sci. 34 (2011) 854.
[7] A. de Villiers, F. Lynen, P. Sandra, J. Chromatogr. A 1216 (2009) 3431.
[8] M. Schwarz, M.C. Rodríguez, D.A. Guillén, C.G. Barroso, J. Sep. Sci. 32 (2009) 1782.
[9] S. Trautvetter, I. Koelling-Speer, K. Speer, Apidologie 40 (2010) 140.
[10] W. Oleszek, A. Stochmal, B. Janda, J. Agric. Food Chem. 55 (2007) 8095.
[11] X. Deng, G. Gao, S. Zheng, F. Li, J. Pharm. Biomed. Anal. 48 (2008) 562.
[12] A. de Villiers, D. Cabooter, F. Lynen, G. Desmet, P. Sandra, J. Chromatogr. A 1216 (2009) 3270.
[13] A. de Villiers, D. Cabooter, F. Lynen, G. Desmet, P. Sandra, J. Chromatogr. A 1218 (2011) 4660.
[14] A. de Villiers, K.M. Kalili, M. Malan, J. Roodman, LC-GC Eur. 23 (2010) 466.
[15] B. Klejdus, J. Vacek, L. Lojková, L. Benesová, V. Kubán, J. Chromatogr. A 1195 (2008) 52.
[16] B. Klejdus, J. Vacek, L. Benesova, J. Kopecky, O. Lapcik, V. Kuban, Anal. Bioanal. Chem. 389 (2007) 2277.
[17] K.M. Kalili, A. de Villiers, J. Chromatogr. A 1216 (2009) 6274.
[18] K.M. Kalili, A. de Villiers, J. Sep. Sci. 33 (2010) 853.
[19] W. Pongsuwan, T. Bamba, K. Harada, T. Yonetani, A. Kobayashi, E. Fukusaki, J. Agric. Food Chem. 56 (2008) 10705.
[20] I. Kapusta, B. Janda, B. Szajwaj, A. Stochmal, S. Piacente, C. Pizza, F. Franceschi, C. Franz, W. Oleszek, J. Agric. Food Chem. 55 (2007) 8485.
[21] C. Cavaliere, P. Foglia, R. Gubbiotti, P. Sacchetti, R. Samperi, A. Laganà, Rapid Commun. Mass Spectrom. 22 (2008) 3089.
[22] T.J. Causon, K. Broeckhoven, E.F. Hilder, R.A. Shellie, G. Desmet, S. Eeltink, J. Sep. Sci. 34 (2011) 877.
[23] G. Desmet, D. Clicq, P. Gzil, Anal. Chem. 77 (2005) 4058.
[24] G. Desmet, P. Gzil, D. Clicq, LC-GC Eur. 18 (2005) 403.
[25] U.D. Neue, LC-GC Eur. 22 (2009) 570.
[26] G. Desmet, D. Clicq, D.T.T. Nguyen, D. Guillarme, S. Rudaz, J.L. Veuthey, N. Vervoort, G. Torok, D. Cabooter, P. Gzil, Anal. Chem. 78 (2006) 2150.
[27] C.R. Wilke, P. Chang, A.I.Ch.E. J. 1 (1955) 264.
[28] M.A. Kelm, J.C. Johnson, R.J. Robbins, J.F. Hammerstone, H.H. Schmitz, J. Agric. Food Chem. 54 (2006) 1571.
[29] D. Guillarme, S. Heinisch, J.L. Rocca, J. Chromatogr. A 1052 (2004) 39.
[30] D. Cabooter, A. Fanigliulo, G. Bellazzi, B. Allieri, A. Rottigni, G. Desmet, J. Chromatogr. A 1217 (2010) 7074.
[31] F. Gritti, I. Leonardis, J. Abia, G. Guiochon, J. Chromatogr. A 1217 (2010) 3819.
[32] F. Gritti, I. Leonardis, D. Shock, P. Stevenson, A. Shalliker, G. Guiochon, J. Chromatogr. A 1217 (2010) 1589.
[33] J.C. Giddings, Dynamics of Chromatography: Principles and Theory, Marcel Dekker, New York, 1965.
[34] F. Gritti, G. Guiochon, J. Chromatogr. A 1166 (2007) 30.
[35] E. Oláh, S. Fekete, J. Fekete, K. Ganzler, J. Chromatogr. A 1217 (2010) 3642.
[36] A. Liekens, J. Denayer, G. Desmet, J. Chromatogr. A 1218 (2011) 4406.
[37] J.J. DeStefano, T.J. Langlois, J.J. Kirkland, J. Chromatogr. Sci. 46 (2008) 254.
[38] C.V. McNeff, B. Yan, D.R. Stoll, R.A. Henry, J. Sep. Sci. 30 (2007) 1672.
[39] H. Chen, C. Horvath, J. Chromatogr. A 705 (1995) 3.
[40] H. Chen, C. Horváth, Anal. Methods Instr. 1 (1993) 213.
[41] S. Heinisch, J.-L. Rocca, J. Chromatogr. A 1216 (2009) 642.
[42] F.D. Antia, C. Horvath, J. Chromatogr. 435 (1988) 1.
[43] F. Lestremau, A. de Villiers, F. Lynen, A. Cooper, R. Szucs, P. Sandra, J. Chromatogr. A 1138 (2007) 120.
[44] A.A. van der Sluis, M. Dekker, M.A.J.S. van Boekel, J. Agric. Food Chem. 53 (2005) 1073.
[45] T. Sultana, G. Stecher, R. Mayer, L. Trojer, M.N. Qureshi, G. Abel, M. Popp, G.K. Bonn, J. Agric. Food Chem. 56 (2008) 3444.
[46] D. Guillarme, J. Ruta, S. Rudaz, J.L. Veuthey, Anal. Bioanal. Chem. 397 (2010) 1069.
[47] J. Billen, P. Gzil, J. De Smet, N. Vervoort, G. Desmet, Anal. Chim. Acta 557 (2006) 11.
[48] S. Fekete, K. Ganzler, J. Fekete, J. Pharm. Biomed. Anal. 54 (2011) 482.
[49] F. Gritti, G. Guiochon, J. Chromatogr. A 1169 (2007) 125.
[50] W.R. Melander, H.J. Lin, J. Jacobson, C. Horváth, J. Phys. Chem. 88 (1984) 4527.
[51] M. Suzuki, M. Sano, R. Yoshida, M. Degawa, T. Miyase, M. Maeda-Yamamoto, J. Agric. Food Chem. 51 (2003) 510.
[52] R. Wang, W. Zhou, X. Jiang, J. Agric. Food Chem. 56 (2008) 2694.
[53] W.R. Bergmann, M.D. Barkley, R.W. Hemingway, W.L. Mattice, J. Am. Chem. Soc. 109 (1987) 6614.
[54] A.C. Fletcher, L.J. Porter, E. Haslam, R.K. Gupta, J. Chem. Soc., Perkin Trans. 1 (1977) 1628.
[55] L.Y. Foo, L.J. Porter, J. Chem. Soc., Perkin Trans. 1 (1983) 1535.
[56] T. Shoji, M. Mutsuga, T. Nakamura, T. Kanda, H. Akiyama, Y. Goda, J. Agric. Food Chem. 51 (2003) 3806.
[57] C. Santos-Buelga, F.A. Garcia-viguera, Tomas-Barberan, in: C. Santos-Buelga, G. Williamson (Eds.), Methods in Polyphenol Analysis, The Royal Society of Chemistry, Cambridge, 2003, p. 102.
[58] K.J. Fountain, U.D. Neue, E.S. Grumbach, D.M. Diehl, J. Chromatogr. A 1216 (2009) 5979.
[59] E.S. Grumbach, J.C. Arsenault, D.R. McCabe, Beginners Guide to Ultra-performance Liquid Chromatography, Waters Corporation, Milford, MA, USA, 2009.
[60] U.D. Neue, HPLC Columns Theory, Technology and Practice, Wiley-VCH, Inc., New York, 1997.
[61] P.D. McDonald, The Quest for Ultra Performance in Liquid Chromatography: Origins of UPLC Technology, Waters Corporation, Milford, MA, USA, 2009.
[62] J.M. Cunliffe, S.B. Adams-Hall, T.D. Maloney, J. Sep. Sci. 30 (2007) 1214.
[63] F. Gritti, C.A. Sanchez, T. Farkas, G. Guiochon, J. Chromatogr. A 1217 (2010) 3000.
[64] A. de Villiers, H. Lauer, R. Szucs, S. Goodall, P. Sandra, J. Chromatogr. A 1113 (2006) 84.
[65] D. Cabooter, A. de Villiers, D. Clicq, R. Szucs, P. Sandra, G. Desmet, J. Chromatogr. A 1147 (2007) 183.
[66] U.D. Neue, J. Chromatogr. A 1079 (2005) 153.

Addendum C

Systematic optimisation and evaluation of on-line, off-line and stop-flow comprehensive hydrophilic interaction chromatography × reversed phase liquid chromatographic analysis of procyanidins, Part I: Theoretical considerations

K.M. Kalili, A. de Villiers, J. Chromatogr. A 1289 (2013) 58-68.

Journal of Chromatography A, 1289 (2013) 58–68

Contents lists available at SciVerse ScienceDirect

Journal of Chromatography A

journal homepage: www.elsevier.com/locate/chroma

Systematic optimisation and evaluation of on-line, off-line and stop-flow comprehensive hydrophilic interaction chromatography × reversed phase liquid chromatographic analysis of procyanidins, Part I: Theoretical considerations

Kathithileni M. Kalili, André de Villiers *

Stellenbosch University, Department of Chemistry and Polymer Science, Private Bag X1, Matieland 7602, South Africa

ARTICLE INFO

Article history:
Available online 17 March 2013

Keywords:
Comprehensive two-dimensional liquid chromatography (LC × LC)
Hydrophilic interaction chromatography (HILIC)
On-line
Off-line
Procyanidins
Stop-flow

ABSTRACT

Comprehensive two-dimensional liquid chromatography (LC × LC) provides significantly improved separation for complex real-life samples. LC × LC can be performed in one of three different ways, using on-line, off-line, or stop-flow configurations. We have previously shown how off-line comprehensive hydrophilic interaction chromatography (HILIC) × reversed-phase liquid chromatography (RP-LC) provides a powerful separation system for procyanidins (PCs), one of the most complex fractions of natural phenolics. In the current contribution, a systematic approach for the optimisation and evaluation of each of the LC × LC methodologies is presented using HILIC × RP-LC analysis of PCs as application. Optimisation was performed using the peak capacities of individual one-dimensional separations measured for different gradient times and flow rates and their combination in each of the three LC × LC modes by taking into account the effects of first dimension under-sampling, the degree of orthogonality between the two dimensions and additional band broadening associated with stop-flow analysis. The performance of all three methods is compared in terms of practical peak capacities, analysis times and peak production rates. One-dimensional LC provided the best performance for separations requiring relatively low peak capacities, whereas the on-line LC × LC system was advantageous for required practical peak capacities up to ~600. For higher resolution, the off-line or stop-flow systems should be used. Especially noteworthy is the fact that, due to slow diffusion of PCs, the contribution of stop-flow to first dimension band broadening was negligible for stop-flow times of up to 15 min. In a separate contribution, the experimental verification of the findings of this study will be reported.

1. Introduction

The performance limit of any given chromatographic technique is ultimately reached when presented with highly complex samples [1]; as sample complexity increases, so does the need for higher resolving power [2,3]. This is especially relevant for high performance liquid chromatography (HPLC) due to the relatively low resolving power of the technique (compared to for example gas chromatography), coupled to the widespread application of HPLC for analysis of complex samples. Multidimensional chromatography may be used to overcome the limitations of traditional one-dimensional (1D) separations due to the ability to increase separation space through the combination of multiple separation mechanisms [1,3,4]. Comprehensive two-dimensional liquid chromatography (LC × LC) in particular is one of the most powerful tools currently available for the separation of complex non-volatile samples, since the entire sample is submitted to two orthogonal separations. This allows for maximum exploitation of selectivity differences between the selected separation modes, resulting in increased separation power [5]. Since its inception, LC × LC has proven effective, if not indispensable, for the detailed characterisation of complex real-life samples [5–9].

Several approaches may be used when coupling separations in LC × LC, namely on-line, off-line and stop-flow (also known as stop-and-go) methods. In on-line LC × LC, fractions from the first dimension are sequentially transferred to the second dimension by means of an interface, usually a high-pressure switching valve. This requires that analysis in the second dimension be completed before transfer of the subsequent fraction. The off-line approach involves collection of fractions from the primary column, followed by their analysis on a secondary column. The stop-flow setup entails direct transfer of each fraction to the 2nd dimension column, followed by stopping the flow in the first dimension while performing the 2nd dimension separation and repeating this procedure throughout

* Corresponding author. Tel.: +27 21 808 3351; fax: +27 21 808 3360.
E-mail address: ajdevill@sun.ac.za (A. de Villiers).

0021-9673/$ – see front matter © 2013 Elsevier B.V. All rights reserved.
http://dx.doi.org/10.1016/j.chroma.2013.03.008

the entire first dimension separation. All three LC × LC systems are associated with a number of advantages and limitations, and usually the choice of configuration depends on the separation problem at hand and availability of the necessary instrumentation.

While on-line and off-line LC × LC strategies have been extensively exploited in recent years, the stop-flow approach is not as popular. This is mainly due to the complexity of this approach, coupled to concerns regarding additional first dimension band broadening during stop-flow periods [10–14]. However, the latter concern has been shown to be of less relevance than expected, especially when relatively large molecules are analysed [13,15]. Yates and co-workers [16–20] developed a multidimensional protein identification technology (MudPIT) strategy based on stop-flow MD-LC and tandem mass spectrometry (MS/MS). Although requiring long analysis times (~28 h), this method allowed detection and identification of up to 5 540 peptides [19] and generated peak capacities of up to 3240 (23 000 when combined with MS/MS) [20]. Blahová et al. [21] employed stop-flow RP-LC × RP-LC for the analysis of phenolic compounds using a 19 min second dimension gradient, although first dimension band broadening due to stop-flow operation was not addressed. Bedani et al. [13] compared on-line and stop-flow size exclusion chromatography (SEC) × RP-LC analyses of peptides, and measured virtually no additional band broadening due to stop-flow operation for stop times of 9.5 min. Fairchild et al. [22] reached the same conclusion for the stop-flow strong cation exchange (SCX) × RP-LC analysis of protein digests for stop times of 3 min. Their theoretical calculations based on estimated diffusion coefficients for typical peptides indicated that total stop-flow LC × LC analysis times of up to 450 min could be used without significant loss of performance [22]. More recently, Dugo et al. developed a stop-flow capillary RP-LC × RP-LC system for proteomic samples [23] as well as a stop-flow HILIC × RP-LC method coupled to MS for phospholipid analysis [24]. Although band broadening due to stop-flow operation was not quantitatively evaluated, good separations were achieved for stop times of more than 10 min, resulting in a practical peak capacity of 955 for a casein tryptic digest [23].

Although most multidimensional separations are designed on a trial and error basis, several LC × LC optimisation strategies have been reported [13,22,25–27]. For instance, Schoenmakers et al. [26] proposed a systematic approach for the design of LC × LC systems. This theoretical method required pre-defined values for the acceptable total analysis time, maximum pressures in the two dimensions and minimum first dimension column diameter to derive optimal operational parameters (such as column dimensions, injection volumes and flow rates) for LC × LC separations. Bedani et al. [13] described a strategy where a previously optimised second dimension separation and the desired two-dimensional peak capacity were used as starting point to derive optimal analytical parameters for the first dimension. Fairchild et al. [22] also used a similar approach, however starting with an optimised first dimension separation, to compare the performance of on-line, off-line and stop-flow LC × LC schemes both in terms of peak capacity and analysis time. These authors kept the first dimension separation parameters constant and systematically varied those of the second dimension as a function of the coupling mode while taking under-sampling and stop-flow band broadening into consideration for the theoretical comparison of each of the set-ups. Vivó-Truyols et al. [27] developed an LC × LC optimisation strategy based on the Pareto-optimality method to derive chromatographic conditions (such as column dimensions, particle sizes and modulation times) by taking efficiency-losses due to first dimension under-sampling and second dimension injection band broadening into account. These authors considered isocratic and gradient separations on conventional and ultrahigh pressure systems, and used this approach to investigate the "trade-off between total analysis time, total peak capacity and total dilution" for each system.

These studies clearly illustrate the important relationships between key experimental parameters in LC × LC optimisation. However, as in most HPLC method development, optimal experimental parameters depend on the separation method(s) used as well as the specific target analytes. This follows from inherent differences between separation modes, such as mobile phase viscosity and the kinetic properties of the specific interactions involved, as well as the effect of analyte properties on optimal chromatographic behaviour [28]. In the case of LC × LC, the derivation of a generic method optimisation strategy is further hampered by aspects such as the mobile phase miscibility and elution strength in the two dimensions. Therefore, while previously reported LC × LC optimisation strategies point to generically applicable relationships between experimental parameters in method development, these should still be applied to the specific column combinations and target analytes in order to provide the most relevant real-life solution.

In our previous work, the off-line coupling of hydrophilic interaction chromatography (HILIC) and reversed-phase liquid chromatography (RP-LC) was shown to provide a powerful separation system for procyandins (PCs) [29] and flavonoids [30,31] owing to the complementary selectivities offered by the two separation techniques. Although this approach provided significantly improved separation of these notoriously challenging compounds, the method required very long analysis times. Therefore, the goal of the current contribution was to develop a systematic optimisation approach that would allow the detailed evaluation and comparison of off-line HILIC × RP-LC with on-line and stop-flow modes as alternative automated systems for PC analysis. A critical comparison of all three systems in terms of analytical throughput, ultimate performance limits as well as the time required to achieve such limits will be presented. The experimental verification of the findings reported here will be presented for cocoa PCs in a separate contribution [32].

2. Theory

Throughout this paper, the notation proposed in [33,34] for parameters related to one- and two-dimensional chromatographic separations is used.

2.1. One-dimensional peak capacities

Peak capacity is commonly used to measure the separation power of chromatographic separations [35]. For one-dimensional gradient separations, the peak capacity ($n_{c,1D}$) is given by [36]:

$$n_{c,1D} = 1 + \frac{t_g}{1/n\sum_1^n w_b} \quad (1)$$

where t_g is the gradient time and w_b is the baseline peak width, averaged for n number of peaks. The peak capacity obtainable on a given column varies as a function of the gradient time, and can be estimated using the following empirical relation [22]:

$$n_{c,1D} = 1 + \frac{at_g}{b + t_g} \quad (2)$$

where, a and b are constants obtained by fitting Eq. (2) to experimental $n_{c,1D}$ data measured for a range of t_g values.

2.2. Two-dimensional peak capacity

For a completely orthogonal LC × LC system, i.e. where two uncorrelated separation mechanisms are coupled, the total

two-dimensional peak capacity ($n_{c,2D}$) is equal to the product of the peak capacities in the first (^1n_c) and second (^2n_c) dimensions [3]:

$$n_{c,2D} = {}^1n_c \times {}^2n_c \quad (3)$$

Practically, truly orthogonal systems are hard to achieve due to retention correlation which commonly exist between separation modes, resulting in incomplete usage of the available separation space [7,37,38]. This aspect should therefore be taken into account when determining the practical peak capacity of LC × LC separations. Several metrics for the quantitation of orthogonality have been reported in literature [37–43], although as yet consensus has not been reached regarding the most accurate method. In this study, we use the procedure formulated by Liu et al. [37], which is based on a geometric approach to factor analysis to account for lack of orthogonality in the calculation of the effective 2D peak capacity ($n'_{c,2D}$) according to:

$$n'_{c,2D} = {}^1n_c{}^2n_c - \frac{1}{2}[{}^2n_c{}^2\tan\gamma + {}^1n_c{}^2\tan\alpha] \quad (4)$$

The reader is referred to [37] for details on how angles γ and α are derived. For the determination of orthogonality according to this method, range-scaled retention times for cocoa PCs identified by LC–ESI-MS ($n = 33$) using the off-line HILIC- and RP-LC separations were used [29,32]. This was done to maximise the number of compounds used in the calculation, since the estimation of orthogonality based on correlation coefficients has been shown to be susceptible to inaccuracies due to limited compound numbers and outliers [38]. A correlation coefficient (r^2) of 0.05 was obtained for these data according to [37].

Band broadening due to under-sampling of first dimension peaks also contributes to loss of peak capacity in LC × LC separations. Truly comprehensive systems require that the resolution achieved in the primary dimension be preserved and that the elution profiles from both dimensions be maintained [3,4,34]. For preservation of first dimension resolution, a sampling rate of three or more fractions per first dimension peak is generally required [31,44,45] (although sampling rates of two or more have been found to provide a better compromise between the sampling rate and second dimension analysis time for the highest overall peak capacity in on-line LC × LC [27,46]). The phenomenon of 1st dimension under-sampling can quantitatively be taken into account by correcting the 1st dimension peak capacity using the method proposed by Li et al. [47]:

$$n'_{c,1D} = \frac{{}^1n_c}{\beta} \quad (5)$$

where $n'_{c,1D}$ is the corrected first dimension peak capacity and β is the under-sampling correction factor. Accordingly, the corrected two-dimensional peak capacity ($n'_{c,2D}$) of an on-line LC × LC separation is determined as follows:

$$n'_{c,2D} = \frac{{}^1n_c{}^2n_c}{\beta} = \frac{{}^1n_c{}^2n_c}{\sqrt{1 + 3.35({}^2t_c{}^1n_c/{}^1t_g)^2}} \quad (6)$$

where ^1n_c is the (uncorrected) 1st dimension peak capacity, ^1t_g is the first dimension gradient time and ^2t_c is the second dimension cycling time (i.e. in the case of gradient analyses, the sum of the gradient time, ^2t_g, and the time required for re-equilibration of the column, $^2t_{re\text{-}eq}$). For off-line and stop-flow LC × LC analyses, ^1t_s is substituted for ^2t_c in Eq. (6), since in these configurations the sampling time is independent of the second dimension cycle time.

Since orthogonality and under-sampling are both important phenomena affecting the effective LC × LC peak capacity, all practical 2D peak capacities reported in this work were corrected using the methods of Liu et al. [37] and [47].

Peak capacities for stop-flow analyses were calculated based on the average peak width obtained in the first dimension after accounting for band broadening due to stop-flow according to Eq. (14) (refer to Section 2.4 further for details) and a new β value was calculated based on this corrected ^1n_c value.

2.3. Analysis time

For on-line LC × LC analysis, the first dimension sampling time (^1t_s) is equal to the second dimension cycling time (^2t_c). In this study, gradient elution was used in the second dimension, and therefore ^2t_c is the sum of ^2t_g and $^2t_{re\text{-}eq}$:

$${}^1t_s = {}^2t_c = {}^2t_g + {}^2t_{re\text{-}eq} \quad (7)$$

The total analysis time for an on-line system ($t_{tot,online}$) is then given by:

$$t_{tot,\ online} = f \times {}^2t_c + {}^2t_c \quad (8)$$

where f is the total number of fractions sampled throughout the first dimension separation window and the additional ^2t_c term accounts for the analysis of the last fraction. For off-line and stop flow analyses, the total analysis times were calculated using Eq. (9).

$$t_{tot,\ offline} = t_{tot,\ stopflow} = f \times {}^2t_c + f \times {}^1t_s \quad (9)$$

2.4. Correction of first-dimension peak capacity to account for band broadening due to stop-flow operation

During stop-flow LC × LC experiments, the overall peak capacity may be affected as a result of additional band broadening that occurs in the first dimension column during the stop-flow periods. The extent of this broadening depends on the effective stop-flow period experienced by each 1st dimension peak as well as the effective diffusion coefficients of the relevant analyte(s). The stop-flow period for each 1st dimension peak (t_{stop}) is determined by the number of stop-flow periods (n_{stop}) prior to its elution and the duration of these periods (which is equal to ^2t_c), i.e.:

$$t_{stop} = n_{stop} \times {}^2t_c \quad (10a)$$

$$= t_{tot} - t_R \quad (10b)$$

with t_R being the total time required to pass through the column with length L during the actual flow period. To determine the additional band broadening due to stop-flow operation, the effective diffusion coefficients of cocoa PCs were calculated according to Knox and Scott [11] using the so-called "arrested elution method" (also referred to as stop-flow or peak parking method). This approach entails elution of a band half-way through the column, followed by a defined stopped-flow period. The band is subsequently eluted from the column at a measured flow rate, after which the (total) peak variance is determined [11]. The principles behind the stop-flow method are briefly outlined below according to [13].

In a continuous flow experiment, band broadening is measured from the peak variance (σ^2_{cont}), which is given by:

$$\sigma^2_{cont} = \frac{t_R^2}{N} \quad (11)$$

where t_R is the retention time and N is the number of theoretical plates.

During arrested elution, molecules still actively diffuse along the length of the column and the longitudinal variance (σ_z^2) due to molecular diffusion while a band resides inside the column (and is the same whether the band is moving or not) is given as [11]:

$$\sigma_z^2 = 2D_{eff}t_{stop} \quad (12)$$

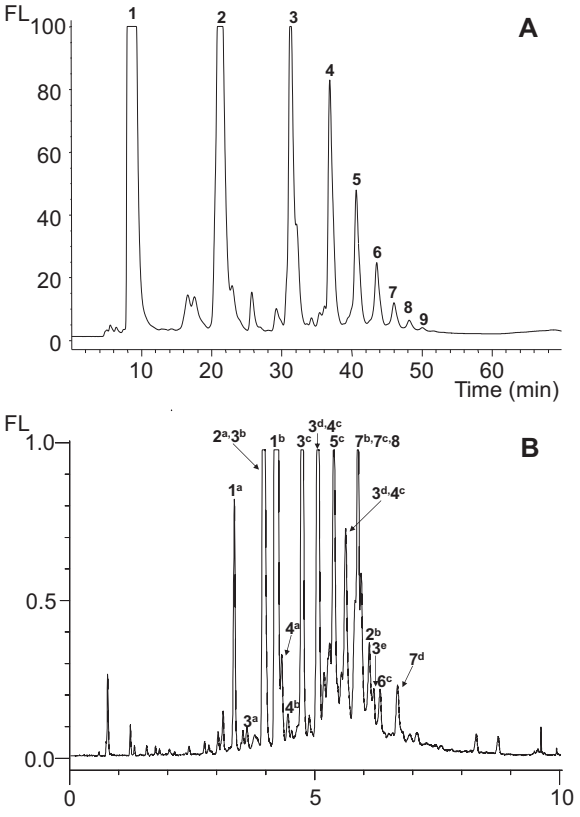

Fig. 1. Chromatograms for the HILIC (A) and RP-LC (B) separation of a cocoa extract under the off-line experimental conditions using fluorescence detection. Peak numbers denote degree of polymerisation (DP) of various procyanidin oligomers as identified by LC–MS [29], with superscripts denoting different isomers. Experimental conditions: HILIC: t_g = 50 min, F = 50 μL/min, V_{inj} = 0.5 μL; RP-LC: t_g = 11.25 min, V_{inj} = 0.5 μL, F = 1.5 mL/min. For further experimental details, refer to Sections 3.4.1 and 3.4.2.

where D_{eff} is the effective diffusion coefficient of the analyte in the column.

In which case, σ_z^2 (in space units) is related to σ_t^2 (in time units) by [13]:

$$\sigma_z^2 = \sigma_t^2 u^2 \quad (13)$$

where u is the linear velocity of the analyte upon elution, and is given as $u = L/t_R$.

The total variance in time units ($\sigma_{t,tot}^2$) of a peak eluted in a stop-flow experiment is the sum of the contributions of band broadening processes due to both continuous- and stop-flow processes, i.e.:

$$\sigma_{t,tot}^2 = \sigma_{t,cont}^2 + \frac{2D_{eff}t_{stop}}{u^2} \quad (14)$$

wherein $2D_{eff}t_{stop}/u^2$ represents the variance due to stop-flow. From this relationship, D_{eff} can be calculated from a plot of $\sigma_{t,tot}^2$ versus t_{stop} (where the y-intercept is equal to $\sigma_{t,cont}^2$).

Using D_{eff} values for the principal 1st-dimensional peaks (labelled 1–9 in Fig. 1A) calculated according to this method, in combination with the known effective stop-flow period for each of these peaks (Eq. (10a)), it is possible to calculate $\sigma_{t,tot}$ for each 1st-dimensional peak. From these values, a new ^1n_c value was calculated according to Eq. (1) using the average w_b (w_b is equal to $4\sigma_{t,tot}$ in this case) to account for additional stop-flow band broadening of each peak. Subsequently, new β values were calculated for each 1st-dimension peak, and the average β value was used to adapt the corrected ^1n_c value for under-sampling according to Eq. (5).

3. Experimental

3.1. Reagents and materials

Cocoa beans were purchased from a local supermarket. Standards of (−)-epicatechin and (±)-catechin as well as HPLC grade methanol, acetonitrile, formic acid, acetic acid and acetone were purchased from Sigma–Aldrich (Steinheim, Germany). HPLC grade hexane was purchased from Burdick & Jackson (Muskegon, USA). Deionised water was obtained using a Milli-Q water purification system (Millipore, Milford, MA, USA). All solutions were filtered through 0.45 μm HVLP membrane filters (Millipore) and degassed in an ultrasonic bath (Branson Model 3510, Danbury, USA) before use.

3.2. Sample preparation

The cocoa sample was prepared according to a previously reported method [29]. For HILIC analyses, the sample was freeze dried and re-dissolved in 80% acetonitrile/20% methanol (v/v).

3.3. Instrumentation

HILIC analyses were performed on a Hewlett Packard 1050 liquid chromatograph equipped with a quaternary pump, an injector, diode array and fluorescence detectors, and controlled by Chemstation software (Agilent, Waldbronn, Germany). Separations were performed on a Develosil Diol-100 column (250 mm × 1 mm i.d., 5 μm d_p, Nomura Chemical Co. Ltd., Aichi, Japan) using a modified method adapted from [29,48].

RP-LC analyses were performed on an Acquity UPLC system equipped with a binary pump, autosampler, column oven, photodiode array (PDA) detector (500 nL flow cell, 10 mm path length) and controlled by Waters Empower software (Waters, Milford, MA, USA).

3.4. Chromatographic methods

3.4.1. HILIC analyses

HILIC separations were performed at room temperature using a binary mobile phase consisted of (A) acetonitrile and acetic acid (99:1, v/v) and (B) methanol, water and acetic acid (94.05:4.95:1, v/v/v). For off-line and stop-flow analyses, 9 μL was injected and a flow rate of 50 μL/min was used with the following gradient: 0–40 min (4–40% B), 40–45 min (40% B isocratic) and 45–50 min (40–4% B). For on-line analyses, the gradient was adapted to keep the ratio of the gradient time to the void time ($^1t_g/t_0$) constant at a flow rate of 25 μL/min. An injection volume (V_{inj}) of 2.5 μL was used. Fluorescence data were acquired at excitation and emission wavelengths of 230 and 321 nm, respectively, and a photomultiplier (PMT) gain of 10 using DAx 8.0 data acquisition software (Van Mierlo software, Amsterdam, The Netherlands).

3.4.2. RP-LC analyses

RP-LC separations were performed on an Agilent Zorbax SB-C18 column (50 mm × 4.6 mm i.d., 1.8 μm d_p) protected with a Phenomenex C18 guard column (4 mm × 3 mm i.d., Torrance, USA). The binary mobile phase consisted of 0.1% formic acid in water (v/v) (A) and acetonitrile (B). For off-line and stop-flow analyses, the following gradient was used: 0–0.13 min (2% B), 0.13–5.40 min (2–18% B), 5.40–9.00 min (18–25% B), 9.00–10.35 min (25–100% B), 10.35–11.25 min (100% B isocratic) and 11.25–12.60 min (100–2% B), at a flow rate of 1.5 mL/min. 0.5 μL was injected. The gradient was adapted at different flow rates and gradient times in on-line analyses to keep the ratio $^2t_g/t_0$ constant. A column temperature of 50 °C was used, and UV chromatograms were recorded at 210,

280, 320 and 370 nm. Fluorescence detection was performed as for HILIC analyses.

3.5. Measurements of D_{eff} for procyanidins

To determine the effective diffusion coefficients for the different PC oligomers, a cocoa extract was analysed on a Develosil Diol-100 column (250 mm × 4.60 mm i.d., 5 μm d_p, Nomura Chemical Co., Ltd.) using the same mobile phases and gradient as outlined for off-line HILIC analyses at a flow rate of 1 mL/min. In these experiments, 10 μL of the sample was injected. Gradient analysis was executed until the specific target band was eluted half-way through the column, after which the flow was stopped and gradient paused for periods of 30, 60, 120, 240 and 480 min. Subsequently, the gradient was resumed at the same flow rate to elute the sample from the column. A 10-port switching valve (Valco Instruments Co. Inc., Houston, Texas, USA) was configured to direct the column effluent to a blocked port during the stop-flow period to prevent forward flow and keep the column pressure constant (supplementary Fig. S1, position 2). After the stop period the valve was switched to direct the flow to the detector for measurement of peak variances (Fig. S1, position 1). These measurements were performed for PC monomers to tetramers and all experiments were performed in triplicate. Peak widths at half height were calculated using the Chemstation software (Agilent).

Supplementary data associated with this article can be found, in the online version, at http://dx.doi.org/10.1016/j.chroma.2013.03.008.

3.6. Calculations

All optimisation and evaluation calculations were performed in Microsoft Excel. Three-dimensional (3D) plots were created with Sigmaplot (version 11.0, Systat Software, Inc., IL, USA).

4. Results and discussion

4.1. Evaluation of one-dimensional separations

Column dimensions, mobile phase compositions, analysis temperatures as well as HILIC and RP-LC gradients as previously reported [29] were adopted in this study with slight modifications as outlined in the experimental section. Compared to [29], slight changes in the HILIC gradient were necessary to provide comparable elution profiles due to differences in dwell volumes between the instruments used in the two studies. Furthermore, the RP-LC gradient was adapted to a shorter column length and different flow rates used in the current study compared to [29]. Fluorescence wavelengths were adapted (Section 3.4.1) for improved sensitivity [49]. Fig. 1 shows the chromatograms for the HILIC- and RP separations of the cocoa extract obtained under the conditions used for the off-line and stop-flow analyses.

As can be seen in Fig. 1A, PCs were separated in order of increasing degree of polymerisation (DP) in HILIC. On the other hand, RP-LC provides separation according to hydrophobicity, with individual PC isomers separated on the C18 phase, although extensive co-elution is observed due to the large number of isomers (Fig. 1B). We have previously shown that the off-line combination of HILIC and RP-LC provides significant resolution gains for complex PC fractions [29].

The HILIC separation used for off-line LC × LC analyses provided a practical peak capacity of ~14, as determined using Eq. (1) for PCs of DP 1–8. In agreement with previous reports on the HILIC separation of PCs [48–51], the peak capacity is quite low. It should be noted that efficiencies in HILIC are generally much lower than in RP-LC [52,53]. This is in part due to slow kinetics of the adsorption process, which, in addition to the partitioning mechanism, governs the HILIC separation, as opposed to the much faster partitioning mechanism which predominates in RP-LC [54,55]. Furthermore, some resolution is sacrificed under the experimental conditions used here, primarily as a result of using a narrow-bore column on (optimised) conventional instrumentation and due to the relatively large injection volumes used in this dimension. Nevertheless, HILIC provides valuable alternative selectivity for combination with RP-LC in LC × LC.

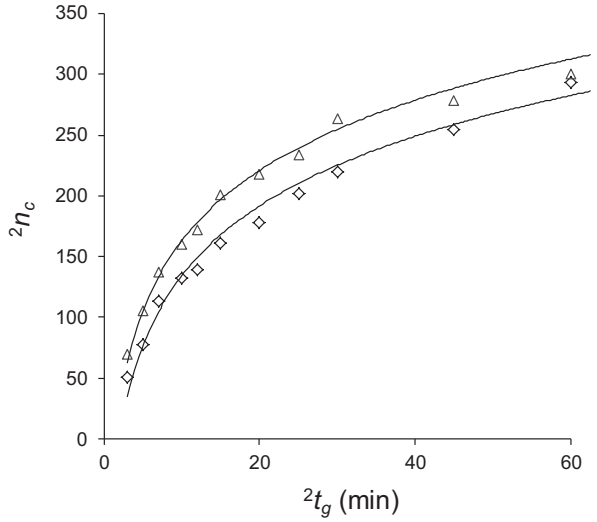

Fig. 2. Experimental data for (2nd dimension) RP-LC peak capacity versus gradient time at 0.8 mL/min (◊) and 1.5 mL/min (△) obtained for a cocoa extract on a Zorbax SB-C18 column (50 mm × 4.6 mm, 1.8 μm) at 50 °C. For further experimental details, refer to Section 3.4.2.

Since RP-LC is used in the second dimension, it was important to determine the relationship between peak capacity and gradient time (^2t_g) in this dimension. This is because the second dimension gradient time, and by extension the cycle time ($^2t_c = {}^2t_g + {}^2t_{re\text{-}eq}$), are important parameters in the optimisation of LC × LC separations. These variables directly determine the sampling time (^1t_s) in on-line LC × LC (and consequently the degree of under-sampling), as well as the second dimension (and by extension overall) peak capacity and total analysis times of on-line, off-line and stop-flow LC × LC. To determine the relationship between ^2n_c and ^2t_g, a cocoa extract was analysed on a 50 mm × 4.60 mm, 1.8 μm Zorbax C18 column and peak capacities were calculated according to Eq. (1) for different gradient times at two flow rates, 0.8 and 1.5 mL/min (higher flow rates were not possible in the on-line configuration due to operating pressures close to the maximum of the column, 600 bar). From the results presented in Fig. 2, it can be seen that a flow rate of 1.5 mL/min provided higher peak capacities for the same gradient time; therefore this flow rate was used throughout this study. From the well-known shape of these curves, it is evident that especially in the region of very short gradient times (i.e. $^2t_g < 5$ min), substantial increases in peak capacity are observed for slight increases in the analysis time. The experimental data obtained at 1.5 mL/min were fit to Eq. (2), which was found to provide the best fit ($r^2 = 0.987$) for the ^2n_c versus ^2t_g data when $a = 357.3$ and $b = 12.3$. This relationship was used in the optimisation of LC × LC experiments to determine ^2n_c for any ^2t_g. It should be noted that optimisation was performed here using a fixed column length in the second dimension. A more complete optimisation will require adding the second dimension column length as additional variable [26,27]; this was not attempted in the current contribution.

4.2. Optimisation of HILIC × RP-LC separations

The primary goal of this work was to devise a systematic approach for the optimisation and evaluation of on-line, off-line and stop-flow HILIC × RP-LC methods for PC analysis. The theoretical basis for these calculations has been outlined in Section 2. In the following sections, the optimisation of each of the three modes of LC × LC operation will be described in detail.

4.2.1. Off-line HILIC × RP-LC analyses

The principal benefit of performing off-line LC × LC is that longer analysis times can be employed in the second dimension to achieve very high peak capacities. This is a consequence of the fact that the two dimensions are executed independently, unlike in the case of on-line analyses.

The coupling of HILIC and RP-LC is however complicated by the fact that HILIC mobile phases are strong eluents in RP-LC (and vice versa) [56]. A consequence of this is that the volume of 1st dimension fractions injected onto the second dimension column should be minimised in order to avoid injection band broadening. This limitation may be partially negated by using columns with carefully matched dimensions in the two dimensions: a narrow-bore column in the first dimension reduces fraction volumes and minimises sample dilution, while a wider-bore column in the second dimension allows higher sample loadability for better sensitivity [6,25,57]. Alternatively, the first dimension flow may be split before the second dimension column (see further), or dilution of the primary column effluent with a weak solvent may be performed [51,58].

For off-line analyses, sample volume and mobile phase incompatibility are less of a concern, since small enough volumes of incompatible solvents can be injected into the 2nd dimension, provided sensitivity is sufficient. However, a consequence of the relative elution strengths of HILIC and RP-LC mobile phases is that the sampling time directly impacts on the sensitivity of off-line LC × LC analyses. The dilution of 1st dimension fractions can be calculated using the following relation:

$$\text{Dilution} = \frac{{}^1F \times {}^1t_s}{{}^2V_{\max}} \tag{15}$$

where ${}^1F$ is the first-dimension flow rate in μL/min, ${}^1t_s$ the first dimension sampling time in min and ${}^2V_{\max}$ is the maximum volume that can be injected in the second dimension in μL. The latter parameter may be estimated based on chromatographic theory (see for example [25]), although this approach requires additional information which may not be readily available, such as the retention factors of compounds in 1st- and 2nd-dimension mobile phases. For this reason, ${}^2V_{\max}$ values were experimentally determined in the current study by injecting various volumes of the sample dissolved in the 1st dimension mobile phase(s) to determine the maximum volume that does not lead to injection band broadening. These experiments produced a value of ~2 μL for ${}^2V_{\max}$. Eq. (15) implies that for a fixed 1st dimension flow rate, the use of longer sampling times would result in a decrease in sensitivity due to the fact that fraction volumes increase, whereas the maximum injection volume on the second dimension column remains constant. An alternative approach would be to evaporate fractions and re-dissolve them in a more suitable solvent, provided this does not compromise the sample integrity [1]. This was not attempted in the current study due to concerns regarding PC stability during evaporation, since these compounds are susceptible to oxidation.

Another important consideration in off-line LC × LC is the overall analysis time. For a fixed sampling time, longer second dimension analyses will always provide higher two-dimensional peak capacities (see Fig. 2), although the gain in performance also decreases with an increase in the total analysis time (a situation which is familiar from 1D LC analysis). A good measure of this compromise is the peak capacity production rate, defined as:

$$\text{Peak production rate} = \frac{n'_{c,2D}}{t_{\text{tot}}} \tag{16}$$

Taking these considerations into account, the following approach was used for the optimisation of off-line LC × LC analyses. The first dimension flow rate and gradient time were kept constant at 50 μL/min and 50 min, respectively, which provided a first dimension peak capacity, ${}^1n_c$, of ~14 according to Eq. (1). For a fixed sampling time, the second dimension gradient time (${}^2t_g$) was used as a primary variable and ${}^2n_c$ calculated according to Eq. (2) for each ${}^2t_g$. The two-dimensional peak capacity was then determined using Eq. (3), followed by correction for under-sampling according to Eq. (5) and orthogonality according to Eq. (4). The total analysis time was calculated according to Eq. (9). Finally, the peak capacity production rate was determined using Eq. (16). Since the sampling time, ${}^1t_s$, determines both first dimension under-sampling and the total analysis time, this procedure was repeated for various sampling times. The results are summarised in Fig. 3.

Fig. 3A shows that the highest corrected two-dimensional peak capacity ($n'_{c,2D} \sim 2943$) is obtained for the longest second dimension cycle time and the shortest sampling time. This is expected considering the effect of ${}^2t_c$ on the 2nd dimension peak capacity (Fig. 2). Furthermore, smaller sampling times result in less under-sampling, and therefore higher corrected 2D peak capacities for a given second dimension cycle time (as seen in the y–z plane in Fig. 3A). It is also evident though that there is little gain in reducing the sampling time below 1 min. For a sampling time of 1 min, the under-sampling correction factor, β, is equal to 1.12, indicating a negligible effect on the first dimension peak capacity for lower sampling times in the case of HILIC analysis of PCs. On the other hand, the price to pay in terms of total analysis time is exorbitant when using shorter sampling times (as seen in the x-y plane of Fig. 3A), since the total analysis time is dependent on the product of the number of fractions collected (i.e. ${}^1t_g/{}^1t_s$) and the second dimension cycle time. This effect is even more pronounced when using longer second dimension cycle times.

Fig. 3B illustrates how the peak capacity production rate varies with the second dimension cycle time, which in turn delivers a unique optimal sampling time for optimal peak capacity production. For example, for a second dimension cycle time of 0.5 min (${}^2t_g$ = 0.375 min), the sampling time resulting in the highest peak capacity production rate of 1.66 peaks/min is 1 min, whereas for a second dimension cycle time of 30 min, the respective values are 2.77 peaks/min and 3.5 min ${}^1t_s$. These data indicate that for off-line analysis, the maximum peak capacity production rate (4.21 peaks/min) corresponds roughly to a second dimension cycle time of 6.5 min and a sampling time of 2.5 min. Note that these conclusions are valid for the specific sample and column combination studied here. For LC × LC operation in general, the optimal conditions will depend on the columns, mobile phases and flow rates used in each dimension, the temperature and analyte properties (most notably analyte diffusion).

It should be noted though that if peak capacity production rate is used as sole criterion, on-line HILIC × RP-LC analysis will provide better results (see Section 4.2.3 further). In fact, in the entire range of practical peak capacities attainable by on-line HILIC × RP-LC (i.e. $n'_{c,2D} < 570$), this approach will deliver higher peak capacity production rates. The benefit of off-line HILIC × RP-LC rather lies in the production of higher overall (corrected) peak capacities at lower peak capacity production rates. This situation is analogous to 1-dimension separations, where the maximum resolution is always obtained at longer analysis times.

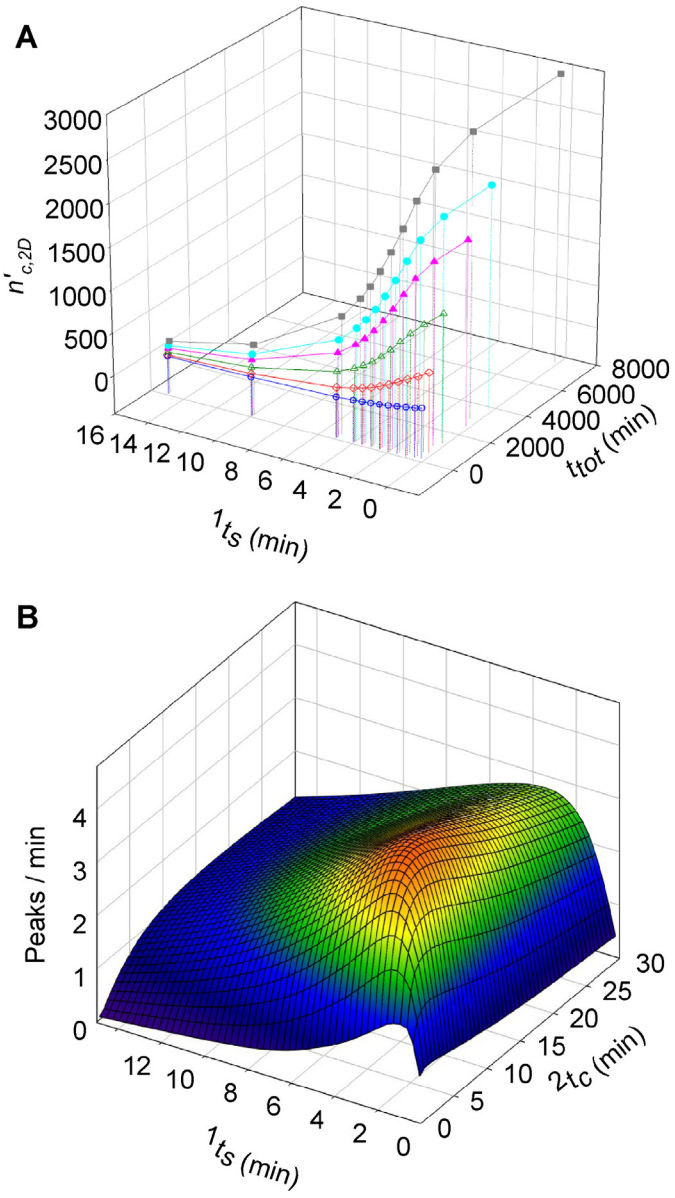

Fig. 3. (A) A 3-dimensional plot illustrating the relationship between total analysis time (t_{tot}, x-axis), corrected 2D peak capacity ($n'_{c,2D}$, z-axis) and 1st dimension sampling time (^1t_s, y-axis) in off-line HILIC × RP-LC analysis of PCs. Values are plotted for second dimension cycle times of 0.5 min (○), 2 min (◊), 5 min (△), 10 min (▲), 15 min (●) and 30 min (■) and (B) a 3-dimensional plot illustrating the relationship between 2nd dimension cycle time (^2t_c, x-axis), 1st dimension sampling time (^1t_s, y-axis) and corrected 2D peak production rate (z-axis) for off-line HILIC × RP-LC analysis of PCs. Experimental conditions: ^1t_g = 50 min, ^1F = 50 μL/min, $^1V_{inj}$ = 9 μL, $^2V_{inj}$ = 0.5 μL, ^2F = 1.5 mL/min. For further experimental details, refer to Sections 3.4.1 and 3.4.2.

4.2.2. Stop-flow HILIC × RP-LC analyses

While the total analysis time, and possibly analyte stability, is the limiting factor in the off-line configuration, the stop-flow approach is constrained by the diffusion properties of the analytes under investigation. This is a result of the fact that molecules are still subjected to longitudinal diffusion during the stop-flow periods, which may cause additional band broadening. As a consequence of this concern and the higher instrumental complexity of the approach compared to off-line LC × LC, the stop-flow design remains the least used hyphenation mode in LC × LC separations. However, while excessive band broadening is possibly a relevant concern for small molecules, its effect is expected to be less detrimental for large molecules such as high MW PCs.

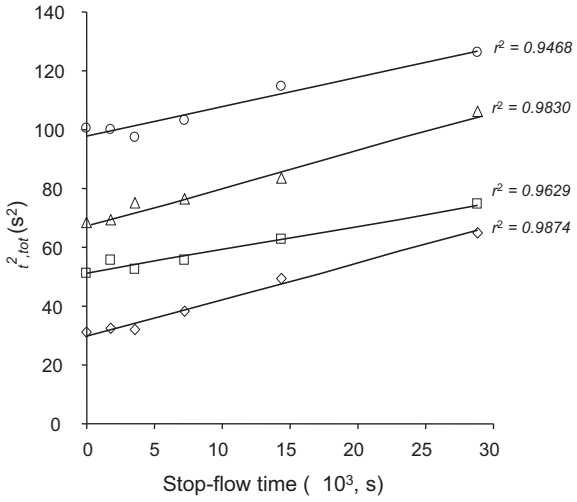

Fig. 4. Evolution in total variance, $\sigma^2_{t,tot}$, as a function of stop-flow time for PC monomers (◊), dimers (□), trimers (△) and tetramers (○) in HILIC. For experimental conditions used to obtain these data, refer to Section 3.5.

To allow the accurate comparison of stop-flow HILIC × RP-LC with the on- and off-line approaches, a quantitative measure of the contribution of stop-flow operation to band broadening in the first dimension is required for the target analytes. This information is also relevant for the optimisation of stop-flow experimental conditions, because the second dimension analysis time determines the stop-flow period and therefore peak capacities in both dimensions.

Band broadening was measured using the so-called arrested elution method as outlined in Section 2.4. Fig. 4 presents plots of total variance, $\sigma^2_{t,tot}$, as a function of stop-flow time as measured on a 4.6 mm i.d. HILIC column for PC monomers to tetramers. Note that the use of a 4.6 mm i.d. column was essential for these experiments, since extra-column band broadening made accurate measurements on a 1 mm i.d. column impossible [59]. From the figure, it is clear that linear correlations were obtained between the peak variance and peak parking times for PCs of DP 1–4. Note that the slopes of these curves are related to the term $2D_{eff}t_{stop}/u^2$, and therefore do not decrease linearly as a function of PC DP. D_{eff} values for monomeric, dimeric, trimeric and tetrameric bands were calculated from experimentally measured variances (% RSD for peak variances ranged between 0.3 and 7.7%, n = 3) depicted in Fig. 4 and the respective experimental linear velocities determined from $u = L/t_R$.

The relationship between DP and D_{eff} for PCs is hard to predict from a fundamental perspective, as D_{eff} will depend on the hydrodynamic radii of the relevant molecules, which are not known. However, the assumption is made here that the trend observed between measured D_{eff}-values and DP for PC monomers to tetramers remains valid for the higher DP PCs. This assumption seems reasonable in the absence of any reason why this trend should significantly be altered for higher MW PC oligomers. Accordingly, effective diffusion coefficients for the higher molecular weight oligomers (DP 5–8) were extrapolated using the relationship between DP and D_{eff} obtained for the oligomers of DP 1–4 ($D_{eff} = 4.91 \times 10^{-10} \times DP^{-2.334}$, $r^2 = 0.961$). D_{eff} values and linear velocities obtained in this manner for the different oligomeric PCs are listed in Table 1.

Fig. 5 portrays the variation of D_{eff} values as a function of DP for the target PCs, and illustrates that D_{eff} decreases as HILIC retention increases with increasing DP. As expected, an increase in molecular weight coincides with a significant decrease in the effective diffusion coefficient. This trend implies that HILIC is an ideal separation mode in the first dimension for stop-flow LC × LC analysis

Table 1
Linear velocities and effective diffusion coefficients (D_{eff}) for different PC oligomers in HILIC as determined using the arrested elution method.

Oligomer	Linear velocity (m/s)	D_{eff} (m^2/s)
Monomers	4.84×10^{-4}	5.95×10^{-10}
Dimers	2.00×10^{-4}	7.07×10^{-11}
Trimers	1.33×10^{-4}	3.25×10^{-11}
Tetramers	1.14×10^{-4}	2.55×10^{-11}
Pentamers	1.04×10^{-4}	1.17×10^{-11} [a]
Hexamers	9.70×10^{-5}	7.63×10^{-12} [a]
Heptamers	9.19×10^{-5}	5.33×10^{-12} [a]
Octamers	8.79×10^{-5}	3.90×10^{-12} [a]

[a] D_{eff} values extrapolated from the experimentally determined values for DP 1–4 according to the following relationship: $D_{eff} = 4.91 \times 10^{-10} \times DP^{-2.334}$.

of PCs, as the most retained compounds exhibit the smallest effective diffusion coefficients, which fortuitously offsets the fact that these compounds will experience the longest effective stop-flow times. This further suggests that relatively long analysis times can be employed in the second dimension to obtain enhanced 2D peak capacities because the effective loss of peak capacity in the first dimension due to stop-flow band broadening is kept to a minimum.

Following estimation of effective diffusion coefficients for different PC oligomers in HILIC, it was possible to obtain an estimate of the effect of stopping the flow on the first dimension peak capacity. The total band broadening for PCs of each DP was calculated using the effective diffusion coefficients (Table 1) and the effective stop-flow time for each DP according to Eq. (10a). These values were used to adapt the first dimension peak capacity to take the effect of stop-flow operation into account as described in Section 2.4.

For further optimisation of stop-flow HILIC × RP-LC analysis, the effect of sampling time and 1st dimension flow rate on the volumes of 1st dimension fractions should be considered. In stop-flow analysis, fraction volumes can be made small enough so as to avoid injection band broadening in the 2nd dimension by reducing the sampling time. However, the total analysis time also increases considerably when transferring many fractions using short sampling times (Eq. (9)). To overcome this limitation, a flow splitter [60] was introduced before the second dimension column (see [32] for experimental details). Flow-splitting is advantageous in that the first dimension flow rate does not directly impact on the second dimension, hence optimisation of individual dimensions can be done virtually independently [60]. The obvious drawback of this approach is a decrease in sensitivity. However, despite the relatively high split ratios (1:50 and 1:33 for on-line (^2t_c = 3 min,

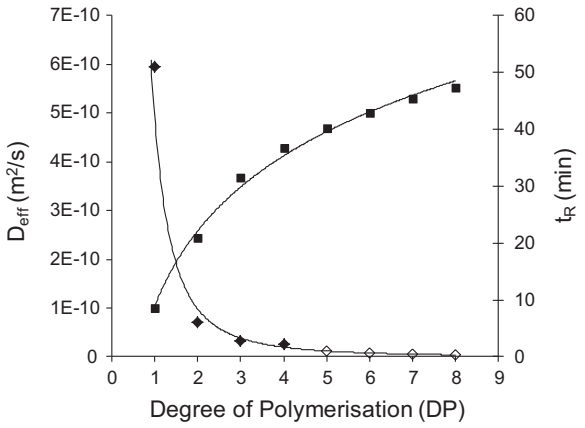

Fig. 5. Plots of DP versus the effective diffusion coefficient (D_{eff}, ♦/◊, primary y-axis) and HILIC retention time, t_R (■, secondary y-axis) for PC oligomers. D_{eff} values for PCs of DP 5–8 (◊) were extrapolated from the experimentally determined values for PCs of DP 1–4 (♦). Experimental conditions: ^1t_g = 50 min, ^1F = 1 mL/min, $^1V_{inj}$ = 10 μL. For further experimental details, refer to Section 3.4.

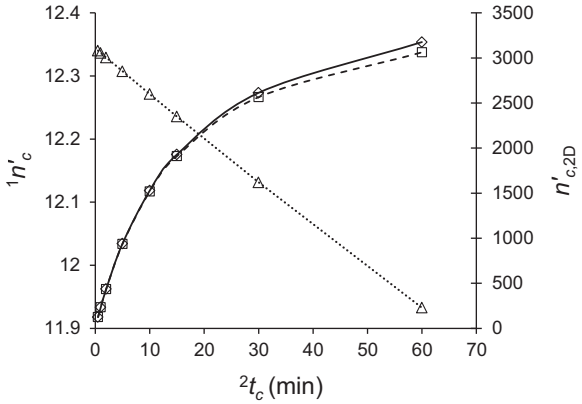

Fig. 6. Plots of first dimension (HILIC) peak capacity corrected for the effect of stop-flow operation ($^1n'_c$, △, primary y-axis) as a function of second dimension cycling time (^2t_c). Corrected 2D peak capacities ($n'_{c,2D}$) are plotted as a function of ^2t_c for the off-line (◊) and stop-flow (□) systems on the secondary y-axis. Experimental conditions: ^1t_g = 50 min, ^1F = 50 μL/min, $^1V_{inj}$ = 9 μL, ^1t_s = 1 min, $^2V_{inj}$ = 0.5 μL, ^2F = 1.5 mL/min. For further experimental details, refer to Sections 3.4.1 and 3.4.2.

see further) and stop-flow analyses, respectively) used in the current study, sufficient sensitivity was obtained and the separation integrity (sample profile) was maintained. This can be ascribed to the fact that on-column dilution is limited by the use of a 1 mm i.d. column in the first dimension, coupled to relatively fast second dimension analyses and the use of fluorescence detection (An alternative approach would be to use capillary columns in the primary dimension to avoid flow splitting and allow quantitative transfers of fractions to the secondary column [56,61,62], although the lower mass loadability of capillary columns does not guarantee better sensitivity).

By assuming the use of a suitable split ratio, constraints placed on the first dimension flow rate and sampling time by the maximum injection volumes permissible in the 2nd dimension are effectively removed. This then allowed optimisation of stop-flow HILIC × RP-LC analysis in a manner analogous to that followed for off-line HILIC × RP-LC. In stop-flow LC × LC, the second dimension cycle time, ^2t_c, determines the stop-flow time for a given 1st dimension peak according to Eq. (10a). Accordingly, corrected 1st dimension peak capacities, $^1n'_c$, were first calculated as a function of 2nd dimension cycle times, ^2t_c. Subsequently, corrected two-dimensional peak capacities were calculated for different ^2t_c times by taking under-sampling and orthogonality into account as for the off-line approach.

Fig. 6 illustrates the effective reduction of the first dimension peak capacity as a function of second dimension cycle time. Even for stop-flow periods of 60 min, the effective first dimension peak capacity is only reduced by 3.3% (primary y-axis). Also added in Fig. 6 (secondary y-axis) are the corrected two-dimensional peak capacities obtained for off-line and stop-flow HILIC × RP-LC analysis as a function of ^2t_c. The curves coincide virtually perfectly for ^2t_c values up to 15, indicating that identical results should be obtained for the two approaches for second dimension cycle time equal to or less than this value. Even for longer cycle times, the discrepancy in corrected two-dimensional peak capacities remains small, reaching a maximum of 3.6% at a ^2t_c value of 60 min. Since all other parameters affecting $n'_{c,2D}$ are identical for off-line and stop-flow LC × LC, this difference is virtually identical to that between 1st dimension peak capacities of the two approaches.

4.2.3. On-line HILIC × RP-LC analysis

In on-line LC × LC, the first dimension sampling time directly determines the second dimension cycle time ($^1t_s = {}^2t_c$) as well as the volume of first-dimension eluent to be injected onto the 2nd

dimension column. As alluded to previously, the volume of each 1st dimension fraction should not exceed a critical value ($^2V_{max}$ = 2 μL) to avoid band broadening due to injection of the sample in a solvent of higher eluotropic strength in the 2nd dimension [56]. In most on-line LC × LC studies, this limitation is addressed by using low flow rates in the first dimension, normally in combination with narrow-bore columns. The maximum flow rate allowable in the first dimension (^1F in μL/min) can be calculated using the following relationship:

$$^1F = \frac{^2V_{max}}{^1t_s} \quad (17)$$

where $^2V_{max}$ is the maximum volume that can be injected in the second dimension in μL and ^1t_s is the sampling time. In the case of HILIC × RP-LC, this implies a flow rate of 2 μL/min for a 1 min sampling time (the flow rate decreases further as sampling time is increased), which is much too low even for the 1 mm i.d. column used in this work. These conditions would result in a significant loss in 1st dimension peak capacity as well as an excessively long 1st dimension and total analysis times (the latter in the order of 21 h if the equivalent gradient profile is used as for the off-line analysis). In order to avoid these undesirable experimental restraints, a flow splitter was once again incorporated after the 1st dimension column to permit the use of higher 1st dimension flow rates in on-line HILIC × RP-LC analyses. This approach effectively de-couples the effect of 1st dimension flow rate on sampling time, allowing the former to become an unconstrained parameter in method optimisation.

For the optimisation of the on-line HILIC × RP-LC system, the following approach was then used. Since the second dimension cycle time, ^2t_c, determines the second dimension peak capacity, the amount of 1st dimension under-sampling (as reflected by β), as well as the overall analysis time (calculated using Eq. (8)), this parameter was utilised as the primary variable in optimisation. For each value of ^2t_c, ^2n_c was calculated using Eq. (2). Furthermore, all corrected 2D peak capacities ($n'_{c,2D}$) were calculated taking the relevant degree of under-sampling (according to Eq. (5)) and orthogonality (according to Eq. (4)) into account.

Initial calculations were based on HILIC operational parameters described in Section 3.4.1 for the off-line- and stop-flow HILIC × RP-LC analyses (i.e. a flow rate of 50 μL/min and a gradient time of 50 min on a 1 mm i.d. column). Under these conditions, a first dimension peak capacity (^1n_c) of ~14 was obtained according to Eq. (1). With this value in hand, it was possible to calculate $n'_{c,2D}$ for different analysis times (t_{tot}) (Fig. 7, curve *b*). The shape of the curve obtained for $n'_{c,2D}$ versus t_{tot} in this figure reflects the compromise between 2nd dimension peak capacities (requiring longer sampling times) and 1st dimension under-sampling (requiring shorter sampling times) inherent to on-line LC × LC. Sampling times (or ^2t_c) of 1 min and 2 min provided corrected 2D peak capacities of ~190 and 272, respectively, while the optimal sampling time was found to be 3 min, which provided a corrected two-dimensional peak capacity of 292. However, these values present small gains in peak capacity compared to a one-dimensional RP separation, which yields a peak capacity of ~280 for an analysis time of 60 min (as illustrated on the secondary *y*-axis in Fig. 7, curve *a*). For this reason, and in view of the fact that the total peak capacity achievable in an on-line LC × LC system is dependent on the first dimension gradient time [63,64], a longer gradient time was subsequently employed to improve the peak capacity for the on-line system.

Accordingly, the HILIC flow rate was decreased to 25 μL/min and the gradient time was increased to a 100 min. These conditions provided a 1st dimension peak capacity of ~28. This significant increase in ^1n_c can be ascribed to a combination of the use of smaller injection volumes (9 μL vs. 2.5 μL for flow rates of 50 and 25 μL/min, respectively) and the fact that the optimal linear velocity for oligomeric PCs are very low under HILIC conditions (unpublished results). In this context it can be noted that for the cocoa sample analysed here, which contains PCs of a wide range of molecular weights (MWs), the selection of an optimal flow rate for all compounds is not possible. This is a consequence of significant differences between diffusion properties of low- and high-MW PCs [65]. As a result, the optimal mobile phase linear velocity (flow rate) is much lower for the higher MW oligomers than for monomeric PCs, for example.

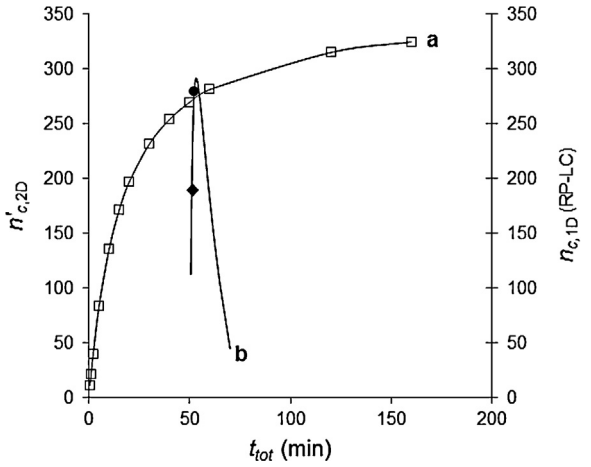

Fig. 7. Plots of the total analysis time (t_{tot}) versus 1D (RP) peak capacity (secondary *y*-axis, curve *a*) and corrected 2D peak capacity ($n'_{c,2D}$, primary *y*-axis, curve *b*) calculated for the on-line HILIC × RP-LC analysis of PCs using a first dimension flow rate and gradient time of 50 μL/min and 50 min, respectively. The black diamond and circle on curve *b* denote second dimension cycle times (^2t_c) of 1 and 2 min, respectively.

Corrected 2D peak capacities were calculated using the modified first dimension analysis conditions, and the results were compared. Fig. 8 depicts the relationship between corrected two-dimensional peak capacity and ^2t_c when 50 min (curve *b*) and 100 min (curve *c*) gradient times (with adapted flow rates) were used in the first dimension. From the two curves, it is evident that for a constant ^2t_c, the total 2D peak capacity increased by a factor 2 when the first dimension gradient time is doubled. This observation follows directly from the increase in 1st dimension peak capacity as outlined above.

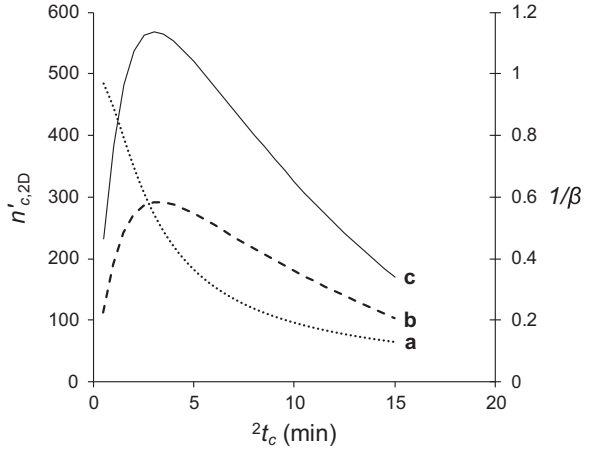

Fig. 8. Plots of second dimension cycling time (^2t_c) versus the inverse of the under-sampling correction factor (1/β, secondary *y*-axis, dotted line, curve *a*) and corrected 2D peak capacity (primary *y*-axis) calculated for the on-line HILIC × RP-LC analysis of PCs when gradient times of 50 min (50 μL/min, dashed line, curve *b*) and 100 min (25 μL/min, solid line, curve *c*) are used in the first dimension.

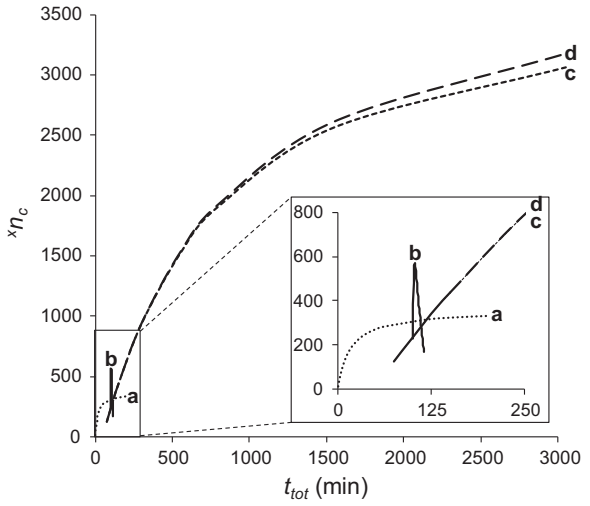

Fig. 9. Plots of one-dimensional RP-LC peak capacity (dotted line, curve *a*) and corrected 2D peak capacities for the on-line- (solid line, curve *b*), stop-flow- (dashed line, curve *c*) and off-line (dashed line, curve *d*) HILIC × RP-LC analyses of cocoa PCs as a function of total analysis time (*x*-axis).

Fig. 8 also indicates that the best compromise between sampling time and overall peak capacity is achieved when a second dimension cycle time of ~3 min is used at a 1st dimension flow rate of 25 μL/min (this value is identical to the optimal sampling time for a higher 1st dimension flow rate (curve *b*), albeit in the latter case delivering lower 2D peak capacity). In order to demonstrate the effect of under-sampling on 2D peak capacity, the inverse under-sampling correction factor ($1/\beta$) was plotted against $^{2}t_c$ (Fig. 8, curve *a*). The degree of under-sampling increases with $^{2}t_c$, as expected. In fact, this curve only approaches unity at around 0.5 min, implying that under-sampling becomes significant for $^{2}t_c$ times above this value. This effect is however balanced by the increase in second dimension peak capacity associated with longer cycle times–the combination of these effects is responsible for the shape of the $n'_{c,2D}$ curve. These results confirm that under-sampling alone should not be used as sole criterion in selecting the optimal sampling time in on-line LC × LC [46].

4.3. Comparison of on-line, off-line and stop-flow HILIC × RP-LC separations

A concise summary of the findings of this study is presented in Fig. 9, which depicts the peak capacities obtainable for the analysis of PCs by one-dimensional RP-LC and HILIC × RP-LC in each of the different modes as a function of the required analysis time, t_{tot}. Curve *a* in this figure shows the performance of one-dimensional RP-LC analysis at 1.5 mL/min as reference (Fig. 2). It should be noted that the RP-LC conditions used here closely approximate the optimal conditions for the analysis of PCs [65].

It is clear that on-line HILIC × RP-LC analysis, under the conditions utilised in the current study, provides increased separation performance compared to one-dimensional analysis for analysis times in the region of 2 h. For required peak capacities in excess of ~300, on-line HILIC × RP-LC delivers much better performance than 1D RP-LC. While higher peak capacities can be obtained by using longer gradient times and column lengths in RP-LC, this performance can only be reached at significantly longer analysis times than required for on-line LC × LC separations providing similar or better peak capacities. In addition, there is some flexibility in the choice of operating conditions for on-line HILIC × RP-LC which allows fine-tuning of the maximum peak capacity vs. analysis time compromise inherent to this technique.

Compared to 1D RP-LC and on-line HILIC × RP-LC, the off-line and stop-flow approaches provide much higher practical peak capacities. Also evident from Fig. 9 is that stop-flow HILIC × RP-LC analysis is a realistic alternative to the off-line approach, a result which follows directly from the band-broadening experiments presented in Section 4.2.2. This performance is however only reached at much longer total analysis times for both methods, and as such comes at the cost of lower peak capacity production rates compared to 1D and on-line methods. However, similar performance in terms of practical peak capacity is not attainable by either of the latter techniques. In the case of 1D RP-LC this is a result of the kinetic limitations resulting from pressure-constrained operation conditions [65]. For on-line HILIC × RP-LC on the other hand, this follows directly from the compromise between first- and second dimension peak capacities resulting from the balance of under-sampling vs. $^{2}t_c$ inherent to this approach. It is important to point out that the shape of the curve for on-line HILIC × RP-LC (curve *b* in Fig. 9) follows from the fact that the first dimension analysis time was kept constant in these calculations. Therefore, as the second dimension analysis time is increased, undersampling becomes progressively more important, eventually resulting in a dramatic loss of resolution. This is in contrast to off-line and stop-flow analysis, where the sampling time is constant (and is independent of the second dimension analysis time).

Based on these results, it can be concluded that for relatively simple PC mixtures, RP-LC will remain the method of choice due to the simplicity of this approach coupled to its good performance for relatively fast analyses. For more complex samples, on-line HILIC × RP-LC is ideally suited as a fast screening method to provide an extra dimension of information in terms of MW and isomeric distribution. For the detailed separation of complex PC mixtures, off-line or stop-flow methods should be used, in this case accepting much longer analysis times. Since PCs found in nature generally comprise highly complex mixtures, it may be argued that the latter two approaches are best suited for the analysis of these compounds in natural products.

5. Conclusions

HILIC × RP-LC shows particular promise for the analysis of complex oligomeric fractions of PCs due to the combination of size- and isomeric separations. The manner in which HILIC and RP-LC are combined will determine the total resolving power, as well as the time required for this performance. In this study, we presented a systematic approach for the optimisation and quantitative comparison of on-line, off-line and stop-flow HILIC × RP-LC modes for the analysis of PCs.

For these molecules, one-dimensional RP-LC provides the best performance for peak capacities up to 300, although this value is misleading as significant co-elution between isomers of different DP occurs. On-line HILIC × RP-LC is beneficial for peak capacities in the region of ~300–600; if higher peak capacities are desired, the off-line or stop-flow modes should be used. The on-line system offers automation, higher throughput and reproducibility, and minimal sample exposure, although these systems require specific interfaces that are more complicated to design and operate. The attainable peak capacity is ultimately limited by the compromise between first dimension sampling rate and second dimension analysis time.

The off-line system offers simplicity and high peak capacities. This technique can be difficult to automate and time-consuming, as additional sample handling steps are usually required, which can also compromise the sample integrity [66]. In the stop-flow set-up, band broadening of first dimension peaks due to stop flow proved insignificant for PCs when an analysis time of 15 min was

used in the second dimension. HILIC is an ideal method to use in the first dimension, as relatively long second dimension analysis times can be employed without significant band broadening in the first dimension, owing to the elution order (increasing size and decreasing diffusion coefficients) of PCs in this mode. Stop-flow HILIC × RP-LC therefore provides an attractive alternative to off-line analysis as it offers automation, minimal sample handling and avoids sample exposure between the two dimensions.

In summary, our results demonstrate that HILIC × RP-LC offers an effective means of increasing the resolving power for PC analysis; the manner in which these separations are coupled depends on the analysis goals in terms of total analysis time and required resolution. It should however be emphasised that complementary separation techniques are required to exploit the benefits of LC × LC, and that optimisation of each of the instrumental configurations must be performed in order to maximally exploit the performance of a selected strategy.

Acknowledgements

The authors thank the National Research Foundation (NRF, South Africa, Grant 70995 to AdV), the International Foundation of Science (IFS, Sweden, Grant F/4904-1 to AdV), SASOL and the Harry Crossley Foundation (bursary to KMK) for funding. W.J. Gerber is thanked for helpful discussions and assistance with some figures used in the paper.

References

[1] F. Erni, R.W. Frei, J. Chromatogr. 149 (1978) 561.
[2] P.C. Iraneta, K.D. Wyndham, D.R. McCabe, T.H. Walter, A review of Waters hybrid particle technology, part 3. Charged surface hybrid (CSH) technology and its use in liquid chromatography Waters white paper, June 2010, 720003469EN, www.waters.com
[3] J.C. Giddings, in: H.J. Cortes (Ed.), Multidimensional Chromatography: Techniques and Applications, Marcel Dekker, Inc., New York, 1990, p. 1.
[4] J.C. Giddings, Anal. Chem. 56 (1984) 1258A.
[5] H.J. Cortes, in: H.J. Cortes (Ed.), Multidimensional Chromatography: Techniques and Applications, Marcel Dekker, Inc., New York, USA, 1990, p. 251.
[6] P. Dugo, F. Cacciola, T. Kumm, G. Dugo, L. Mondello, J. Chromatogr. A 1184 (2008) 353.
[7] S.P. Dixon, I.D. Pitfield, D. Perrett, Biomed. Chromatogr. 20 (2006) 508.
[8] D.R. Stoll, X. Li, X. Wang, P.W. Carr, S.E.G. Porter, S.C. Rutan, J. Chromatogr. A 1168 (2007) 3.
[9] R.A. Shellie, P.R. Haddad, Anal. Bioanal. Chem. 386 (2006) 405.
[10] J.H. Knox, J. Chromatogr. A 831 (1999) 3.
[11] J.H. Knox, H.P. Scott, J. Chromatogr. 282 (1983) 297.
[12] B. Tran, E. Lundanes, T. Greibrokk, Chromatographia 64 (2006) 1.
[13] F. Bedani, W.T. Kok, H.-G. Janssen, J. Chromatogr. A 1133 (2006) 126.
[14] K. Miyabe, H. Kobayashi, D. Tokuda, N. Tanaka, J. Sep. Sci. 29 (2006) 2452.
[15] A.M. Striegel, J. Chromatogr. A 932 (2001) 21.
[16] A.J. Link, J. Eng, D.M. Schieltz, E. Carmack, G.J. Mize, D.R. Morris, B.M. Garvik, J.R. Yates III, Nat. Biotechnol. 17 (1999) 676.
[17] W.H. McDonald, R. Ohi, D.T. Miyamoto, T.J. Mitchison, J.R. Yates III, Int. J. Mass Spectrom. 219 (2002) 245.
[18] M.P. Washburn, R. Ulaszek, C. Deciu, D.M. Schieltz, J.R. Yates, Anal. Chem. 74 (2002) 1650.
[19] M.P. Washburn, D. Wolters, J.R. Yates III, Nat. Biotechnol. 19 (2001) 242.
[20] D.A. Wolters, M.P. Washburn, J.R. Yates, Anal. Chem. 73 (2001) 5683.
[21] E. Blahová, P. Jandera, F. Cacciola, L. Mondello, J. Sep. Sci. 29 (2006) 555.
[22] J.N. Fairchild, K. Horvath, G. Guiochon, J. Chromatogr. A 1216 (2009) 1363.
[23] E. Sommella, F. Cacciola, P. Donato, P. Dugo, P. Campiglia, L. Mondello, J. Sep. Sci. 35 (2012) 530.
[24] P. Dugo, N. Fawzy, F. Cichello, F. Cacciola, P. Donato, L. Mondello, J. Chromatogr. A (2013) http://dx.doi.org/10.1016/j.chroma.2012.12.042
[25] F. Bedani, P.J. Schoenmakers, H.-G. Janssen, J. Sep. Sci. 35 (2012) 1697.
[26] P.J. Schoenmakers, G. Vivo-Truyols, W.M.C. Decrop, J. Chromatogr. A 1120 (2006) 282.
[27] G. Vivo-Truyols, S.J. van der Wal, P.J. Schoenmakers, Anal. Chem. 82 (2010) 8525.
[28] A. de Villiers, F. Lynen, P. Sandra, J. Chromatogr. A 1216 (2009) 3431.
[29] K.M. Kalili, A. de Villiers, J. Chromatogr. A 1216 (2009) 6274.
[30] K.M. Kalili, A. de Villiers, J. Sep. Sci. 31 (2010) 853.
[31] T. Beelders, K.M. Kalili, E. Joubert, D. de Beer, A. de Villiers, J. Sep. Sci. 35 (2012) 1808.
[32] K.M. Kalili, A. de Villiers, J. Chromatogr. A (2013), http://dx.doi.org/10.1016/j.chroma.2013.03.009.
[33] P.J. Marriot, P. Schoenmakers, Z. Wu, LC–GC Eur. 25 (2012) 266.
[34] P. Schoenmakers, P. Marriott, J. Beens, LC–GC Eur. 16 (2003) 335.
[35] J.C. Giddings, Anal. Chem. 39 (1967) 1027.
[36] U.D. Neue, J. Chromatogr. A 1079 (2005) 153.
[37] Z. Liu, D.G. Patterson, M.L. Lee, Anal. Chem. 67 (1995) 3840.
[38] M. Gilar, P. Olivova, A.E. Daly, J.C. Gebler, Anal. Chem. 77 (2005) 6426.
[39] P.J. Slonecker, X. Li, T.H. Ridgway, J.G. Dorsey, Anal. Chem. 68 (1996) 682.
[40] M.R. Schure, J. Chromatogr. A 1218 (2011) 293.
[41] M. Gilar, J. Fridrich, M.R. Schure, A. Jaworski, Anal. Chem. 84 (2012) 8722.
[42] M. Gray, G.R. Dennis, P. Wormell, R.A. Shalliker, P. Slonecker, J. Chromatogr. A 975 (2002) 285.
[43] N.E. Watson, J.M. Davis, R.E. Synovec, Anal. Chem. 79 (2007) 7924.
[44] R.E. Murphy, M.R. Schure, J.P. Foley, Anal. Chem. 70 (1998) 1585.
[45] J.V. Seeley, J. Chromatogr. A 962 (2002) 21.
[46] K. Horie, H. Kimura, T. Ikegami, A. Iwatsuka, N. Saad, O. Fiehn, N. Tanaka, Anal. Chem. 79 (2007) 3764.
[47] X. Li, D.R. Stoll, P.W. Carr, Anal. Chem. 81 (2009) 845.
[48] M.A. Kelm, J.C. Johnson, R.J. Robbins, J.F. Hammerstone, H.H. Schmitz, J. Agric. Food Chem. 54 (2006) 1571.
[49] R.J. Robbins, J. Leonczak, J.C. Johnson, J. Li, C. Kwik-Uribe, R.L. Prior, L. Gu, J. Chromatogr. A 1216 (2009) 4831.
[50] A. Yanagida, H. Murao, M. Ohnishi-Kameyama, Y. Yamakawa, A. Shoji, M. Tagashira, T. Kanda, H. Shindo, Y. Shibusawa, J. Chromatogr. A 1143 (2007) 153.
[51] L. Montero, M. Herrero, M. Prodanov, E. Ibanez, A. Cifuentes, Anal. Bioanal. Chem. (2012), http://dx.doi.org/10.1007/s00216-012-6567-5.
[52] T. Ikegami, K. Tomomatsu, H. Takubo, K. Horie, N. Tanaka, J. Chromatogr. A 1184 (2008) 474.
[53] A. D'Attoma, C. Grivel, S. Heinisch, J. Chromatogr. A 1262 (2012) 148.
[54] B. Chauve, D. Guillarme, P. Cleon, J-L. Veuthey, J. Sep. Sci. 33 (2010) 752.
[55] H. Tanaka, X. Zhou, O. Masayoshi, J. Chromatogr. A 987 (2003) 119.
[56] P. Jandera, T. Hajek, M. Stankova, K. Vynuchalova, P. Cesla, J. Chromatogr. A 1268 (2012) 91.
[57] P.Q. Tranchida, P. Dugo, G. Dugo, L. Mondello, J. Chromatogr. A 1054 (2004) 3.
[58] Y. Wang, X. Lu, G. Xu, J. Sep. Sci. 31 (2008) 1564.
[59] F. Lestremau, D. Wu, R. Szucs, J. Chromatogr. A 1217 (2010) 4925.
[60] M.R. Filgueira, Y. Huang, K. Witt, C. Castells, P.W. Carr, Anal. Chem. 83 (2011) 9531.
[61] T. Takeuchi, J. Chromatogr. 499 (1990) 549.
[62] H. Cortes, J. Chromatogr. 626 (1992) 3.
[63] Y. Huang, H. Gu, M. Filgueira, P.W. Carr, J. Chromatogr. A 1218 (2011) 2984.
[64] L.W. Potts, D.R. Stoll, X. Li, P.W. Carr, J. Chromatogr. A 1217 (2010) 5700.
[65] K.M. Kalili, D. Cabooter, G. Desmet, A. de Villiers, J. Chromatogr. A 1236 (2012) 63.
[66] I. François, A. de Villiers, P. Sandra, J. Sep. Sci. 29 (2006) 492.

Addendum D

Systematic optimisation and evaluation of on-line, off-line and stop-flow comprehensive hydrophilic interaction chromatography × reversed phase liquid chromatographic analysis of procyanidins, Part II: Application to cocoa procyanidins

K.M. Kalili, A. de Villiers, J. Chromatogr. A 1289 (2013) 69-79.

Journal of Chromatography A, 1289 (2013) 69–79

Contents lists available at SciVerse ScienceDirect

Journal of Chromatography A

journal homepage: www.elsevier.com/locate/chroma

Systematic optimisation and evaluation of on-line, off-line and stop-flow comprehensive hydrophilic interaction chromatography × reversed phase liquid chromatographic analysis of procyanidins. Part II: Application to cocoa procyanidins

Kathithileni M. Kalili, André de Villiers *

Stellenbosch University, Department of Chemistry and Polymer Science, Private Bag X1, Matieland 7602, South Africa

ARTICLE INFO

Article history:
Received 1 November 2012
Received in revised form 13 February 2013
Accepted 8 March 2013
Available online 17 March 2013

Keywords:
Cocoa
Comprehensive two-dimensional liquid chromatography (LC × LC)
On-line
Off-line
Procyanidins
Stop-flow

ABSTRACT

Procyanidins present a severe analytical challenge due to their structural complexity and diversity. Comprehensive two-dimensional hydrophilic interaction chromatography × reversed-phase liquid chromatography (HILIC × RP-LC) provides a highly efficient separation system for procyanidins. In the first part of this contribution a systematic approach for the optimisation and evaluation of HILIC × RP-LC analyses in on-line, off-line and stop-flow modes was presented. The three systems were compared in terms of peak capacity, the number of peaks produced per unit time as well as the total analysis time required to carry out such analyses by taking under-sampling, degree of orthogonality and stop-flow band-broadening into account. In this paper, the experimental verification of these findings using cocoa procyanidins as an application is presented. The results show that while optimisation procedures based on theoretical considerations remain largely valid in practice, several important experimental considerations should also be taken into account to achieve maximum performance in all three modes of HILIC × RP-LC. On-line analysis provides an effective tool for the screening of procyanidin content within reasonable times, provided that under-sampling of first dimension peaks is minimised. Off-line- and stop-flow HILIC × RP-LC analyses on the other hand are more suited for the detailed analysis of complex procyanidin fractions, with the latter being shown to be a promising automated alternative providing the same performance as the off-line approach. Experimental data presented verify the conclusion that stop-flow operation has a negligible effect on first dimension band broadening under the optimised experimental conditions used.

1. Introduction

Procyanidins (PCs) are a class of widely occurring natural phenolic compounds comprising monomeric, oligomeric and polymeric flavan-3-ol isomeric structures. These secondary metabolites are known to display a diverse range of biological and physiological activities, and hence extensive research has been devoted to them [1]. PCs possess anti-oxidant, anti-microbial, anti-inflammatory, anti-carcinogenic and anti-hypertensive activities, amongst others [2–4].

Considering their biological importance and widespread distribution in nature, there is a need for accurate analytical methods for PC determination. As a consequence of their diversity in terms of constituent monomeric units ((+)-catechin, (−)-epicatechin, (epi)catechin gallates and additional derivatives), coupled to the fact that monomeric units may be linked in one of three different configurations (Fig. 1), the number of isomeric structures of oligomeric PCs increase exponentially with the degree of polymerisation (DP) [5]. While bulk spectrophotometric- and precipitation methods can be used to obtain information on the total (average) procyanidin composition of natural extracts [6–9], separation is required for further investigation of their exact chemical composition. Detailed analysis of individual PC compounds is essential in light of the fact that biological activity depends on the structures of individual PC molecules [10]. High performance liquid chromatography (HPLC) is currently the method of choice for PC analysis. Reversed phase liquid chromatography (RP-LC) is most commonly used for this purpose, often in combination with fluorescence or electrospray-ionisation mass spectrometric (ESI-MS) detection [11]. While RP-LC provides good separation performance, these methods show limitations when analysing highly complex mixtures of PCs due to co-elution of compounds of different DPs.

* Corresponding author. Tel.: +27 21 808 3351; fax: +27 21 808 3360.
E-mail address: ajdevill@sun.ac.za (A. de Villiers).

0021-9673/$ – see front matter © 2013 Elsevier B.V. All rights reserved.
http://dx.doi.org/10.1016/j.chroma.2013.03.009

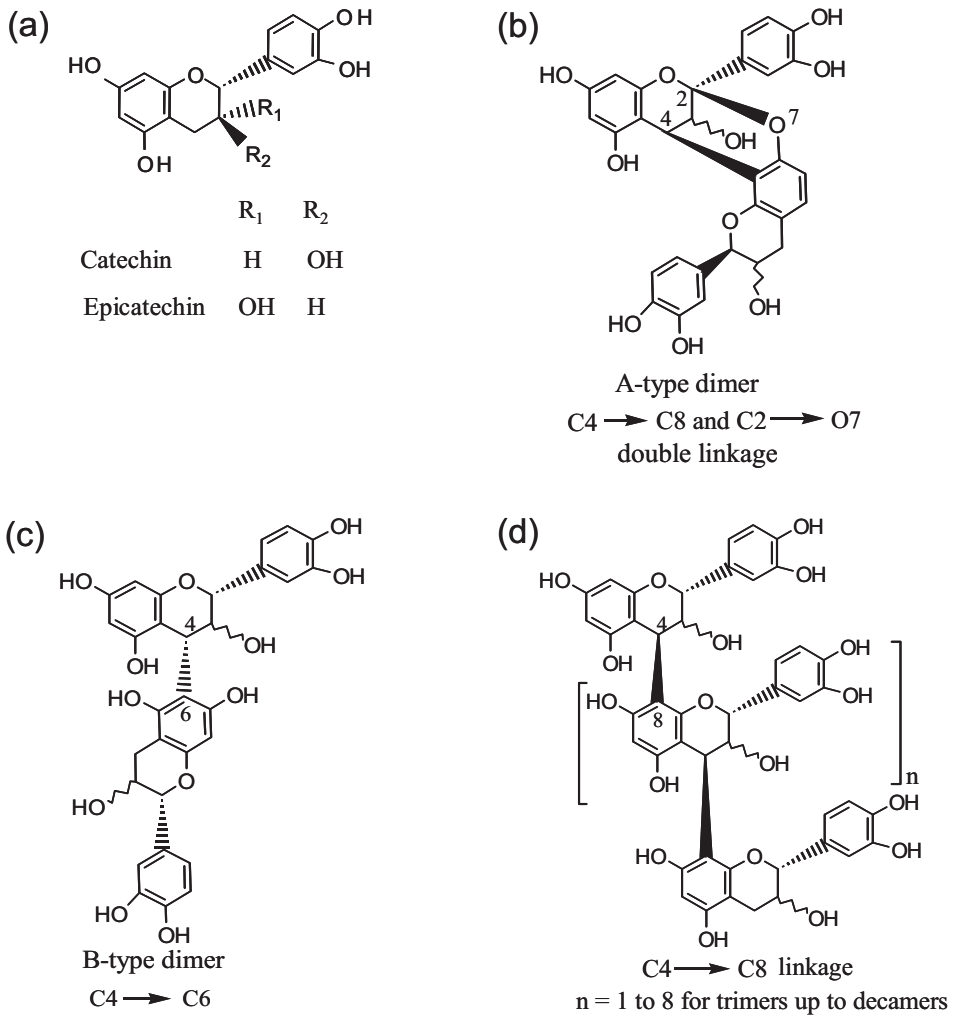

Fig. 1. Structures for (a) monomeric, (b) A-type dimeric, (c) C4 → C6 B-type dimeric and (d) C4 → C8 B-type higher oligomeric procyanidins.

On the other hand, normal phase liquid chromatography (NP-LC) and hydrophilic interaction chromatography (HILIC) have in recent years effectively been used to separate PCs according to DP [2,12–20]. Isomeric separation is however not possible using these techniques. Therefore, despite considerable effort dedicated to PC analysis during the past two decades, complete resolution of especially the high molecular weight (HMW) PCs by HPLC remains elusive [21]. This limitation can be ascribed to the large number of isomeric structures found in crude phenolic extracts, coupled to the relatively low separation power provided by conventional HPLC methods. As a consequence, MS and tandem MS (MS/MS) have been extensively used in PC analysis. However, MS does not allow differentiation of isomeric structures, and ESI-MS shows limitations in terms of quantitative analysis of complex samples. Improved methods for the separation of PCs therefore remain one of the great challenges in research related to PCs today [22].

Coupling multiple separation techniques is an established approach to improve the separation power of chromatographic methods. This is due to the increased separation space obtained through the combination of complementary separation mechanisms [23–25]. We have previously explored the comprehensive combination of HILIC and RP-LC separations for PC analysis [26]. Off-line HILIC × RP-LC was found to provide a powerful method for the analysis of cocoa PCs due to the combination of molecular weight (MW) and isomeric information obtained. In addition, this approach has also proven useful for the separation of different phenolic classes such as prodelphinidins, flavonols, phenolic acids, flavanones, chalcones, flavones and isoflavones in green [27] and rooibos [28] teas. Although HILIC × RP-LC analysis delivered significantly improved resolution, this benefit was realised at the expense of very long analysis times which are a characteristic of off-line comprehensive two-dimensional liquid chromatography (LC × LC).

LC × LC may be performed in one of three different ways: using on-line, off-line or stop-flow configurations. Each of these modes of operation offer distinct advantages for specific types of analyses. In a related paper [29], a systematic approach for the optimisation and evaluation of on-line-, off-line- and stop-flow HILIC × RP-LC methods for PC analysis was presented based on the complex interplay of several experimental parameters and their effects on the one- and two-dimensional separations. In the current report, the findings of this paper are confirmed experimentally using cocoa PCs as application. The potential of each of the HILIC × RP-LC configurations for real-life PC analysis will be discussed.

2. Experimental

2.1. Reagents and materials

Cocoa beans were purchased from a local supermarket. Standards of (−)-epicatechin and (±)-catechin as well as HPLC grade methanol, acetonitrile, formic acid, acetic acid and acetone were purchased from Sigma–Aldrich (Steinheim, Germany). HPLC grade

hexane was purchased from Burdick & Jackson (Muskegon, USA). Deionised water was obtained using a Milli-Q water purification system (Millipore, Milford, MA, USA). All solutions were filtered through 0.45 μm HVLP membrane filters (Millipore) and degassed in an ultrasonic bath (Branson Model 3510, Danbury, USA) before use.

2.2. Sample preparation

The cocoa sample was prepared as reported previously [26]. The sample was freeze dried and re-dissolved in 80% acetonitrile/20% methanol (v/v) for injection in HILIC.

2.3. Instrumentation

For all LC × LC analyses, a Hewlett Packard 1050 HPLC system equipped with a quaternary pump, autosampler, diode array and fluorescence (model 1046 A) detectors and controlled by Chemstation software (Agilent Technologies, Waldbronn, Germany) was used in the first dimension. The system volume was reduced by replacing all connectors with minimal lengths of 0.1 mm i.d PEEK tubing. In the second dimension, an Acquity UPLC system equipped with a binary pump, autosampler, column oven, photodiode array (PDA) detector (500 nL flow cell, 10 mm path length) and controlled by Waters Empower software (Waters, Milford, MA, USA) was used.

LC–MS analyses were performed on an Acquity UPLC system equipped with a binary solvent manager and autosampler (Waters). The UPLC system was connected via an ESI source to a Waters Ultima API quadrupole time-of-flight (Q-TOF) mass spectrometer. Detection was carried out in negative ionisation mode with a capillary voltage of −3.7 kV and a cone voltage of 35 V. A source temperature of 100 °C and a mass scan range of 250–2000 mass-to-charge (m/z) ratios were used. Data were acquired and analysed using MassLynx v.4.0 software (Waters). Calibration was performed using a sodium formate solution. For HILIC analyses, a desolvation temperature of 300 °C was applied. The desolvation and cone gas flows (both N_2) were 300 L/h and 50 L/h, respectively. For RP-LC analyses, the desolvation temperature was 350 °C, and desolvation and cone gas flows were 350 L/h and 50 L/h, respectively. For RP-LC–ESI-MS analyses, the eluent was split 1:7 before introduction into the ionisation chamber. This Q-TOF instrument was not equipped with a lock-spray function for accurate mass measurements, and therefore m/z values are reported to one decimal place.

2.4. Chromatographic methods

2.4.1. One-dimensional methods

2.4.1.1. Hydrophilic interaction chromatography (HILIC) analyses. Separations were performed on a Develosil Diol-100 column (250 mm × 1 mm i.d., 5 μm d_p, Nomura Chemical Co., Aichi, Japan) using a method [26] adapted from Kelm et al. [17]. The gradient was slightly modified compared to [26] to obtain a similar separation on the 1050 HPLC instrument used here. The binary mobile phase consisted of (A) acetonitrile and acetic acid (99:1, v/v) and (B) methanol, water and acetic acid (94.05:4.95:1, v/v/v) and gradient elution as outlined in Section 2.4.2. All HILIC separations were performed at ambient temperature. Fluorescence data were acquired using the DAx 8.0 data acquisition software (Van Mierlo Software, Amsterdam, The Netherlands), with excitation and emission wavelengths at 230 and 321 nm, respectively, and a photomultiplier (PMT) gain of 10.

2.4.1.2. Reversed-phase liquid chromatography (RP-LC) analyses. RP-LC separations were performed on an Agilent Zorbax SB-C18 column (50 mm × 4.6 mm i.d., 1.8 μm) protected with a Phenomenex C18 guard column (4 mm × 3 mm i.d., Torrance, USA) using gradient conditions detailed in Section 2.4.2. Gradients were adapted to the 50 mm column and different flow rates from [26]. The binary mobile phase consisted of 0.1% formic acid in water (v/v) (A) and acetonitrile (B). A column temperature of 50 °C was used in all cases, and UV chromatograms were recorded at 210, 280, 320 and 370 nm. Fluorescence data were acquired as specified for HILIC analyses.

2.4.2. Two-dimensional methods

2.4.2.1. Off-line HILIC × RP-LC analyses. HILIC separations were performed using the following linear gradient: 4–40% B (0–40 min), 40% B isocratic (40–45 min), 40–4% B (45–50 min), followed by column re-equilibration. The flow rate was 50 μL/min and 9 μL was injected. One-minute fractions (corresponding to 50 μL each) of the HILIC effluent were automatically collected over the entire separation window using a programmable BIO-RAD Model 2110 fraction collector (Corston, UK). The collected fractions were immediately transferred to 1.5 mL vials containing 250 μL inserts and kept under N_2 until analysed by gradient RP-LC.

In the second dimension, a linear gradient was performed as follows: 2% B (0–0.13 min), 2–18% B (0.13–5.40 min), 18–25% B (5.40–9.00 min), 25–100% B (9.00–10.35 min), 100% B until 11.25 min before returning to the initial conditions at 12.60 min. The column was re-equilibrated for 2.40 min before the next analysis. A flow rate of 1.5 mL/min was used and 1.5 μL was injected using the partial loop with needle overfill mode with 0.1% formic acid as the weak needle wash.

2.4.2.2. Stop-flow HILIC × RP-LC analyses. For stop-flow analyses, a 10-port 2-position high pressure switching valve (1000 bar maximum pressure, 150 μm bore, Valco Instruments Co. Inc., Houston, Texas, USA) was used. In valve position 1 (Fig. 2A), the HILIC column effluent was directed via a flow splitter (set at a split ratio of ∼1:33) to the RP column. A T-piece union equipped with different lengths of 0.0025″ i.d. PEEK tubing was used for flow-splitting. The split ratio was set by adjusting the lengths of tubing and measuring the ratio of the column eluate and the waste effluent using a Hamilton GC injection syringe (Reno, Nevada, USA).

The column, flow rate, gradient profile and injection volume in the first dimension were identical to those used for off-line HILIC × RP-LC analysis (Section 2.4.2.1 above). In stop-flow analyses, sampling times of 1 min were also used, which in combination with the flow splitter ensured an effective injection volume of ∼1.5 μL in the second dimension. Following transfer of HILIC fractions during 1 min periods, the valve was switched to position 2 and the flow in the first dimension was simultaneously stopped. In this position, the HILIC column was connected to a blocked port of the 10-port valve to maintain a constant pressure in the first dimension during the stop-flow period. While in position 2, RP-LC separation of the previously transferred fraction was performed using identical experimental conditions as outlined for off-line HILIC × RP-LC analyses (Section 2.4.2.1). Following completion of each second dimension analysis and re-equilibration of the column (second dimension cycle time = 15 min), the valve was switched to position 1 and the flow in the first dimension started at the same time for the transfer of the next fraction. Care was taken to ensure identical starting times on both instruments.

2.4.2.3. On-line HILIC × RP-LC analyses. For on-line LC × LC analyses, the same 10-port switching valve as for the stop-flow set-up was used as the interface between the two dimensions. The valve was configured in a symmetrical manner [30] and equipped with two 5-μL loops (Fig. 2B). The valve was switched every 2 or 3 min through the UPLC external events. The HILIC separation was effected by a series of linear gradients of B into A as follows: 4–40%

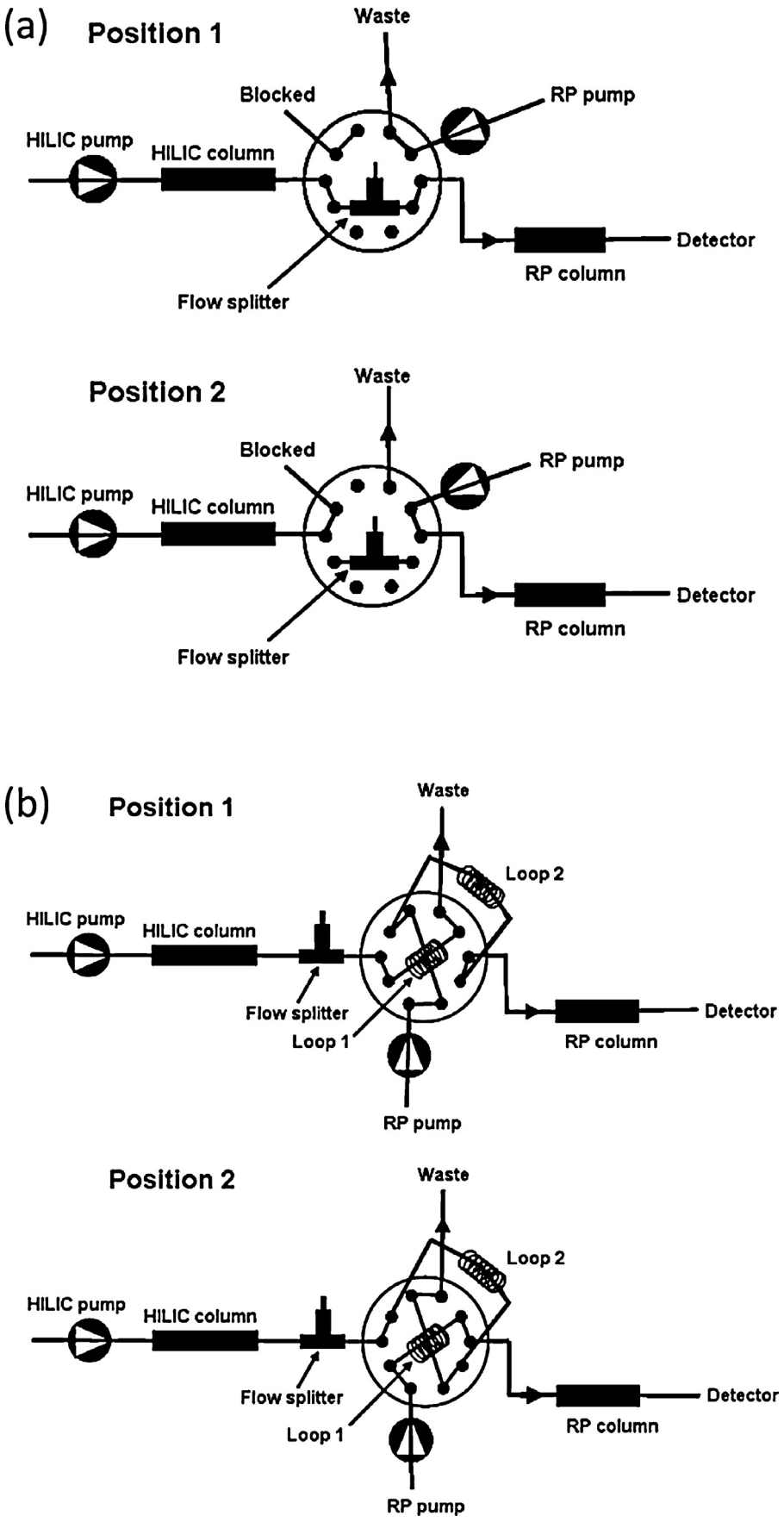

Fig. 2. A schematic illustration of the instrumental configurations used for (a) stop-flow and (b) on-line HILIC × RP-LC experiments.

B (0–80 min), 40% B isocratic (80–90 min), 40–4% B (90–100 min), followed by column re-equilibration. The flow rate was 25 μL/min and an injection volume of 2.5 μL was used. The HILIC flow was split post-column through a tee union at split ratios of ~1:33 (for a 2 min sampling time, ^1t_s) and ~1:50 (for ^1t_s = 3 min).

For RP separation, two gradient methods corresponding to 2 and 3 min cycling (^2t_c) times were used. For a 2 min cycle time, a linear gradient was performed as follows: 2% B (0–0.02 min), 2–18% B (0.02–0.10 min), 18–25% B (0.10–1.10 min), 25–100% B (1.10–1.20 min), 100–2% B (1.20–1.30 min). The column was re-equilibrated for 0.70 min before the next analysis. For a 3 min cycling time, a linear gradient was performed as follows: 2% B (0–0.03 min), 2–18% B (0.03–0.15 min), 18–25% B (0.15–1.65 min), 25–100% B (1.65–1.80 min), 100–2% B (1.80–1.95 min). The column was re-equilibrated for 1.05 min before the next analysis. The flow rate was 1.5 mL/min for both cycle times.

2.5. Calculations

All optimisation and evaluation calculations were performed in Microsoft Excel. Raw fluorescence data for the RP analyses were exported into STATISTICA 10 (Statsoft Inc., USA) to create 2-D contour plots.

3. Results and discussion

3.1. One-dimensional separations and identification of cocoa procyanidins

For the identification of cocoa PCs, one-dimensional HILIC- and RP-LC separations were coupled to negative mode ESI-Q-TOF-MS detection. Optimal experimental conditions in each dimension as determined in [29] for on-line, off-line and stop-flow HILIC × RP-LC were used for this purpose (refer to Section 2.4 for details). In order to identify PCs in HILIC × RP-LC analyses, mass spectral information for individual oligomers were correlated with retention times and fluorescence data in both HILIC and RP-LC dimensions. In this manner, all the major peaks observed in HILIC × RP-LC contour plots could be identified, although the exact structures of isomers could not be determined.

PC oligomers were detected as singly- or multiply-charged ions under both HILIC and RP-LC conditions. Singly charged ions were commonly observed as base peaks of the spectra for low MW compounds (DP 1–4), while multiply charged ions predominated for the HMW PCs, as previously reported [26]. Extracted ion chromatograms (EICs) obtained using the off-line HILIC– and RP-LC–ESI-MS conditions are presented in Fig. 3. Fig. 3A confirms that in HILIC, separation occurs on the basis of polarity, resulting in increasing retention as a function of DP for PCs [17,18]. While this method gives information on the MW distribution of PCs in the sample, compounds with the same molecular weight (or identical polarity, as is the case for isomeric PCs of the same DP) co-elute under these conditions. In contrast, RP-LC provides separation of isomers, as is evident from multiple compounds with the same mass-to-charge (m/z) depicted in the RP-LC–ESI-MS EICs shown in Fig. 3B. A high degree of co-elution is also observed and especially HMW compounds are poorly resolved.

In addition to the more common B-type PC oligomers, several A-type isomers were also detected at low levels [26]. These compounds are easily distinguished by MS due to their different MWs, as well as chromatographically due to different polarities, resulting in lower retention in HILIC and higher retention times in RP-LC [26]. Furthermore, several A-type glycosylated procyanidins were also detected. Chromatographic and mass spectrometric

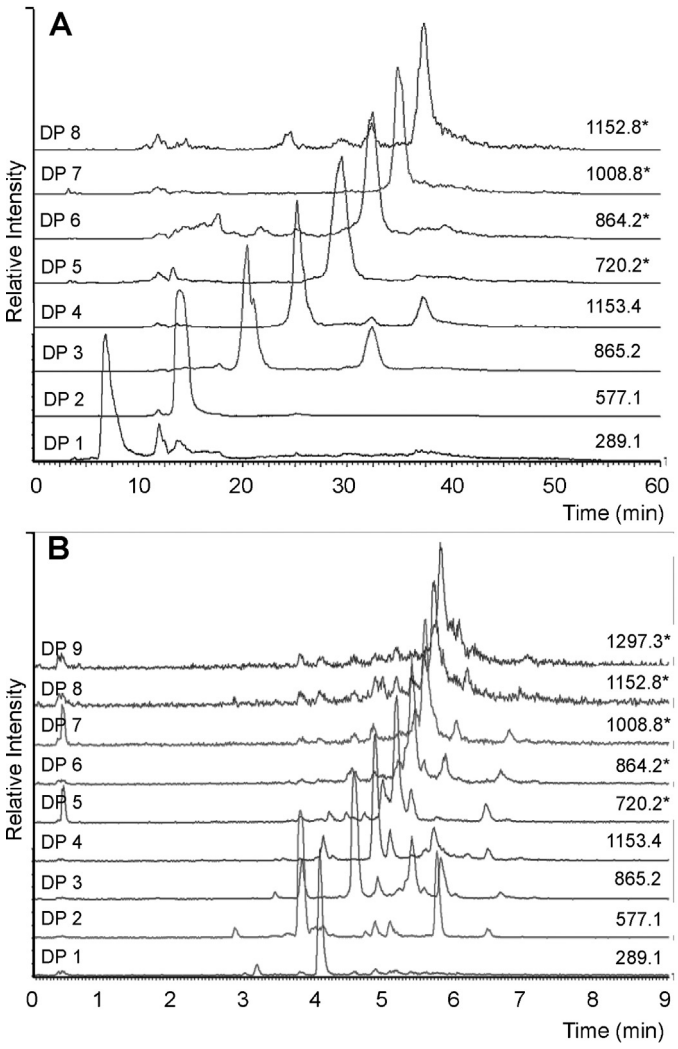

Fig. 3. Extracted ion chromatograms (EICs) for procyanidin oligomers obtained from the HILIC–ESI-MS (A) and RP-LC–ESI-MS (B) analyses of a cocoa extract. Experimental conditions for these analyses were as used for off-line HILIC × RP-LC analyses. For further details, refer to Section 2.4.2.1. * denotes multiply charged species.

characteristics of these compounds are in accordance with O-β-D-galactopyranosyl-epicatechin-(2α → 7,4α → 8)-epicatechin and O-L-arabinopyranosyl-epicatechin-(2α → 7,4α → 8)-epicatechin previously identified in cocoa by Porter et al. [31].

As is evident from the EICs for the different PC oligomers in RP-LC, a large number of isomeric structures were detected in the cocoa extract. Co-elution occurs in both HILIC and RP separations and as a result 1-D LC–MS mass spectra often contain information for multiple PC molecules [26]. Clearly, due to the similarity of PC mass spectra and the inability of MS to distinguish between isomeric compounds, improved chromatographic resolution is required to allow detailed investigation of individual PC structures.

3.2. Comprehensive HILIC × RP-LC analyses

In the first part of this contribution [29], a systematic approach for the optimisation and evaluation of on-line, off-line and stop-flow HILIC × RP-LC analyses using experimental data for PCs was reported. The aim of the current contribution was to experimentally verify the conclusions based on theoretical calculations for the specific system and sample under investigation. In the following sections, experimental data for each of the LC × LC systems will be presented and compared to the results obtained in the

optimisation studies. Note that optimisation was performed using values for one- and two-dimensional peak capacities following correction for under-sampling, extent of orthogonality and stop-flow band broadening [29], and may therefore be expected to provide an accurate reflection of the experimental reality.

3.2.1. Off-line and stop-flow HILIC × RP-LC analyses

The optimisation of off-line- and stop-flow HILIC × RP-LC analyses were based on the theoretical calculations reported previously [29]. To enable a quantitative comparison of these methods, identical sampling times as well as flow rates and gradient times were employed in each dimension for off-line and stop-flow systems (refer to Sections 2.4.2.1 and 2.4.2.2 for experimental details).

In the first dimension, a 50 min gradient and flow rate of 50 μL/min were used [29]. Based on calculations taking into account the effect of sampling time, $^{1}t_s$, on the overall practical peak capacity ($n'_{c,2D}$), a sampling time of 1 min was used to ensure sufficient sampling rates while keeping the number of fractions to a minimum to avoid unnecessarily long analysis times. Accordingly, 1-min fractions were collected (for off-line analyses) or transferred directly to the second dimension column for stop-flow analyses. Under the HILIC conditions used here, peak widths ranged between 1.94 and 7.67 min, which corresponds to a sampling rate of two or more fractions for every first dimension peak, and a total number of fractions, f, of 50. The under-sampling correction factor, β, is equal to 1.12 under these conditions, which ensures acceptable losses in first dimension peak capacity due to insufficient sampling of HILIC peaks. Note that in the case of stop-flow analyses, any additional band broadening in the first dimension resulting from stopping of the flow would in fact result in a reduction of the extent of under-sampling. This aspect was taken into consideration in the optimisation strategy by quantitative measurement of stop-flow band broadening to correct the effective first dimension peak capacity before correcting for under-sampling [29].

For a given sampling time, the highest practical peak capacity is achieved for the longest second dimension cycle time, $^{2}t_c$, as demonstrated in [29]. The latter refers to the time required to complete the gradient separation and re-equilibrate the second dimension column, i.e. $^{2}t_c = {}^{2}t_g + {}^{2}t_{re\text{-}eq}$. However, this performance is achieved at excessively long analysis times (e.g. ~25.8 h for the off-line set-up when $^{1}t_s$ = 1 min and $^{2}t_c$ = 30 min). For this reason, a second dimension cycle time of 15 min ($^{2}t_g$ = 11.25 min) was selected as this provided high resolution at more acceptable total analysis times (~13.3 h) and better peak capacity production rates (in both off-line and stop-flow LC × LC analyses, $^{2}t_c$ primarily affects the second dimension peak capacity and total analysis time, and not first dimension under-sampling as is the case for on-line analysis). Longer second dimension analysis times do however influence band broadening in the first dimension due to stop-flow operation, although this effect was shown to be virtually negligible for $^{2}t_c$ times up to 60 min [29].

For off-line analyses, 1.5 μL of each collected fraction was injected onto the second dimension column. To ensure similar second dimension injection volumes in stop-flow HILIC × RP-LC, the mobile phase flow was split after the first dimension column using a split ratio of ~1:33 (see Fig. 2A for details on the experimental configuration used for stop-flow analyses). This step was essential to allow the use of equivalent flow rates in the first dimension and avoid band broadening due to injection of large volumes of the strong HILIC solvent in the second dimension during stop-flow analysis.

Contour plots for the off-line and stop-flow HILIC × RP-LC analyses of a cocoa extract obtained under these conditions are presented in Fig. 4. Note that the contour plot axes are swapped compared to conventional representation of LC × LC data, with the second dimension RP-LC separation on the *x*-axis. This was done because RP-LC provides more detailed information in terms of isomeric separation, and therefore this form of presentation facilitates interpretation of contour plots of PCs.

The similar performance of these two methodologies confirms theoretical calculations based on additional first-dimension band broadening of PCs determined using the effective diffusion coefficients measured for these molecules [29]. Comparison of Fig. 4A and B indicates that very similar elution profiles were obtained for the two systems in both dimensions, as can also be visualised from the detailed sections of the two contour plots shown of the right hand side of the main figures. This observation verifies that band broadening in the first dimension due to the stop-flow approach is negligible, at least for the stop-flow periods used here for the oligomeric PCs. By confirming theoretical predictions of the effect of stop-flow operation on first dimension band broadening, these results validate the approach used for this purpose in [29].

It can be noted that HILIC retention times are slightly shifted to later times in the stop-flow contour plot, which implies that the average first dimension flow rate was slightly lower during this experiment. We believe that this is due to the relatively slow ramping of the flow when the first dimension flow is resumed during stop-flow experiments, causing the average flow rate to be slightly less than in the continuous flow off-line experiment. This phenomenon was anticipated, although measurements showed a negligible difference compared to the off-line approach when the flow was directed to a blocked port of the switching valve during stop-flow periods. This aspect should however be considered when designing stop-flow LC × LC systems, since this discrepancy will depend on the specific instrumentation used. This could also explain the slightly higher peak intensities and seemingly broader peaks observed for the stop-flow system. However, this aspect can relatively easily be corrected in practice through the use of a slightly higher flow rate in the first dimension, selected such that the average flow rate is the same as that in the continuous flow system [32].

3.2.2. On-line HILIC × RP-LC analysis

For on-line LC × LC separations where mobile phases in the two dimensions are not compatible (i.e. non-miscible or where the mobile phase in one dimension is a strong eluent in the other and vice versa), small fraction volumes are required to avoid injection band broadening in the second dimension. Depending on the first dimension column internal diameter and sampling time used, this may dictate the use of flow rates significantly below the optimal linear velocity [33], and therefore result in a considerable loss of peak capacity in this dimension. Reducing the first dimension column diameter may allow operation closer to the optimal flow rate, although there is a price to pay in terms of loadability and susceptibility to extra-column band broadening effects.

Although the use of sub-optimal first dimension flow rates results in smaller fraction volumes and broader first-dimension peaks, thus relaxing the constraints on the sampling time required to minimise under-sampling, it is important to note that this gain is always more than offset by the loss in first dimension peak capacity (for example, doubling the first dimension peak width will reduce the first dimension peak capacity by half, but have a smaller effect on the degree of under-sampling). In such cases, the total two-dimensional peak capacity is mostly determined by the second dimension peak capacity [34,35].

One approach to overcome these constraints is to employ a flow splitter before the second dimension column. This allows the use of higher flow rates in the first dimension without affecting the choice of sampling time (in the absence of a splitter, the first dimension flow rate is related to the maximum allowable injection volume onto the second dimension column ($^{2}V_{max}$) and the sampling time,

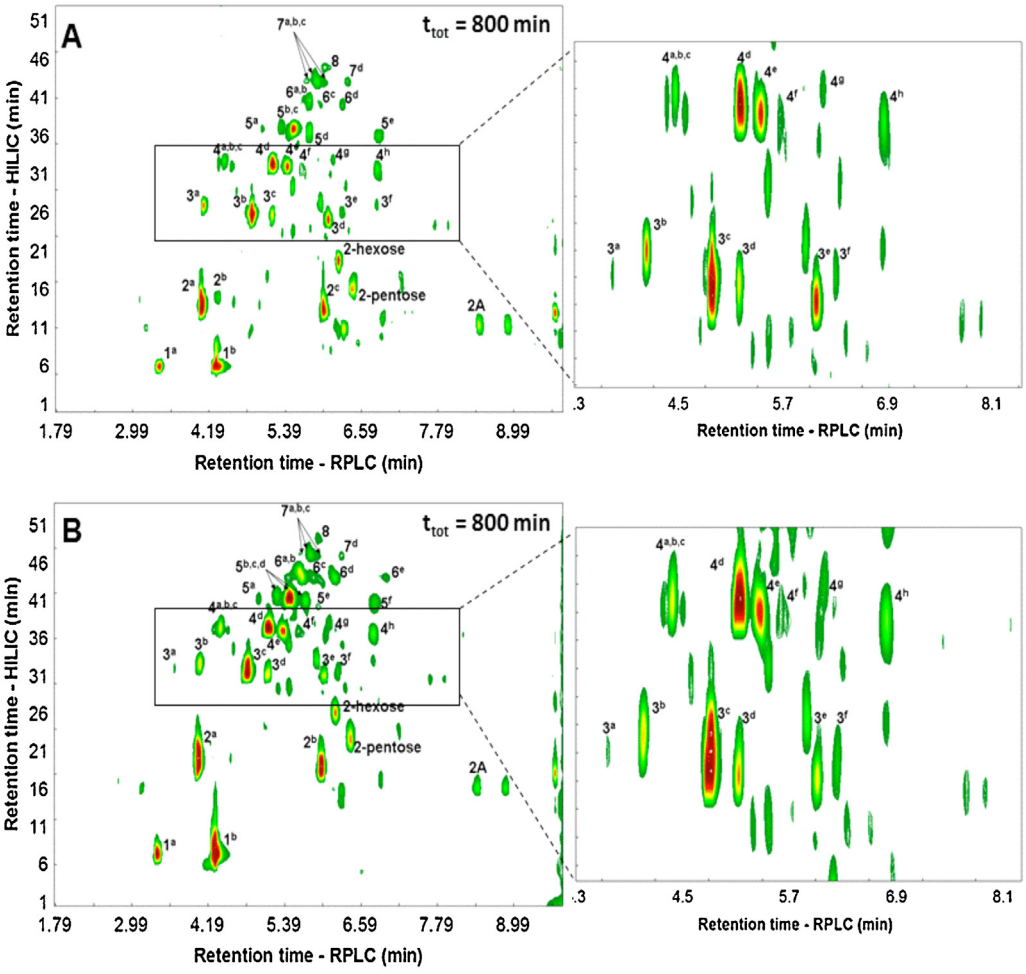

Fig. 4. Fluorescence contour plots obtained for the HILIC × RP-LC analysis of a cocoa extract using off-line (A) and stop-flow (B) configurations. Peak numbers indicate the degree of polymerisation (DP) of PC isomers and letters differentiate isomers of the same DP. For experimental details, refer to Sections 2.4.2.1 and 2.4.2.2.

^1t_s, as outlined in [29]). However, splitting the flow has the obvious drawback of reducing the sensitivity for a given first dimension column diameter and flow rate. The use of narrower first dimension columns or lower flow rates in this dimension to negate the requirement of splitting would not necessarily increase the sensitivity due to the reduced sample capacity and broader first dimension peaks, respectively. In the current study, sensitivity was of less concern due to the use of a highly concentrated extract coupled to sensitive and selective fluorescence detection and fast second dimension analyses.

Calculations reported in [29] show that much better performance is obtained for on-line HILIC × RP-LC when using a first dimension flow rate of 25 μL/min and a gradient time of 100 min. The optimisation of on-line HILIC × RP-LC analyses was therefore performed using a fixed first-D flow rate of 25 μL/min and various second dimension cycle times (^2t_c). In on-line LC × LC, the second dimension cycle time corresponds to the first dimension sampling time, $^2t_c = {}^1t_s$. Calculations indicated that a second dimension cycling time of 3 min would provide the highest corrected two-dimensional peak capacity for the HILIC × RP-LC system used here (refer to [29] and Figure 8 therein).

At this point it is worth noting that the two-dimensional peak capacities used in the theoretical optimisation of HILIC × RP-LC analyses were corrected for lack of orthogonality (as outlined in [29]) as well as first dimension under-sampling, in the latter case according to the following relationship [34]:

$$n'_{c,2D} = \frac{{}^1n_c{}^2n_c}{\beta} = \frac{{}^1n_c{}^2n_c}{\sqrt{1 + 3.35(({}^2t_c{}^1n_c)/{}^1t_g)^2}} \quad (1)$$

where ^1n_c is the (uncorrected) first dimension peak capacity, ^1t_g is the first dimension gradient time and ^2t_c and ^2n_c the second dimension cycle time and peak capacity, respectively. In this equation, ^1n_c was determined using the average peak width in the first dimension [36]:

$$n_{c,1D} = 1 + \frac{t_g}{(1/n)\sum_1^n w_b} \quad (2)$$

where t_g is the gradient time and w_b is the average baseline peak width, calculated for n number of peaks. In the case of HILIC analysis of PCs, peak widths vary as a function of retention time, with later eluting compounds generally showing smaller values of w_b. Clearly, the amount of under-sampling will vary across the gradient, and the corrected peak capacity obtained in this manner, while presenting a correct (average) measure of the overall separation power, may not as accurately reflect the effective separation of all compounds in the contour plot.

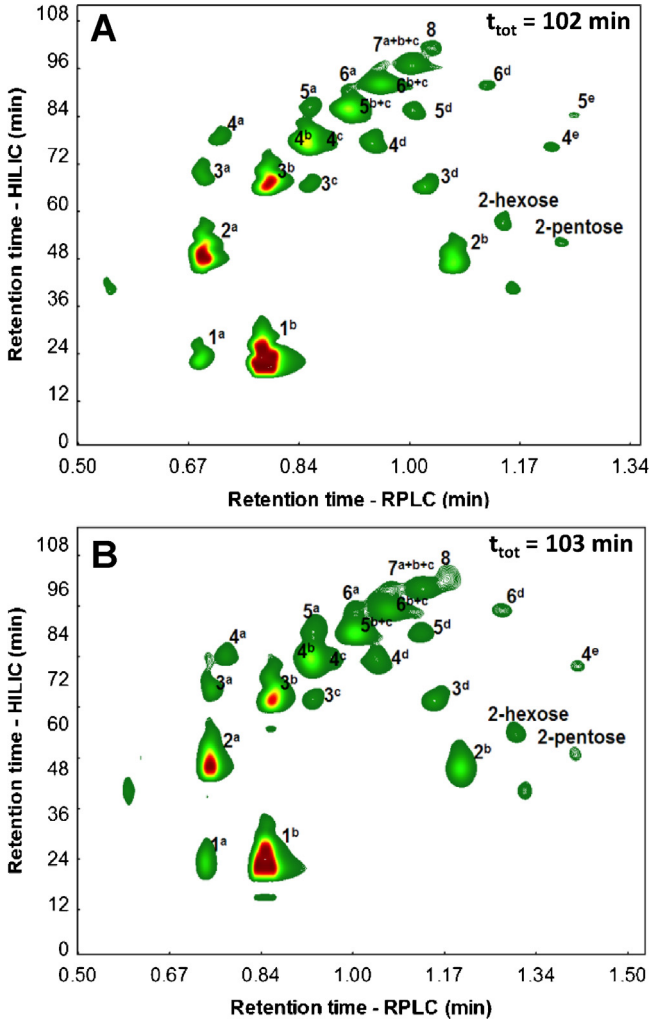

Fig. 5. Fluorescence contour plots for the on-line HILIC × RP-LC analysis of cocoa procyanidins using 2 min (A) and 3 min (B) sampling times and second dimension cycle times. Peak numbers indicate DP and letters distinguish isomers with the same DP. For experimental details, refer to Section 2.4.2.3.

In fact, judging from the first dimension peak widths in HILIC (Fig. 3A), a sampling time of 3 min implies a higher degree of under-sampling for the later eluting compounds (DP 6 to 8, w_b = 2.91–3.05 min). For this reason, sampling times of 2 and 3 min were selected for the on-line HILIC × RP-LC experiments to allow a quantitative comparison of these two experimental conditions. For a 2 min sampling time, at least two fractions were sampled for every first dimension peak, whereas the sampling rate was reduced to ≤ one fraction(s) per peak for the narrowest peaks when using a 3 min cycling time.

Fig. 5 presents contour plots for the on-line HILIC × RP-LC analyses obtained using the two sampling times (and related second dimension cycle times). It is important to point out that these two analyses differ in terms of the split ratio used prior to the second dimension column: since a constant first dimension flow rate was used, the split ratio had to be adapted according to the sampling time.

Both these contour plots demonstrate an evident reduction in separation performance compared to off-line and stop-flow HILIC × RP-LC analyses (Fig. 4). This is expected as a result of the combination of shorter sampling times and longer second dimension analyses for off-line and stop-flow analyses. Especially the latter consideration is particularly evident from comparison of Figs. 4 and 5, since much better isomeric separation is achieved in the RP-LC dimension for off-line and stop-flow methods.

In fact, a considerable portion of the time available for second dimension separation is used to re-equilibrate the column before the transfer of the next fraction: ${}^2t_c = {}^2t_g + {}^2t_{re\text{-}eq}$. For first dimension sampling times of 2 and 3 min, the corresponding gradient times (${}^2t_g$) are only 1.2 and 1.8 min, respectively. Attempts to shorten ${}^2t_{re\text{-}eq}$ were unsuccessful, as this resulted in unacceptable retention time shifts in the second dimension. Any slight shifts in second dimension retention would in fact contribute to band broadening in this dimension since each peak is sampled multiple times. Also important to note in this context is the importance of using low delay-volume instrumentation, as this increases the time available for separation in the second dimension [37,38]. RP-LC separations in this work were performed on a UPLC instrument ($V_{delay} \sim 70$ μL) at a flow rate of 1.5 mL/min, which provides very short delay times in the second dimension.

The contour plots for sampling times of 2 and 3 min appear relatively similar at first glance. However, close inspection shows an important loss in resolution in the first (HILIC) dimension, especially for high molecular weight compounds (DP 5–8) in the case of a 3 min sampling time. This is supported by the first dimension peak capacity values corrected for under-sampling (see Table 1 further). This effect is however offset by longer second dimension separations, which provide increased resolution in the RP-LC dimension. As a consequence, very similar practical two-dimensional peak capacities are obtained for sampling times of 2 and 3 min (Table 1).

However, in the specific case of HILIC × RP-LC analysis of PCs, the HILIC separation provides essential information in terms of the MW of PC isomers. As a result, even a small reduction in HILIC resolution severely impacts on the overall two-dimensional separation, since RP-LC analysis in the second dimension does not guarantee a complete separation of isomers of differing DP. This situation progressively becomes worse for the high MW PCs, since the large number of isomers for these compounds cannot be separated by RP-LC. MS data presented in Fig. 3B shows that even for relatively long RP gradients (${}^2t_g$ = 11.25 min), extensive overlap occurs for PC isomers of DP 7–9. For these compounds, pre-separation according to MW in the HILIC dimension is therefore particularly beneficial. However, resolution for the high-DP PCs also decreases in HILIC, and as a result under-sampling becomes more pronounced for these compounds. The effective two-dimensional separation of these compounds is therefore not accurately reflected in theoretical peak capacity calculations due to the use of the average under-sampling correction factor obtained for the first dimension separation.

In HILIC × RP-LC analysis of PCs, the first dimension separation provides a very low peak capacity, therefore the total 2-D peak capacity is mainly determined by the second dimension. Despite this, however, the overall practical peak capacity is critically dependent on the first dimension sampling rate as well as the degree of correlation between the selected separation mechanisms. Our results also confirm that the total 2-D peak capacity achievable in an on-line system is dependent on the first dimension gradient time [35,39]. Furthermore, these data demonstrate that the use of a longer cycling time in the second dimension of on-line LC × LC is only beneficial up to a point where it does not severely impact the first dimension sampling rate.

Under optimal conditions, the on-line system provides peak capacities greater than could be achieved even by highly optimised one-dimensional separations, while the structured contour plots obtained offer a very useful method for the visual interpretation of PC content of a given sample. It is also worth pointing out that peak capacity calculations do not reflect the type of information provided in each dimension: in the case of HILIC × RP-LC analysis of PCs, the MW information provided by HILIC separation is especially

Table 1
Summary of theoretical [29] and practical performance values for the off-line, stop-flow and on-line HILIC × RP-LC analysis of cocoa PCs.

Parameter	Value							
	Off-line		Stop-flow		On-line			
	15 min		15 min		2 min		3 min	
	Theoretical	Experimental	Theoretical	Experimental	Theoretical	Experimental	Theoretical	Experimental
[a]HILIC peak capacity, ^1n_c	14 (12[b])	14 (12[b])	14 (14[c]) (12[b])	14 (14[c]) (12[b])	28 (20[b])	28 (20[b])	28 (15[b])	28 (15[b])
[a]RP-LC peak capacity, ^2n_c	172	157	172	125	33	28	47	39
[d]Theoretical peak capacity, $n_{c,2D}$	2376	2170	2350	1710	916	788	1304	1082
[e]Practical peak capacity, $n'_{c,2D}$	2185	1994	2162	1568	813	699	1161	962
[f]Practical peak capacity, $n'_{c,2D}$	2119	1936	2101	1528	640	551	711	591
[g]Practical peak capacity, $n'_{c,2D}$	1929	1760	1913	1387	537	462	569	470
[h]Total analysis time (min)	800	800	800	800	102	102	103	103
[i]Peak production rate (peaks/min)	2.41	2.20	2.39	1.73	5.27	4.53	5.53	4.56

[a] Calculated according to Neue [36] using experimentally measured baseline peak widths.
[b] ^1n_c corrected for under-sampling in accordance with Li et al. [34].
[c] ^1n_c corrected for stop-flow band broadening as outlined in [29].
[d] $n_{c,2D} = {}^1n_c \times {}^2n_c$.
[e] Calculated according to Liu et al. [40] to take lack of orthogonality into account.
[f] Calculated according to Li et al. [34] to account for under-sampling of first dimension peaks.
[g] Accounting for both orthogonality (Liu et al. [40]) and under-sampling (Li et al. [34]).
[h] Calculated as outlined in [29].
[i] Calculated based on peak capacities corrected for orthogonality and under-sampling.

useful in identification of individual PC isomers. As such, it can be argued that even a RP-LC separation providing an equivalent practical peak capacity, would not be as useful as on-line HILIC × RP-LC for PC analysis.

It is therefore evident that in the specific case of HILIC × RP-LC analysis of PCs, maintaining the first dimension separation is of more relevance than indicated by theoretical calculations. While these calculations do provide a useful strategy for parameter optimisation in LC × LC, they may not necessarily guarantee optimum performance in practice. In this example, the potential of multi-dimensional separation is only fully realised when the separation integrity is maintained from one dimension to the other, stressing the need for careful selection of optimal analysis parameters for a given application.

3.2.3. *Comparison of practical peak capacities for on-line, off-line and stop-flow HILIC × RP-LC analyses*

In order to compare the practical performance of each of the HILIC × RP-LC systems with theoretical predictions reported in [29], raw experimental data for the second dimension chromatograms used to construct contour plots in Figs. 4 and 5 were used to calculate the true ^2n_c values. It is impractical to measure actual first dimension peak widths from raw two-dimensional data in the absence of a separate first-dimension detector, which was not used here. Therefore, first dimension peak capacities were determined from one-dimensional HILIC separations performed under identical conditions (gradient times, flow rates and injection volumes) as those used for on-line and off-line/stop-flow conditions, respectively (these ^1n_c values are identical to those used in the theoretical calculations). One-dimensional peak capacity values were then translated to practical two-dimensional peak capacities following correction for first-dimension under-sampling [34], limited orthogonality [40] as well as stop-flow band broadening as outlined in [29]. Peak capacities calculated in this manner for the three LC × LC systems are compared to theoretical values calculated in [29] in Table 1.

These data indicate that for all three systems, a slight reduction in ^2n_c was observed compared to theoretical values. The latter were determined from an experimental plot of ^2n_c as a function of gradient time, ^2t_g, on the column used in the second dimension ([29] and Fig. 2 therein). Therefore the reason for this discrepancy in ^2n_c values is most likely injection band broadening associated with the injection of sample fractions in HILIC mobile phase. Indeed, for off-line analysis, where second dimension injection volumes are determined by instrumental injection accuracy, experimental values are only slightly lower. This deviation likely falls within the error associated with peak integration and calculation of peak capacities.

In the case of stop-flow and on-line analyses, however, the actual second dimension injection volume is determined by the effective split ratio. In practice it is very hard to accurately adjust the split ratio within the limits imposed under the conditions used here (V_{inj} = 1.5 ± 0.5 μL). The values presented in Table 1 show that for the stop-flow HILIC × RP-LC analysis, ^2n_c values were ~28% lower than theoretical values, indicating that the injection volumes on the second dimension column were slightly higher than the target value. This is supported by comparison of peak widths obtained for the one-dimensional RP-LC analysis of a cocoa extract (V_{inj} = 1.5 μL) and selected second dimension chromatograms of the same compounds obtained under stop-flow HILIC × RP-LC conditions.

At this point it is relevant to emphasise that when using a flow splitter in LC × LC, the split ratio directly affects not only the second dimension performance, but also the overall sensitivity of the method. For applications where the latter consideration is more important, the inherent compromise between sensitivity and chromatographic performance will result in inevitable sacrifice of resolution in order to obtain the desired sensitivity. Our results indicate the extreme sensitivity of second dimension separation performance to even slight variations in the volume of HILIC fractions injected, implying that in the case of HILIC × RP-LC analysis this compromise becomes critically important. In this regard the design of a more accurate and reproducible splitting device would be beneficial.

Despite the relatively minor differences observed between experimental and theoretical values reported in Table 1, the trends in the data are entirely consistent, and allow several general conclusions to be drawn regarding HILIC × RP-LC analysis of PCs. First, all three comprehensive HILIC × RP-LC methods provide higher peak capacities than one-dimensional LC separations. In the case of on-line HILIC × RP-LC, corrected 2-D peak capacities are almost double the value obtained by one-dimensional RP-LC. However, as alluded to previously, the information obtained from on-line HILIC × RP-LC contour plots is much more pertinent in the case of PC analysis than could be obtained even for a one-dimensional separation providing

the same peak capacity. This is a result of the combination of MW and isomeric information provided by the coupling of HILIC and RP-LC separations. As recently demonstrated for grape seed proanthocyanidins [41], the combination of on-line HILIC × RP-LC separation with MS/MS detection provides a powerful method for the detailed analysis of these molecules. Practical peak capacity values (corrected for under-sampling only) found here for cocoa are very similar to those reported by Montero et al. [41] for on-line HILIC × RP-LC–MS/MS. It should be noted though that the efficient separation of these molecules remains essential due to the fact that MS does not allow differentiation between isomers.

The same applies for off-line and stop-flow HILIC × RP-LC methods, while these also provide much higher resolving power compared to the on-line system. In fact, for complex mixtures of PCs where maximum resolution is essential, off-line or stop-flow should preferentially be used. Comparison of Figs. 4 and 5 clearly illustrates the limitations of on-line HILIC × RP-LC for complex mixtures of PCs. On the other hand, the benefits of on-line HILIC × RP-LC analysis are obtained for conventional analysis times in the order of 100 min. This method therefore delivers much higher peak capacity production rates and as such is ideally suited for screening analysis of PCs.

Comparison of the off-line and stop-flow methods show that both systems are characterised by very high peak capacities with similar peak production rates, and that no significant loss in resolution occurs in the stop-flow methodology. These results indicate that stop-flow is indeed an attractive alternative approach to off-line LC × LC, as it provides automation and minimal sample handling and exposure between the two dimensions, thus minimising the risk of sample contamination and/or degradation. This aspect is especially important for PC analysis, since these compounds are susceptible to oxidative alteration upon exposure to air for extended periods of time.

Comparison of peak capacity production rates reported here with previous LC × LC literature [42,43] points to relatively low values in the current contribution. This may be ascribed largely to the low peak capacities provided by HILIC separations (see [29] for a discussion on this issue). However, another aspect relevant in this regard is the optimisation of the second dimension column length and flow rate (not attempted in this study). Depending on the maximum pressure and flow rate constraints in this dimension, further improvements in the overall performance of HILIC × RP-LC separations in all three modes may be envisioned.

Finally, it is relevant to note that good reproducibility of retention times in both dimensions were obtained using the experimental configurations used here: %RSD values for RP-LC retention times ($n = 3$) were less than 2% for LC × LC separations, while the corresponding values in HILIC were <8% and ±2 modulation periods in one- and two-dimensional modes, respectively. Although it is hard to quantify the sensitivity of the HILIC × RP-LC separations in the absence of reference standards, comparison of the contour plots with one-dimensional separations (refer to [29] and Fig. 1 therein) demonstrates that even minor PC constituents are detected in the two-dimensional separations, confirming that HILIC × RP-LC is suitable for the analysis of PCs in natural products at their normal levels of occurrence.

4. Conclusions

Complete resolution of complex procyanidin fractions is not possible using conventional 1-D LC methods. HILIC × RP-LC has been shown to be an exceptionally powerful approach for PC analysis. In a previous report, an extensive theoretical evaluation of on-line, stop-flow and off-line HILIC × RP-LC methods was presented. In this contribution, the experimental confirmation of these conclusions was demonstrated for cocoa PCs. All three approaches were shown to be much more powerful than 1-D LC due to the combination of orthogonal separations. HILIC provides MW information which is especially useful in terms of simplification of data interpretation. RP-LC on the other hand provides isomeric information, whereas the pre-separation in HILIC avoids co-elution of PCs of different DP.

For on-line LC × LC, the compromise between under-sampling and second dimension analysis time is critical. In the specific case of HILIC × RP-LC analysis, our data indicate that the information provided by HILIC is more important than reflected by theoretical peak capacity calculations (where equal weights are given to separation performance in both dimensions). This implies that under-sampling should be minimised as far as possible for these analyses. Off-line and stop-flow HILIC × RP-LC analyses provide much higher performance, but at the cost of significantly longer analysis times. Because the sampling time is independent of second dimension analysis time, the use of longer RP-LC analysis times is especially beneficial in terms of isomeric separation. Stop-flow HILIC × RP-LC gave very similar results to the off-line approach, confirming predictions based on PC band-broadening as a function of stop-flow time. Therefore, this is an attractive automated alternative to off-line, especially for labile compounds such as phenolics.

Comparison of all practical performance of all three systems shows that on-line HILIC × RP-LC provides much higher peak capacity production rates, although the performance of this approach is insufficient for the detailed analysis of complex PC fractions and therefore better suited for a fast screening method. Off-line and stop-flow analyses provide much higher, and similar, resolving power at peak capacity production rates roughly half those obtained by the on-line system. These approaches should be used for detailed analysis of complex PC fractions. The stop-flow system requires the use of additional hardware and may be experimentally more complicated but offers the advantages of complete automation and less risk of sample alteration.

Acknowledgements

The authors thank the National Research Foundation (NRF, South Africa, Grant 70995 to AdV), the International Foundation of Science (IFS, Sweden, Grant F/4904-1 to AdV), SASOL and the Harry Crossley Foundation (bursary to KMK) for funding. D. Cabooter is thanked for help with the experimental setup. M.A. Stander is thanked for assisting with the LC–MS analysis.

References

[1] D. Ramljak, L.J. Romanczyk, L.J. Metheny-Barlow, N. Thompson, V. Knezevic, M. Galperin, A. Ramesh, R.B. Dickson, Mol. Cancer Ther. 4 (2005) 537.
[2] T.L. Lunder, in: M.-T. Huang, C.-T. Ho, C.Y. Lee (Eds.), Phenolic Compounds in Food and Their Effects on Health II, American Chemical Society, New York, 1992, p. 114.
[3] J.F. Hammerstone, S.A. Lazarus, A.E. Mitchell, R. Rucker, H.H. Schmitz, J. Agric. Food Chem. 47 (1999) 490.
[4] G.E. Adamson, S.A. Lazarus, A.E. Mitchell, R.L. Prior, G. Cao, P.H. Jacobs, B.G. Kremers, J.F. Hammerstone, R.B. Rucker, K.A. Ritter, H.H. Schmitz, J. Agric. Food Chem. 47 (1999) 4184.
[5] R. Mayer, G. Stecher, R. Wuerzner, R.C. Silva, T. Sultana, L. Trojer, I. Feuerstein, C. Krieg, G. Abel, M. Popp, O. Bobleter, G.K. Bonn, J. Agric. Food Chem. 56 (2008) 6959.
[6] P. Schofield, D.M. Mbugua, A.N. Pell, Anim. Feed Sci. Technol. 91 (2001) 21.
[7] I. Mueller-Harvey, Anim. Feed Sci. Technol. 91 (2001) 3.
[8] W. Hümmer, P. Schreier, Mol. Nutr. Food Res. 52 (2008) 1381.
[9] M. Naczk, F. Shahidi, J. Chromatogr. A 1054 (2004) 95.
[10] G. Tucker, K. Robards, Crit. Rev. Food Sci. Nutr. 48 (2008) 929.
[11] R. Flamini, Mass Spectrom. Rev. 22 (2003) 218.
[12] J. Rigaud, M.T. Escribano-Bailon, C. Prieur, J.-M. Souquet, V. Cheynier, J. Chromatogr. A 654 (1993) 255.
[13] M. Natsume, N. Osakabe, M. Yamagishi, T. Takizawa, T. Nakamura, H. Miyatake, T. Hatano, T. Yoshida, Biosci. Biotechnol. Biochem. 64 (2000) 2581.

[14] A. Yanagida, T. Kanda, T. Takahashi, A. Kamimura, T. Hamazono, S. Honda, J. Chromatogr. A 890 (2000) 251.
[15] L. Gu, M. Kelm, J.F. Hammerstone, G. Beecher, D. Cunningham, S. Vannozzi, R.L. Prior, J. Agric. Food Chem. 50 (2002) 4852.
[16] T. Shoji, M. Mutsuga, T. Nakamura, T. Kanda, H. Akiyama, Y. Goda, J. Agric. Food Chem. 51 (2003) 3806.
[17] M.A. Kelm, J.C. Johnson, R.J. Robbins, J.F. Hammerstone, H.H. Schmitz, J. Agric. Food Chem. 54 (2006) 1571.
[18] A. Yanagida, H. Murao, M. Ohnishi-Kameyama, Y. Yamakawa, A. Shoji, M. Tagashira, T. Kanda, H. Shindo, Y. Shibusawa, J. Chromatogr. A 1143 (2007) 153.
[19] R.J. Robbins, J. Leonczak, J. Li, J.C. Johnson, T. Collins, C. Kwik-Uribe, H.H. Schmitz, J. AOAC Int. 95 (2012) 1153.
[20] P.J. Sarnoski, J.V. Johnson, K.A. Reed, J.M. Tanko, S.F. O'Keefe, Food Chem. 131 (2012) 927.
[21] S. Tourino, E. Fuguet, O. Jauregui, F. Saura-Calixto, M. Cascante, J.L. Torres, Rapid Commun. Mass Spectrom. 22 (2008) 348.
[22] M.D. Mercurio, P.A. Smith, J. Agric. Food Chem. 56 (2008) 5528.
[23] F. Erni, R.W. Frei, J. Chromatogr. 149 (1978) 561.
[24] J.C. Giddings, in: H.J. Cortes (Ed.), Multidimensional Chromatography: Techniques and Applications, Marcel Dekker, Inc., New York, 1990, p. 1.
[25] J.C. Giddings, Anal. Chem. 56 (1984) 1258A.
[26] K.M. Kalili, A. de Villiers, J. Chromatogr. A 1216 (2009) 6274.
[27] K.M. Kalili, A. de Villiers, J. Sep. Sci. 33 (2010) 853.
[28] T. Beelders, K.M. Kalili, E. Joubert, D. de Beer, A. de Villiers, J. Sep. Sci. 35 (2012) 1808.
[29] K.M. Kalili, A. de Villiers, J. Chromatogr. A (2013), http://dx.doi.org/10.1016/j.chroma.2013.03.008.
[30] A. van der Horst, P.J. Schoenmakers, J. Chromatogr. A 1000 (2003) 693.
[31] L.J. Porter, Z. Ma, B.G. Chan, Phytochemistry 30 (1991) 1657.
[32] F. Bedani, W.T. Kok, H.-G. Janssen, J. Chromatogr. A 1133 (2006) 126.
[33] P. Dugo, F. Cacciola, T. Kumm, G. Dugo, L. Mondello, J. Chromatogr. A 1184 (2008) 353.
[34] X. Li, D.R. Stoll, P.W. Carr, Anal. Chem. 81 (2009) 845.
[35] L.W. Potts, D.R. Stoll, X. Li, P.W. Carr, J. Chromatogr. A 1217 (2010) 5700.
[36] U.D. Neue, J. Chromatogr. A 1079 (2005) 153.
[37] A.P. Schellinger, D.R. Stoll, P.W. Carr, J. Chromatogr. A 1064 (2005) 143.
[38] P.W. Carr, D.R. Stoll, X. Wang, Anal. Chem. 83 (2011) 1890.
[39] Y. Huang, H. Gu, M. Filgueira, P.W. Carr, J. Chromatogr. A 1218 (2011) 2984.
[40] Z. Liu, D.G. Patterson, M.L. Lee, Anal. Chem. 67 (1995) 3840.
[41] L. Montero, M. Herrero, M. Prodanov, E. Ibáñez, A. Cifuentes, Anal. Bioanal. Chem (2012), http://dx.doi.org/10.1007/s00216-012-6567-5.
[42] M.R. Filgueira, Y. Huang, K. Witt, C. Castells, P.W. Carr, Anal. Chem. 83 (2011) 9531.
[43] J.N. Fairchild, K. Horvath, G. Guiochon, J. Chromatogr. A 1216 (2009) 1363.

Addendum E

Towards unravelling grape tannin composition: Application of on-line hydrophilic interaction chromatography × reversed phase liquid chromatography – time-of-flight mass spectrometry to grape seed analysis

K.M. Kalili, J. Vestner, M.A. Stander, A. de Villiers, Anal. Chem. 85 (2013) 9107-9115.

analytical chemistry

Article

pubs.acs.org/ac

Toward Unraveling Grape Tannin Composition: Application of Online Hydrophilic Interaction Chromatography × Reversed-Phase Liquid Chromatography−Time-of-Flight Mass Spectrometry for Grape Seed Analysis

Kathithileni M. Kalili,[†] Jochen Vestner,[†,‡] Maria A. Stander,[§,⊥] and André de Villiers*[,†]

[†]Stellenbosch University, Department of Chemistry and Polymer Science, Private Bag X1, Matieland, Stellenbosch, Western Cape 7602, South Africa

[‡]Hochschule Geisenheim University, Center of Analytical Chemistry and Microbiology, Department of Microbiology and Biochemistry, Von-Lade-Str. 1, 65366 Geisenheim, Germany

[§]Stellenbosch University, Central Analytical Facility, Private Bag X1, Matieland, Stellenbosch, Western Cape 7602, South Africa

[⊥]Stellenbosch University, Department of Biochemistry, Private Bag X1, Matieland, Stellenbosch, Western Cape 7602, South Africa

Supporting Information

ABSTRACT: Despite the significant importance of tannins in viticulture and enology, relatively little is known about the detailed chemical composition of these molecules. This is due to challenges associated with the accurate analytical determination of the highly structurally diverse proanthocyanidins which comprise tannins. In this contribution, we address this limitation by demonstrating how online comprehensive two-dimensional liquid chromatography (LC × LC) coupled to high resolution mass spectrometry (HR-MS) can be exploited as a powerful analytical approach for the detailed characterization of grape seed tannins. Hydrophilic interaction chromatography (HILIC) and reversed-phase liquid chromatography (RP-LC) were employed in the two dimensions to provide complementary information in terms of separation according to hydrophilicity and hydrophobicity, respectively. Online coupling of HILIC × RP-LC with fluorescence detection and electrospray ionization MS delivered high resolution analysis in a practical analysis time, while allowing selective detection and facilitating compound identification. Time-of-flight (TOF) MS provided high acquisition rates and sensitivity coupled to accurate mass information, which allowed detection of procyanidins up to a degree of polymerization (DP) of 16 and a degree of galloylation up to 8 in a red grape seed extract. This analytical methodology promises to shed new light on these important grape constituents and potentially on their evolution during wine production.

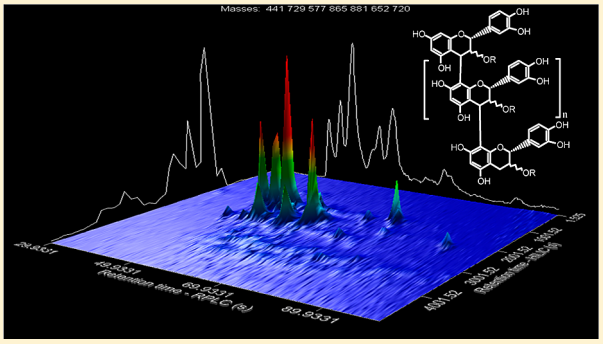

Condensed tannins (proanthocyanidins, PACs) are natural oligomeric and polymeric phenolic compounds formed through condensation of flavan-3-ol units.[1,2] PACs are subdivided into various classes with procyanidins (PCs), based on (epi)catechin units, and prodelphinidins (PDs), comprising (epi)gallocatechin units, being the most common.[2,3] Galloylated PACs are formed by esterification with gallic acid (Figure S1, Supporting Information). PACs are widely distributed in nature and often constitute the largest portion of phenolic constituents in common foods such as grapes, cocoa, apples, berries, wine, etc.[1,4] Natural PACs vary in terms of degree of polymerization (DP); for example, PC oligomers of DP > 10 have been detected in cocoa[5,6] and apples,[7,8] while this value is >30 for grape seeds and skins.[9−11] PACs have been the subject of extensive research due to a broad spectrum of beneficial health effects associated with their consumption.[10−12]

In viticulture and enology, PACs are particularly important: these molecules form the so-called "tannins", which are responsible for much of the "body" and aging properties of especially red wine.[13,14] Tannins are defined by their ability to complex proteins, a property which is thought to contribute to the astringency and mouth-feel of wines by precipitation of salivary proteins.[15] Wine tannins originate from the grape; grape seed tannins consist of partly galloylated PCs, while grape skin tannins also contain PDs. Grape-derived PACs are involved in several reactions during wine aging, which generally improve the properties of red wine, such as the incorporation of anthocyanins in the tannin structure which alters and stabilizes red wine color.[16,17]

Received: June 12, 2013
Accepted: August 26, 2013
Published: August 26, 2013

dx.doi.org/10.1021/ac401896r | Anal. Chem. 2013, 85, 9107−9115

Clearly, tannins play a vital role in determining wine character, and the chemical composition of tannins is known to affect their sensory properties. For example, perceived astringency of PACs increases with increasing DP as well as percentage galloylation.[18] Yet, despite commendable progress in phenolic research during the past 25 years, the lack of suitable analytical methods for tannin determination currently represents a major bottleneck. As generalized by Mercurio et al.,[19] the "quantification and characterization of tannins remains one of the great analytical challenges in natural products chemistry".

In terms of analytical methods, bulk spectrophotometric and precipitation methods using a variety of reagents may be used to determine the total tannin content.[12,19−21] However, for the diverse wine tannins, the assumptions made regarding chemical reactivity often lead to inaccurate results.[12,20−22] Acid-catalyzed depolymerization assays such as thiolysis and phloroglucinol degradation provide information on the mean degree of polymerization (mDP) and type of constitutive units of grape PACs,[10,23,24] but these assays do not provide any structural information for individual tannin molecules.[25] Reversed-phase liquid chromatography (RP-LC) with mass spectrometric (MS) detection allows characterization of individual oligomers.[26] However, failure of RP-LC to resolve higher molecular weight (MW) isomers hampers the study of polymeric tannins.[27] Separation of tannins according to MW has been achieved by normal phase LC (NP-LC) and hydrophilic interaction chromatography (HILIC), although isomers are not separated.[5,8,28−30] As summarized by Tourino et al.,[27] "polymeric procyanidins...cannot be separated through conventional HPLC". High resolution analytical techniques are therefore critically required to allow the in-depth investigation of these complex molecules.

Comprehensive two-dimensional liquid chromatography (LC × LC) has in recent years been applied for the high resolution separation of complex sample mixtures. This is based on the combination of independent separation mechanisms to explore different sample dimensionalities and deliver improved resolution.[31,32] LC × LC has also been applied for phenolic analysis.[33−36] The combination of HILIC and RP-LC has been shown to provide a particularly powerful separation method for PACs,[6,37] including grape seed PACs,[38] by combining HILIC separation according to DP and isomeric separation by RP-LC. The application of online HILIC × RP-LC-DAD−MS/MS has recently been reported for the analysis of grape seed PACs, with promising results.[39] This approach allowed identification of 46 PACs, although the use of suboptimal chromatographic conditions limited the application range in terms of DP and isomeric separation. We have recently reported[40,41] a systematic optimization procedure for online, off-line, and stop-flow HILIC × RP-LC methods for PC analysis, which highlighted several important experimental considerations for optimal separation using each configuration. The goal of the work reported herein was to extend the developed online HILIC × RP-LC methodology to grape seed tannins. The combination of optimized separations in both dimensions with high resolution time-of-flight (TOF) MS detection will be shown to provide a powerful methodology for the detailed investigation of grape seed tannins.

EXPERIMENTAL SECTION

Reagents and Materials. Grapes (*Vitis vinifera*, cv. Cabernet Sauvignon) of the 2011 harvest were obtained from the Institute of Wine Biotechnology (IWBT, Stellenbosch University) and stored frozen until analysis. (−)-Epicatechin and (±)-catechin standards, phloroglucinol, hydrochloric acid, sodium acetate, HPLC grade methanol, acetone, acetonitrile, formic acid, and acetic acid were purchased from Sigma Aldrich (Steinheim, Germany). Ascorbic acid was purchased from Hopkin & Williams S.A. (Johannesburg, South Africa). Deionized water was obtained using a Milli-Q water purification system (Millipore, Milford, MA, USA).

Sample Preparation. Grape berries were hand-pressed, and seeds were washed free of the pulp and skin using deionized water, flash-frozen in liquid nitrogen, and ground into a fine powder using a blender. Extraction of PACs was performed as previously reported:[6] 10 g of the homogenized material was extracted three times each with 15 mL of 70% acetone in water (v/v) and 15 mL of 70% methanol in water (v/v). The extracts were combined, and the organic solvents were removed by rotary evaporation at 40 °C. For 1-D RP-LC analyses, this aqueous extract was used. For 1-D HILIC and HILIC × RP-LC analyses, the sample was freeze-dried and redissolved in 70/30 acetonitrile/methanol (v/v).

Phloroglucinolysis. Phloroglucinolysis was performed as reported previously.[42] Briefly, the phloroglucinol reaction mixture contained 0.1 g ascorbic acid and 0.5 g of phloroglucinol in 5 mL of 0.2 N HCl in methanol. One mg of the freeze-dried grape seed extract was reacted with 200 μL of the phloroglucinol reaction mixture for 20 min at 50 °C. The reaction was stopped by adding 5 volumes (1 mL) of 40 mM aqueous sodium acetate.

Instrumentation. An Acquity UPLC system equipped with a fluorescence detector and controlled by MassLynx software (Waters, Milford, MA, USA) was used. Fluorescence data were acquired using excitation and emission wavelengths of 230 and 321 nm, respectively. The system was coupled to a Waters Synapt Q-TOF mass spectrometer operated in negative ionization mode. A capillary voltage of −3.0 kV, a sampling cone voltage of 15 V, and an extraction cone voltage of 4.0 V were used. The source and desolvation temperatures were set to 120 and 275 °C, respectively. Nitrogen was used as desolvation gas at a flow rate of 650 L/h. The instrument was calibrated using a sodium formate solution, and a scan range of 200 to 2000 m/z was used. Leucine enkephalin (m/z = 554.2615) was used as the lock mass. Mass accuracy was within 5 ppm for singly charged ions.

For HILIC × RP-LC-FL−ESI-MS separations, a second UPLC system controlled by Empower was used. The two instruments were interfaced through a 10-port 2-position high pressure switching valve (1000 bar maximum pressure, 150 μm bore, Valco Instruments Co. Inc., Houston, Texas, USA) equipped with two 5 μL loops. HPLC-UV quantification of phloroglucinolysis products was performed on an HP 1090 liquid chromatograph equipped with a diode-array detector (Agilent Technologies, Waldbronn, Germany).

Chromatographic Conditions. *Online HILIC × RP-LC-FL−ESI-MS Analyses.* HILIC analyses were performed at ambient temperature on a Develosil Diol-100 column (250 mm × 1 mm i.d., 5 μm d_p, Nomura Chemical Co., Aichi, Japan) using a mobile phase comprising (A) acetonitrile and acetic acid (99:1, v/v) and (B) methanol, water, and acetic acid (94.05:4.95:1, v/v/v). The gradient was as follows: 4−40% B (0−80 min), 40% B isocratic (80−90 min), 40−100% B (90−100 min). The flow rate was 0.025 mL/min, and 5 μL was injected. RP-LC separations were achieved on an Agilent

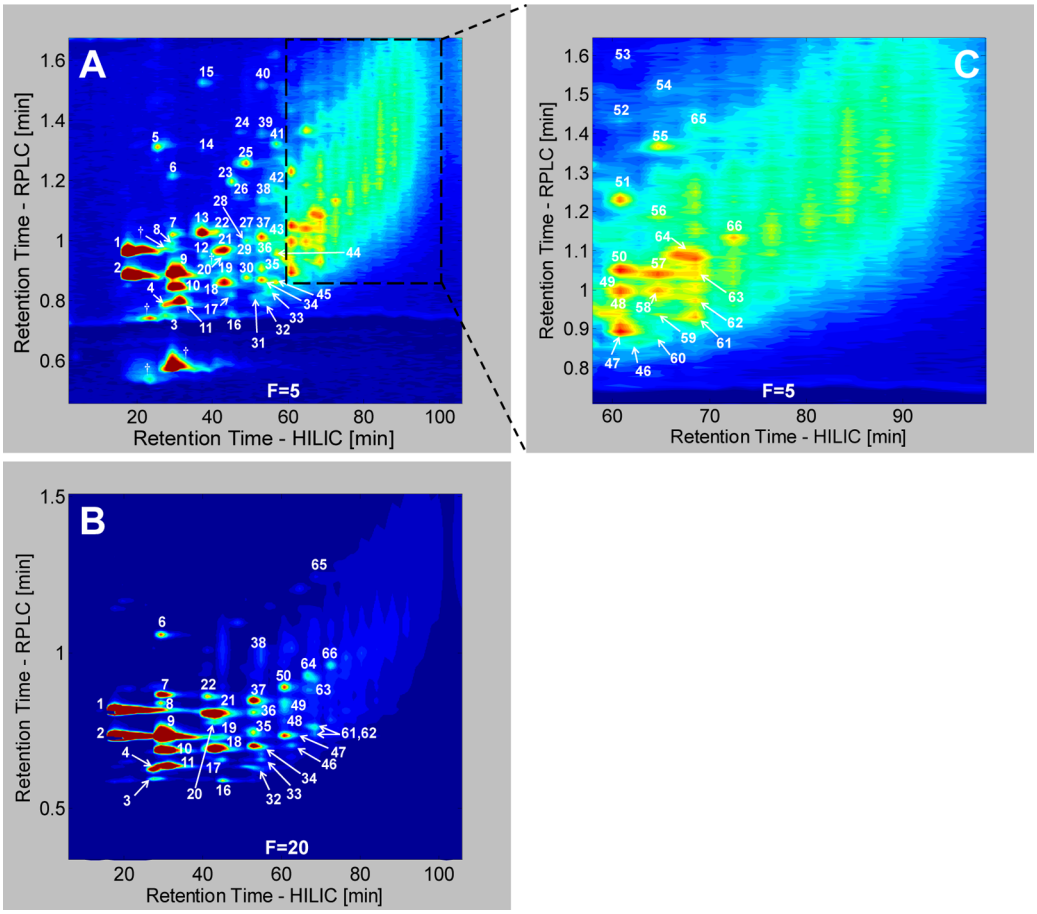

Figure 1. Total ion chromatogram (TIC) (A) and fluorescence (B) contour plots obtained for the HILIC × RP-LC-FL–ESI-MS analysis of a red grape seed extract. (C) presents a detail of the TIC contour plot highlighting the separation of high MW PACs. Peak numbers correspond to Table 1; † denotes unidentified compounds. F denotes the scale of the *z*-axes.

Zorbax SB-C18 column (50 mm × 4.6 mm i.d., 1.8 μm) protected with a Phenomenex prefilter (Torrance, USA). A linear gradient using 0.1% formic acid in water (v/v) (A) and acetonitrile (B) mobile phases was performed as follows: 2% B (0–0.02 min), 2–18% B (0.02–0.20 min), 18–25% B (0.20–1.10 min), and 25–100% B (1.10–1.20 min) (total analysis time including re-equilibration, 2.0 min). The column was thermostatted at 50 °C, and the flow rate was 1.5 mL/min.

The two columns were connected using a 10-port switching valve configured in a symmetrical manner.[43] The HILIC effluent was split ~1:24 prior to the valve, which was switched every 2 min via the UPLC external events, resulting in a first dimension sampling time of 2 min and a second dimension injection volume of 2 μL (i.e., 1 μL/min × 2 min). The RP-LC column effluent was split ~1:1.14 after the FL detector, resulting in a flow of ~700 μL/min to the MS. A schematic illustration of the instrumental configuration is presented in Figure S2, Supporting Information.

RP-LC-UV–ESI-MS Analysis of Phloroglucinolysis Samples. Phloroglucinolysis products were analyzed by RP-LC-UV–MS on a Phenomenex Kinetex C18 column (50 mm × 4.6 mm i.d., 2.6 μm) using 0.1% formic acid in water (v/v) (A) and acetonitrile (B) mobile phases and the following gradient: 2% B (0–0.13 min), 2–18% B (0.13–5.40 min), 18–25% B (5.40–9.00 min), 25–100% B (9.00–10.35 min), and 100% B (10.35–11.25 min). The analysis was carried out at room temperature using a flow rate of 1 mL/min, and 4 μL was injected. UV detection was performed at 280 nm, and MS conditions were the same as those described in "Instrumentation" except that a scan range of 120–1500 was used. The mDP was estimated in accordance with Kennedy and Jones.[42]

Data Processing. Raw MS data for online HILIC × RP-LC–ESI-MS analyses were converted to network common data form (NetCDF) using MetAlign (www.metalign.nl, Wageningen, The Netherlands) and imported into Matlab 7.14 (The Mathworks, Natick, MA, USA) for processing and visualization. Fluorescence data were converted to comma separated value files (CSV) before processing in Matlab. Small shifts between second dimension chromatograms were aligned using the interval correlation optimized shifting algorithm (*i*coshift).[44] Visualization of contour plots was performed in Matlab using built-in functions. The *z*-axes of contour plots were scaled by the maximum intensity value of the data matrix divided by a certain factor, indicated as F in the relevant figures. Three-dimensional surface plots were obtained using ChromaTOF software (LECO Africa, Kempton Park, South Africa).

RESULTS AND DISCUSSION

Considerations on HILIC × RP-LC Separation of Proanthocyanidins. The current study extends previous work[6,36,37,40,41] on the HILIC × RP-LC separation of phenolics to the analysis of grape seed PACs by online HILIC × RP-LC in combination with high resolution MS detection. Effective LC × LC operation requires careful consideration of several inter-

dx.doi.org/10.1021/ac401896r | *Anal. Chem.* 2013, 85, 9107–9115

Table 1. Summary of the Procyanidins and Galloylated Procyanidins Tentatively Identified in Red Grape Seeds by HILIC×RP-LC–ESI-MS[a]

peak no.	DP[b]	DG[c]	t_R[d] (HILIC)	t_R[d] (RP-LC)	$[M - H]^-$	$[M - 2H]^{2-}/2$
1, 2	1	0	17.64	0.89, 0.97	**289.0714**	
3, 4[e]	1		27.44	0.75, 0.79	**451.1248**	
5		1	25.48	1.32	**441.0816**	
6–11	2	0	29.40	0.80, 0.85, 0.90, 0.99, 1.03, 1.22	**577.1349**	
12–15		1	37.24	0.93, 1.03, 1.31, 1.53	**729.1442**	
23		2	45.08	1.21	**881.1578**	440.0738
16–22	3	0	45.08	0.75, 0.83, 0.87, 0.90, 0.95, 0.98, 1.03	**865.1970**	
24–31		1	49.00	0.81, 0.88, 0.95, 1.00, 1.04, 1.15, 1.26, 1.37	**1017.2070**	508.1001
39, 40, 67, 68		2	52.92	1.01, 1.15, 1.36, 1.53	1169.2195	**584.0989**
72		3	58.80	1.27	1321.2405	**660.1138**
32–38	4	0	52.92	0.80, 0.83, 0.87, 0.91, 0.98, 1.03, 1.14	**1153.2610**	576.1260
41–45		1	56.84	0.86, 0.96, 1.05, 1.18, 1.32	1305.2622	**652.1315**
51–53, 69–71		2	60.76	0.91, 1.00, 1.09, 1.24, 1.44, 1.59	1457.2726	**728.1377**
73–77		3	64.68	1.09, 1.20, 1.30, 1.37, 1.42	1609.3081	**804.1466**
78		4	66.64	1.36		**880.1536**
46–50	5	0	60.76	0.87, 0.90, 0.95, 1.00, 1.05, 1.44	1441.3137	**720.1582**
54–60		1	64.68	0.88, 0.95, 1.00, 1.06, 1.17, 1.37, 1.58	1593.3317	**796.1641**
61–65	6	0	68.60	0.90, 0.95, 1.05, 1.09, 1.42		**864.1880**
66	7	0	72.52	1.14		**1008.2220**

[a]Only compounds detected as distinct chromatographic peaks are listed (for the remainder of the identified compounds, refer to Table S1, Supporting Information). Base peak ions are highlighted in bold. [b]DP: Degree of polymerization of procyanidins. [c]DG: Degree of galloylation. [d]t_R: retention time. [e](Epi)catechin monoglycosides.

related parameters;[40,45] a detailed optimization strategy for HILIC × RP-LC separation of PCs in online-, off-line, or stop-flow modes has been presented elsewhere.[40,41] Since online HILIC × RP-LC provides a fast, automated system ideally suited for combination with MS detection, this approach was used here for grape seed tannins. In the interest of brevity, a concise motivation of the experimental conditions used will be presented.

Several previous studies[6,36,37,46] have demonstrated that HILIC and RP-LC offer complementary separation mechanisms and, therefore, a high degree of orthogonality for the separation of phenolic compounds. In the case of PCs, HILIC provides separation on the basis of size or DP, whereas RP-LC separation occurs on the basis of isomeric composition.[6,39–41] However, HILIC mobile phases are strong eluents in RP-LC, which limits the injection volume for HILIC fractions on a 4.6 × 50 mm RP-LC column to ~2 μL.[6,40] To address this, a 1 mm i.d. column was used in the first dimension at a flow rate of 25 μL/min, and a 1:24 flow-splitter was incorporated before the switching valve.[40] Note that, owing to the use of a highly concentrated extract and minimal on-column dilution in the first dimension, sufficient sensitivity was obtained using this approach.

In online LC × LC, the first dimension sampling time (^1t_s) dictates the second dimension cycle time (^2t_c, the time required for the gradient and re-equilibration), since separation in the two dimensions is carried out simultaneously. ^1t_s also defines the volume of each first-dimension fraction as well as the extent of first dimension under-sampling: a sampling rate of 3 or more fractions per first dimension peak is generally required.[47–49] The sampling time should therefore be optimized relative to ^2t_c, since longer second dimension separations provide improved resolution. First dimension peak widths ranged from 3.08 to 7.61 min (average 5.17 min); a sampling time of 2 min therefore provided the best compromise between ^1t_s and ^2t_c for online HILIC × RP-LC analysis of PCs.[40] In the second dimension, a 1.8 μm column was used at a temperature of 50 °C to provide optimal performance for PCs at a flow rate of 1.5 mL/min.[40] Finally, for optimal online operation using the column dimensions used here, the instrumental extra-column volume was carefully minimized.

In a previous report on the HILIC × RP-LC analysis of grape seed PACs,[39] a first dimension flow rate of 15 μL/min was used on a 1 mm i.d. Diol column. However, relatively poor separation of PACs was obtained, presumably as a result of the effect of instrumental delay volume. Furthermore, no split was used in this work, and therefore, the second dimension injection volume was 19.5 μL (for a sampling time of 1.3 min), which resulted in significant second dimension band broadening, especially for the first HILIC fractions. The optimized experimental conditions used in the current study delivered much better separation for all grape seed PACs.

Online HILIC × RP-LC-FL–MS Analysis of Grape Seed Proanthocyanidins. Figure 1 presents the total ion chromatogram (TIC) and fluorescence contour plots obtained for the HILIC × RP-LC-FL–MS analysis of a red grape seed extract under optimal conditions. Compound labeling in this figure corresponds to Table 1. At first glance, the extreme complexity of the sample is evident. However, owing to the independent retention mechanisms offered by HILIC and RP-LC, their combination in LC × LC results in a well-structured elution pattern displaying a size separation in the HILIC dimension (as seen along the *x*-axis in Figure 1) and an isomeric separation in the RP-LC dimension (on the *y*-axis).[6,36,37,39] (One-dimensional HILIC- and RP-LC separations of the grape seed extract are presented in Figure S3, Supporting Information.) The advantages of HILIC × RP-LC separation are evident when considering the extensive coelution which occurs in each of the dimensions individually. For example, compounds with similar molecular weights are not resolved in HILIC, whereas a high degree of coelution between isomers of differing DPs is observed in the RP-LC dimension. Furthermore, the benefit of

dx.doi.org/10.1021/ac401896r | Anal. Chem. 2013, 85, 9107–9115

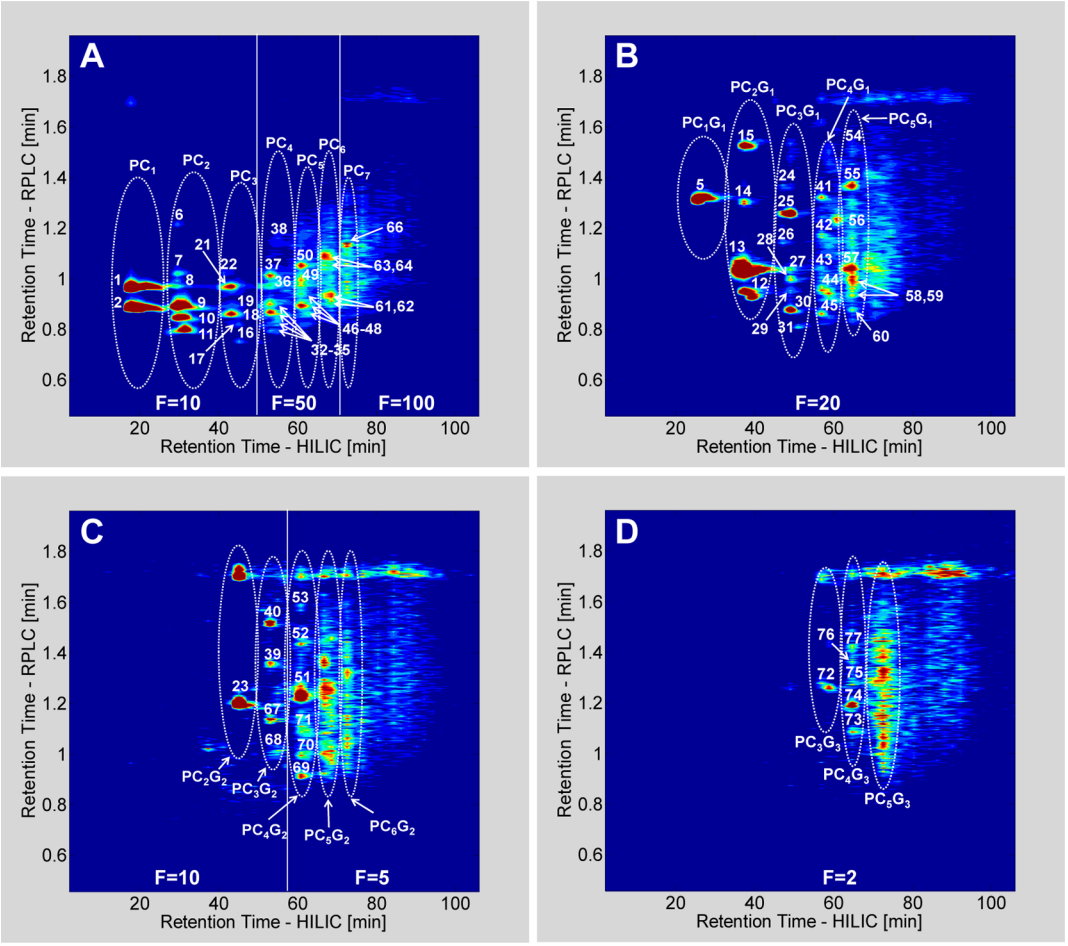

Figure 2. Extracted ion contour plots for (A) procyanidins, (B) monogalloylated procyanidins, (C) digalloylated procyanidins, and (D) trigalloylated procyanidins obtained by HILIC × RP-LC–MS analysis of a red grape seed extract. Peak numbers correspond to Table 1 and F indicates the scaling factor used in the *z*-axis. In the notation PC_xG_y, *x* represents the procyanidin degree of polymerization and *y* represents the degree of galloylation.

portraying data in contour plot format is apparent, as a clear picture of the PAC content of grape seeds, in terms of both MW and isomeric distribution, is provided in two dimensions.

Comparison of the fluorescence and TIC contour plots shows that the former detector is much more selective for PCs. In fact, the lack of fluorescence response of galloylated PCs is beneficial in the sense that this facilitates the identification of PCs. However, the decrease in fluorescence response of PCs as a function of DP^{50} means that high MW compounds (DP > 9) of this class are not detected.

In terms of identification of compounds, MS detection is indispensable. The most attractive feature of HILIC × RP-LC–MS analysis is the fact that the benefits of one method can be exploited where the other methods are limited. For example, HILIC and MS cannot distinguish between compounds of identical MW (particularly stereoisomers such as PACs), whereas these isomers are separated on the basis of hydrophobicity by RP-LC. On the other hand, compounds varying in MW which coelute in RP-LC are easily distinguished in HILIC and MS dimensions. This approach therefore combines HILIC fractionation according to size and subsequent isomeric separation by RP-LC with the structural elucidation properties of MS. HILIC preseparation removes the constraint that MS spectra of high MW PACs contain fragments corresponding to PACs of lower DP. The reduction in peak overlap provided by HILIC × RP-LC separation therefore provides greater confidence in compound identification.

The use of high resolution mass spectrometry (HR-MS) furthermore provides an additional means of tentatively identifying compounds based on accurate mass measurements, which is especially important for multiply charged species such as the higher MW PACs. Tables 1 and S1, Supporting Information, list the PACs detected in the red grape seed extract. Low MW compounds (DP ≤ 4) were mostly detected as singly charged ions, with doubly charged molecular ions observed for DP 5 to 10 and triply charged species predominant for DP ≥ 11.

A total of 78 PACs could be identified as single chromatographic peaks, corresponding to the numbered compounds in Table 1 and the figures. These include 33 PCs, 25 monogalloylated, 11 digalloylated, 6 trigalloylated, and 1 tetragalloylated PCs as well as 2 (epi)catechin monoglycosides. In addition, the high MS sensitivity allowed identification of low level PCs of DP up to 12 as well as monogalloylated-octagalloylated PCs of DP as high as 16. Highly polymerized compounds identified, but for which isomeric separation in the RP-LC dimension was not possible (see further), are listed in Table S1, Supporting Information.

MS detection provides an effective means of obtaining an overview of the chemical composition of each class of PACs by means of extracted ion contour plots. Examples for different PC

dx.doi.org/10.1021/ac401896r | *Anal. Chem.* 2013, 85, 9107–9115

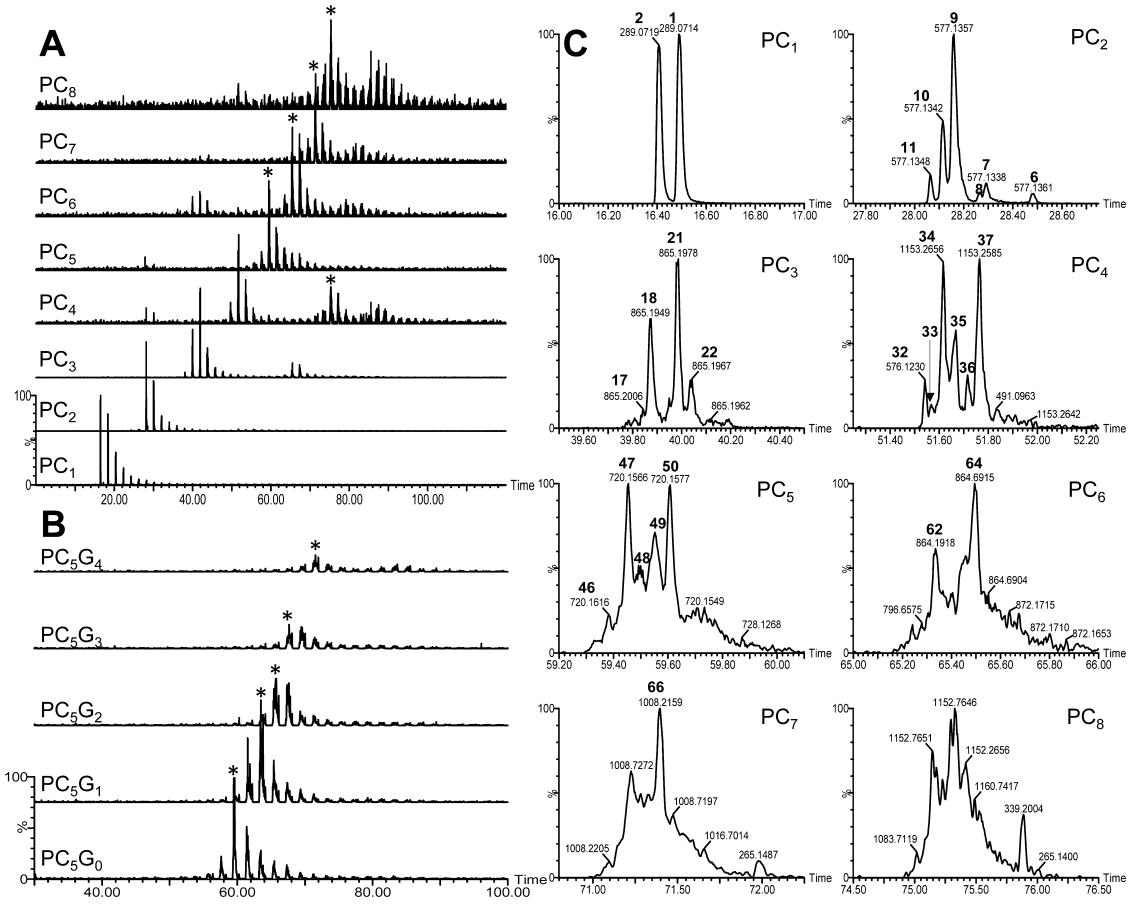

Figure 3. Raw HILIC × RP-LC–MS data illustrating the elution patterns for (A) procyanidin oligomers and (B) pentametric procyanidins as a function of degree of galloylation (DG). (*) indicates doubly charged species. (C) shows extracted ion chromatograms (EICs) corresponding to individual 2 min second dimension RP-LC separations obtained for procyanidins of degrees of polymerization (DPs) of 1–8. In the notation PC_x and PC_xG_y, x indicates procyanidin DP and y represents DG. Peak numbers correspond to Table 1.

and galloylated PC oligomers are presented in Figure 2. This form of representation provides a clear picture of both the molecular weight and isomeric distributions of each class.

The chromatographic behavior of PCs and galloylated PCs in each dimension can be visualized in terms of the raw extracted ion chromatograms (EICs) presented in Figure 3. In this figure, consecutive "peaks" in fact correspond to individual second dimension chromatograms, each containing several isomeric compounds (Figure 3C). Higher HILIC retention results in longer retention times in the raw EICs. From the EICs for PCs shown in Figure 3A, it is evident that PCs were clearly separated according to DP in HILIC. A similar elution pattern is evident for pentameric PCs as a function of degree of galloylation (DG) (Figure 3B), implying that HILIC retention increases with DG, as expected on the basis of the relative polarity of these compounds (see also Figure 2). HILIC separation according to DG for the same DP is less efficient, with partial overlap occurring between compounds with different DG. This figure also illustrates that at least five fractions of each first dimension peak (i.e., each extracted mass) are analyzed in the second dimension. Therefore, the requirement of ~3 fractions per first dimension peak is more than satisfied.[47−49]

While the separation according to size was generally maintained in the HILIC dimension, RP-LC separation of the higher MW PACs progressively worsened with increasing DP. This follows directly from the exponential increase in the number of isomers with DP.[51] This phenomenon is emphasized in representative one-dimensional RP-LC EICs obtained for PCs of increasing DP (Figure 3C). In this figure, the challenges associated with the separation of high MW PCs are clearly evident: beyond DP 5, the 2 min RP-LC gradient separation is no longer sufficient to provide isomeric separation; this is despite the fact that HILIC preseparation effectively removes interference from PCs of different DP. For PCs of DP > 5, unresolved "humps" involving a large number of isomeric compounds are observed. This situation is exacerbated by the galloylated PCs also present in grape seeds, with extensive overlap occurring between these classes of compounds. Figure S4, Supporting Information, illustrates the relative retention of pentameric and hexameric PCs with various DGs in terms of the relevant EICs. The superimposition of both these chemical distribution profiles, i.e., according to DP and DG, coupled to the increase in the number of isomeric structures with increasing DP, is responsible for the extensive coelution observed for high MW compounds in the contour plots.

As an extreme example of the complexity of grape seed PACs, a mass spectrum obtained from the region of the contour plot corresponding to the high MW PACs is presented in Figure 4. In this figure, the presence of triply charged ions for PC oligomers of DP 10–12 with various degrees of galloylation is observed. Careful study of this mass spectrum highlights the complexity of the sample. For instance, for a fixed DG = 3, PACs of DP 10–12 are detected ~96 mass units apart

dx.doi.org/10.1021/ac401896r | Anal. Chem. 2013, 85, 9107–9115

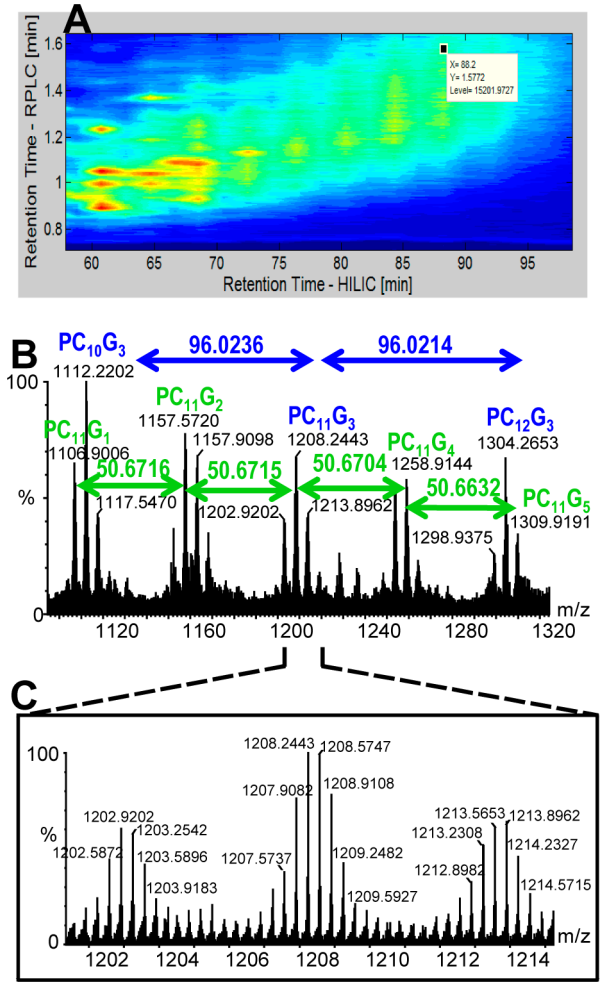

Figure 4. Example of the mass spectrum for high MW proanthocyanidins obtained by HILIC × RP-LC–ESI-MS analysis of a red grape seed extract. (A) shows the relevant region of the contour plot, with the black square indicating the coordinates where the mass spectrum was obtained. (B) The region of the mass spectrum illustrating the presence of PACs of DP 10–12 with different degrees of galloylation. In the PC_xG_y notation, *x* signifies PC DP and *y* the DG. Blue arrows and labels correspond to trigalloylated PCs of DP 10–12, while green arrows and labels assign undecameric PCs with various DGs. All compounds in the figure were detected as triply charged species, as confirmed in (C).

(indicated by the blue arrows in Figure 4), consistent with the addition of an (epi)catechin unit for a triply charged species. In the same mass spectrum, triply charged species for PACs with a DP of 11 and degrees of galloylation from 1 to 5 are detected, distinguished by increments of 51 mass units (green arrows in Figure 4) with each additional gallate unit. This figure indicates that, despite the power of HILIC × RP-LC separation, coelution of high MW grape seed PACs still occurs, involving compounds differing by up to three degrees of polymerization and five degrees of galloylation.

These data point to the fact that, in the case of grape seed PACs, the complexity of the sample outweighs the resolving power of online HILIC × RP-LC–MS. Decoupling the two separation modes in either off-line or stop-flow configurations would improve chromatographic resolution due to better isomeric separation provided by longer second dimension analyses.[6,40,41] While this will effectively extend the DP range of PACs that can be separated, complete separation of PCs of DP > 5 in RP-LC is not possible for RP-LC separations under 30 min.[6] For these compounds, the number of isomers simply exceeds the separation power of even highly optimized RP-LC separations.

MS/MS detection in combination with HILIC × RP-LC separation shows promise for the characterization of individual low DP compounds[39] by potentially providing information on the hydroxylation patterns and type of interflavan linkages.[52,53] However, the complexity of grape seed PACs means that limited useful information is provided for high MW compounds due to their extensive coelution in RP-LC. The use of multiple MS/MS functions during the short second dimension separations is limited by lack of sensitivity. Furthermore, MS/MS operation results in a loss of second dimension resolution due to insufficient data acquisition rates. For these reasons, HR-MS is better suited to the screening of the overall composition of grape seed PACs.

On the basis of mass spectral data, the grape seed extract contained PCs of DP up to 16 with a degree of galloylation up to 8 (Table S1, Supporting Information). Submission of the same extract to phloroglucinolysis ("Phloroglucinolysis" and Figure S5, Supporting Information) indicated a mDP of 3.6 for this sample (Table S2, Supporting Information). This is roughly in accordance with previous values[42,54] reported for grape seeds and indicates that by far the largest proportion of grape seed PACs are low MW compounds. In light of this, the apparent complexity of the high MW PACs detected by HILIC × RP-LC–MS emphasizes that grape tannins are much more complex than suggested by average DP determinations. These data also highlight a further challenge in the determination of high MW PACs in grape seeds: their low molar percentage, coupled to their isomeric heterogeneity, implies much lower absolute concentrations and therefore lower sensitivity for these compounds. PACs of DP up to 32 and extent of galloylation up to 19 have previously been reported[11] in grape seeds. The fact that such high MW compounds were not detected in the present report may be due to several reasons, including their low levels of occurrence, the mass scan range used, or their limited solubility in acetonitrile used in the redissolution of the freeze-dried extracts. The low solubility of high MW PACs in HILIC solvents represents a potential limitation of the current methodology, as the sample should be dissolved in a relatively hydrophobic solvent for efficient injection in this dimension.

Nevertheless, the developed methodology clearly demonstrates sufficient sensitivity for the analysis of a diverse range of PACs in grape seeds and has previously been shown to be sufficiently reproducible for routine analysis.[41] This approach can therefore in essence be extended to quantitative analysis[55] of grape seed PACs, although this would be hampered by the lack of commercially available standards and differences in extinction coefficients.[50] Future HILIC × RP-LC–MS analysis of grape skin PACs, which comprise higher MW compounds and also contain additional PDs,[54] would also be interesting. Off-line HILIC × RP-LC analysis of green tea PACs[51] has confirmed that PDs can successfully be separated from the PCs and galloylated PCs by this approach.

■ CONCLUSIONS

To obtain a better understanding of the biological and organoleptic properties of grape and wine tannins, chromatographic separation is essential, considering that these properties are dependent on individual molecules. In this study, an online HILIC × RP-LC-FL–HR-MS methodology was developed to

dx.doi.org/10.1021/ac401896r | Anal. Chem. 2013, 85, 9107–9115

allow an in-depth study of grape seed tannins. Combining HILIC and RP-LC presented the advantage of prefractionating compounds according to size before their subsequent isomeric separation, which reduced compound overlap and simplified data interpretation. Hyphenating LC × LC to HR-MS added an independent dimension which allowed peak assignment based on two independent chromatographic retention times as well as accurate mass data. HR-MS confirmed the presence of a broad spectrum of PACs in a grape seed extract, with PACs up to DP 16 and a DG up to 8 detected. Partially as a result of the constraints of continuous online LC × LC operation (as opposed to stop-flow operation), complete separation of these compounds could not be obtained. Nevertheless, the developed methodology represents the most powerful single analytical method for the characterization of grape seed PAC chemical composition reported to date.

Given the importance of PACs in wine chemistry, this approach shows promise as a means of addressing the current analytical limitations for tannin characterization. Future extension to the analysis of grape skin and wine tannins could therefore shed more light on these influential components and their alteration during wine production.

■ ASSOCIATED CONTENT

Supporting Information

Additional information as noted in text. This material is available free of charge via the Internet at http://pubs.acs.org.

■ AUTHOR INFORMATION

Corresponding Author

*E-mail: ajdevill@sun.ac.za. Tel: (+27) 21 808 3351. Fax: (+27) 21 808 3360.

Notes

The authors declare no competing financial interest.

■ ACKNOWLEDGMENTS

The authors acknowledge Sasol, the NRF (Grant 70995 to A.d.V.), IFS (Grant F/4904-1 to A.d.V.), Stellenbosch University, and the Harry Crossley Foundation for funding. Chandré Willemse is thanked for experimental assistance and Edmund Luckay (IWBT) for the donation of the grapes. Alexander Whaley (LECO Africa) is thanked for assistance with ChromaTOF software.

■ REFERENCES

(1) Santos-Buelga, C.; Scalbert, A. *J. Sci. Food Agric.* **2000**, *80*, 1094−1117.
(2) Ferreira, D.; Slade, D. *Nat. Prod. Rep.* **2002**, *19*, 517−541.
(3) Aron, P. M.; Kennedy, J. A. *Mol. Nutr. Food Res.* **2008**, *52*, 79−104.
(4) Manach, C.; Scalbert, A.; Morand, C.; Remesy, C.; Jimenez, L. *Am. J. Clin. Nutr.* **2004**, *79*, 727−747.
(5) Kelm, M. A.; Johnson, J. C.; Robbins, R. J.; Hammerstone, J. F.; Schmitz, H. H. *J. Agric. Food Chem.* **2006**, *54*, 1571−1576.
(6) Kalili, K. M.; de Villiers, A. *J. Chromatogr., A* **2009**, *1216*, 6274−6284.
(7) Yanagida, A.; Kanda, T.; Shoji, T.; Ohnishi-Kameyama, M.; Nagata, T. *J. Chromatogr., A* **1999**, *855*, 181−190.
(8) Yanagida, A.; Murao, H.; Ohnishi-Kameyama, M.; Yamakawa, Y.; Shoji, A.; Tagashira, M.; Kanda, T.; Shindo, H.; Shibusawa, Y. *J. Chromatogr., A* **2007**, *1143*, 153−161.
(9) Sun, B. S.; Leandro, M. C.; Ricardo da Silva, J. M.; Spranger, M. I. *J. Agric. Food Chem.* **1998**, *46*, 1390−1396.
(10) Hayasaka, Y.; Waters, E. J.; Cheynier, V.; Herderich, M. J.; Vidal, S. *Rapid Commun. Mass Spectrom.* **2003**, *17*, 9−16.
(11) Spranger, I.; Sun, B.; Mateus, A. M.; de Freitas, V.; Ricardo da Silva, J. M. *Food Chem.* **2008**, *108*, 519−532.
(12) Hümmer, W.; Schreier, P. *Mol. Nutr. Food Res.* **2008**, *52*, 1381−1398.
(13) Kennedy, J. A.; Saucier, C.; Glories, Y. *Am. J. Enol. Vitic.* **2006**, *57*, 239−248.
(14) Obradovic, D. In *ASVO proceedings*; ASVO: Adelaide, South Australia, 2005; p 23−27.
(15) Waterhouse, A. L. *Ann. N.Y. Acad. Sci.* **2002**, *957*, 21−36.
(16) Dell'Agli, M.; Busciala, A.; Bosisio, E. *Cardiovasc. Res.* **2004**, *63*, 593−602.
(17) Pati, S.; Losito, I.; Gambacorta, G.; La Notte, E.; Palmisano, F.; Zambonin, P. G. *J. Mass Spectrom.* **2006**, *41*, 861−871.
(18) Vidal, S.; Francis, I. L.; Guyot, S.; Marnet, N.; Kwiatkowski, M.; Cheynier, V.; Waters, E. *J. Sci. Food Agric.* **2003**, *83*, 564−573.
(19) Mercurio, M. D.; Smith, P. A. *J. Agric. Food Chem.* **2008**, *56*, 5528−5537.
(20) Schofield, P.; Mbugua, D. M.; Pell, A. N. *Anim. Feed Sci. Technol.* **2001**, *91*, 21−40.
(21) Mueller-Harvey, I. *Anim. Feed Sci. Technol.* **2001**, *91*, 3−20.
(22) Herderich, M. J.; Smith, P. A. *Austr. J. Grape Wine Res.* **2005**, *11*, 205−214.
(23) Rigaud, J.; Perez-Ilzarbe, X.; Ricardo da Silva, J. M.; Cheynier, V. *J. Chromatogr.* **1991**, *540*, 401−405.
(24) Matthews, S.; Mila, I.; Scalbert, A.; Pollet, B.; Lapierre, C.; Hervé du Penhoat, C. L. M.; Rolando, C.; Donnelly, D. M. X. *J. Agric. Food Chem.* **1997**, *45*, 1195−1201.
(25) Labarbe, B.; Cheynier, V.; Brossaud, F.; Souquet, J.-M.; Moutounet, M. *J. Agric. Food Chem.* **1999**, *47*, 2719−2723.
(26) Flamini, R. *Mass Spectrom. Rev.* **2003**, *22*, 218−250.
(27) Tourino, S.; Fuguet, E.; Jauregui, O.; Saura-Calixto, F.; Cascante, M.; Torres, J. L. *Rapid Commun. Mass Spectrom.* **2008**, *22*, 3489−3500.
(28) Rigaud, J.; Escribano-Bailon, M. T.; Prieur, C.; Souquet, J.-M.; Cheynier, V. *J. Chromatogr., A* **1993**, *654*, 255−260.
(29) Hammerstone, J. F.; Lazarus, S. A.; Mitchell, A. E.; Rucker, R.; Schmitz, H. H. *J. Agric. Food Chem.* **1999**, *47*, 490−496.
(30) Yanagida, A.; Kanda, T.; Takahashi, T.; Kamimura, A.; Hamazono, T.; Honda, S. *J. Chromatogr., A* **2000**, *890*, 251−259.
(31) Giddings, J. C. *J. Chromatogr., A* **1995**, *703*, 3−15.
(32) Dugo, P.; Mondello, L.; Cacciola, F.; Donato, P. In *Comprehensive Chromatography in Combination with Mass Spectrometry*; Mondello, L., Ed.; John Wiley & Sons, Inc.: Hoboken, NJ, 2011; pp 331−390.
(33) Cacciola, F.; Jandera, P.; Blahová, E.; Mondello, L. *J. Sep. Sci.* **2006**, *29*, 2500−2513.
(34) Dugo, P.; Cacciola, F.; Herrero, M.; Donato, P.; Mondello, L. *J. Sep. Sci.* **2008**, *31*, 3297−3308.
(35) Kivilompolo, M.; Hyötyläinen, T. *J. Sep. Sci.* **2008**, *31*, 3466−3472.
(36) Beelders, T.; Kalili, K. M.; Joubert, E.; de Beer, D.; de Villiers, A. *J. Sep. Sci.* **2012**, *35*, 1808−1820.
(37) Kalili, K. M.; de Villiers, A. *J. Sep. Sci.* **2010**, *33*, 853−863.
(38) de Villiers, A.; Kalili, K. M. In *12th International Symposium on Hyphenated Techniques in Chromatography and Chromatographic Analyzers (HTC-12) and Second International Symposium on Hyphenated Techniques for Sample Preparation (HTSP-2)*, Brugge, Belgium, CIP Koninklijke Bibliotheek van België (Royal Library Albert I): Brussels, Belgium, 2012; p 42.
(39) Montero, L.; Herrero, M.; Prodanov, M.; Ibáñez, E.; Cifuentes, A. *Anal. Bioanal. Chem.* **2013**, *405*, 4627−4638.
(40) Kalili, K. M.; de Villiers, A. *J. Chromatogr., A* **2013**, *1289*, 58−68.
(41) Kalili, K. M.; de Villiers, A. *J. Chromatogr., A* **2013**, *1289*, 69−79.
(42) Kennedy, J. A.; Jones, G. P. *J. Agric. Food Chem.* **2001**, *49*, 1740−1746.
(43) van der Horst, A.; Schoenmakers, P. J. *J. Chromatogr., A* **2003**, *1000*, 693−709.

(44) Tomasi, G.; Savorani, F.; Engelsen, S. B. *J. Chromatogr., A* **2011**, *1218*, 7832−7840.
(45) Stoll, D. R. *Anal. Bioanal. Chem.* **2010**, *397*, 979−986.
(46) Jandera, P.; Hajek, T.; Stankova, M.; Vynuchalova, K.; Cesla, P. *J. Chromatogr., A* **2012**, *1268*, 91−101.
(47) Murphy, R. E.; Schure, M. R.; Foley, J. P. *Anal. Chem.* **1998**, *70*, 1585−1594.
(48) Seeley, J. V. *J. Chromatogr., A* **2002**, *962*, 21−27.
(49) Horie, K.; Kimura, H.; Ikegami, T.; Iwatsuka, A.; Saad, N.; Fiehn, O.; Tanaka, N. *Anal. Chem.* **2007**, *79*, 3764−3770.
(50) Hurst, W. J.; Stanley, B.; Glinski, J. A.; Davey, M.; Payne, M. J.; Stuart, D. A. *Molecules* **2009**, *14*, 4136−4146.
(51) Mayer, R.; Stecher, G.; Wuerzner, R.; Silva, R. C.; Sultana, T.; Trojer, L.; Feuerstein, I.; Krieg, C.; Abel, G.; Popp, M.; Bobleter, O.; Bonn, G. K. *J. Agric. Food Chem.* **2008**, *56*, 6959−6966.
(52) Gu, L.; Kelm, M. A.; Hammerstone, J. F.; Zhang, Z.; Beecher, G.; Holden, J.; Haytowitz, D.; Prior, R. L. *J. Mass Spectrom.* **2003**, *38*, 1272−1280.
(53) Li, H.-J.; Deinzer, M. L. *Anal. Chem.* **2007**, *79*, 1739−1748.
(54) Mattivi, F.; Vrhovsek, U.; Masuero, D.; Trainotti, D. *Austr. J. Grape Wine Res.* **2009**, *15*, 27−35.
(55) Dugo, P.; Cacciola, F.; Donato, P.; Airado-Rodriguez, D.; Herrero, M.; Mondello, L. *J. Chromatogr., A* **2009**, *1216*, 7483−7487.

SUPPORTING INFORMATION FOR THE MANUSCRIPT:

Towards unravelling grape tannin composition: Application of on-line hydrophilic interaction chromatography × reversed phase liquid chromatography – time-of-flight mass spectrometry to grape seed analysis.

Kathithileni M. Kalili[1], Jochen Vestner[1,2], Maria A. Stander[3,4] and André de Villiers[1,*]

[1]Stellenbosch University, Department of Chemistry and Polymer Science, Private Bag X1, Matieland 7602, South Africa

[2]Hochschule Geisenheim University, Center of Analytical Chemistry & Microbiology, Department of Microbiology and Biochemistry, Von-Lade-Str. 1, 65366 Geisenheim, Germany

[3]Stellenbosch University, Central Analytical Facility, Private Bag X1, Matieland 7602, South Africa

[4]Stellenbosch University, Department of Biochemistry, Private Bag X1, Matieland 7602, South Africa

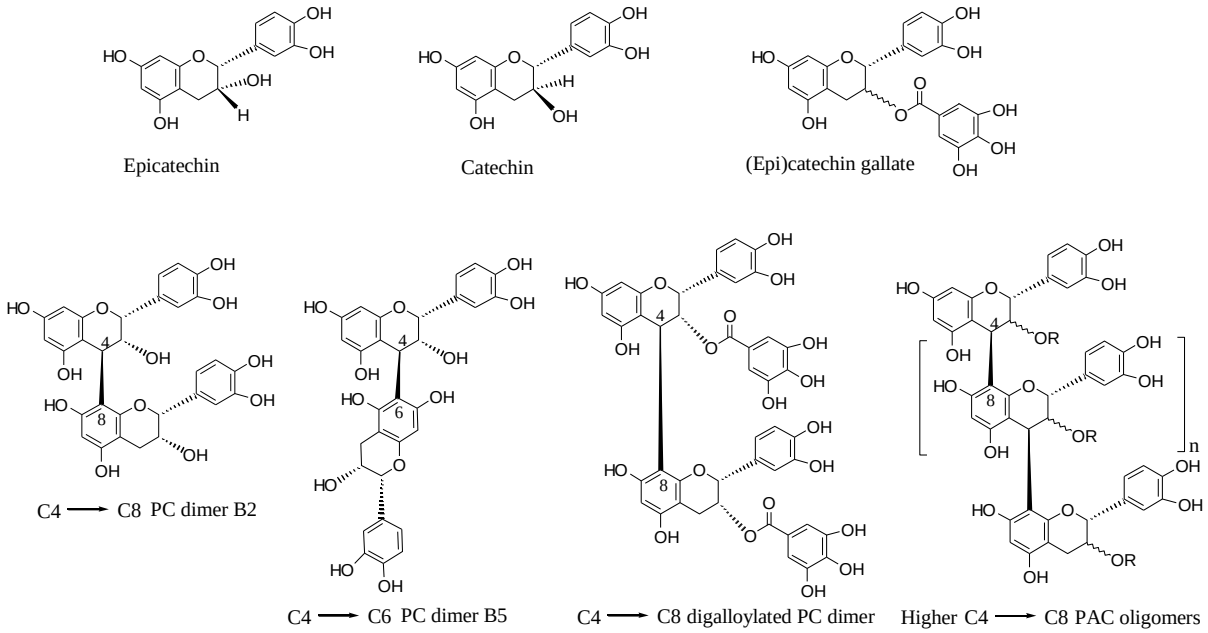

Figure S1. Chemical structures for proanthocyanidins (PACs) commonly found in grape seeds.

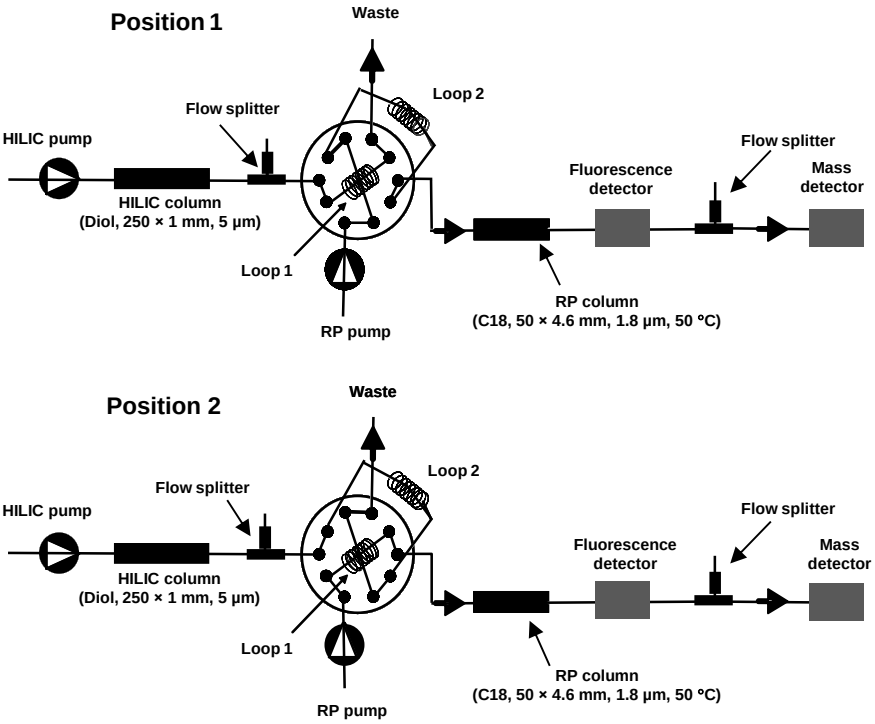

Figure S2. Schematic illustration of the instrumental configuration used for on-line HILIC×RP-LC-FL−ESI-MS analyses.

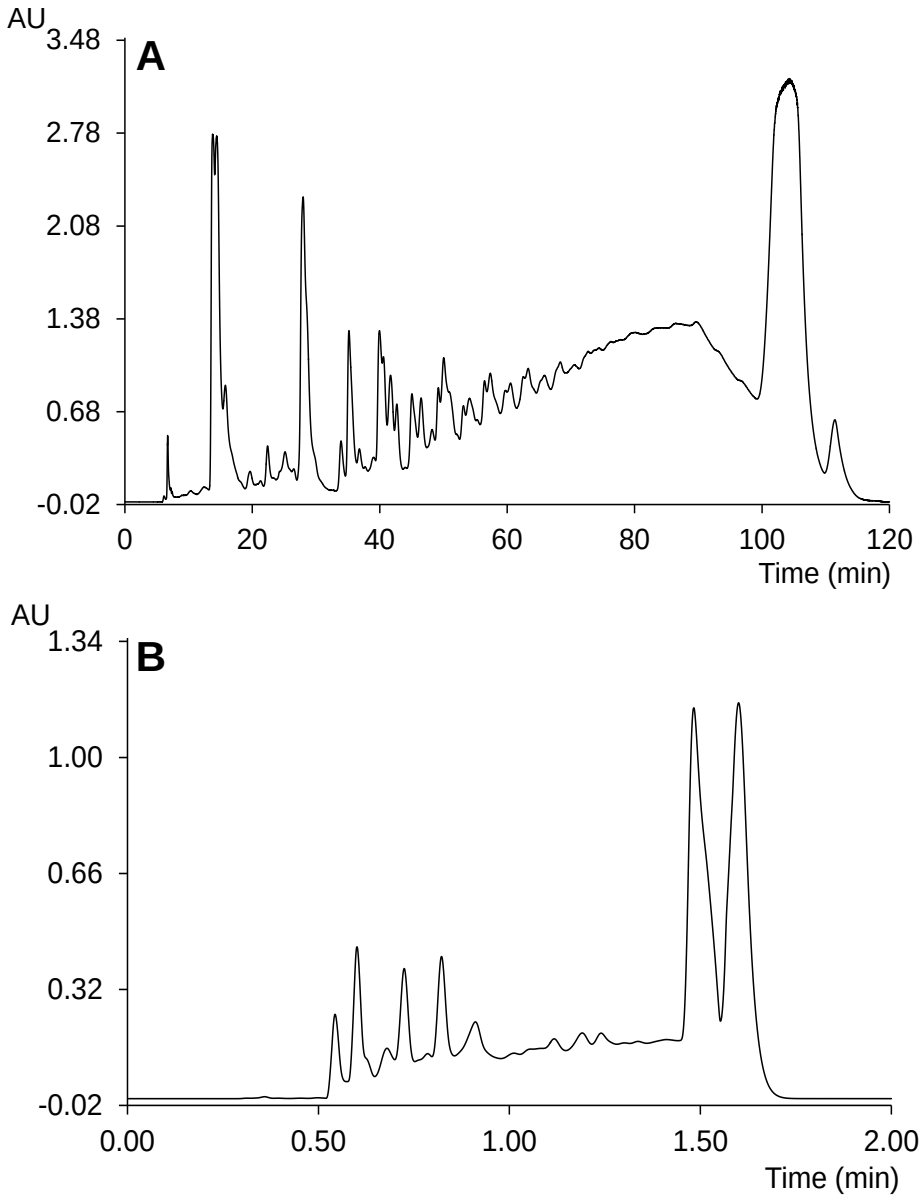

Figure S3. One-dimensional UV chromatograms (280 nm) obtained for the HILIC (A) and RP-LC (B) analysis of a red grape seed extract. Gradient conditions are the same as those specified in section 2.5 with injection volumes of 2.5 and 1 µL for HILIC and RP-LC, respectively.

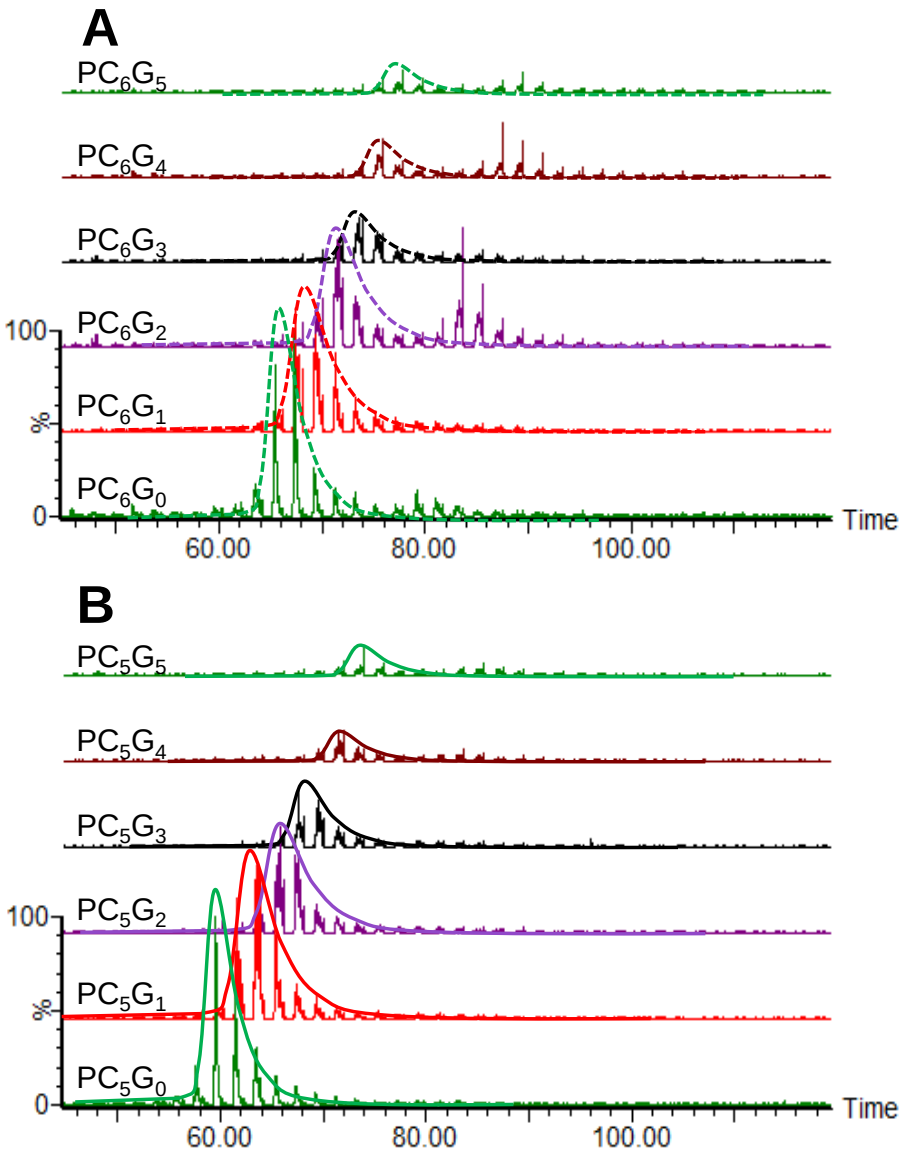

Figure S4. Raw extracted ion chromatograms obtained from HILIC×RP-LC−MS analysis of grape seeds, illustrating the elution patterns for doubly charged ions for (A) hexameric- and (B) pentameric procyanidin oligomers as a function of degree of galloylation (DG). Simulated effective first dimension HILIC peaks are represented by solid (pentameric) and dotted (hexameric) lines. In the notation PC_xG_y, *x* indicates procyanidin degree of polymerization and *y* denotes DG.

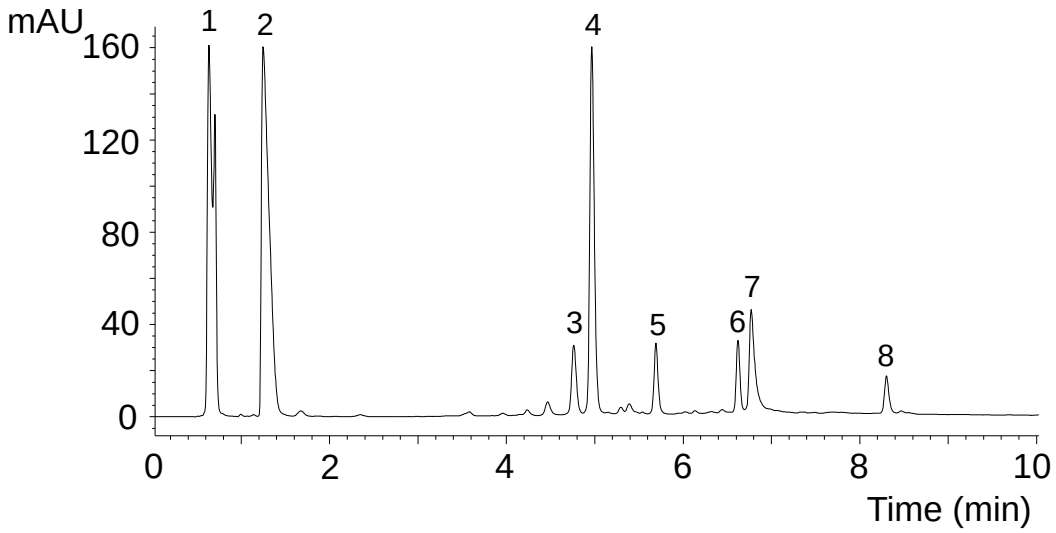

Figure S5. HPLC-UV chromatogram obtained for the analysis of the phloroglucinolysis degradation products of the red grape seed extract. Peak labels (as identified by RP-LC−MS) correspond to: 1-ascorbic acid, 2-phloroglucinol, 3-catechin phloroglucinol adduct, 4-epicatechin phloroglucinol adduct, 5-catechin, 6-epicatechin, 7-epicatechin gallate phloroglucinol adduct and 8-epicatechin gallate. For experimental details, refer to section 2.5.2.

Table S1: Summary of additional proanthocyanidins detected by HILIC×RP-LC–ESI-MS analysis of a red grape seed extract. This table lists the compounds for which individual chromatographic peaks could not be identified due to co-elution of several isomeric structures in the second dimension separation. For the remainder of compounds detected as individual peaks, refer to **Table 1** in the manuscript. Base peak ions are highlighted in bold.

Label	#DP	*DG	$[M-2H]^{2-}/2$	$[M-3H]^{3-}/3$	$[M-4H]^{4-}/4$
PC_5G_2	5	2	**872.1691**	-	-
PC_5G_3		3	**948.1784**	-	-
PC_5G_4		4	**1024.1893**	-	-
PC_5G_5		5	**1100.1990**	-	-
PC_6G_1	6	1	**940.1940**	-	-
PC_6G_2		2	**1016.2027**	-	-
PC_6G_3		3	**1092.2084**	-	-
PC_6G_4		4	**1168.2169**	778.4746	-
PC_6G_5		5	**1244.2247**	829.1492	-
PC_6G_6		6	**1320.2330**	879.8198	-
PC_7G_1	7	1	**1084.2240**	722.4805	-
PC_7G_2		2	**1160.2362**	773.1595	-
PC_7G_3		3	**1236.2448**	823.8293	-
PC_7G_4		4	**1312.2494**	874.4942	-
PC_7G_5		5	1388.2670	**925.1715**	-
PC_7G_6		6	1464.2540	**975.8384**	-
PC_7G_7		7	-	**1026.5112**	-
PC_8G_0	8	0	**1152.2560**	767.8298	-
PC_8G_1		1	**1228.2583**	818.5050	-
PC_8G_2		2	**1304.2643**	869.1717	-
PC_8G_3		3	1380.2662	**919.8462**	-
PC_8G_4		4	1456.2882	**970.5224**	-
PC_8G_5		5	1532.2815	**1021.1870**	-
PC_8G_6		6	1608.2871	**1071.8735**	-
PC_8G_7		7	-	**1122.5299**	-
PC_8G_8		8	-	**1173.2019**	-
PC_9G_0	9	0	**1296.2778**	863.8510	-
PC_9G_1		1	1372.2877	**914.5180**	-
PC_9G_2		2	1448.2800	**965.1956**	-
PC_9G_3		3	1524.2889	**1015.8644**	-
PC_9G_4		4	1600.2766	**1066.5366**	-
PC_9G_5		5	1676.3145	**1117.2109**	-
PC_9G_6		6	-	**1167.8811**	-
PC_9G_7		7	-	**1218.5630**	-
PC_9G_8		8	-	**1269.2179**	-
$PC_{10}G_0$	10	0	1440.2990	**959.8712**	-
$PC_{10}G_1$		1	1516.3007	**1010.5452**	-
$PC_{10}G_2$		2	1592.2966	**1061.2170**	-
$PC_{10}G_3$		3	1668.3236	**1111.8861**	-

$PC_{10}G_4$		4	1744.3245	**1162.5548**	-
$PC_{10}G_5$		5	-	**1213.2310**	-
$PC_{10}G_6$		6	-	**1263.9098**	947.6565
$PC_{10}G_7$		7	-	**1314.5651**	-
$PC_{10}G_8$		8	-	**1365.2373**	-
$PC_{11}G_0$	11	0	-	**1055.8816**	-
$PC_{11}G_1$		1	1660.3298	**1106.5630**	-
$PC_{11}G_2$		2	1736.3188	**1157.2375**	-
$PC_{11}G_3$		3	1812.3025	**1207.9082**	-
$PC_{11}G_4$		4	-	**1258.5731**	-
$PC_{11}G_5$		5	-	**1309.2476**	-
$PC_{11}G_6$		6	-	**1359.9125**	-
$PC_{11}G_7$		7	-	**1410.5817**	-
$PC_{11}G_8$		8	-	**1461.2620**	-
$PC_{12}G_0$	12	0	-	**1151.9089**	-
$PC_{12}G_1$		1	1804.3363	**1202.5898**	-
$PC_{12}G_2$		2	-	**1253.2571**	-
$PC_{12}G_3$		3	-	**1303.9169**	-
$PC_{12}G_4$		4	-	**1354.6042**	1015.6978
$PC_{12}G_5$		5	-	**1405.2516**	-
$PC_{12}G_6$		6	-	**1455.9237**	-
$PC_{12}G_7$		7	-	**1506.6000**	-
$PC_{12}G_8$		8	-	**1557.2876**	-
$PC_{13}G_0$	13	0	-	-	-
$PC_{13}G_1$		1	-	**1298.5895**	-
$PC_{13}G_2$		2	-	**1349.2756**	-
$PC_{13}G_3$		3	-	**1399.9513**	-
$PC_{13}G_4$		4	-	**1450.6306**	-
$PC_{13}G_5$		5	-	**1501.2808**	-
$PC_{13}G_6$		6	-	**1551.9612**	-
$PC_{13}G_7$		7	-	**1602.6183**	-
$PC_{13}G_8$		8	-	**1653.3196**	1239.7177
$PC_{14}G_0$	14	0	-	-	-
$PC_{14}G_1$		1	-	**1394.6107**	-
$PC_{14}G_2$		2	-	**1445.2883**	1083.7351
$PC_{14}G_3$		3	-	**1495.9569**	1121.7063
$PC_{14}G_4$		4	-	**1546.6333**	1159.7158
$PC_{14}G_5$		5	-	**1597.2981**	1197.7429
$PC_{14}G_6$		6	-	**1647.9626**	1235.7478
$PC_{14}G_7$		7	-	**1698.6550**	1273.7394
$PC_{14}G_8$		8	-	**1749.3209**	-
$PC_{15}G_0$	15	0	-	-	-
$PC_{15}G_1$		1	-	**1490.6309**	-
$PC_{15}G_2$		2	-	**1541.3120**	1155.7352
$PC_{15}G_3$		3	-	**1591.9846**	-
$PC_{15}G_4$		4	-	**1642.6521**	-

$PC_{15}G_5$		5	-	**1693.3280**	1269.7494
$PC_{16}G_0$	16	0	-	-	-
$PC_{16}G_1$		1	-	**1586.6537**	-
$PC_{16}G_2$		2	-	**1637.3256**	-
$PC_{16}G_3$		3	-	**1687.9915**	-
$PC_{16}G_4$		4	-	**1738.6830**	-
$PC_{16}G_5$		5	-	**1789.3674**	1341.7789

[#]DP: Degree of polymerization of procyanidins, [*]DG: Degree of galloylation

Table S2: Summary of phloroglucinolysis data obtained for the red grape seed extract.

Label	Compound	Molar %	% Terminal unit	% Extension unit
3	Catechin-phloroglucinol	13.5		
4	Epicatechin-phloroglucinol	52.4		
5	Catechin	12.7	46	19
6	Epicatechin	12.3	44	73
7	(Epi)catechin gallate-phloroglucinol	6.3		
8	(Epi)catechin gallate	2.9	10	8
*mDP		3.6		

*mDP: mean degree of polymerization

The data reported in **Table S2** indicate that the grape seed tannins are principally composed of catechin, epicatechin and epicatechin gallate. Catechin and epicatechin were the main terminal units (46 and 44%, respectively), followed by epicatechin gallate (10%). Epicatechin was the major extension unit (73%), followed by catechin (19%) and epicatechin gallate (8%).

Addendum F

Comprehensive two-dimensional liquid chromatography coupled to the ABTS radical scavenging assay: A powerful method for the analysis of phenolic antioxidants

K.M. Kalili, F. Lynen, S. de Smet, T. van Hoeylandt, A. de Villiers, 2013, submitted for publication in Anal. Bioanal. Chem.

Comprehensive two-dimensional liquid chromatography coupled to the ABTS radical scavenging assay: A powerful method for the analysis of phenolic antioxidants

Kathithileni M. Kalili[1], Seppe De Smet[2], Tim van Hoeylandt[2], Frédéric Lynen[2] and André de Villiers[1,*]

[1]Department of Chemistry and Polymer Science, Stellenbosch University, Private Bag X1, Matieland 7602, South Africa.
[2]Separation Science Group, Department of Organic Chemistry, Ghent University, Krijgslaan 281 S4, 9000 Ghent, Belgium.

*Tel: +27 21 808 3351, Email: ajdevill@sun.ac.za

Abstract

The on-line combination of comprehensive two-dimensional liquid chromatography (LC×LC) with the 2,2'-azino-bis(3-ethylbenzothiazoline)-6 sulfonic acid (ABTS) radical scavenging assay was investigated as a powerful method to determine the free radical scavenging activities of individual phenolics in natural products. The combination of hydrophilic interaction chromatography (HILIC) separation according to polarity and reversed-phase liquid chromatography (RP-LC) separation according to hydrophobicity is shown to provide much higher resolving power than one-dimensional (1-D) separations, which, combined with on-line ABTS detection, allows the detailed characterisation of antioxidants in complex samples. Careful optimisation of the ABTS reaction conditions was required to maintain the chromatographic separation in the antioxidant detection process. Both on-line and off-line HILIC×RP-LC–ABTS methods were developed, with the former offering higher throughput and the latter higher resolution. Even for the fast analyses used in the second dimension of on-line HILIC×RP-LC, good performance for the ABTS assay was obtained. The combination of LC×LC separation with an on-line radical scavenging assay increases the likelihood of identifying individual radical scavenging species compared to conventional LC–ABTS assays. The applicability of the approach was demonstrated for cocoa, red grape seed and green tea phenolics.

Keywords:

antioxidant activity, ABTS, comprehensive two-dimensional liquid chromatography (LC×LC), natural products, phenolic compounds, radical scavenging assay

1. Introduction

Antioxidants are molecules with recognised biological and industrial uses. Traditionally, antioxidants have been used in food, pharmaceutical and cosmetic products primarily for preservation purposes, although recent increased use of particularly natural antioxidants is coupled to their beneficial physiological properties [1]. Extensive research has shown that a diet rich in fruits and vegetables reduces the risk of ageing and degenerative diseases such as diabetes, cardiovascular diseases and cancer, amongst others [2,3]. These protective effects are closely linked with the antioxidant activity of phenolic compounds, which are major constituents of fruits and vegetables [2-6]. As a result, increased research has been focused on natural products, either in search of new (or more potent) natural nutraceuticals or for the formulation of so called “functional products” enriched with known bioactive extracts [1,7].

Although substantial evidence exists regarding the *in vitro* antioxidant capacities of whole phenolic extracts, comparatively little is known of the antioxidant activities of individual compounds. This is especially so in the case of highly condensed oligomeric and polymeric structures commonly encountered in phenolic extracts [8], and is largely due to the complexity of these compounds, which makes their analysis extremely challenging. While previous studies have shown that biological activity is influenced by a large number of factors and cannot be judged based on antioxidant activity alone, this property is still viewed as a fundamental aspect of functional food research and a potent indicator of bioactivity [1,2]. Therefore, extensive effort has been dedicated to the development of simple, fast and accurate methods for the determination of antioxidant or radical scavenging activities of phenolics in natural products.

Several assays based on a variety of radical species have been developed for the determination of antioxidant activity *in vitro* [9-14]. These can be broadly classified into three groups: (i) assays that target specific reactive oxygen- or nitrogen-containing species similar to those encountered in biological systems, (ii) assays based on non-biological radicals, and (iii) assays based on electrochemical determination [11,15,16]. Although assays based on reactive oxygen or nitrogen species closely mimic *in vivo* conditions and would, in theory, provide a much more accurate estimation of the antioxidant activity of a compound *in vivo*, these reactions can be hard to control and require relatively long reaction times, and are therefore not suitable for routine antioxidant screening [11,15].

Conversely, assays based on stable non-biological radicals have increased in popularity due to their simplicity and relative ease of use [14]. Of these, the free radical decolourising assays based on the 1,1-diphenyl-2-picrylhydrazyl (DPPH) and 2,2'-azino-bis(3-ethylbenzothiazoline)-6 sulfonic acid

(ABTS) radicals have found widespread application in the routine screening of radical scavengers in complex samples. When coupled to high performance liquid chromatography (HPLC), these assays facilitate identification of active compounds in complex mixtures following their chromatographic separation. In fact, HPLC coupled on-line to a radical scavenging assay, UV and/or mass spectrometric (MS) detection currently represents the most widely used and effective strategy for routine screening and identification of individual antioxidants in complex samples. While both DPPH and ABTS assays have been used with some success in combination with HPLC, the latter demonstrates better sensitivity, faster reaction kinetics (i.e. on the time-scale of LC separations) and applicability to both hydrophilic and lipophilic antioxidants over a wider range of pH and solvent composition [15,17-21].

Despite the benefits of this approach, one-dimensional HPLC often provides incomplete separation for highly complex natural products. As a consequence of inevitable co-elution, accurate determination of radical scavenging activities of individual compounds is hampered. By coupling multiple LC separations in a 2-dimensional separation, the combination of different selectivities greatly improves the chances of obtaining pure compounds [22-24]. Comprehensive 2-dimensional LC (LC×LC), wherein the entire sample is subjected to two non-correlated separation mechanisms [25], provides the maximum performance gain. Previous work has demonstrated that LC×LC separation combining hydrophilic interaction chromatography (HILIC) and reversed-phase liquid chromatography (RP-LC) provides improved resolution for phenolic compounds in complex natural product extracts [26-29]. In the current study, the potential of HILIC×RP-LC separation coupled on-line to the ABTS radical scavenging assay was investigated as a more powerful approach for the identification of radical scavenging species in natural products.

2. Experimental

2.1. Reagents and materials

Cocoa beans were purchased from a local supermarket. Red grapes (*Vitis vinifera*, cv. Cabernet Sauvignon) were obtained from the Institute of Wine Biotechnology (IWBT, Stellenbosch University). HPLC grade methanol, acetonitrile, acetic acid, formic acid as well as sodium chloride (NaCl), disodium hydrogen phosphate (Na_2HPO_4), potassium chloride (KCl), potassium dihydrogen phosphate (KH_2PO_4), 2,2'-azino-bis(3-ethylbenzothiazoline-6-sulphonic acid) diammonium salt (ABTS), manganese (IV) oxide (MnO_2), (-)-epicatechin and (±)-catechin were purchased from Sigma Aldrich (Bornem, Belgium). Deionised water was prepared using a Milli-Q water purification system (Millipore,

Milford, MA, USA). All solutions were filtered through 0.22 µm nylon membrane filters (Millipore) before use.

2.2. Sample preparation

The cocoa and red grape seed extracts were prepared according to a previously reported method [26]. For HILIC analyses, the extracts were freeze-dried and re-dissolved in 70% acetonitrile and 30% methanol (*v/v*). For RP-LC analyses, the freeze-dried extracts were re-dissolved in 10% methanol in water (*v/v)*.

2.3. Instrumentation

One-dimensional HILIC– and RP-LC–ABTS as well as off-line HILIC×RP-LC–ABTS analyses were performed on a Shimadzu LC-10AD liquid chromatograph equipped with a binary pump, two UV detectors and a column oven, controlled by LCsolution software (Shimadzu Corporation, Kyoto, Japan). Solvents were degassed by a 7600 Solvent Degasser (Jones Chromatography, Cardiff, UK) and injections were performed using a Hewlett Packard 1050 injector (Agilent Technologies, Waldbronn, Germany). The ABTS solution was delivered by an Alliance 2695 HPLC system (Waters, Milford, MA, USA).

For on-line HILIC×RP-LC–ABTS, HILIC analyses were performed on the Shimadzu LC system described above while RP-LC separations were performed on an Agilent 1100 liquid chromatograph equipped with a binary pump, degasser, autosampler, column oven, photodiode array (PDA) detector and controlled by Chemstation software (Agilent). The two instruments were interfaced through a 10-port 2-position high pressure switching valve (Valco Instruments Co. Inc., Houston, Texas, USA) equipped with two 5 µL loops. The ABTS solution was added using a Hewlett Packard 1050 pump (Agilent). A schematic representation of the instrumental configurations used for one-dimensional HILIC– and RP-LC–ABTS and off- and on-line HILIC×RP-LC–ABTS analyses is shown in **Fig. 1**.

LC–MS experiments were perfomed on a Waters Acquity UPLC system equipped with a binary pump, degasser, autosampler, column oven, PDA detector and controlled by MassLynx software v4.1 (Waters). The UPLC system was coupled to a Waters Synapt Q-TOF mass spectrometer through an electrospray ion (ESI) source operated in negative ionisation mode. The capillary voltage was -2.5 kV, the sampling cone voltage 15 V and the extraction cone voltage 4.0 V. The source and desolvation temperatures were 120 and 275 °C, respectively. The cone and desolvation gas (both N_2) flow rates were 50 and 650 L/h, respectively. A sodium formate solution was used to calibrate the instrument and a mass-to-charge ratio (*m/z*) range of 200 and 2000 was scanned.

2.4. Chromatographic methods

*2.4.1. One-dimensional and off-line LC×LC–*ABTS *analyses*

HILIC separations were performed at ambient temperature on a Nomura Chemical Develosil Diol-100 column (250 mm × 1 mm i.d., 5 µm d_p, Aichi, Japan) using a previously reported method [26]. The binary mobile phase consisted of (A) acetonitrile and acetic acid (99:1, *v/v*) and (B) methanol, water and acetic acid (94.05:4.95:1, *v/v/v*). The following gradient was used at a flow rate of 50 µL/min: 4–40% B (0–45 min), 40% B isocratic (45–50 min), 40–100% B (50–55 min). An injection volume of 10 µL was used in the off-line analyses. One-minute fractions of the HILIC effluent, corresponding to 50 µL each, were collected using a Waters (WFC II) fraction collector.

RP-LC analyses were performed on a Kinetex C18 column (50 mm × 4.6 mm, 2.6 µm d_p, Phenomenex, Torrance, USA) protected with a Krudkatcher pre-filter (Phenomenex). A binary mobile phase consisting of (A) 0.1% formic acid in water (*v/v*) and (B) acetonitrile was used and separations were performed using a previously reported gradient method [30,31]: 2% B (0–0.13 min), 2–18% B (0.13–5.40 min), 18–25% B (5.40–9.00 min), 25–100% B (9.00–10.35 min), 100% B (10.35–11.25 min). The column temperature was 50 °C and the flow rate was 0.8 mL/min. 1.5 µL of each HILIC fraction was injected, and UV data were recorded at 280, 320 and 370 nm by the first UV detector (after the RP-LC column) and 414 nm by the second UV detector (after the reaction coil).

One-dimensional RP-LC–ABTS analyses were performed under identical conditions as outlined above. For one-dimensional HILIC–ABTS analyses, an injection volume of 0.5 µL was used while other experimental conditions were the same as outlined above.

*2.4.2. On-line LC×LC–*ABTS *analyses*

HILIC conditions were the same as outlined above for the off-line method, except that a flow rate of 25 µL/min was used; the gradient was adapted to keep the ratio of the gradient time to the void time (t_g/t_0) constant and 2.5 µL was injected. RP-LC analyses were performed as for the off-line system, except that a flow rate of 1.5 mL/min was used with the following gradient: 2% B (0–0.02 min), 2–18% B (0.02–0.20 min), 18–25% B (0.20–1.10 min), 25–100% B (1.10–1.20 min), 100–2% B (1.20–1.30 min) (total analysis time including re-equilibration, 2.0 min). The HILIC effluent was split ~1:32 before the 10-port switching valve, which was switched every 2 minutes using external events from the Agilent 1100 instrument. Under these conditions roughly 1.5 µL of each 2-minute HILIC fraction was injected onto the RP column.

2.4.3. ABTS radical scavenging detection

The ABTS solution was prepared according to [18] with minor adjustments. Briefly, 0.07 mM ABTS was added to 500 mL of a phosphate buffered saline (PBS) solution containing 137 mM NaCl, 10 mM Na_2HPO_4, 2 mM KCl and 2 mM KH_2PO_4, and stirred for 2 minutes. 1 g MnO_2 was added and the solution was stirred for an additional 10 min at room temperature before filtering through a 0.22 µm nylon membrane filter. The ABTS solution was kept in an ice-bath and protected from light with aluminium foil and was prepared freshly every 12 h. A 2.8 m × 0.25 mm i.d. polytetrafluoroethylene (PTFE) reaction coil, coiled as described by Kuhlman *et al* [32], was used for the post-column reaction in all cases except for one-dimensional HILIC–ABTS analyses, where a 1 m × 0.25 mm i.d. reaction coil was used. The reaction coil and the ABTS solvent line were protected from light using aluminium foil. The ABTS solution was added before the reaction coil at a flow rate of 0.8 mL/min for RP-LC–ABTS and off-line HILIC×RP-LC–ABTS analyses; for on-line HILIC×RP-LC–ABTS analyses the reagent flow rate was 0.5 mL/min and for one-dimensional HILIC–ABTS analyses it was 0.1 mL/min. The reaction was monitored at 414 nm in all cases using the second UV detector.

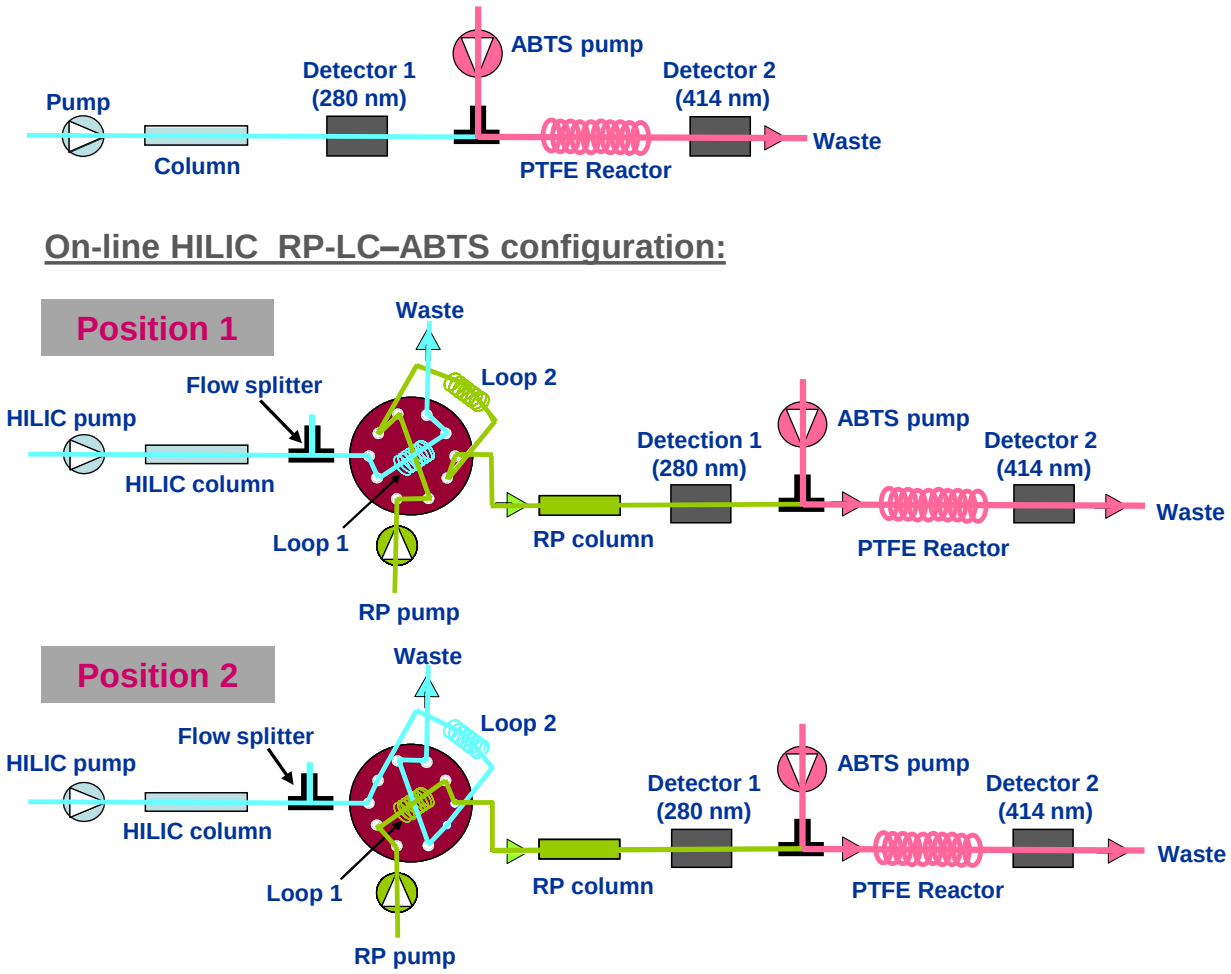

Fig. 1 A schematic illustration of the instrumental configurations used for 1-D LC–ABTS and off-line- and on-line HILIC×RP-LC–ABTS analyses. A 2.8 m × 0.25 mm i.d. PTFE reaction coil was used in all configurations except one-dimensional HILIC–ABTS analyses, where a 1 m × 0.25 mm i.d. reaction coil was used

2.5. Data handling

Raw off-line HILIC×RP-LC–ABTS data were exported into Statistica 10 (Statsoft Inc., USA) to construct contour plots. On-line HILIC×RP-LC–ABTS data were exported as comma separated (CSV) files before importing into GC Image 1.9b7 (Zoex Corporation, Houston, USA) to create contour plots.

3. Results and discussion

3.1. HPLC−ABTS optimisation

The choice of HILIC×RP-LC separation for hyphenation with selective radical scavenging detection was based on previous research which highlighted the improved separation offered by the combination of HILIC and RP-LC for the separation of complex phenolic extracts, including cocoa, grape seeds and green and rooibos teas [26,29-31]. Cocoa, grape seed and green tea extracts were used as applications in the current study to allow evaluation of radical scavenging activities for a diverse range of phenolic compounds previously identified in these samples [26,27,29]. Cocoa and grape seed contain mainly procyanidins and galloylated procyanidins (**Fig. 2**) of various degrees of polymerisation (DPs). These compounds are notoriously hard to separate due to their isomeric complexity. Green tea also contains low molecular weight (MW) proanthocyanidins as well as a variety of flavonols and phenolic acids. HILIC×RP-LC conditions were the same as in [30,31], with minor changes as outlined in the experimental section. A 2.6 µm superficially porous column was used in the second dimension, since this column has been shown to provide similar performance to fully porous sub-2µm phases for fast, high-resolution separations at lower pressures [33].

(a) **(b)**

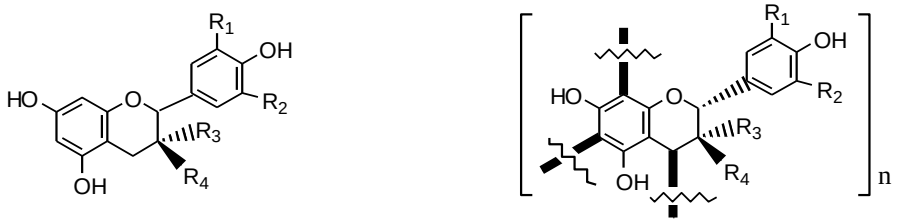

Compound	R_1	R_2	R_3	R_4
Catechin	H	OH	H	OH
Epicatechin	H	OH	OH	H
Epigallocatechin	OH	OH	OH	H
Epicatechin gallate	H	OH	Gallic acid ester	H
Epigallocatechin gallate	OH	OH	Gallic acid ester	H

Fig. 2 General chemical structures for (**a**) monomeric and (**b**) oligomeric proanthocyanidins

Although hyphenation of HPLC with the DPPH assay has been widely used for the determination of radical scavenging activities of phenolics, the ABTS assay was selected in this study for hyphenation with LC×LC for several reasons. Most importantly, ABTS offers faster reaction kinetics and better sensitivity [15,17-21], both aspects which are of paramount importance for combination with the fast separations in the second dimension of especially on-line LC×LC.

Prior to the on-line coupling of LC×LC with the ABTS assay, optimisation of parameters such as the reaction time, reaction coil dimensions (length and internal diameter (i.d.)) and the ABTS flow rate was performed. The choice of reaction coil dimensions is critically important: long reaction coils provide longer reaction times (and therefore better sensitivity), while narrower reaction coils minimise band broadening and thus loss of chromatographic efficiency [34]. Furthermore, backpressure increases with both the reaction coil length and a decrease in i.d. [34]. Since the aim of this study was to couple the ABTS assay to LC×LC separation, where fast, high efficiency and high pressure analyses are performed in the second dimension, a narrow and short reaction coil was essential to reduce extra-column band broadening and operating pressure. At the same time, sufficient reaction times are required for acceptable sensitivity. Three 2.8 m PTFE reaction coils with internal diameters of 0.18, 0.25 and 0.38 mm were evaluated using the off-line RP-LC gradient. A 2.8 m × 0.25 mm i.d. reaction coil provided the best compromise between sensitivity and band broadening. Initially, a 0.02 mM ABTS concentration was used. However, due to the relatively high concentrations of phenolics in the samples analysed in this study, an increase in the ABTS concentration (to 0.07 mM) was necessary to avoid saturation of the ABTS signal. Representative HILIC– and RP-LC–ABTS chromatograms obtained for the cocoa extract are shown in **Fig. 3**. Considering that HILIC separations were performed on a 1 mm i.d. column for which extra-column band broadening is exceptionally problematic (as this relates to both the flow rate and the column volume relative to the extra-column volume of the instrument [35]), the performance of the optimised reaction coil is especially good. Similarly, for the RP-LC separation, the performance of the reaction coil is much better than conventional reaction coil dimensions used for 1-D HPLC–ABTS assays.

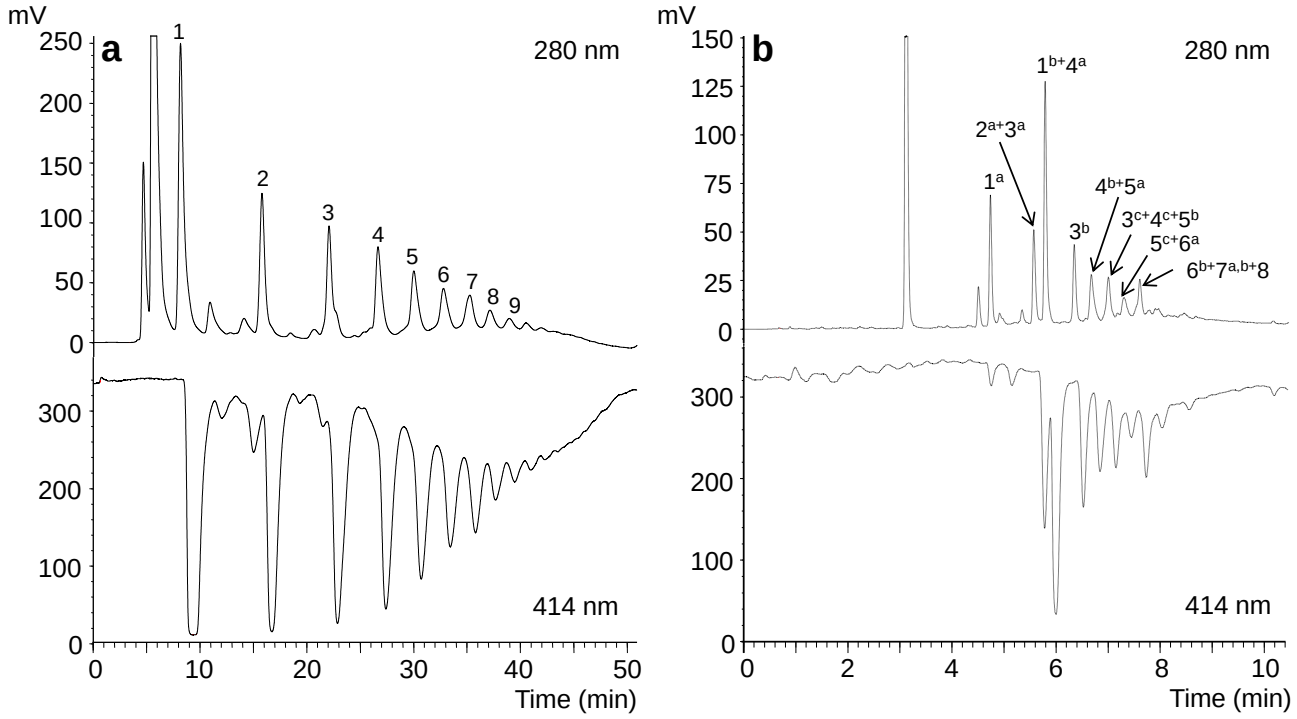

Fig. 3 UV chromatograms obtained at 280 (detector 1, post-column) and 414 nm (detector 2, post-reaction coil) for the one-dimensional HILIC–ABTS (**a**) and RP-LC–ABTS (**b**) analyses of a cocoa extract. Peak numbers denote the degree of polymerisation (DP) of procyanidins and letters differentiate isomers of the same DP as identified by LC–ESI-MS [30,31]. Analysis conditions are as specified in the experimental section

3.2. HILIC×RP-LC–ABTS analysis of cocoa, grape seed and green tea phenolics

Following optimisation of the ABTS detection parameters, HILIC×RP-LC separations were coupled to the post-column reaction coil with the ABTS radical solution added through a T-union after the first detector as described in the experimental section (see also **Fig. 1)**. Contour plots for the on-line and off-line HILIC×RP-LC–ABTS analyses of cocoa, grape seed and green tea phenolics are shown in **Figs 4 and 5**, respectively. A comparison of contour plots obtained at 280 and 414 nm for each of these samples clearly shows that this methodology provides a quick way of identifying radical scavenging species in complex mixtures. For example, UV-active compounds labelled **A-F** in **Figs 4 and 5** lack radical scavenging activity (or exhibit much slower reaction kinetics) based on their absence in the corresponding contour plots at 414 nm. These results confirm that the ABTS assay is sufficiently fast for combination with LC×LC, as all compounds were detected with good sensitivity for reaction times of 4.26 and 5.32 s in the on-line and off-line analyses, respectively.

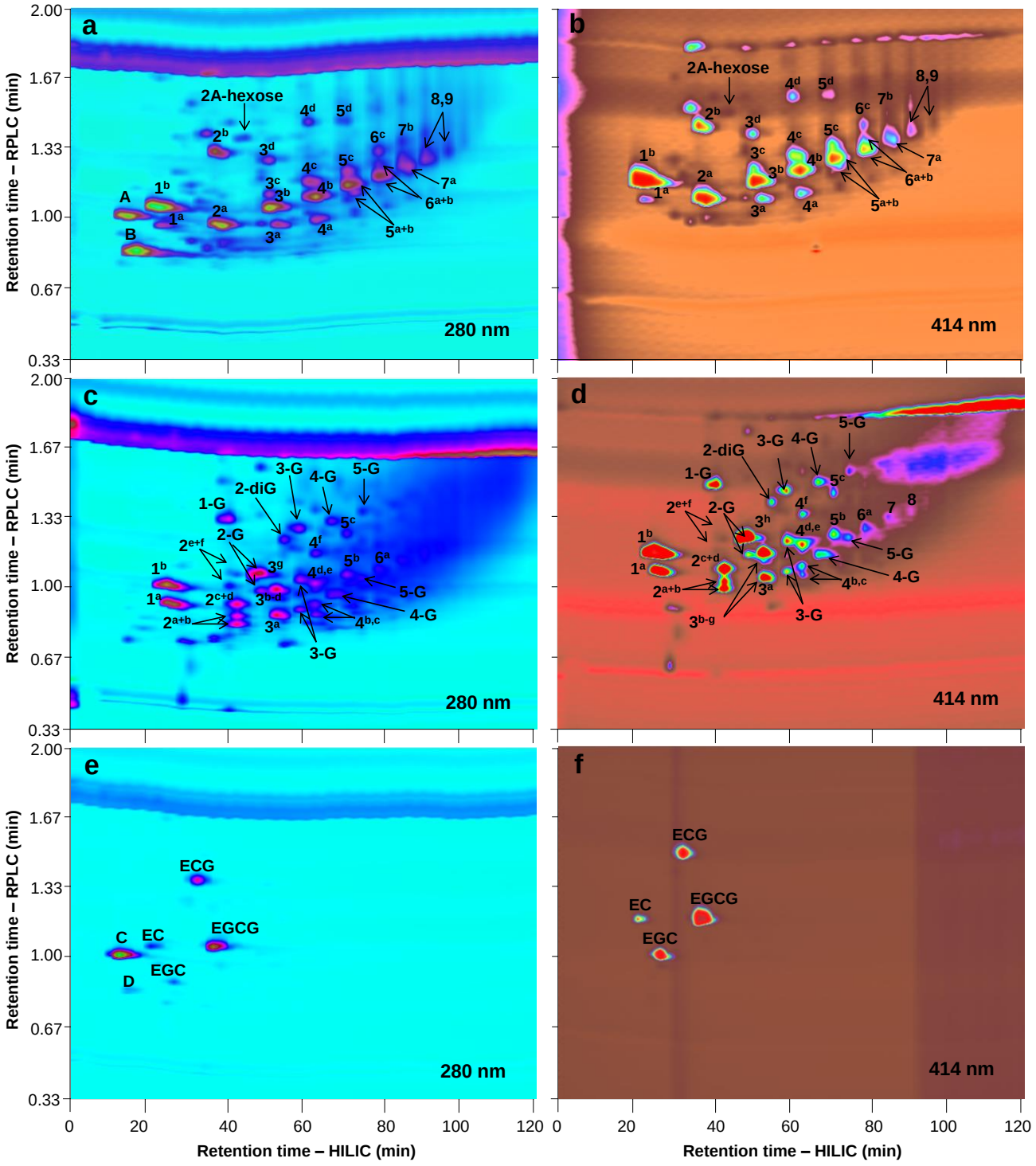

Fig. 4 UV contour plots obtained at 280 (detector 1, post-column) and 414 nm (detector 2, post-reaction coil) for the on-line HILIC×RP-LC–ABTS analysis of cocoa (**a** and **b**), red grape seed (**c** and **d**) and green tea (**e** and **f**) extracts. Peak annotation: Figures **a**-**d**: numbers indicate procyanidin degree of polymerisation (DP), small letters differentiate isomers with the same DP. G and diG

indicate mono- and digalloylated procyanidins, respectively [30,31]. Figures **e** and **f**: EC: epicatechin, ECG: epicatechin gallate, EGC: epigallocatechin, EGCG: epigallocatechin gallate. Compounds were identified by LC–ESI-MS. Refer to the experimental section for analytical conditions

From the contour plots, it is also evident that extensive co-elution occurs in both HILIC and RP-LC separations, something which is not immediately obvious from the 1-D HPLC chromatograms shown in **Fig. 3**. For example, proanthocyanidins with the same degree of polymerisation (DP) are not resolved in the HILIC dimension, while co-elution of proanthocyanidins of different DPs is evident in the RP-LC dimension (**Fig. 4a and c**). A similar observation can be made for the green tea sample, where epicatechin (EC) and epigallocatechin gallate (EGCG) co-elute in the RP-LC dimension.

When comparing on-line and off-line HILIC×RP-LC–ABTS analyses of cocoa and grape seed (**Figs 4 and 5**), much better resolution is evident for the latter separations. This follows from the longer second dimension separations used in the off-line mode, since the second dimension analysis time is independent of the sampling time in this configuration [30,31]. While the benefit in terms of separation performance is evident, it should be noted that off-line analysis under these conditions takes ~13.75 h, compared to 120 min for the on-line separation.

As a quantitative measure of the performance gain offered by LC×LC separation, the peak capacity may be used. Peak capacity is a theoretical measure of the number of compounds that can be separated at a given resolution (typically 1) [36]. The peak capacities for the 1-D HILIC and RP-LC methods used in this work are 14 and 157, respectively (calculated for the cocoa extract using the off-line conditions) [31]. As approximation, the peak capacity of an LC×LC separation is the product of the peak capacities in each dimension, although this represents an overestimation in most cases. Practical peak capacities, taking into account the effects of the first dimension under-sampling and limited orthogonality between dimensions, for the on-line and off-line methods used have previously been determined as 462 and 1760, respectively [31]. While it should be considered that some performance loss occurs due to the ABTS detection process (compare UV traces at 280 and 414 nm in **Figs 3** and **6**), these values still provide an approximate measure of the gain in resolving power offered by HILIC×RP-LC–ABTS compared to conventional one-dimensional HPLC–ABTS methods.

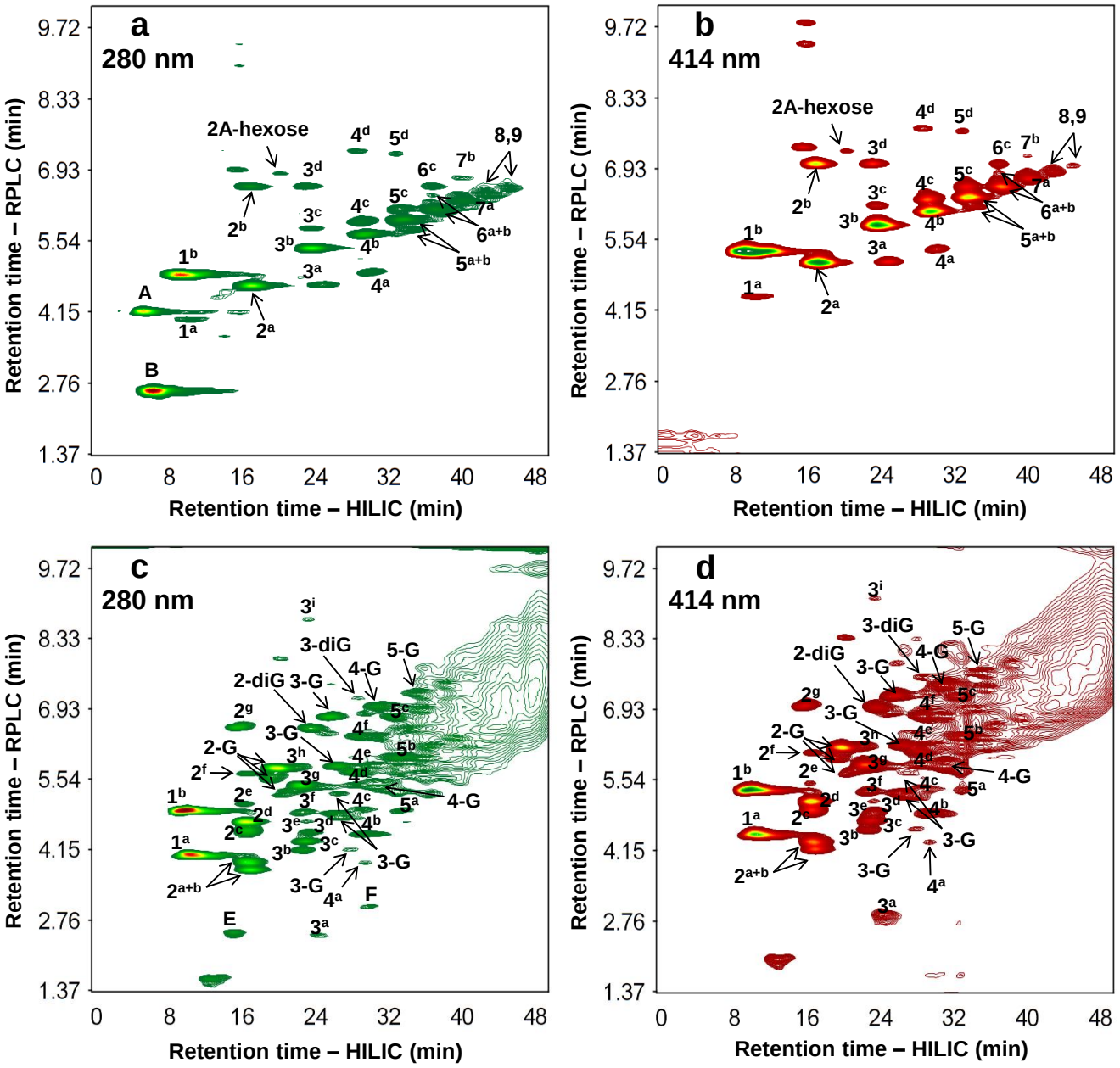

Fig. 5 UV contour plots obtained at 280 (detector 1, post-column) and 414 nm (detector 2, post-reaction coil) for the off-line HILIC×RP-LC–ABTS analyses of cocoa (**a** and **b**) and red grape seed (**c** and **d**) extracts. Peak annotation corresponds to **Fig. 4**. Refer to the experimental section for analytical conditions

An illustration of the complexity of the grape seed sample can be seen in **Fig. 6**, which compares RP-LC UV chromatograms obtained for HILIC fractions 29 (corresponding mainly to tetrameric procyanidins and galloylated trimeric procyanidins) and 36 (corresponding to proanthocyanidins of DP

> 6). These figures point to the extent of overlap occurring in the HILIC dimension (all compounds detected in a single chromatogram co-elute in a single 1-minute HILIC fraction). Furthermore, even for the longer (off-line) RP-LC gradient used here, separation of all compounds in each fraction could not be obtained, especially in the case of the higher MW fraction. This implies that measuring radical scavenging activity for this sample by either HILIC–ABTS or RP-LC–ABTS would deliver inaccurate results due to inevitable peak overlap. HILIC×RP-LC–ABTS is demonstrably a better approach for assessment of radical scavenging activities of individual compounds in highly complex samples since component overlap is significantly reduced by the two-dimensional separation.

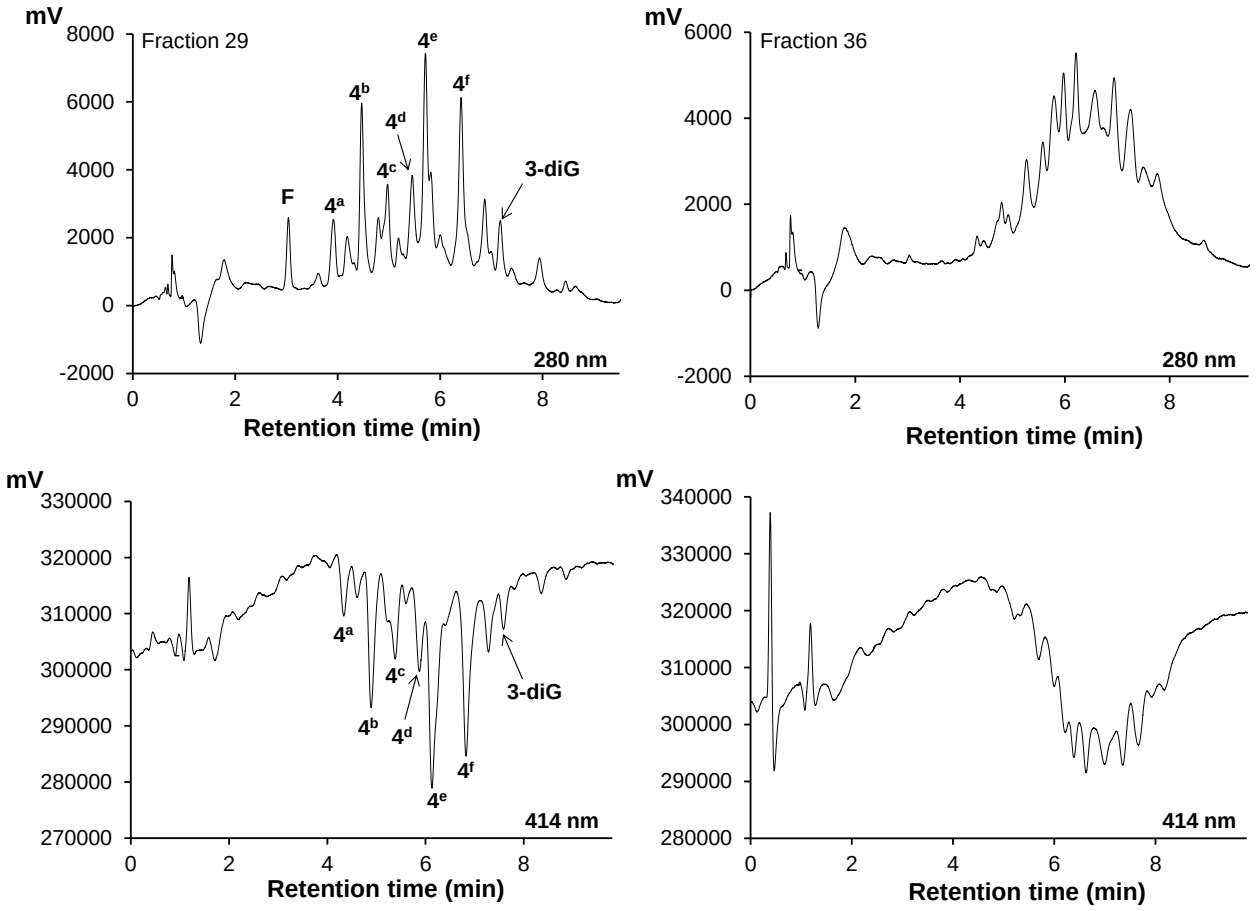

Fig. 6 UV contour plots obtained at 280 (top, detector 1 post-column) and 414 nm (bottom, detector 2 post-reaction coil) for the RP-LC separation of fractions 29 and 36 in the off-line HILIC×RP-LC–ABTS analysis of a grape seed extract. Peak annotation corresponds to **Fig. 5**

Judging from the contour plots at 280 and 414 nm, it can be concluded that cocoa and grape seed proanthocyanidins as well as a few compounds detected in the green tea extract are effective radical

scavengers. Visual inspection of relative peak intensities between the two contour plots suggests that the activity is directly proportional to the relative concentrations of individual compounds in the sample. For this reason, it appears as if low molecular weight compounds are the most important radical scavengers in these samples, although this is misleading since radical scavenging activity should be judged on an equimolar basis [8]. The radical scavenging activity of a compound is commonly expressed in terms of its trolox equivalent antioxidant capacity (TEAC) value, whereby compound activity is calculated relative to a 1 mM trolox solution [18,37]. Although not attempted in the current work, quantification of radical scavenging activity by this strategy is entirely compatible with LC×LC separation. Several studies [38-40] have demonstrated the feasibility of quantitative LC×LC; the same principles can be applied to obtain quantitative TEAC values in combination with LC×LC separation.

The feasibility of hyphenating LC×LC separation with on-line radical scavenging assays paves the way for several future studies. For quantitative analysis, the use of a capillary column in the first dimension would avoid the need for splitting the first dimension flow. While this will not necessarily affect the sensitivity because of the smaller sample capacity of capillary columns, it would improve quantification accuracy. Off-line LC×LC can also be upscaled to allow a more powerful method for the isolation and further structural characterisation of active compounds. Another possibility is to split the flow after the second dimension column to perform simultaneous mass spectrometry (MS) (and/or MS/MS) and radical scavenging detection. Since MS requires only a flow of ~0.3 mL/min, this would not severely impact on the sensitivity of the radical scavenging assay.

4. Conclusions

In this study, the potential of combining HILIC×RP-LC separation with an on-line radical scavenging assay has been demonstrated. This methodology represents a powerful analytical strategy for the measurement of radical scavenging activities of individual compounds in complex mixtures. Compared to one-dimensional LC–ABTS methods, where extensive peak overlap may occur, LC×LC separation provides a much higher likelihood of obtaining pure chromatographic peaks. On-line HILIC×RP-LC–ABTS offers high throughput and is suitable for analysis of samples with relatively simple antioxidant profiles. Alternatively, this method can be used as a quick tool for the screening of bioactive molecules in complex natural products. Off-line HILIC×RP-LC–ABTS provides high resolution, therefore shows promise as a relatively fast alternative to tedious and time-consuming conventional assay-guided isolation of bioactive compounds from complex matrices. Future research should focus on the quantitative analysis of radical scavenging activities by LC×LC–ABTS to allow determination of structural-radical scavenging relationships.

Acknowledgements

KMK and AdV gratefully acknowledge Stellenbosch University, Sasol and the National Research Foundation (NRF, Grant 70995 to AdV) for funding. SDS and TVH gratefully acknowledge the Agency for Innovation by Science and Technology in Flanders (IWT) for financial support. Dalene de Beer is thanked for advice on the antioxidant assays, and Edmund Luckay (IWBT) for the donation of the grape sample.

References

[1] Kusznierewicz B, Piasek A, Bartoszek A, Namiesnik J (2011) Phytochem Anal 22:392-402
[2] Szajdek A, Borowska EJ (2008) Plant Foods Hum Nutr 63:147-156
[3] Iriti M, Faoro F (2009) In: Watson RR (ed) Complementary and Alternative Therapies and the Aging Population: An evidence-based approach. Elsevier Inc., San Diego
[4] Shahidi F, Wanasundara PKJPD (1992) Crit Rev Food Sci Nutr 32:67-103
[5] Koşar M, Dorman HJD, Başer KHC, Hiltunen R (2004) J Agric Food Chem 52:5004-5010
[6] Dudonné AS, Vitrac X, Coutière P, Woillez M, Mérillon J-M,(2009) J Agric Food Chem 57:1768-1774
[7] Joubert E, Manley M, Botha M (2008) Phytochem Anal 19:169-178
[8] Spranger I, Sun B, Mateus AM, de Freitas V, Ricardo-da-Silva JM (2008) Food Chem 108:519-532
[9] Huang D, Ou B, Prior RL (2005) J Agric Food Chem 53:1841-1856
[10] Magalhaes LM, Segundo MA, Reis S, Lima JLFC (2008) Anal Chim Acta 613:1-19
[11] Karadag A, Ozcelik B, Saner S (2009) Food Anal Meth. 2:41-60
[12] Moon J-K, Shibamoto T (2009) J Agric Food Chem 57:1655-1666
[13] Laguerre M, Decker EA, Lecomte J, Villeneuve P (2010) Curr Opin Clin Nutr Metab Care 13:518-525
[14] Gülçin I (2012) Arch Toxicol 86:345-391
[15] Niederländer HAG, van Beek TA, Bartasiute A, Koleva II (2008) J Chromatogr A 1210:121-134
[16] Malherbe CJ, de Beer D, Joubert E (2012) Int J Mol Sci 13:3101-3133
[17] Re R, Pellegrini N, Proteggente A, Apnnal A, Yang M, Rice-Evans C (1999) Free Radic Biol Med 26:1231-1237
[18] Koleva II, Niederländer HAG, van Beek TA (2001) Anal Chem 73:3373-3381
[19] Floegel A, Kim D-O, Chung S-J, Koo SI, Chun OK (2011) J Food Comp Anal 24:1043-1048
[20] Martysiak-Lrowska D, Wenta W (2012) Acta Sci Pol Technol Aliment 11:83-89
[21] Li F, Zhang L-D, Li B-C, Yang J, Yu H, Wan J-B, Wang Y-T, Li P (2012) Free Radic Res 46:286-294
[22] Bushey MM, Jorgenson JW (1990) Anal Chem 62:161-167
[23] Davis JM, Giddings JC (1985) Anal Chem 57:2168-2177
[24] Davis JM, Giddings JC (1985) Anal Chem 57:2178-2187
[25] Giddings JC (1990) In: Cortes HJ (ed) Multidimensional Chromatography: techniques and applications. Marcel Dekker Inc., New York
[26] Kalili KM, de Villiers A (2009) J Chromatogr A 1216:6274-6284
[27] Kalili KM, de Villiers A (2010) J Sep Sci 33:853-863
[28] Beelders T, Kalili KM, Joubert E, de Beer D, de Villiers A (2012) J Sep Sci 35:1808-1820
[29] Kalili KM, Vestner J, Stander MA, de Villiers A (2013) Anal Chem 85:9107-9115
[30] Kalili KM, de Villiers A (2013) J Chromatogr A 1289:58-68
[31] Kalili KM, de Villiers A (2013) J Chromatogr A 1289:69-79
[32] Kuhlmann O, Krauss G-J (1997) J Pharm Biomed Anal 16:553-559
[33] Kalili KM, Cabooter D, Desmet G, de Villiers A (2012) J Chromatogr A 1236:63-76
[34] Kucera P, Umagat H (1983) J Chromatogr 255:563-579
[35] Lestremau F, Wu D, Szücs R (2010) J Chromatogr A 1217:4925-4933
[36] Giddings JC (1984) Anal Chem 56:1258A-1270A
[37] Pannala AS, Rice-Evans C (2001) Methods in Enzymology 335:266-272
[38] Kivilompolo M, Hyötyläinen T (2007) J Chromatogr A 1145:155-164
[39] Kivilompolo M, Oburka V, Hyötyläinen T (2008) Anal Bioanal Chem 391:373-380
[40] Dugo P, Cacciola F, Donato P, Airado-Rodríguez D, Herrero M, Mondello L (2009) J Chromatogr A 1216:7483-7487